Design and Synthesis of Benzimidazole Core Moieties and Structure Activity Relationship Studies Based on *In Vitro* Evaluation as Anticancer Drugs

Thesis submitted

by

Alka Sharma
(Regd. No. 901009004)

In fulfilment of the requirement

for the degree of

Doctor of Philosophy

Under the supervision of

Dr. Kamaldeep Paul
(Associate Professor)

School of Chemistry and Biochemistry
Thapar University
Patiala – 147 004
Punjab, India

December, 2014

Candidate's Declaration

I, hereby declare that the work presented in the thesis entitled "**Design and Synthesis of Benzimidazole Core Moieties and Structure Activity Relationship Studies Based on *In Vitro* Evaluation as Anticancer Drugs**" in fulfilment of the requirement for the award of the Degree of Doctor of Philosophy, School of Chemistry and Biochemistry, Thapar University, Patiala, is an authentic record of my own work carried out under the supervision of Dr. Kamaldeep Paul, Assistant Professor, School of Chemistry and Biochemistry, Thapar University, Patiala, India. The matter embodied in this thesis has not been submitted in part or full to any other university or institute for the award of any degree in India or Abroad.

Alka Sharma

Alka Sharma

Kamaldeep Paul.

(Supervisor)

Dr. Kamaldeep Paul
Associate Professor
School of Chemistry and Biochemistry
Thapar University, Patiala - 147 004
Punjab (India)

Certificate

This is to certify that thesis entitled "**Design and Synthesis of Benzimidazole Core Moieties and Structure Activity Relationship Studies Based on *In Vitro* Evaluation as Anticancer Drugs**", being submitted by Alka Sharma in the fulfilment of the requirement for the award of Degree of Doctor of Philosophy to the School of Chemistry and Biochemistry, Thapar University, Patiala, is a record of candidate's own work carried out by her under my supervision and guidance. The matter presented in this thesis has not been submitted in part or full for the award of any degree in any other University or Institute.

(Supervisor)

Dr. Kamaldeep Paul
Associate Professor
School of Chemistry and Biochemistry
Thapar University, Patiala - 147 004
Punjab (India)

(Supervisor)

Dr. Bonamali Pal
Professor & Head
School of Chemistry and Biochemistry
Thapar University, Patiala - 147 004
Punjab (India)

Dedicated to
My
Beloved Family

All that I am, or hope to be, I owe to my angel mother.

Abraham Lincoln

Acknowledgements

I humbly prostrate myself before the Almighty God for his grace and enduring blessings which enabled me to complete this work successfully with my full satisfaction.

First and foremost, I would like to express my sincere gratitude to my adored research supervisor ***Dr. Kamaldeep Paul,*** *for introducing me to this exciting field of science and for his valuable guidance, continuous support, motivation and patience throughout the Ph.D. work. I have learnt extensively from his, including how to regard an old question from a new perspective and how to approach a problem by systematic thinking. His persistent courage and confidence will always inspire me, and I hope to continue to work with his noble thoughts. I am really glad to be associated with a person like him in my life.*

I am profoundly obliged to ***Dr. Bonamali Pal****, Associate Professor and Head, School of Chemistry and Biochemistry, Thapar University, Patiala for their good wishes and motivation.*

I would like to thank ***Dr. Vijay Luxami*** *and* ***Dr. Sanjai Saxena*** *for their fruitful discussion and my doctoral committee for their encouragement, constructive criticism and inspirations.*

Special regards to my beginning teachers and teachers of the School of Chemistry and Biochemistry for providing suggestions and taking interest in the progress of work along with lab facility. Deep sense of gratitude to all because of whose teaching at different stages of education has made it possible for me to see this day.

I am thankful to my lab-mates and other close friends ***Dr. Rohit Singh, Dr. Inderpreet Singh, Bhupendra Thakur, Rekha Gupta, Kuldeep Kaur, Happy, Dr. Gurmeet Singh****,*

Dr. Dinesh Kumar, Dr. ***Jaspal Singh, Navjot kaur, Shilpa Narang, Sandeep Kaur, Ruchika Thakur, Dr. Anil, Chawan, Chinu, Dr. Mandeep kaur, Dr. Rupinder Makker, Rajesh Kumar, Sandeep kumar, Akul Sen Gupta, Richa Rani, Prinka, Richa goel, Gulshan, Alka goel, Meenakshi, Yuvraj*** *for always standing by my side and sharing a great relationship as compassionate friends. I will forever cherish the warmth shown by them, whose smiling face always made me refreshing.*

I would like to thank ***other staff*** *of the School of Chemistry and Biochemistry, Thapar University, Patiala for the constant official help and cooperation.*

Most of the results described in this thesis would not have been possible without the help of laboratories at the institutes like, ***SAI,*** *Thapar University, Patiala,* ***SAIF****, Punjab University, Chandigarh,* ***IISER****, Mohali Research Institute and* ***NCI,*** *USA is gratefully acknowledged for investigating antitumor activities.*

I gratefully acknowledge, ***University Grant Commission (UGC)****, Government of India, for providing me financial support in the initial years.*

I would like to pay high regards to my most lovable mother ***Mrs. Kiran Tejpal,*** *my father* ***Mr. Tirath Ram Tejpal****, my brother* ***Amit Tejpal*** *and my sweet sister* ***Arti Sharma*** *for their love, affection, patience and blessings. This Ph. D. thesis is a result of the extraordinary will, efforts and sacrifices of my parents. I am extremely happy to fulfil their ultimate desire that today, I achieve.*

Despite all this co-operation rendered generously by one and all, I am solely responsible for any and all the errors and short comings of this dissertation.

_____

Alka Sharma

Table of Contents

List of Abbreviations

ATP	Adenosine triphosphate
ATCC	American Type Culture Collection
ALK5	Activin receptor-like kinase 5
AMPK	Adenosine Monophosphate-Activated Protein Kinase
ACAT1	Acyl-coenzyme A:cholesterol acyltransferase 1
A. niger	*Aspergillus niger*
A. clavatus	*Aspergillus clavatus*
ArH	Aromatic hydrogen
B. cereus	*Bacillus cereus*
CDK1	Cyclin dependent kinase 1
CD3+	Cluster of differentiation 3
C. albicans	*Candida albicans*
CDK1	Cyclin dependent kinase 1
Cs_2CO_3	Cesium carbonate
DNA	Deoxyribonucleic acid
DMN	Dimethylnitrosamine
DGAT1	Diglyceride acyltransferase 1
DMSO	Dimethyl sulfoxide
E. histolytica	*Entamoeba histolytica*
EtOH	Ethanol
Et_3N	Triethylamine
EIMS	Electron Impact Mass Spectrometry
E. coli	Escherichia coli
5-FU	5-Fluorouracil
G. intestinalis	*Giardia intestinalis*
GI_{50}	Growth Inhibitory
Hsp90	Heat shock protein 90
Her2	Human epidermal growth factor receptor 2
hFOB	Human fetal normal osteoblastic
IC_{50}	Inhibition Concentration
K_2CO_3	Potassium carbonate
LTT	Lipid tolerance test

LC_{50}	Lethal concentrations
LE	Ligand efficiency
LOO	Leave-one-out
MIC	Minimum Inhibitory Concentration
M. tuberculosis	Mycobacterium tuberculosis
MTT	3-(4,5-dimethylthiazol-2-yl)-2,5-diphenyltetrazolium bromide
MCF-7	Michigan Cancer Foundation-7
mTOR	Mammalian target of rapamycin
µM	micro molar
mg	milligram
min	minutes
mL	millilitre
MG-MID	Mean graph mid-point
M. P.	Melting point
MR	Molar refractivity
Na^tOBu	Sodium tert-butoxide
NaOH	Sodium hydroxide
NaH	Sodium hydride
NCI	National Cancer Institute
OS	Osteogenic sarcoma
$Pd(PPh_3)_4$	Tetrakis(triphenylphosphine)palladium(0)
$Pd(PPh_3)_2Cl_2$	Bis(triphenylphosphine)palladium(II) dichloride
$Pd_2(dba)_3$	Tris(dibenzylideneacetone)dipalladium(0)
PC-3	Prostate cancer
PBMC	Peripheral blood mononuclear cells
P. aeruginosa	Pseudomonas aeruginosa
PK	Pharmacokinetic
p38MAP	P38 mitogen-activated protein kinases
POCl3	Phosphorus oxychloride
PM3	Parametric Method-3
pdb	Protein data bank
QSAR	Quantitative structural-activity relationship

RNA	Ribonucleic acid
RNR	Ribonucleotide reductase
$RMSE_{cv}$	Root mean square error of cross-validated
Ser	Serine
S. aureus	*Staphylococcus aureus*
S. pyogenus	*Streptococcus pyogenes*
S. dysenteriae	*Shigella dysenteriae*
SRB	Sulforhodamine B
Thr	Threonine
T. vaginalis	*Trichomonas vaginalis*
THF	Tetrahydrofuran
TLC	Thin layer chromatography
TGI	Total growth inhibitory
Topo I	Topoisomerase -1
Topo II	Topoisomerase -1
V. cholerae	*Vibrio cholerae*
VEGFR	Vascular endothelial growth factor receptor

INTRODUCTION

We are living through an exciting era for drug discovery and development-one that is full of vast opportunities and challenges. Cancer is inescapably one of the most studied but yet unexplained non communicable human disease. It is an idiopathic disease; doctors and scientists are constantly trying to evolve new effective drugs for its treatment. There is no other disease which parallel cancer in diversity of its origin, nature and treatment.

Cancer is a multifaceted disease characterized by a remarkably high degree of adaptability and resilience.[1] The medical term for cancer is neoplasm, which means "a relatively autonomous growth of tissues".[2] It is a collective term for a group of diseases characterized by the loss of control of the growth, division and spread of a group of cells. It can form an encapsulated benign tumor, leading to invasion and destruction of adjacent tissues. On the other hand, nonencapsulated malignant tumors grow rapidly, and can spread to various regions of the body and metastasize. Cancer therapy is mostly based on surgery, radiotherapy, hormone and chemotherapy. However, the clinical results are often only a short prolongation in patient survival.[3] A schematic description of current cancer treatment involves surgery for local resection, radiotherapy targeted for the destruction of the remaining cancer cells in the normal tissues surrounding the excised cancer, and systemic chemotherapy aimed at elimination of isolated cancer cells within normal tissues and distant metastases. Over the years, the design of cancer chemotherapy has become increasingly sophisticated. Yet there is no cancer treatment that is 100% effective against disseminated cancer. At present cancer therapy interfering with a single biological molecule or pathway has been successfully utilized.[4] Most chemotherapy regimens include the sequential use of several drugs, such as kinase inhibitors, monoclonal antibodies for cancer cell surface receptors, and cytotoxic drugs. The protein kinases including serine-threonine kinases, known as mitotic kinases, include cyclin dependent kinase 1 (CDK1), polo kinases, NIMA kinases, WARTS/LATS1 kinases, and Aurora kinases that play an important role in different stages of cell division.[5] The serine/threonine (Ser/Thr) kinases and tyrosine kinases are enzymes that phosphorylate either serine or threonine residues or tyrosine residues on a variety of proteins, many of which are involved in signal transduction pathways associated with a variety of cellular processes.[6,7] These kinases have been implicated in a number

of signalling pathways contributing to disease states, including cancer,[8,9] psoriasis,[10] atherosclerosis,[11] and chronic inflammatory diseases such as rheumatoid arthritis and inflammatory bowel disease.[12,13] Despite numerous drug discovery projects targeting kinases and considerable investments during the past few decades, only a few compounds have reached the market, leaving many potential cancer targets still undrugged. Subpopulations of treatment-resistant cancer cells will invariably occur during chronic administrations of any of these chemotherapeutic agents.

Aurora kinases are a family of three highly homologous serine-threonine protein kinases that play a critical role in regulating many of the processes that are pivotal to mitosis. The first homologue of the Aurora kinase family was identified using a genetic screen to find mutations in yeast that induce an increase-in-ploidy phenotype.[14] The Aurora kinases have shown to be promising clinically relevant anticancer targets. Depletion or inhibition of Aurora A and B by RNA, dominant negative kinase mutant or neutralizing antibodies results in critical disruption of mitosis and a block in proliferation leading to cell death in human cancer cell lines. Such compounds also exhibit less severe side effects as compared to the compounds targeting general microtubule dynamics, since they are not expected to interfere with proper function of interphase

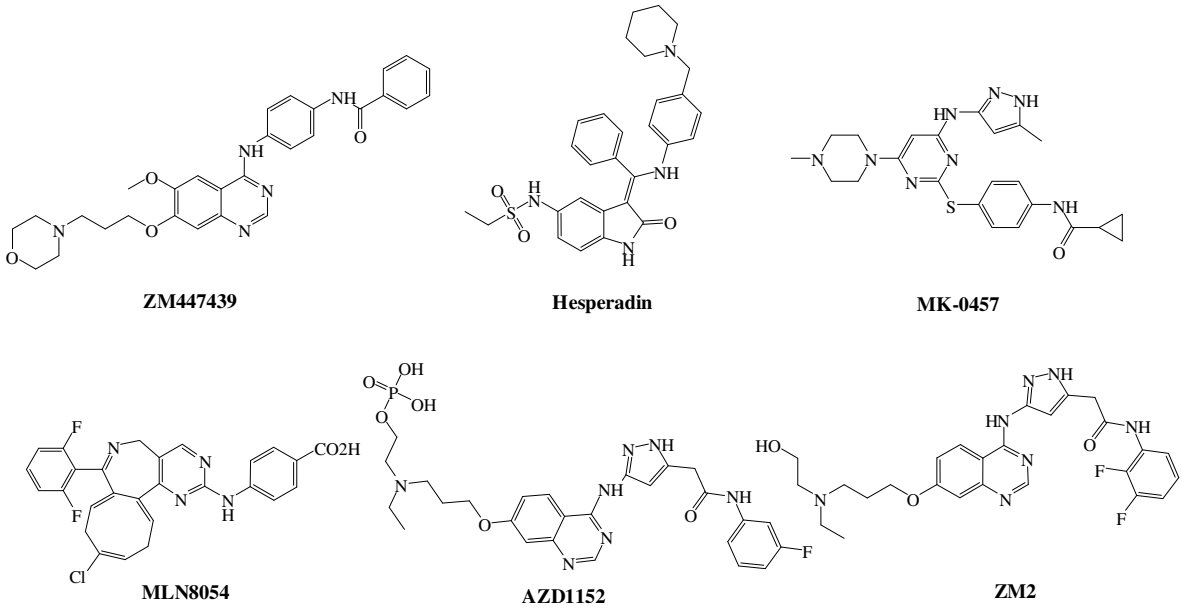

Figure-I

cells. In the present scenario, this strategy has intensively been used for identifying selective inhibitors as potential anticancer drugs based upon Aurora kinase. In recent years, several small molecule ATP-competitive inhibitors have been described that target the Aurora kinase family. Moreover, *in vivo* studies with Aurora inhibitors viz., MK-0457/VX-680,[15] PHA-739358,[16] MLN8237,[17] AZD1152[18] etc. **(figure-I)** in various animal models have shown tumor regression and are now in different stages of clinical development of various cancers.

Nitrogen-containing heterocycles are present in a wide variety of bioactive natural products and biological molecules that may be good drug candidates.[19] Specifically, quinazolines, purines and benzimidazoles, and their derivatives, which belong to the N-containing heterocyclic compounds, have caused universal concerns due to their widely and distinct pharmaceutical activities. The chemistry of quinazoline compounds has more than centuries old history; however the intense search for biologically active substances in this series began only in the last few decades. Researchers have determined a wide range of biological and pharmacological activities of quinazoline derivatives, including anticancer,[20] anti-inflammation,[21] anti-bacterial,[22] analgesic,[23] anti-virus,[24] anti-cytotoxin,[25] anti-spasm,[23] anti-tuberculosis,[26] anti-oxidation,[27] antimalarial,[28] anti-hypertension,[29] anti-obesity,[30] anti-psychotic,[31] anti-diabetes,[32] etc. The hybrid synthesis of small-molecule library is now a widespread method to provide large numbers of candidates for drug discovery program.[33]

The purine ring is a ubiquitous recognition motif in biological systems. Purines are also components of nucleotides that are monomeric building blocks of the DNA or RNA nucleic acid poly-chains. Therefore, the synthesis and chemical modifications of purines are of substantial interest. Purine motifs have attracted a great deal of research interest due to their preponderance in pharmaceutically indispensable compounds.[34] Substituted purine especially, 2,6-disubstituted purine known to be very important medicinal and pharmaceutical intermediate.[35]

Benzimidazoles are also categorized in the important pharmacophores and privileged sub-structures in medicinal chemistry owing to their involvement as a key component for various biological activities.[36] Thus, a series of quinazoline/purine and benzimidazole hybrids were prepared with introduction of aromatic, aliphatic and heterocyclic moieties at the 2-position of quinazoline and purine rings to improve its potency and selectivity. Substitution of these hybrids

with different primary and secondary amines remarkably increase their activity beyond their normal scope.

Thus, in the present research programme, the new series of hybrid molecules of quinazoline-benzimidazoles and purine-benzimidazoles have been synthesized, evaluated for their *in-vitro* anticancer activity as well as Aurora kinase inhibitors and the roles of their different structural fragments in affecting the properties have been studied on the basis of structure activity relationship (SAR). The presentation of present work in this dissertation has been divided into following parts:

Chapter 1: Review of Literature

Chapter 2: Quinazoline-Benzimidazole Hybridization

Chapter 3: Purine-Benzimidazole Hybridization

Chapter 4: Pd-Catalyzed Coupling Reaction of 2,4-Dichloroquinazoline

REFERENCES

1. Hanahan, D.; Weinberg, R. A. *Cell* **2011**, *144*, 646.
2. Ahluwalia, V. K.; Chopra, M. (**2008**) Medicinal Chemistry. Ane Books India. *13*, 239.
3. Avendano, C.; Menendez, J. C. (**2008**) Medicinal Chemistry of Anticancer Drugs. Elsevier B. V. *1*, 1.
4. (a) Sawyers, C. *Nature* **2004**, *432*, 94; (b) Petrelli, A.; Giordano, S. *Curr. Med. Chem.* **2008**, *15*, 422.
5. Dar, A. A.; Goff, L. W.; Majid, S.; Berlin, J.; El-Rifai, W. *Mol Cancer Ther.* **2010**, *9*, 1.
6. Hunter, T. *Methods Enzymol.* **1991**, *200*, 3.
7. Pearson, R. B.; Kemp, B. E. *Methods Enzymol.* **1991**, *200*, 62.
8. Bruton, V. G.; Workman, P. *Cancer Chem. Pharmacol.* **1993**, *32,* 1.
9. Powis, G. *Pharmacol. Ther.* **1994**, *62,* 57.
10. Elder, J. J.; Fisher, G. L.; Lindquist, P. B.; Bennet, G. L.; Pittelkow, M. R.; Coffey, R. J.; Ellingsworth, L.; Denryneck, R.; Voorhees, J. J. *Science* **1989***, 243*, 811.
11. Ross, R. *Nature* **1993***, 362*, 801.
12. Lee, J. C.; Badger, A. M.; Griswold, D. E.; Dunnington, D.; Truneh, A.; Votta, B.; White, J. R.; Young, P. R.; Bender, P. E. *Ann. N. Y. Acad. Sci.* **1993,** *696*, 149.

13. Badger, A. M.; Bradbeer, J. N.; Votta, B.; Lee, J. C.; Adams, J. L.; Griswold D. E. *J. Pharm. Exp. Ther.* **1996,** *279*, 1453.

14. Chan C. S.; Botstein, D. *Genetics* **1993**, *135*, 677.

15. (a) Cheetham, G. M.; Charlton, P. A.; Golec, J. M.; Pollard, J. R. *Cancer Lett.* **2007**, *251*, 323; (b) Harrington, E. A.; Bebbington, D.; Moore, J.; Rasmussen, R. K.; Ajose-Adeogun, A. O.; Nakayama, T.; Graham, J. A.; Demur, C.; Hercend, T.; Diu-Hercend, A.; Su, M.; Golec, J. M.; Miller, K. M. *Nat. Med.* **2004***, 10,* 262.

16. (a) Fancelli, D.; Moll, J.; Varasi, M.; Bravo, R.; Artico, R.; Berta, D.; Bindi, S.; Cameron, A.; Candiani, I.; Cappella, P.; Carpinelli, P.; Croci, W.; Forte, B.; Giorgini, M. L.; Klapwijk, J. *J. Med. Chem.* **2006**, *49,* 7247; (b) Carpinelli, P.; Ceruti, R.; Giorgini, M. L.; Cappella, P.; Gianellini, L.; Croci, V.; Degrassi, A.; Texido, G.; Rocchetti, M.; Vianello, P.; Rusconi, L.; Storici, P.; Zugnoni, P.; Arrigoni, C. *Mol. Cancer Ther.* **2007**, *6,*3158.

17. Manfredi, M. G.; Ecsedy, J. A.; Meetze, K. A.; Balani, S. K.; Burenkova, O.; Chen, W.; Galvin, K. M.; Hoar, K. M.; Huck, J. J.; LeRoy, P. J.; Ray, E. T.; Sells, T. B. *Proc. Natl. Acad. Sci. U.S.A.* **2007**, *104*, 4106.

18. (a) Mortlock, A. A.; Foote, K. M.; Heron, N. M.; Jung, F. H.; Pasquet, G.; Lohmann, J. J.; Warin, N.; Renaud, F.; De Savi, C.; Roberts, N. J.; Johnson, T.; Dousson, C. B.; Hill, G. B.; Perkins, D. *J. Med. Chem.* **2007**, *50*, 2213; (b) Wilkinson, R. W.; Odedra, R.; Heaton, S. P.; Wedge, S. R.; Keen, N. J.; Crafter, C.; Foster, J. R.; Brady, M. C.; Bigley, A.; Brown, E.; Byth, K. F.; Barrass, N. C.; Mundt, K. E. *Clin. Cancer Res.* **2007**, *13,* 3682.

19. (a) Xiao, X.; Antony, S.; Pommier, Y.; Cushman, M. *J. Med. Chem.* **2006**, *49*, 1408; (b) Cinelli, M. A.; Morrell, A.; Dexheimer, T. S.; Scher, E. S.; Pommier, Y.; Cushman, M. *J. Med. Chem.* **2008**, *51*, 4609; (c) Oh, S.; Park, S. B. *Chem. Commun.* **2011**, *47*, 12754.

20. Henderson, E. A.; Bavetsias, V.; Theti, D. S.; Wilson, S. C.; Clauss, R.; Jackman, A. L. *Bioorg. Med. Chem.* **2006**, *14*, 5020.

21. Alagarsamy, V.; Solomon, V. R.; Dhanabal, K. *Bioorg. Med. Chem.* **2007**, *15*, 235.

22. Rohini, R.; Reddy, P. M.; Shanker, K.; Hu, A.; Ravinder, V. *Eur. J. Med. Chem.* **2010**, *45*, 1200.

23. Jatav, V.; Kashaw, S.; Mishra, P. *Med .Chem. Res.* **2008**, *17*, 205.

24. Aly, A. A. *Chin. J. Chem.* **2003**, *21*, 339.
25. Li, H.; Huang, R.; Qiu, D.; Yang, Z.; Liu, X.; Ma, J.; Ma, Z. *Prog. Nat. Sci.* **1998**, *8*, 359.
26. Nandy, P.; Vishalakshi, M. T.; Bhat, A. R. *Indian J. Heterocycl. Chem.* **2006**, *15*, 293.
27. Saravanan, G.; Alagarsamy, V.; Prakash, C. R. *Int. J. Pharm. Pharm. Sci*. **2010**, *2*, 83.
28. Lakhan, R.; Singh, O. P.; Singh, J. R. L. *J. Indian Chem. Soc.* **1987**, *64*, 316.
29. Hess, H. J.; Cronin, T. H.; Scriabine, A. *J. Med. Chem.* **1968**, *11*, 130.
30. Sasmal, S.; Balaji, G.; Kanna Reddy, H. R.; Balasubrahmanyam, D.; Srinivas, G.; Kyasa, S.; Sasmal, P. K.; Khanna, I.; Talwar, R.; Suresh, J.; Jadhav, V. P.; Muzeeb, S.; Shashikumar, D.; Harinder Reddy, K.; Sebastian, V. J.; Frimurer, T. M.; Rist, Ø.; Elster, L.; Hogberg, T. *Bioorg. Med. Chem. Lett.* **2012**, *22*, 3157.
31. Alvarado, M.; Barceló, M.; Carro, L.; Masaguer, C. F.; Raviña, E. *Chem. Biodivers.* **2006**, *3*, 106.
32. Malamas, M. S.; Millen, J. *J. Med. Chem.* **1991**, *34*, 1492.
33. Dax, S. L.; Youngman, M. A. (**2001**) Solid-Phase Organic Synthesis. Czarnik, A. W. Wiley: New York, *1*, 45.
34. (a) Zeng, Q.; Huang, B.; Danielsen, K.; Shukla, R.; Nagy, T. *Org. Process Res. Dev.* **2004**, *8*, 962; (b) Vandekerckhove, S.; D'hooghe, M. *Bioorg. Med. Chem*. **2013**, *21,* 3643.
35. Legraverend, M.; Grierson, D. S. *Bioorg. Med. Chem.* **2006**, *14*, 3987.
36. (a) Sharma, A.; Luxami, V.; Paul, K. *Bioorg. Med. Chem. Lett.* **2013**, *23*, 3288; (b) Paul, K.; Sharma, A.; Luxami, V. *Bioorg. Med. Chem. Lett.* **2014**, *24*, 624.

CHAPTER-1

REVIEW OF LITERATURE

Medicinal chemistry or pharmaceutical chemistry is a discipline at the intersection of chemistry and pharmacology, involved with design, synthesis and development of new chemical entities suitable for therapeutic use. It also includes the study of existing drugs, their biological properties, structure-activity relationship (SAR) and quantitative structural-activity relationship (QSAR).

The chemistry of heterocyclic compounds has continuously exploring the field of organic and medicinal chemistry. The synthesis of heterocyclic compounds has always drawn the attention of scientist over the years mainly because of important biological properties associated with them. Heterocyclic compounds are widely distributed in nature which is essential to life, from straight chain aliphatic to branch cyclic and aromatic compounds. Among the various heterocyclic compounds, nitrogen containing heterocycles play an important role in medicinal chemistry as most of the drugs are mainly nitrogen heterocycles. The efficiency of these nitrogen containing heterocycles such as quinazoline, purine and benzimidazole are well reported as they show broad spectrum of biological activity.[1]

1.1. BIOLOGICAL ACTIVITY OF QUINAZOLINE BASED MOLECULES

Quinazoline nucleus is an interesting molecule among the most important classes of aromatic bicyclic compounds with two nitrogen atoms in their structure. Quinazoline derivatives, which belong to the N-containing heterocyclic compounds, have caused universal concerns due to their widely and distinct pharmaceutical activities. Medicinal chemists synthesized a variety of quinazoline compounds with different biological activities by introducing various active groups to the quinazoline moiety and determined the potential applications of these derivatives in fields of biology, pesticide and medicine.

Wang *et. al.*[2] reported compound **1a** as highly potent quinazoline derivative for *in vitro* cytotoxic activity with GI_{50} value in the range of 1.9−3.2 nM. This compound was further evaluated as new tubulin-polymerization inhibitors having significant potency against tubulin assembly with IC_{50} value of 0.77 μM, and substantial inhibition of colchicine binding (99% at 5 μM). Compound **1a** and N-methylated analogue **1b** were also analyzed in nude mouse MCF7 xenograft models to validate their antitumor activities. Compound **1b** exhibited

significant *in vivo* activity (tumor inhibitory rate 51%) at a dose of 4 mg/kg without prominent toxicity, whereas **1a** unpredictably resulted in toxicity and death at the same dose.

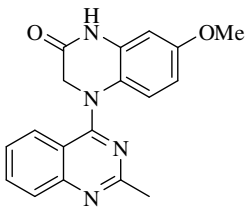

1a

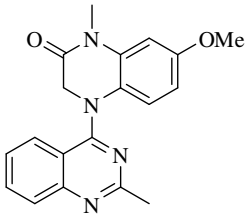

1b

Jiang *et. al.*[3] reported the newly designed synthesis of series of novel 2-(2-arylmethylene)hydrazinyl-4-aminoquinazoline derivatives **2**. Compound **2** showed cytotoxicity against various *in vitro* cancer cell lines viz., H-460, HT-29, HepG2 and SGC-7901 with IC_{50} values of 0.031 µM, 0.015 µM, 0.53 µM and 0.58 µM respectively.

Patel *et. al.*[4] reported the synthesis of N-phenyl-benzothiazolyl acetamide fused quinazoline derivatives through Suzuki coupling reaction and evaluated for their *in vitro* antimycobacterial activity (MIC, 6.25 µg/mL) against M. tuberculosis $H_{37}Rv$. Compound **3** has also been screened against prostate cancer PC3 cell line in order to improve their anticancer activity.

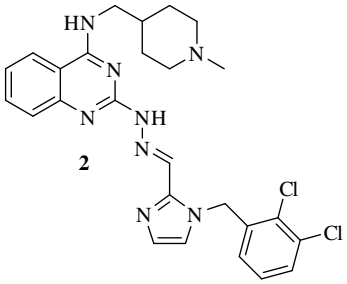

2

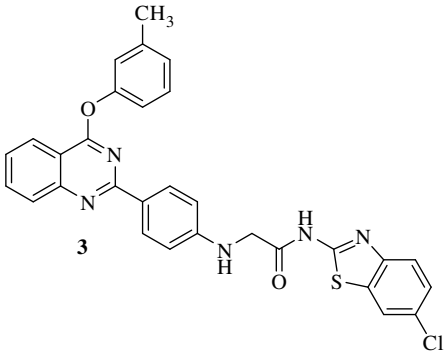

3

Palop *et. al.*[5] synthesized the 2,4-disubstituted quinazolines and pyrido[2,3-d]pyrimidine derivatives. These compounds were screened for their *in vitro* cytotoxic activity using the 3-(4,5-dimethylthiazol-2-yl)-2,5-diphenyltetrazolium bromide (MTT) assay against human prostate cancer cell lines (PC-3, ATCC, Manassas, VA). Some of compounds (**4a**-**g**) showed potent growth inhibitory activity with IC_{50} value less than 8.0 µM against PC-3 cancer cell line and were even more potent than standard drug methylseleninic acid with IC_{50} value of 8.4 µM. Among these series of compounds, **4b** and **4d-g** were more active than topotecan with IC_{50} value below 4.0 µM. Caspase-3 activity and cell cycle regulation studies revealed that compound **4d** provoked an increase in caspase-3 level associated with cell cycle perturbation in a time-dependent manner.

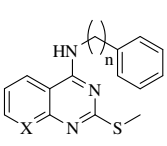

4a; X = N, n = 5 IC_{50} = 5.8 µM

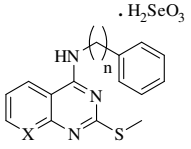

4b; X = C, n = 4 IC_{50} = 3.8 µM
4c; X = N, n = 5 IC_{50} = 7.0 µM

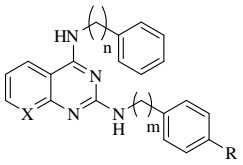

4d; X = C, n = 1, m = 1, R = 4-SCH_3 IC_{50} = 1.7 µM
4e; X = N, n = 1, m = 1, R = 4-SCH_3 IC_{50} = 1.5 µM

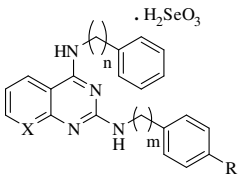

4f; X = C, n = 1, m = 1, R = 4-SCH_3 IC_{50} = 1.6 µM
4g X = N, n = 1, m = 1, R = 4-SCH_3 IC_{50} = 1.8 µM

Verhaeghe *et. al.*[6] synthesized 4-chlorophenyl-2-trichloromethyl-quinazoline **5** in a convenient and efficient way and evaluated towards *in vitro* antiplasmodial potential. Compound **5** has been shown good activity with IC_{50} value of 0.9 µM against the K1-multi-resistant *Plasmodium falciparum* strain as compared with chloroquine with doxycycline as a reference drug. In these series of compounds, trichloromethyl group plays an important role in antiplasmodial activity while the modulation of the thiophenol moiety prominence the toxicity/activity ratio.

Thorat *et. al.*[7] reported the designed and synthesis of 2,4-diaminoquinazoline derivatives and screened their biological activities as heat shock protein 90 (Hsp90) inhibitors. Compound **6** showed excellent anti-proliferative activities against DU-145, HT-29, HCT-116, A375P and MCF-7 cancer cell lines with IC_{50} values of 1.07 µM, 0.86 µM, 0.84 µM, 3.90 µM and 3.14 µM respectively. Compound **6** was found to be the most potent in diminishing the Her2 protein appearance levels and induced Hsp70 protein appearance levels significantly.

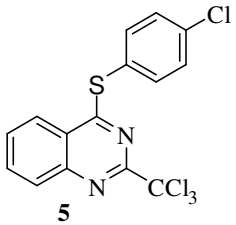

5

(IC_{50}= 0.9 µM)

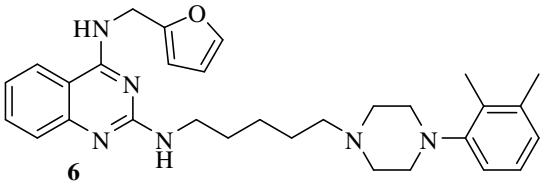

6

IC_{50} ; DU-145 = 1.07 µM
HT-29 = 0.86 µM
HCT-116 = 0.84 µM
A375P = 3.90 µM
MCF-7 = 3.14 µM

Sagiv-Barfi *et. al.*[8] synthesized N-*p*-tolyl-2-(3,4,5-trimethoxyphenyl)quinazolin-4-amine **7** that exhibited significant ability to inhibit T cell proliferation from human peripheral blood mononuclear cells (PBMC) and Jurkat cells, with IC_{50} in the sub-micromolar range. It also induced G2 arrest, as well as an increase in the sub-G1 population of cells. Compound **7** has also been influenced cell growth factors that are unique to CD3+ T cells. The apparent

selective effect of compound **7** on T cells and its lower activity adjacent to other cell types indicated that compound **7** may be a potential lead for an inhibitor of graft rejection.

Gellibert *et. al.*[9] reported a series of novel 2,4-disubstituted quinazoline derivatives as potent and selective ALK5 inhibitors over p38MAP kinase. Compound **8** has shown significant *in vivo* activity in an acute rat model of DMN-induced liver fibrosis when administered orally at 5 mg/kg. Compound **8** was also tested against a panel of more than 15 kinases like AMPK, CDK2, CSK1, CSK2, GSK3, JNK1, LCK, MKK1, MSK1, MAPK2, P70S6K, P38β, P38γ, P38δ, PKC, PDK1, Phos.K, ROCK and SGK. Although good selectivity was obtained against most of them while significant percentage of inhibition (93%) was observed for ROCK1 at 10 μM.

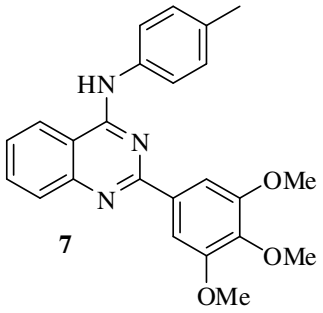

7

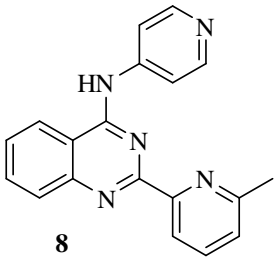

8

Sirisoma *et. al.*[10] synthesized 2-chloro-N-(4-methoxy/methylphenyl)quinazolin-4-amine (**9a-c)** and evaluated for their *in vitro* anticancer activity. Compound **9b** has been found to be the most potent inhibitor of cancer cell growth with EC_{50} value of 2 nM for T47D and HCT-116 cells which was about 3-fold and >1000 fold more potent than **9a** and **9c** respectively. Compound **9b** has also been inhibited tubulin polymerization and effective in cells overexpressing ABC transporter Pgp-1. It has also showed excellent activity on the human breast MX-1 and prostate cancer PC-3 mouse models.

Smits *et. al.*[11] synthesized the class of quinazoline analogue **10** containing sulfonamide moiety at C4 position. Subsequently, a QSAR model for the affinity of this new series of H_4R ligands was developed with good predictive ability in the nanomolar range for the affinity of quinazolines with variations in the sulfonamide moiety. Compound **10** administered in rat, significantly reduced the inflammation caused by the injection of carrageenan in the paw, thereby demonstrating the *in vivo* anti-inflammatory property of this promising class of quinazoline H_4R inverse agonists.

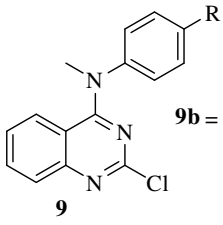

9b = EC_{50} = 2 nM (T47D cells)
EC_{50} = 2 nM (HCT-116 cells)

9

9a; R = H, **9b;** R= OMe, **9c;** R = Me

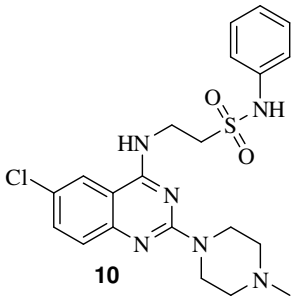

10

Hour *et. al.*[12] synthesized a series of 6-fluoro-2-(3-fluorophenyl)-4-substituted anilinoquinazoline compounds. Compound **11** (LJJ-10) proved to be most active in inhibiting cell proliferation in most of the cancer cell lines. Moreover, compounds bearing F, OCH_3 and NH substituents at 4-anilino moiety, may bind with proteins in cancer cells. LJJ-10 induced significantly dose-dependent growth inhibition and apoptotic cell death. The IC_{50} value of LJJ-10 in human osteogenic sarcoma U-2 OS cells was much lower than that in human fetal normal osteoblastic hFOB cells, suggested that LJJ-10 could be an efficacious and safer anti-cancer agent for treatment of human osteogenic sarcoma. Moreover, further structural modification of compound **11** might lead to the discovery of more active anilinoquinazoline with good selectivity against various cancer cell lines. Use of 30 μM of LJJ-10 significantly inhibited the cell growth and cell death and triggered apoptosis through the activation of caspase-8, caspase-9 and caspase-3 cascades in U-2 OS cells.

Desai *et. al.*[13] synthesized a series lactum bearing quinazoline derivatives for antibacterial activity. Antibacterial property of the synthesized compounds has showed very good inhibition; compounds **12a** and **12e** have revealed outstanding activity towards *S. aureus, E. coli, P. aeruginosa* and *S. pyogenus*. Compound **12b** showed good activity against *E. coli* while compound **12a** showed good activity against *S. pyogenus*. But the systematic substitution at various positions and other derived compounds has shown remarkable antifungal properties. The compounds **12b** and **12d** have been exhibited good activity towards *A. niger, A. clavatus* and *C. albicans*. Compound **12c** has also showed good activity against *A. clavatus* and *C. albicans* and the remaining compounds have shown poor antifungal activity indicating less biological importance for a synthetic chemist.

Chandrika *et. al.*[14] synthesized N- and O-propargylated quinazoline compounds **(13a)** and their reaction with different azides via click chemistry to get a series of novel perfluoro-

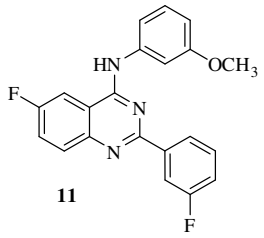

11

Cell lines	IC_{50} (μM)
HL-60	35.40
U937	39.62
HT-29	40.35
Colo 205	44.68
U-2-OS	30.26
MCF-7	46.33
MDA-MB-231	47.05

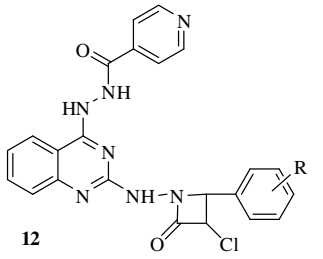

12

12a; R = 4-CH_3
12b; R = 4-Cl
12c; R = 2-NO_2
12d; R = 4-$N(CH_3)_2$
12e; R = 2-OH

alkyl-1*H*-1,2,3-triazol-4-yl substituted O-/N-quinazolines (**13b-e**). All the synthesized compounds were screened against gram-positive and gram-negative bacteria as well as fungal strains. Compounds **13b** and **13c** showed significant activity against bacterial strains with MIC value in the range of 9.37-37.5 μg/ml and compounds **13a**, **13d** and **13e** showed promising activity against fungi with MIC value in the range of 7-12 μg/ml.

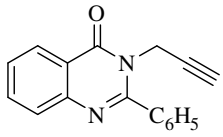

13a

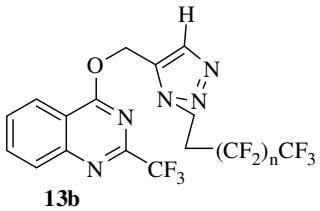

13b

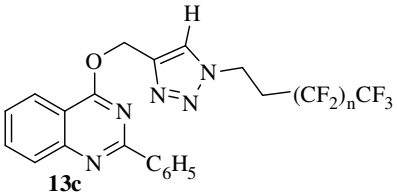

13c

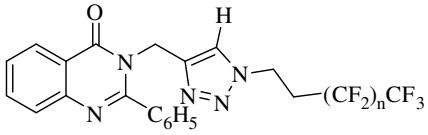

13d

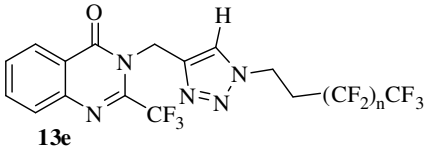

13e

Sirisoma *et. al.*[15] synthesized a series of N-methyl-4-(4-methoxyanilino)quinazolines inducing promising anticancer agents via modifications at the 5-, 6- and 7-positions of the quinazoline and replacement of the quinazoline by other nitrogen-containing heterocycles. It has been found that a small group such as OCH_3 at 5-position **(14a)** was found to be well tolerated while a small group like an amino at 6-position **(14b)** was preferred. Substitution at the 7-position showed much less activity than at the 6-position. Replacement of the carbon at the 8-position or both the 5- and 8-positions with nitrogen led to about 10-fold reductions in potency. Replacement of the quinazoline ring with a quinoline ring resulted in 100-fold reductions in activity while a benzo[d][1,2,3]triazine, or an isoquinoline ring showed that the nitrogen at the 1-position is important for activity, while the carbon at the 2-position can be replaced by a nitrogen and the nitrogen at the 3-position can be replaced by a carbon indicated that there is no effect with removal of heteroatom. Thus, several 5- or 6-substituted analogous, such as **14a** and **14b**, were found to have potencies approaching that of lead compound.

Marvania *et. al.*[16] synthesized a series of N-mustard-quinazoline conjugates bearing a urea or hydrazine carboxamide linker and evaluated for their antitumor activities.

Compound **15a-c** was selected for further antitumor activity against human breast carcinoma MX-1 and prostate PC-3 xenograft in animal model. Among compounds selected for evaluating their antitumor activity, quinazoline derivative **15c** with chloro at 3-position and fluoro at 4-position has been found to be the most potent compound. It has been demonstrated that the newly synthesized N-mustard-quinazoline conjugates are generally less potent than the N-mustard-quinoline conjugates. The newly synthesized compounds are able to induce DNA cross-linking through alkaline agarose gel shift assay and inhibited cell cycle arrest at G2/M phase.

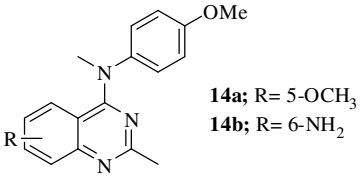

14

14a; R= 5-OCH_3
14b; R= 6-NH_2

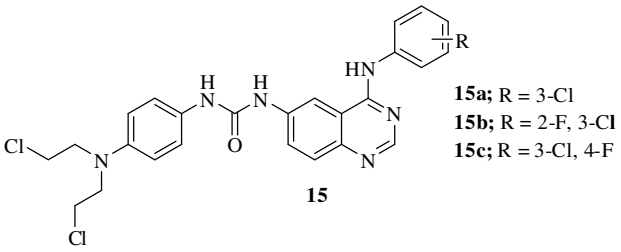

15

15a; R = 3-Cl
15b; R = 2-F, 3-Cl
15c; R = 3-Cl, 4-F

Sharma *et. al.*[17] synthesized a series of novel quinazolinone derivatives in medicinal chemistry based on the concept of molecular hybridization. Compounds **16a-b** and **17** showed very consistent and promising leishmanicidal activity against intracellular amastigotes with IC_{50} value in the range of 0.65 ± 0.2 - 7.76 ± 2.1 μM as compared to miltefosine (IC_{50} = 8.4 ± 2.1 μM). These compounds have also showed *in vivo* efficacy in the golden hamster model and displayed no toxicity for macrophages and vero cells. Moreover, activation of Th1 type and suppression of Th2 type immune responses and induction in nitric oxide generation proved that **16a** and **16b** induce murine macrophages to prevent survival of parasites. Compounds **16a** and **16b** exhibited significant *in vivo* inhibition of parasite 73.15 ± 12.69% and 80.93 ± 10.50% against *Leishmania donovani*/hamster model.

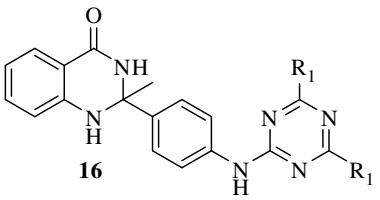

16

16a; R_1 = piperidine,
16b; R_1 = tetrahydroisoquinoline.

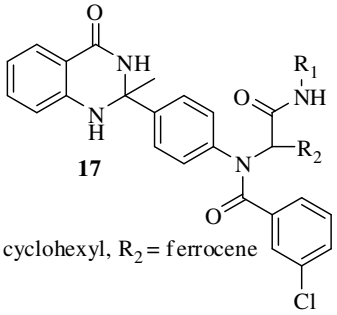

17

R_1 = cyclohexyl, R_2 = ferrocene

Naik *et. al.*[18] reported a series of (E)-N'-(2-(2-(substituted benzaldehyde) hydrazinyl) quinazoline-4-yl)isonicotinohydrazide compounds. Compounds **18a**, **18d** and **18e** are active against *S. aureus*, as compare to standard chloremphenicol and compounds **18b**, **18g** and **18i**

are inactive against *S. aureus*, as compared to standard Ampicillin. Compounds **18e**, **18f** and **18j** are active against *P. aeruginosa* while compounds **18a**, **18d** and **18e** has been shown activity against *S. pyogenus* as compared to standard Ampicillin. The compounds **18b**, **18i** and **18j** have also exhibited outstanding activity towards *C. albicans*, *A. niger* and *A. clavatus*. The remaining compounds have shown poor antifungal activity indicating less biological importance for a synthetic chemist.

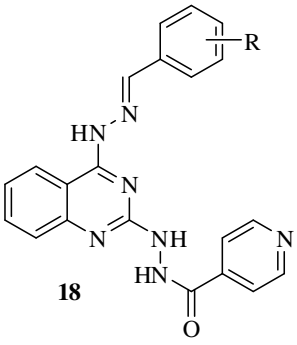

18

18a; R = 4-CH_3
18b; R = 3-CH_3-4-OH
18c ; R = 4-Cl
18d; R = 2-NO_2
18e; R = 2,4-Cl_2
18f; R = 2-OCH_3
18g; R = 4-NO_2
18h; R = 4-H
18i; R = 4-$N(CH_3)_2$
18j; R = 2-OH

1.2. BIOLOGICAL ACTIVITY OF PURINE BASED MOLECULES

Purines have been a profitable source of inspiration for medicinal chemists for many years. As a result, a broad variety of bioactive purine derivatives has been designed, which has led to the launch of several powerful drugs with diverse applications.

Hollinshead *et. al.*[19] have been synthesized a series of novel 4-methyl piperazinyl purine compounds that found to be highly potent and fully efficacious agonists of the human CB2 receptor with excellent selectivity against CB1. Compound **19** has possessed good biopharmaceutical properties and demonstrated robust oral activity in rodent models of joint pain.

Lee *et. al.*[20] reported a series of 1-ethyl-3,8-disubstituted-6-(3-methylmorpholino)-9*H*-purin-2-yl)pyrimidin-2-yl)urea and their derivatives that imparted selectivity for mTOR over the related PI3Kα and δ kinases. Substituted morpholine at the hinge binding region, and replacement of the aminopyrimidine with a phenyl urea on related pyrimidine scaffolds were reported to increase mTOR potency and selectivity over PI3 kinases. The selectivities were due to the S-methyl morpholine packing against a unique Trp2239 residue in mTOR and the ethyl urea interacting hydrophobically with the Cβ and Cγ atoms of the Glu2190 side chain. Thus, the morpholine/aminopyrimdine of **20** was replaced with (S)-3-methyl-morpholine/ethyl phenyl urea to provide a more potent and selective mTOR inhibitor **21a**. Relative to **20**, **21a** was eightfold more potent (mTOR K_i = 9.5 nM) and exhibited 21- and

17-fold selectivities for mTOR over PI3Kα and PI3Kδ respectively. Initial SAR exploration by truncation of the 2-hydroxyethyl side chain led to methyl analog **21b**, which showed comparable mTOR potency (K_i = 7 nM) with decreased PI3Kα and PI3Kδ potencies. Removal of the C-8 tertiary alcohol resulted in **21c**, with similar potencies for mTOR (K_i = 12 nM) and PI3Kα (K_i = 370 nM), and a slight decrease in PI3Kδ potency (IC_{50} = 890 nM).

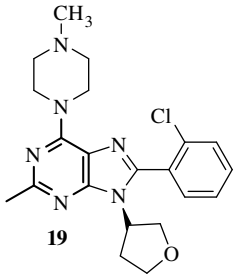

19

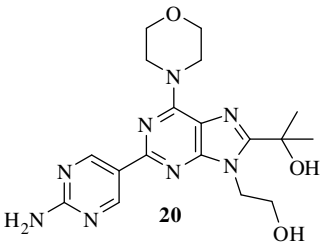

20

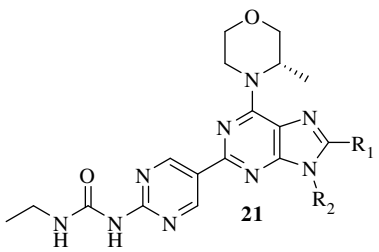

21

21a; R_1 = -CH(CH$_2$)$_2$OH, R_2 = -CH$_2$CH$_2$OH
21b; R_1 = -CH(CH$_2$)$_2$OH, R_2 = -CH$_3$
21c ; R_1 = H, R_2 = -CH$_3$

Nair *et. al.*[21] reported that *o*-fluorophenylmethyl derived triazole, **22b**, effectively suppressed Aβ-induced neurotoxicity as compared to **22a** in hippocampal slice cultures, while the pentafluoroaryl derived triazole **22c** has virtually no neuroprotective effect. Importantly, the neuroprotective effect of compound **22b** has been comparable to Flavopiridol and Roscovitine. DarwinDock/GenDock docking calculations showed that the Roscovitine and the triazoles **22b** and **22c** all bind at the same active site region of the CDK5/p25 complex. The comparable neuroprotective effect of Roscovitine and compound **22b** has reflected in their similar binding affinities, whereas the unfavourably low binding affinity for compound **22c** made it practically inefficient neuroprotector. These docking simulations also supported the involvement of the CDK5/p25 complex in the cell cycle re-entry, a leading cause of the neuronal degeneration.

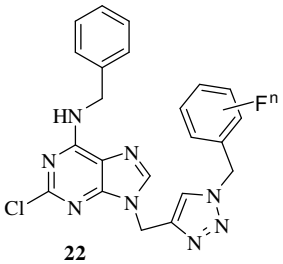

22

22a; n = 0
22b; n = 1; o-fluoro-
22c; n = 5

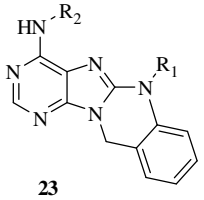

23

23a; R_1= H, R_2 = phenyl
23b; R_1= *N*,*N*-diethylaminoethyl HCl, R_2 = phenyl
23c; R_1= *N*-ethylmorpholine HCl, R_2 = phenyl
23d; R_1= *N*-ethylmorpholine HCl, R_2 = 2-chlorophenyl
23e; R_1= *N*-ethylmorpholine HCl, R_2 = 2-bromophenyl
23f; R_1= *N*-ethylmorpholine HCl, R_2 = benzyl

Verones *et. al.*[22] synthesized 4-amino-tetrahydroquinazolino[3,2-*e*]purine derivatives **(23a-f)** toward Src tyrosine kinase in enzymatic assays along with their antiproliferative activity toward the murine leukemia L1210 cell line. In order to improve solubility and antiproliferative profiles of 4-anilino-derivatives, basic atom incorporated into a linear side chain (**23b**). This study provided a new promising scaffold with moderate enzymatic inhibitory activities for further development of new anticancer drugs targeting Src tyrosine kinase.

Pathak *et. al.*[23] synthesized a series of 6-oxo and 6-thio purine derivatives and screened against *Mycobacterium tuberculosis* (Mtb). Compounds **24a-c** having a decyl/dodecyl chains at the C-6 position of purine showed good activity against Mtb $H_{37}Rv$. Based on their activity, compounds **24d–h** possessing N^9 substitution were synthesized and screened. Structural diversity using D- and L-amino acids in compounds **24h** and **25** did not increase the activity significantly. The diversity analogous (**26a-e)** showed significant high % inhibition but also produced high MIC_{90} values in the Mtb $H_{37}Rv$ screen.

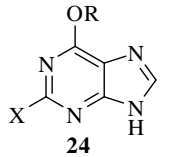

24

24a; X = H, R = $(CH_2)_9CH_3$
24b; X = NH_2, R = $(CH_2)_9CH_3$
24c; X = NH_2, R = $(CH_2)_{11}CH_3$
24d; X = Cl, R = C_6H_4-4-CH_3
24e; X = Cl, R = C_6H_4-3-CH_3
24f; X = Cl, R = CH_2-C_6H_{11}
24g, X = Cl, R = CH_2-C_6H_3-3-Cl,4-Cl
24h; X = H, R = $(CH_2)_{11}CH_3$,

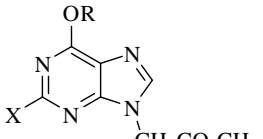

25

X=NH_2; R = $(CH_2)_9CH_3$

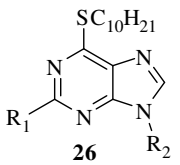

26

26a; R_1 = $NHCOCH_2$, R_2 = H
26b; R_1 = NH_2, R_2 = $CH_2CH(OH)CH_2OH$
26c; R_1 = NH_2, R_2 = CH_2Ph
26d; R_1 = $SC_{10}H_{21}$, R_2 = $CH_2OCH_2CH_2OH$
26e; R_1 = NH_2, R_2 = C_2H_5

Zatloukal *et. al.*[24] synthesized 2,6,9-trisubstituted purine derivatives of Roscovitine, currently being evaluated in clinical trials as potential anticancer drugs, as inhibitors of cyclin-dependent kinases (CDKs). Many of the prepared compounds proved to be more potent at limiting the proliferation of the tested cancer cell lines than Roscovitine and Olomoucine II. Compound **27** blocked cell cycle progression and induced apoptosis in cells as a result of transcriptional perturbations due to reduced phosphorylation of Ser-2 and Ser-5 in the C-terminal domain of RNAP-II, caused by inhibition of CDK7 and CDK9.

Mallari et. al.[25] synthesized a series of purine-nitrile inhibitors **(28a-e)** in order to enhance *in vivo* ADME parameters. This group studied the efficacy of these compounds in two murine models of African trypanosomiasis. Several inhibitors were tested for acute

toxicity in mice, and all were determined to be non-toxic at doses up to 200 mg/kg. Compound **28e** was found to be non-toxic at oral dose upto 1000 mg/kg. Based upon pharmacokinetic (PK) modelling of the initial inhibitor series, structural modifications were made to optimize for *in vivo* stability. This compound displayed peak concentrations in plasma and brain tissue of approximately 10 µM and 20 µM respectively. This inhibitor has been efficacious in a murine disease model, significantly extending the survival time of *Trypanosoma brucei brucei* infected mice relative to a vehicle control. However, the same compound was not efficacious in *Trypanosoma brucei rhodesiense* infected mice, most likely due to lower potency against the human parasite relative to *Trypanosoma brucei brucei*. This inhibitor is significant in that it represented one of the only example of a novel anti-trypanocidal chemotype that is CNS permeable, orally available, and efficacious *in vivo* against *Trypanosoma brucei brucei*.

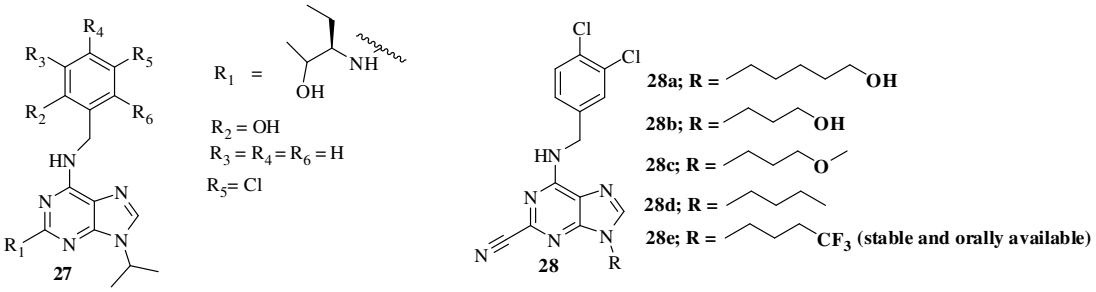

27 28

Vandromme *et. al.*[26] synthesized a series of 2-aminocarbonyl purines using palladium catalyzed cross-coupling reaction either with amides or amines in the presence of carbon monoxide. Moderate *in vitro* inhibitory activities against CDK1 and CDK5 were observed for the most active compounds with respective IC_{50} value of 0.9 µM and 1.3 µM for the compound **29**, 1.2 µM and 0.9 µM for compound **30** and 1.7 µM and 2 µM for compound **31**.

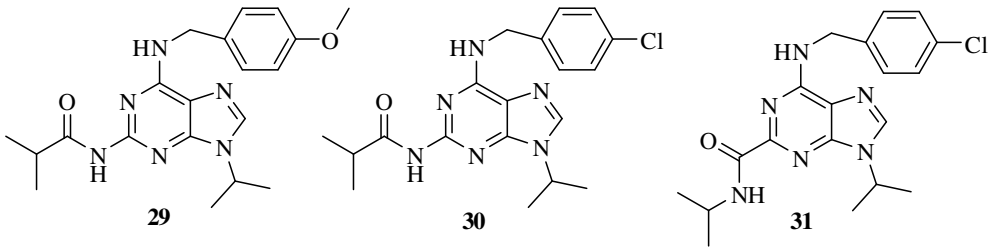

29 30 31

Tunçbilek *et. al.*[27] synthesized a novel series of 8,9-disubstituted adenines, 6-substituted aminopurines (**32a–d**), 9-(*p*-fluorobenzyl)-6-substituted aminopurines (**33a-b**) and 9-cyclopentyl-6-substituted aminopurine (**34a-k** and **35**) compounds and screened for their antimicrobial activities against *Staphylococcus aureus*, methicillin-resistant *S. aureus* (MRSA, standard and clinical isolate), *Bacillus subtilis*, *Escherichia coli* and *Candida albicans*.

Substitution at 6-position with amino group having without any substitution at 9-position of the purine structure and 9-substituted amino purine displayed excellent activity against *C. albicans* with MIC 3.12 µg/ml. These compounds displayed better antifungal activity than that of standard oxiconazole. Furthermore, compound **34d** carrying 4-chlorobenzylamino group at the 6-position of the purine moiety exhibited comparable antibacterial activity with that of the clinically used ciprofloxacin drug.

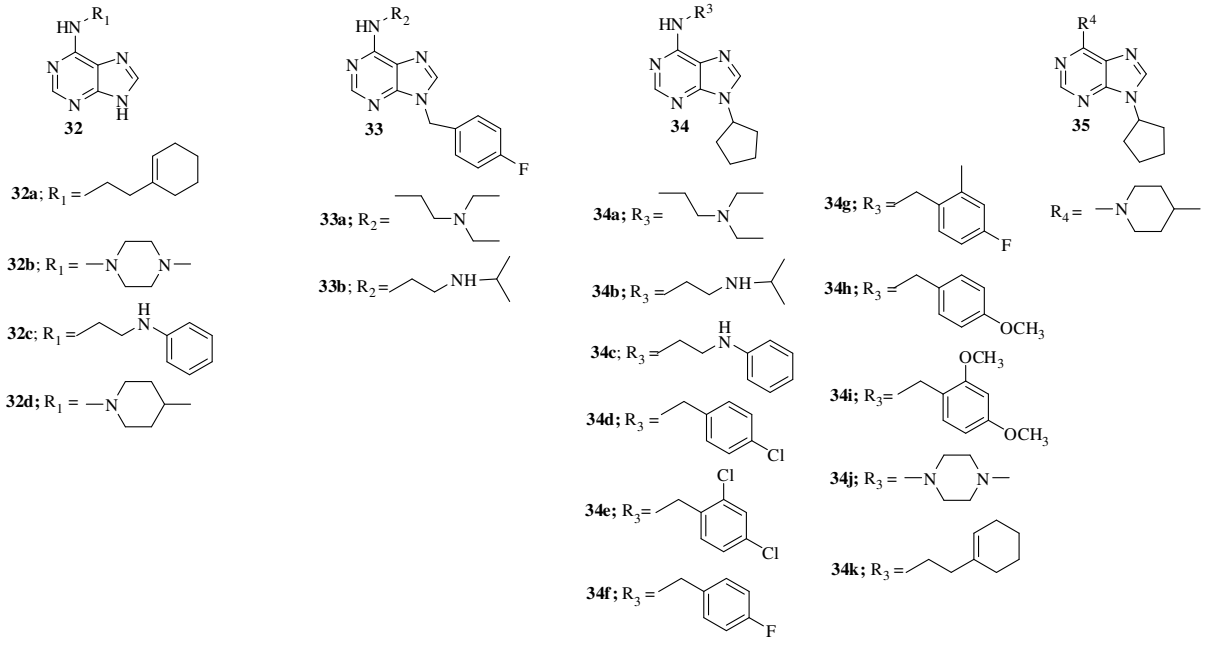

Trova *et. al.*[28] synthesized N^2-((1s,4s)-4-aminocyclohexyl)-N^6-((6-(3-fluorophenyl)pyridin-3-yl)methyl)-9-isopropyl-9*H*-purine-2,6-diamine (**36a)** and N^6-((6-(1*H*-pyrazol-1-yl)pyridin-3-yl)methyl)-N^2-((1s,4s)-4-aminocyclohexyl)-9-isopropyl-9*H*-purine-2,6-diamine (**36b)** and inhibited the cyclin dependent kinases as well as demonstrated potent antiproliferative activity. Derivatives **36a** and **36b** have also been shown respective 1250-fold and 1000-fold improvements in the growth inhibition of HeLa cells compared to Roscovitine.

Gucky *et. al.*[29] reported the synthesis and screening of a novel series of 2-substituted-6-biarylmethylamino-9-cyclopentylpurine derivatives for CDK inhibitory activity and antiproliferative effects. The most potent compound **37b** exhibited strong cytotoxicity in the human melanoma cell line G361 than compound **37a** that correlated with robust CDK1 and CDK2 inhibition and caspase activation. *In silico* modelling of **37b** in the active site of CDK2 revealed a high interaction energy, which believed to be due to the 6-heterobiarylmethylamino substitution of the purine moiety.

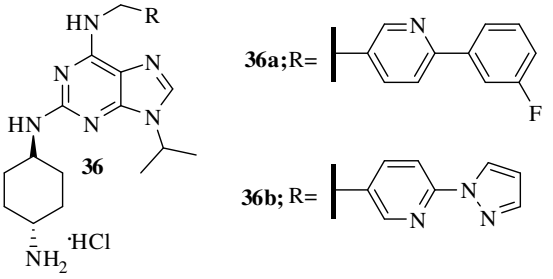

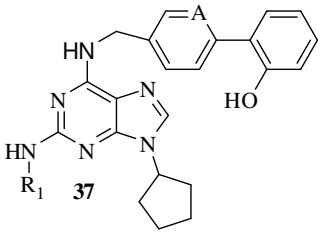

37a; A= CH, R_1= 4-aminocyclohexyl
37b; A= N, R_1= 4-aminocyclohexyl

Gundersen *et. al.*[30] reported the synthesis of 6-arylpurine carrying a benzyl group and furan group at 9-position of purine ring **(38)**. This compound has been prepared by Stille coupling between appropriately substituted 6-chloropurines and aryl(tributyl)tin. Compound **38** was screened for antibacterial activity against *Mycobacterium tuberculosis* H_{37}Rv. It has also shown activity against several singly drug-resistant strains of *M. tuberculosis* with lowest minimum inhibitory concentration (MIC) value of 0.78 µg/mL and also exhibited relatively low cytotoxicity.

Dolecková *et. al.*[31] synthesized a series of 2,9-disubstituted-6-guanidinopurines, structurally related to the cyclin-dependent kinase (CDK) inhibitors Olomoucine and Roscovitine. The most active compound **39b** possessed an identical side chain in the C2 position to Roscovitine; this compound displayed approximately five fold higher inhibitory activity toward CDK2/cyclin E and more than ten fold increase in cytotoxicity in MCF7 cells. Interestingly and in contrast to previously described findings, (S)-6-guanidinopurine derivatives were generally more active than their (R)-counterparts. Kinase selectivity profiling of (R)- and (S)-enantiomers **39a** and **39b** respectively, revealed that introduction of a guanidino group at the 6 position of the purine moiety decreased selectivity towards protein kinases compared to Roscovitine.

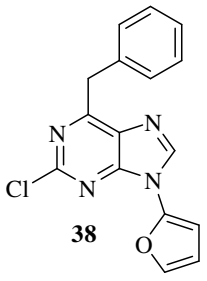

38

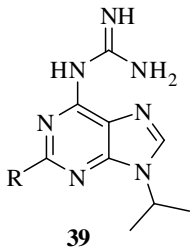

39

39a; R = *R*-NHCH(Et)CH_2OH
39b; R = *S*-NHCH(Et)CH_2OH

Venkatesan *et. al.*[32] synthesized a series of imidazolopyrimidine derivatives **(40-43)** and screened for inhibition against of PI3-Kinase (PI3 K) and mTOR activity. These

compounds were found to be ATP competitive with good tumor cell growth inhibition, and suppression of pathway specific biomakers such as phosphorylation of Akt at T308.

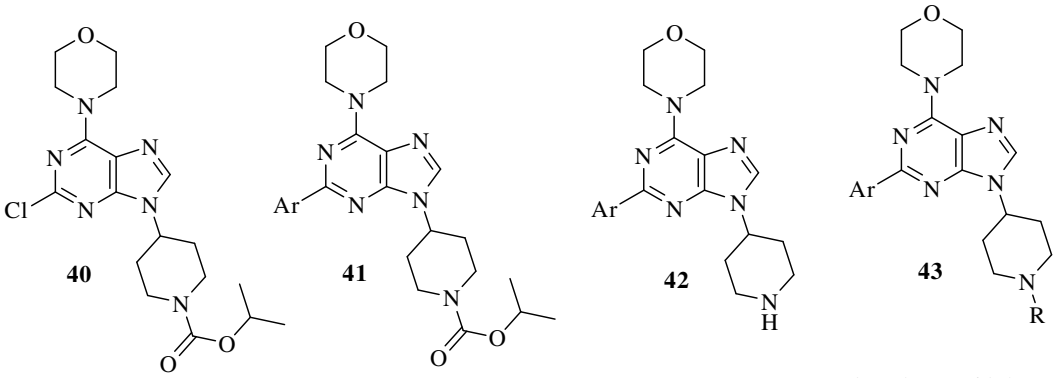

Morales *et. al.*[33] reported 2,6-dichloro-7-(ethoxycarbonylmethyl)-7*H*-purines **(44a)** and 2,6-dichloro-9-(ethoxycarbonylmethyl)-9*H*-purines **(44b)** with notable anti-proliferative activity against human breast, colon and melanoma cancerous cell lines. The results showed that these compounds are potent cytotoxic agents against all tumour cell lines assayed, showing single-digit micromolar IC_{50} values. The selective activities of compounds **44a** and **44b** against the melanoma cell line A-375, via apoptosis, supposed to be a great advantage for future therapeutic use.

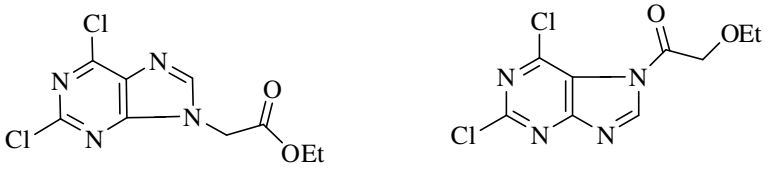

1.3. BIOLOGICAL ACTIVITY OF BENZIMIDAZOLE BASED MOLECULES

There is also growing interest over the past years for the synthesis of benzimidazole-based heterocycles due to the crucial role of benzimidazole unit in the functions of biologically important molecules. Benzimidazole is a bicyclic in nature which consists of the fusion of benzene and imidazole rings. Nowadays, benzimidazole and its derivatives are moiety of choice which possesses many pharmacological properties.

Wang *et. al.*[34] synthesized a series of benzimidazole-2-urea derivatives that were recognized as a new tubulin inhibitors to potently suppress the proliferation of a panel of human cancer cells with low nM IC_{50} values. Compound **45** also inhibited NCI-H460

spindles formation and induced cell cycle arrest at G2/M phase at 0.10 μM. Computational study suggested that compound **45** interacted with β tubulin in a novel binding mode.

This group has also designed and synthesized a series of bis-benzimidazole derivatives. Compound **46** possessed the best potential, its IC_{50} value has been found to be 5.95 mmol/L in mononuclear tumor cell line U937 and 5.58 mmol/L for cervical cancer cell HeLa. Fluorescence and UV–Vis studies also showed that compound **46** could bind into the minor groove of DNA.[35]

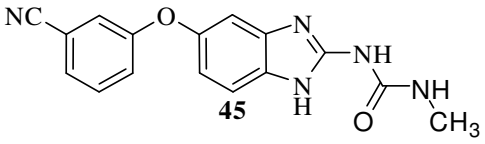

45

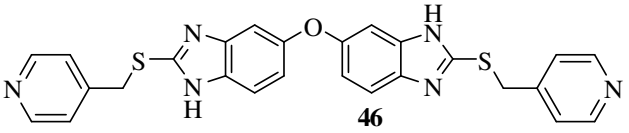

46

Bacharaju *et. al.*[36] designed and synthesized a series of novel benzimidazole dithiocarbamate and chalcone dithiocarbamate scaffold and evaluated for their antimitotic activities. Compounds **47** and **48** displayed the most promising antimitotic activity with IC_{50} values of 1.66 μM and 1.52 μM respectively. Although these molecules showed less potency compared to cisplatin, toxicity wise these molecules can be considered as potent antimitotic derivatives.

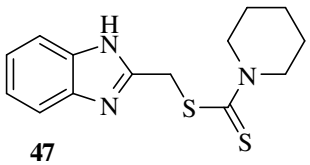

47

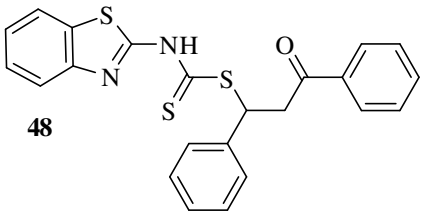

48

He *et. al.*[37] reported a series of novel diglyceride acyltransferase 1 (DGAT1) inhibitors in the benzimidazole class with a pyridyl-oxy-cyclohexanecarboxylic acid moiety. Compound **49** showed excellent potency on DGAT1 inhibitor with excellent selectivity against acyl-coenzyme A : cholesterol acyltransferase 1 (ACAT1). In addition, compound **49** significantly reduced triglyceride excursion in lipid tolerance tests (LTT) in both mice and dogs at low plasma exposure. *In vivo* study in mice with des-fluoro analogue **50** indicated that these series of compounds appeared to distribute in intestine preferentially over plasma.

Bandyopadhyay *et. al.*[38] reported the synthesis of 1,2-disubstituted benzimidazoles and 2-substituted benzothiazoles by using Al_2O_3–Fe_2O_3 nanomaterials as heterogeneous

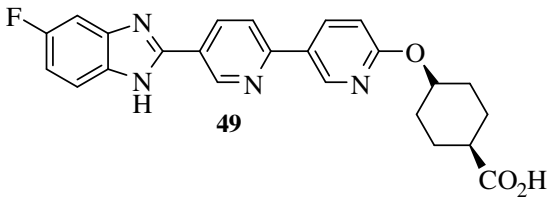

49

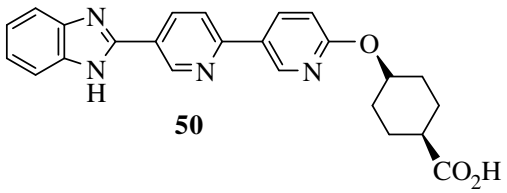

50

catalyst and evaluated against Gram-positive bacteria *Staphylococcus aureus*, *Bacillus cereus* and Gram-negative bacteria *Vibrio cholerae*, *Shigella dysenteriae* and *Escherichia coli*. Bio-evaluation studies revealed that compounds **51a**, **52a** and **52c** exhibited moderate to good antibacterial activity against all the tested bacterial stains. The compounds **51a**, **51c** and **52a** have shown improved inhibitory activity compared with standard antibacterial drug ciprofloxacin against *V. cholerae*, *B. cereus* and *S. dysenteriae* respectively. Additionally, compounds **51a-d** and **52b** displayed complete bactericidal activity within 24 h, whereas ciprofloxacin took 48 h to kill those bacteria completely. These antibacterial results indicated that substitution in the ring and water solubility of the target compounds could further enhance their inhibitory activities.

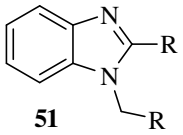

51

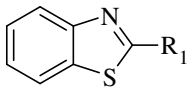

52

51a; R = C_6H_5
51b; R = 3-EtO-4-C_6H_3
51c; R = 5-Br-2-HOC_6H_3
51d; R = 4-$F_3COC_6H_4$

52a; R_1 = 2-EtC_6H_4
52b ; R_1 = 4-HOC_6H_4
52c ; R_1 = 4-$EtOC_6H_4$

Wittman *et. al.*[39] synthesized 1*H*-benzimidazol-2-yl-1*H*-pyridin-2-one analogous as inhibitor of insulin-like growth factor I receptor kinase with *in vivo* antitumor activity. Compound **53** has been shown novel small-molecule inhibitor of the insulin-like growth factor receptor kinase with equal potency against the insulin receptor. Compound **53** effectively inhibited proliferation of IGR-1R Sal cell line *in vitro* and disrupts protein kinase B (Akt/PKB) and mitogen-activated protein kinases (MAPK) phosphorylation. Compound **53** has been shown highly protein bound in mouse and human plasma.

Lee *et. al.*[40] synthesized a series of 2,5-disubstituted benzimidazole derivatives and evaluated for their diacylglycerol acyltransferase (DGAT) inhibitory activity using microsome from rat liver. Compound **54** showed the most promising DGAT inhibitory effect with IC_{50} value of 4.4 μM, which also demonstrated considerable inhibition of triglyceride formation in HepG2 cells as well as increased *in vivo* efficacy.

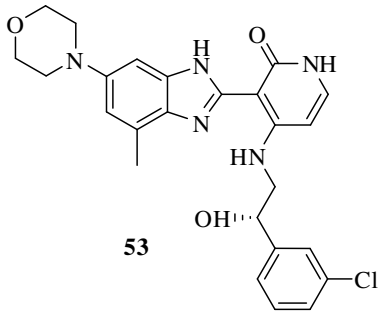

53

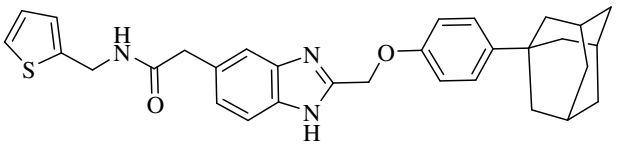

54

Villanueva *et. al.*[41] synthesized a series of 2-{[2-(1*H*-imidazol-1-yl)ethyl]sulfanyl}-1*H*-benzimidazole derivatives. The novel compounds were characterized by using various spectrometric and spectroscopic techniques. Biological assays revealed that these compounds have been shown strong activity against *Trichomonas vaginalis*, *Giardia intestinalis* and *Entamoeba histolytica*, better than metronidazole structure. Compound **55** was found to be most active against *G. Intestinalis* with IC_{50} value of 0.0083 ± 0.0023 μM.

Subramanian *et. al.*[42] synthesized a novel series of orally bio-available benzimidazole reverse amides as Pan RAF kinase inhibitors. Compound **56** demonstrated *in vivo* target inhibition with good antitumor activity. Further work on this scaffold has been done to improve the inhibition of cellular proliferation, ERK phosphorylation, hERG, and plasma stability that led to identify Pan RAF kinase inhibitor, which has since entered human clinical trials.

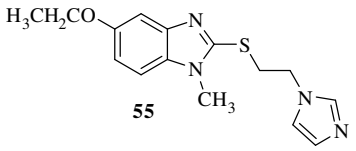

55

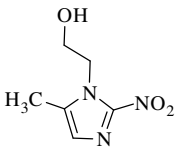

(metronidazole)

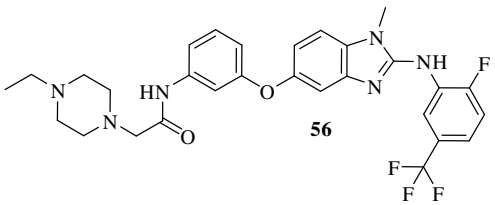

56

Thus, research on quinazoline, purine and benzimidazole moieties has been revealed to possess various pharmacological activities along with wide range of biological activity. It was our interest to make novel derivatives of the fused benzimidazole with quinazoline and purine nucleus and evaluate their *in vitro* anticancer activity. Therefore, in the present research programme, we have combined the basic features of quinazoline, purine and benzimidazole (**fig 1**) to develop new hybrid molecules (Model I and Model II, **fig 2**) which could act more effectively as anticancer agents and Aurora kinase inhibitors that help in finding the availability of anticancer drugs.

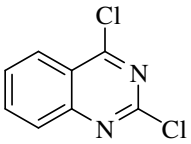

2,4-dichloroquinazoline

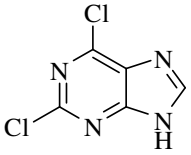

2,6-dichloro-9*H*-purine

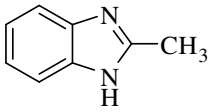

2-methyl-1*H*-benzo[*d*]imidazole

Figure-1

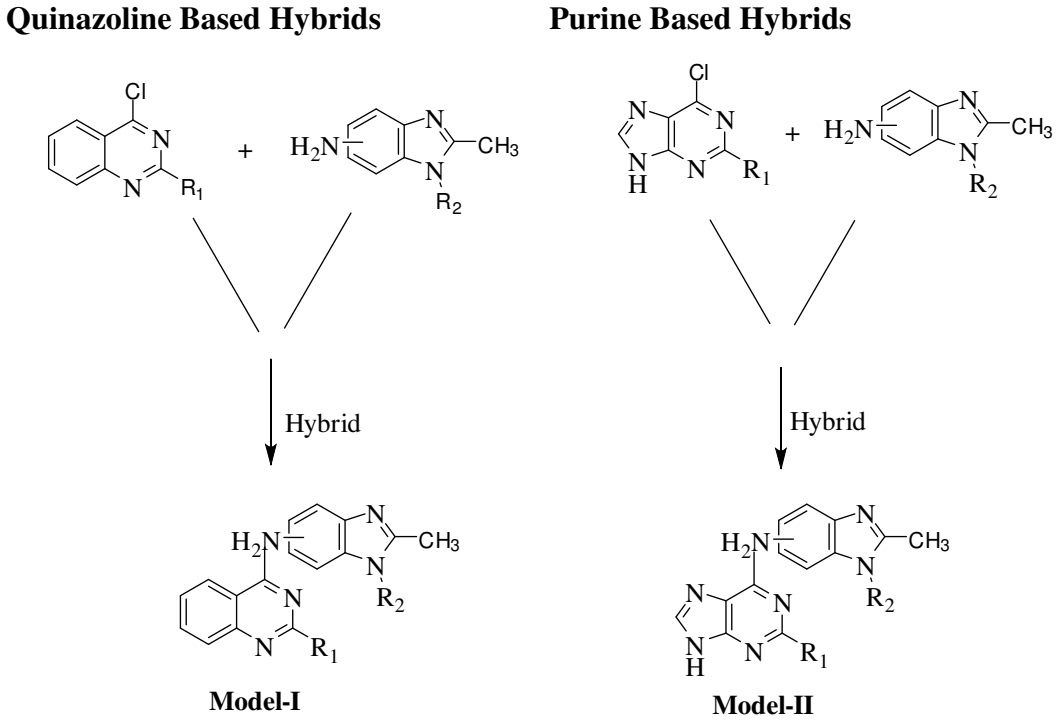

R_1 = Heterocyclic moieties; **R_2 =** Alkyl groups

Figure-2

REFERENCES

1. Tripathi, R. P.; Saxena, N.; Tiwari, V. K.; Verma, S. S.; Chaturvedi, V.; Manju, Y. K.; Srivastva, A. K.; Gaikwad, A.; Sinha, S. *Bioorg. Med. Chem.* **2006**, *14*, 8186; (b) Aggarwal, K.; Vij, K.; Khurana, J. M. *RSC Adv.* **2014**, *4*, 13313; (c) Bhushan, R.; Shuchi, D. *J. Chromatography A.* **2010**, *1217*, 6382; (d) Vandekerckhove, S.; Muller, C.; Vogt, D.; Lategan,C.; Smith, P. J.; Chibale, K.; De Kimpe, N.; D'hooghe, M. *Bioorg. Med. Chem. Lett.* **2013**, *23*, 318.

2. Wang, X. F.; Guan, F.; Ohkoshi, E.; Guo, W.; Wang, L.; Zhu, D. Q.; Wang, S. B.; Wang, L. T.; Hamel, E.; Yang, D.; Li, L.; Qian, K.; Morris-Natschke, S. L.; Yuan, S.; Lee, K. H.; Xie, L. *J. Med. Chem.* **2014**, *57*, 1390.
3. Jiang, N.; Zhai, X.; Zhao, Y.; Liu, Y.; Qi, B.; Tao, H.; Gong, P. *Eur. J. Med. Chem.* **2012**, *54*, 534.
4. Patel, A. B.; Chikhalia, K. H.; Kumari, P. *Res. Chem. Intermed.* **2014**, *14*, 1542.
5. Palop, J. A.; Plano, D.; Moreno, E.; Sanmartína, C. *ARKIVOC* **2014**, *2*, 187.
6. Verhaeghe, P.; Dumètre, A.; Castera-Ducros, C.; Hutter, S.; Laget, M.; Fersing, C.; Prieri, M.; Yzombard, J.; Sifredi, F.; Rault, S.; Rathelot, P.; Vanelle, P.; Azas, N. *Bioorg. Med. Chem. Lett.* **2011**, *21*, 6003.
7. Thorat, D. A.; Doddareddy, M. R.; Seo, S. H.; Hong, T. J.; Cho, Y. S.; Hahn, J. S.; Pae, A. N. *Bioorg. Med. Chem. Lett.* **2011**, *21,* 1593.
8. Barfi, I. S.; Weiss, E.; Levitzki, A. *Bioorg. Med. Chem.* **2010**, *18,* 6404.
9. Gellibert, F.; Fouchet M. H.; Nguyen, V. L.; Wang, R.; Krysa, G.; de Gouville, A. C.; Huet, S.; Dodic, N. *Bioorg. Med. Chem. Lett.* **2009**, *19,* 2277.
10. Sirisoma, N.; Kasibhatla, S.; Pervin, A.; Zhang, H.; Jiang, S.; Willardsen, J. A.; Anderson, M. B.; Baichwal, V.; Mather, G. G.; Jessing, K.; Hussain, R.; Hoang, K.; Pleiman, C. M.; Tseng, B.; Drewe, J.; Cai, S. X. *J. Med. Chem.* **2008**, *51,* 4771.
11. Smits, R. A.; Adami, M.; Istyastono, E. P.; Zuiderveld, O. P.; Van Dam, C. M. E.; de Kanter, F. J. J.; Jongejan, A.; Coruzzi, G.; Leurs, R.; de Esch, I. J. P. *J. Med. Chem.* **2010**, *53*, 2390.
12. Hour, M. J.; Yang, J. S.; Chen, T. L.; Chen, K. T.; Kuo, S. C.; Chung, J. G.; Lu, C. C.; Chen, C. Y.; Chuang, Y. H. *Eur. J. Med. Chem.* **2011,** *46*, 2709.
13. Desai, P. S.; Naik, P. J. *Discovery* **2014**, *17*, 7.
14. Chandrika, P. M.; Yakaiah, T.; Gayatri, G.; Kumar, K. P.; Narsaiah, B.; Murthy, U.S.N.; Rao, A. R. R. *Eur. J. Med. Chem.* **2010,** *45*, 78.
15. Sirisoma, N.; Pervin, A.; Zhang, H.; Jiang, S.; Willardsen, J. A.; Anderson, M.; Mather, G.; Pleiman, C. M.; Kasibhatla, S.; Tseng, B.; Drewe, J.; Cai, S. X. *Bioorg. Med. Chem. Lett.* **2010**, *20*, 2330.
16. Marvania, B.; Lee, P. C.; Chaniyara, R.; Dong, H.; Suman, S.; Kakadiya, R.; Chou, T. C.; Lee, T. C.; Shah, A.; Su, T. L. *Bioorg. Med. Chem.* **2011,** *19*, 1987.
17. Sharma, M.; Chauhan, K.; Shivahare, R.; Vishwakarma, P.; Suthar, M. K.; Sharma, A.; Gupta, S.; Saxena, J. K.; Lal, J.; Chandra, P.; Kumar, B.; Chauhan, P. M. S. *J. Med. Chem.* **2013**, *56*, 4374.

18. Naik, P. J.; Desai, P. S. *J. Environ. Res. Develop.* **2014**, *8*, 437.
19. Hollinshead, S. P.; Astles, P. S.; Chambers, M. G.; Johnson, M. P.; Palmer, J.; Tidwell, M. W. *Bioorg. Med. Chem. Lett.* **2012,** *22*, 4962.
20. Lee, W.; Ortwine, D. F.; Bergeron, P.; Lau, K.; Lin, L.; Malek, S.; Nonomiya, J.; Pei, Z.; Robarge, K. D.; Schmidt. S.; Sideris, S.; Lyssikatos, J. P. *Bioorg. Med. Chem. Lett.* **2013,** *23*, 5097.
21. Nair, N.; Kudo, W.; Smith, M. A.; Abro, R.; Goddard, W. A.; Reddy, V. P. *Bioorg. Med. Chem. Lett.* **2011,** *21*, 3957.
22. Verones, V.; Flouquet, N.; Farce, A.; Carato, P.; Leonce, S.; Pfeiffer, B.; Berthelot, P.; Lebegue, N. *Eur. J. Med. Chem.* **2010,** *45*, 5678.
23. Pathak, A. K.; Pathak, V.; Seitz, L. E.; Suling, W. J.; Reynolds, R. C. *Bioorg. Med. Chem.* **2013,** *21*, 1685.
24. Zatloukal, M.; Jorda, R.; Gucký, T.; Reznícková, E.; Voller, J.; Pospísil, T.; Malínková, V.; Adamcová, H.; Krystof, V.; Strnad, M. *Eur. J. Med. Chem.* **2013,** *61*, 61.
25. Mallari, J. P.; Zhu, F.; Lemoff , A.; Kaiser, M.; Lu, M.; Brun, R.; Guy, R. K. *Bioorg. Med. Chem.* **2010,** *18*, 8302.
26. Vandromme, L.; Legraverend, M.; Kreimerman,S.; Lozach, O.; Meijer, L.; Grierson, D. S. *Bioorg. Med. Chem.* **2007,** *15*, 130.
27. Tunçbilek, M.; Alagöz, Z. A.; Altanlar, N.; Karayel, A.; Ozbey, S. *Bioorg. Med. Chem.* **2009,** *17*, 1693.
28. Trova, M. P.; Barnes, K. D.; Alicea, L.; Benanti, T.; Bielaska, M.; Bilotta, J.; Bliss, B.; Duong, T.; Haydar, S.; Her, R. J.; Hui, Y.; Johnson, M.; Lehman, J. M.; Peace, D.; Rainka, M.; Snider, P.; Salamone, S.; Tregay, S.; Zheng, X.; Friedrich, T. D. *Bioorg. Med. Chem. Lett.* **2009,** *19*, 6613.
29. Gucký, T.; Jorda, R.; Zatloukal, M.; Bazgier, V.; Berka, K.; Reznícková, E.; Beres, T.; Strnad, M.; Krystof, V. *J. Med. Chem.* **2013**, *56*, 6234.
30. Gundersen, L. L.; Nissen-Meyer, J.; Spilsberg, B. *J. Med. Chem.* **2002**, *45*, 1383.
31. Dolecková, I.; Cesnek, M.; Dracinský, M.; Brynda, J.; Voller, J.; Janeba, Z.; Krystof, V. *Eur. J. Med. Chem.* **2013**, *62*, 443.
32. Venkatesan, A. M.; Dehnhardt, C. M.; Chen, Z.; Santos, E. D.; Santos, O. D.; Bursavich, M.; Gilbert, A. M.; Ellingboe, J. W.; Kaloustian, S. A.; Khafizova, G.; Brooijmans, N.; Mallon, R.; Hollander, I.; Feldberg, L.; Lucas, J.; Yu, K.; Gibbons, J.; Abraham, R.; Mansou, T. S. *Bioorg. Med. Chem. Lett.* **2010,** *20*, 653.

33. Morales, F.; Ramírez, A.; García, A. C.; Morata, C.; Marchal, J. A.; Campos, J. M. *Eur. J. Med. Chem.* **2014,** *76*, 118.
34. Wang, W.; Kong, D.; Cheng, H.; Tan, L.; Zhang, Z.; Zhuang, X.; Long, H.; Zhou, Y.; Xu, Y.; Yang, X.; Ding, K. *Bioorg. Med. Chem. Lett.* **2014,** *24*, 4250.
35. Wang, X. J.; Yang, M. L.; Zhang, L. P.; Yao, T.; Chen, C.; Mao, L. G.; Wang, Y.; Wuc, J. *Chinese Chem. Lett.* **2014,** *25*, 589.
36. Bacharaju, K.; Jambula, S. R.; Sivan, S.; JyostnaTangeda, S.; Manga, V. *Bioorg. Med. Chem. Lett.* **2012,** *22*, 3274.
37. He, S.; Hong, Q.; Lai, Z.; Wu, Z.; Yu, Y.; Kim, D. W.; Ting, P. C.; Kuethe, J. T.; Yang, G. X.; Jian, T.; Liu, J.; Guiadeen, D.; Krikorian, A. D.; Sperbeck, D. M.; Sonatore, L. M.; Wiltsie, J.; Chung, C. C.; Gibson, J. T.; Lisnock, J. M.; Murphy, B. A.; Gorski, J. N.; Liu, J.; Chen, D.; Chen, X.; Wolff, M.; Tong, S. X.; Madeira, M.; Karanam, B. V.; Shen, D. M.; Balkovec, J. M.; Pinto, S.; Nargund, R. P.; DeVita, R. J. *Med. Chem. Lett.* **2013**, *4*, 773.
38. Bandyopadhyay, P.; Sathe, M.; Ponmariappan, S.; Sharma, A.; Sharma, P.; Srivastava, A. K.; Kaushik, M. P. *Bioorg. Med. Chem. Lett.* **2011**, *21*, 7306.
39. Wittman, M.; Carboni, J.; Attar, R.; Balasubramanian, B.; Balimane, P.; Brassil, P.; Beaulieu, F.; Chang, C.; Clarke, W.; Dell, J.; Eummer, J.; Frennesson, D.; Gottardis, M.; Greer, A.; Hansel, S.; Hurlburt, W.; Jacobson, B.; Krishnananthan, S.; Lee, F. Y.; Li, A.; Lin, T. A.; Liu, P.; Ouellet, C.; Sang, X.; Saulnier, M. G.; Stoffan, K.; Sun, Y.; Velaparthi, U.; Wong, H.; Yang, Z.; Zimmermann, K.; Zoeckler, M.; Vyas, D. *J. Med. Chem.* **2005**, *48,* 5639.
40. Lee, K.; Goo. J.; Jung, H. Y.; Kim, M.; Boovanahalli, S. K.; Park, H. R.; Kim, M. O.; Kim, D. H.; Lee, H. S.; Choi, Y. *Bioorg. Med. Chem. Lett.* **2012,** *22*, 7456.
41. Villanueva, J. P.; Campos, A. H.; Mulia, L. Y.; Cuesta, C. M.; Lucio, O. M.; Luis, F. H.; Castillo, R. *Bioorg. Med. Chem. Lett.* **2013,** *23*, 4221.
42. Subramanian, S.; Costales, A.; Williams, T. E.; Levine, B.; McBride, C. M.; Poon, D.; Amiri, P.; Renhowe, P. A.; Shafer, C. M.; Stuart, D.; Verhagen, J.; Ramurthy, S. *ACS Med. Chem. Lett.* **2014**, *5*, 989.

CHAPTER-2

Quinazoline-Benzimidazole Hybridization

2.1. INTRODUCTION

Cancer is causing a major health problem in developing as well as undeveloped countries.[1-9] The increase in cancer incidence led to the search for latest, safer and efficient anticancer agents, aiming the prevention or the cure of this deadly disease. In the past decade, the development of new anticancer therapeutic tools had achieved enormous advancements. Thus approaches for the treatment of cancer that has moved towards targeting the molecular modifications, occur in tumor cells. These modifications have been concentrated on the development of both small molecules and biological agents that shown significant activity without toxicity associated with conventional chemotherapy.[10] Most of chemotherapeutics presently used in cancer therapy are agents that inhibit tumor growth by inhibiting the replication or transcription of DNA. In the path of identifying new chemical substances which may lead to the designing of novel antitumor agents, nitrogen-containing heterocycles are of particular interest.[11] Among these, quinazolines and benzimidazoles are important classes of heterocyclic compounds that are the most common motifs present in drugs and bioactive compounds with a broad spectrum of pharmacological activities.[12] Quinazolines symbolize an important category of marketed targeted cancer therapy. Several attempts were made for improving their antitumor activities by modifying the quinazoline moiety. Quinazoline derivatives have also attracted attention due to their broad range of pharmacological activities such as antifungal,[13] antimalarial,[14] anti-inflammatory,[15] anticonvulsant,[16] antibacterial,[17] antihypertensive[18] and anticancer.[19,20] Several of these compounds exhibited dihydrofolate reductase and tyrosine kinase[21] inhibitors such as erlotinib, gefitinib, caneratinib, vandetanib and lapatinib (**Figure 1**). Some quinazoline derivatives interact with tubulin[22] and interfere with its polymerization, others act by modulating Aurora kinase activity[23] or have an effect in critical phases in the cell cycles[24] or act as apoptosis inducers.[25] The reported significance of such synthons generated the interest to exploit this valuable structure in the designing and synthesis of new quinazoline analogue as antitumor agents.

Similarily, benzimidazole, a heteroaromatic organic compound also created an interest in medicinal and biological properties such as antitumor,[26] antibacterial,[27] antihypertensive,[28] anti-inflammatory,[29] vasodilator[30] and antiviral[31] agents. Benzimidazole

derivatives are known inhibitors of cyclin dependent kinase or tyrosine kinase and useful for inhibiting cell proliferation for the treatment of cancer.[32]

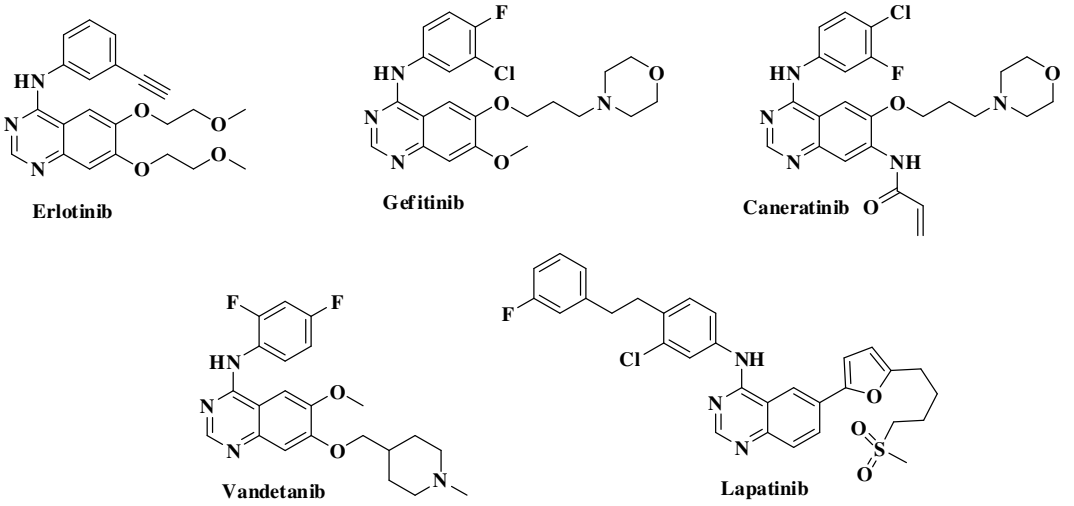

Figure 1

Molecular hybridization is a relatively new terminology in the field of medicinal chemistry with the fusion of two or more pharmacophoric biologically active subunits from the molecular structure of ligands/prototypes previously reported that have an inhibitory effect against the target protein or disease. The newly designed architecture can lead to compounds having improved affinity and efficiency than the parent compounds with reduced side effects, while retaining the desired characteristics of original template. Various literature reports have been explored to this methodology in designing of newer analogues as potential candidates for biological evaluation.[33]

In the present investigation, we have combined the structural artifacts of benzimidazole and quinazoline moieties to make a hybrid and substituted them with different secondary and primary amines in order to observe the effect of electron-donor and acceptor nitrogen groups within the moieties. These hybrid molecules consisted of planar heterocyclic ring (quinazoline) as central core that can act as a scaffold to carry two functionalized branches at positions 2 and 4, in such a way to accommodate a benzimidazole ring at 4-position and secondary/primary amines at 2-position of quinazoline. Introduction of alkyl and allyl groups at 1- or 3-position of benzimidazole are also known to increase lipid solubility of polar compounds, a character very much needed for the activity.

Objective:

Various methods for the synthesis of quinazoline moiety with different substitution at C2 and C4 positions have been documented in the literature. It has been found that most of the study has been done with pyrazole, morpholine, piperidine, piperazine etc. at 4-position of quinazoline as anticancer agents, but no report has been given about the synthesis and evaluation of benzimidazole linked with quinazoline (at 4-position). Regioisomeric alkylation of benzimidazole moiety has not been reported for different electronic environment towards the quinazoline ring. As a part of our research programme that aimed at developing amino benzimidazole at 4-position of quinazoline ring with secondary and primary amines at 2-position, became interesting to develop new and highly potent hybrid compounds.

2.2. DESIGNING

Knowledge from other quinazoline-based kinase inhibitors, such as gefitinib, we have planned to synthesize several series of analogous of quinazoline-benzimidazole hybrids, in which there is the addition of two hydrogen acceptor atoms and increasing the lipophilicity by the introduction of allyl group on benzimidazole. It has been suggested that our compound might bind into the protein molecule and extended benzimidazole group occupy the selectivity pocket that play an important role in its activity and selectivity. The physical properties can also be modulated by further substitution of hydrophilic moieties at the 2-position of the quinazoline ring. In these hybrid compounds, we have found two regions: hydrophobic region and hydrogen bond region that can balance the hydrophilicity and lipophilicity.

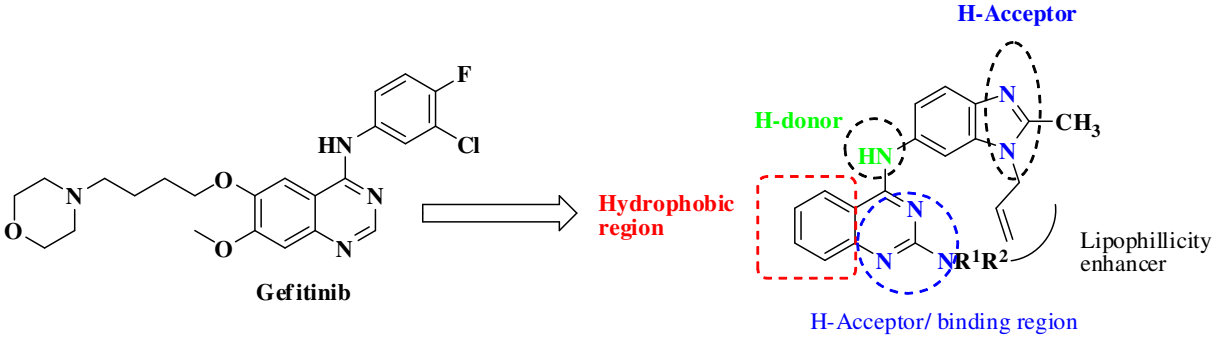

Figure 2: Design of quinazoline-benzimidazole hybrids

2.3. CHEMISTRY

2.3.1. Synthesis of quinazoline-benzimidazole hybrids with secondary amines

2.3.1.1. Synthesis of 1/3-allyl-2-methyl-1*H*/3*H*-benzimidazol-5-ylamine (4a, 4b)

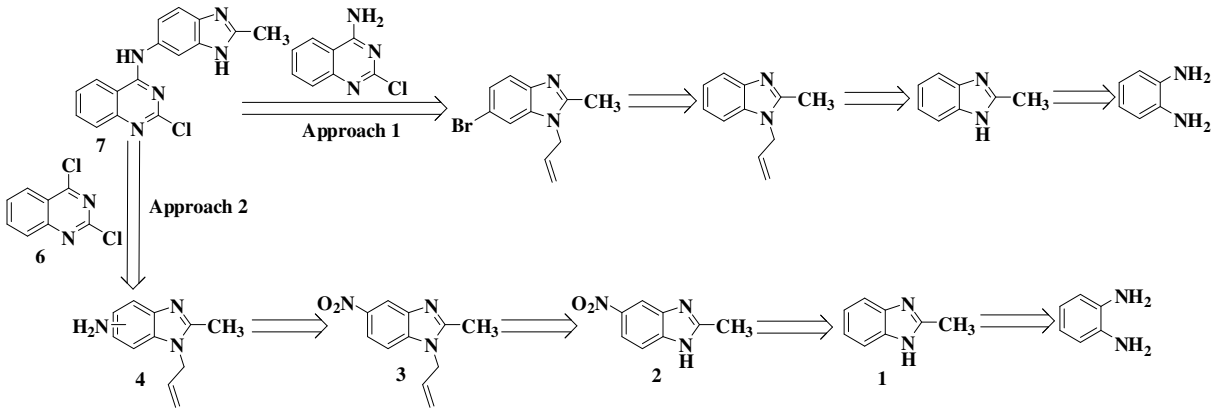

Scheme 1. Retrosynthetic approach for the synthesis of target molecules

A reterosynthetic investigation in achieving compound **7** has been shown in **scheme-1**. For the synthesis of target quinazoline-benzimidazole hybrid compound, first approach 1 has been followed. *o*-Phenylenediamine was treated with acetic acid followed by allylation with allyl bromide in the presence of sodium hydride to get 1-allyl-2-methyl-1*H*-benzo[*d*]imidazole followed by bromination at 6-position to get 1-allyl-6-bromo-2-methyl-1*H*-benzo[*d*]imidazole. Different reaction conditions have been used for the nucleophilic substitution reaction at 4-position of 2-chloro-4-aminoquinazoline with 1-allyl-6-bromo-2-methyl-1*H*-benzo[*d*]imidazole but in all the cases, reactions were unsuccessful. This might be due to the contribution of lone pairs of electrons of nitrogen with quinazoline ring. So, different approach has been used to achieve the target quinazoline-benzimidazole hybrid molecules (Approach 2).

o-Phenylenediamine (1 g, 0.009 mol) was treated with acetic acid (4 ml) at 100 °C for 24 h. After completion of the reaction, work up was done with 10% NaOH to make the reaction mixture alkaline. Filtered the solid product, washed with water and dried over sodium sulphate to give brown coloured 2-methylbenzimidazole (**1**) in 82% yield (mp. 177-180 °C). Nitration has been done with equal amounts of nitric acid and concentrated sulphuric acid in 2-methylbenzimidazole at 0 °C for 5 h. After completion of the reaction, crushed ice was added to the reaction mixture, filtered the solid product, washed with water several times and dried to give orange coloured 2-methyl-5-nitro-1*H*-benzimidazole **(2)** with 80% yield. 2-Methyl-5-nitro-1*H*-benzimidazole (9 g, 0.05 mol) was then treated with allyl bromide (9.17g,

0.075 mol) in the presence of sodium hydride (3.03g, 0.126 mol) and THF at room temperature for 8 h. The reaction mixture was extracted with chloroform, concentrated to give yellow solid of mixture of **3a** and **3b** (m.pt. 195-200 °C). ^{1}H NMR spectrum showed 6H singlet at δ 2.56 of 2×CH_3, 4H multiplet at δ 4.93 of 2xN-CH_2, two 2H double doublets at δ 4.98 and 5.22 of 2xallylCH_2, 2H multiplet at δ 6.01 of 2×allyl–CH, two 2H doublets at δ 7.56 and 8.42 and 2H multiplet at δ 8.09 of 2×aromatic-H. ^{13}C NMR spectrum showed the signals at δ 13.5 (CH_3), 13.6 (CH_3), 45.6 (allyl-NCH_2), 45.7 (allyl-NCH_2), 106.5 (allyl-NCH_2-<u>CH</u>-CH_2), 109.8, 114.3 (ArH), 116.7 (allyl-CH_2), 116.8 (allyl-CH_2), 117.0, 117.3, 118.2, 131.7, 131.9, 134.3, 139.4, 141.4, 142.2, 142.5, 146.8, 155.9, 157.3 (ArH). These spectral data corroborate the mixture of 3-allyl-2-methyl-5-nitro-3*H*-benzimidazole (**3a)** and 1-allyl-2-methyl-5-nitro-1*H*-benzimidazole (**3b**). 1/3-Allyl-2-methyl-5-nitro-1*H*/3*H*-benzimidazole (0.039 mol) was reduced with stannous chloride (0.135 mol) and 2 N HCl at 110 °C for 7 h. The reaction was monitored by TLC. After the completion of the reaction, the suspension was neutralized with 2N NaOH and diluted with ethanol. Filtered the solid product to remove salts, extract the filtrate with chloroform and concentrated to get mixture of products which were separated through column chromatography using ethylacetate : methanol (9.5:0.5) as eluents to afford pure solid regioisomeric **4a** with 65% yield (EIMS, m/z: 188 (M^++1)) and **4b** with 25% yield (EIMS, m/z: 188 (M^++1)) (**Scheme 2**).

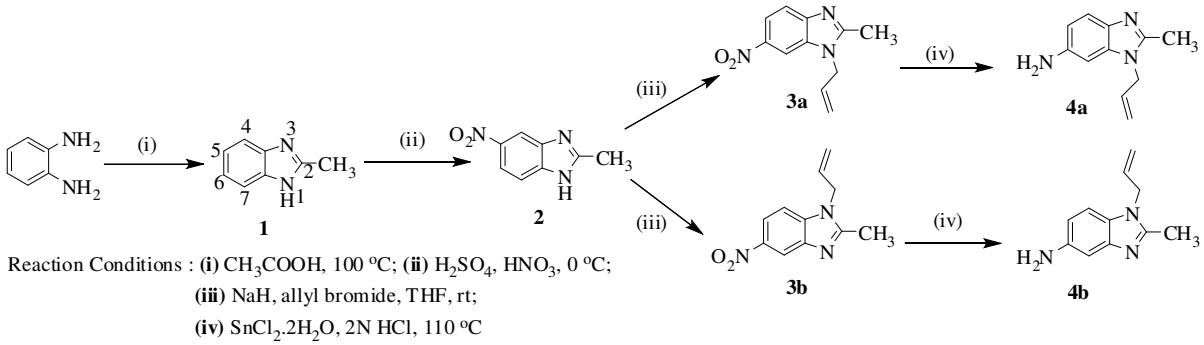

Scheme 2. Synthetic route for the preparation of compounds **4a** and **4b**

^{1}H NMR spectrum of **4a** showed the 3H singlet at δ 2.50 of CH_3, 2H broad singlet at δ 3.56 for NH_2 (exchangeable with D_2O), 2H doublet at δ 4.57 of N-CH_2, two 1H doublets at δ 4.95 and 5.19 of allyl–CH_2, 1H multiplet at δ 5.89 of allyl-CH, two 1H doublets at δ 6.51 and 7.46, and 1H double doublet at δ 6.60 of aromatic-H. ^{13}C NMR spectrum of this compound showed the signals at δ 13.6 (CH_3), 45.6 (allyl-NCH_2), 94.9 (allyl-NCH_2-<u>CH</u>-CH_2), 111.7 (ArH), 117.1 (allyl-CH_2), 119.4, 131.7, 136.0, 136.1, 142.3, 149.9 (ArH). IR spectrum also

showed two bands at 3380 and 3270 cm^{-1} due to NH_2. On the basis of these spectral data, this compound has been assigned the structure of 3-allyl-2-methyl-3*H*-benzimidazol-5-ylamine **(4a)**. Similarly, ^1H NMR spectrum of **4b** showed the 3H singlet at δ 2.53 of CH_3, 2H broad singlet at δ 3.74 for NH_2 (exchangeable with D_2O), 2H multiplet at δ 4.64 of allyl-NCH_2, two 1H double doublets at δ 4.93 and 5.21 of allyl-CH_2, 1H multiplet at δ 5.91 of allyl-CH, 1H double doublet at δ 6.64 and two 1H doublets at δ 7.02 and 7.04 of aromatic-H. ^{13}C NMR spectrum of this compound showed the signals at δ 13.7 (CH_3), 45.8 (allyl-NCH_2), 104.4 (allyl-NCH_2-<u>CH</u>-CH_2), 109.5, 111.9 (ArH), 117.1 (allyl-CH_2), 129.1, 131.9, 141.8, 143.6, 151.6 (ArH). IR spectrum also showed two bands at 3380 and 3272 cm^{-1} due to NH_2. On the basis of these spectral data, this compound has been assigned the structure of 1-allyl-2-methyl-1*H*-benzimidazole-5-ylamine (**4b**).

Complete and unambiguous assignments for all ^1H and ^{13}C resonances could be achieved on the basis of chemical shift considerations, coupling information and NOE difference spectra. Discrimination between **4a** and **4b** were achieved by considering 2D NOE difference experiments. The observation of NOE between singlet H4 and N-CH_2 of **4a** indicated that the allyl group is close proximity to the NH_2 group (**Figure 3**) while in case of compound **4b** that show positive NOEs signals of N-CH_2 protons and doublet of aromatic

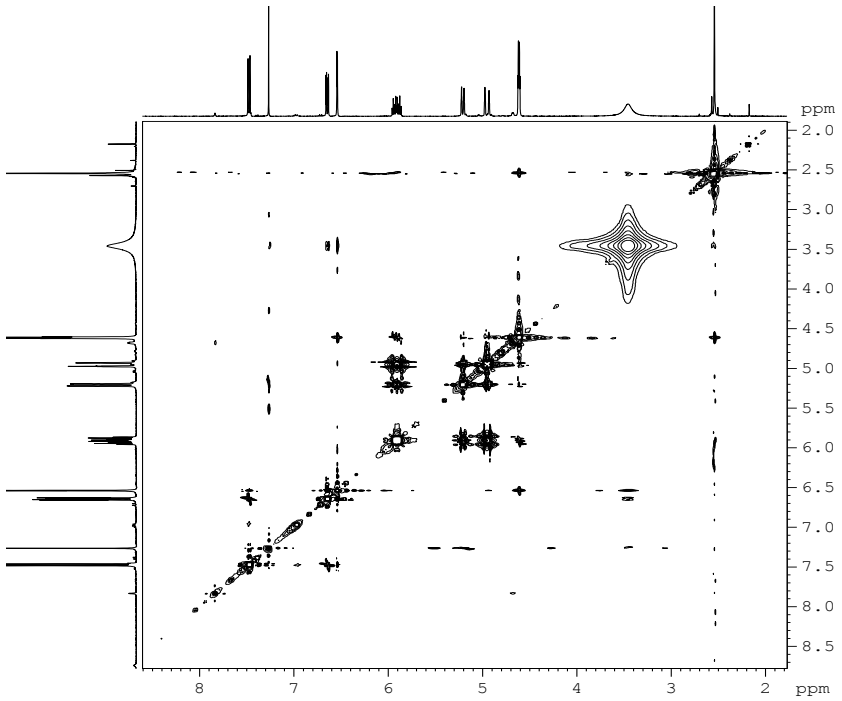

Figure 3. 2D NOE spectrum of 3-allyl-2-methyl-3*H*-benzimidazol-5-ylamine **(4a).**

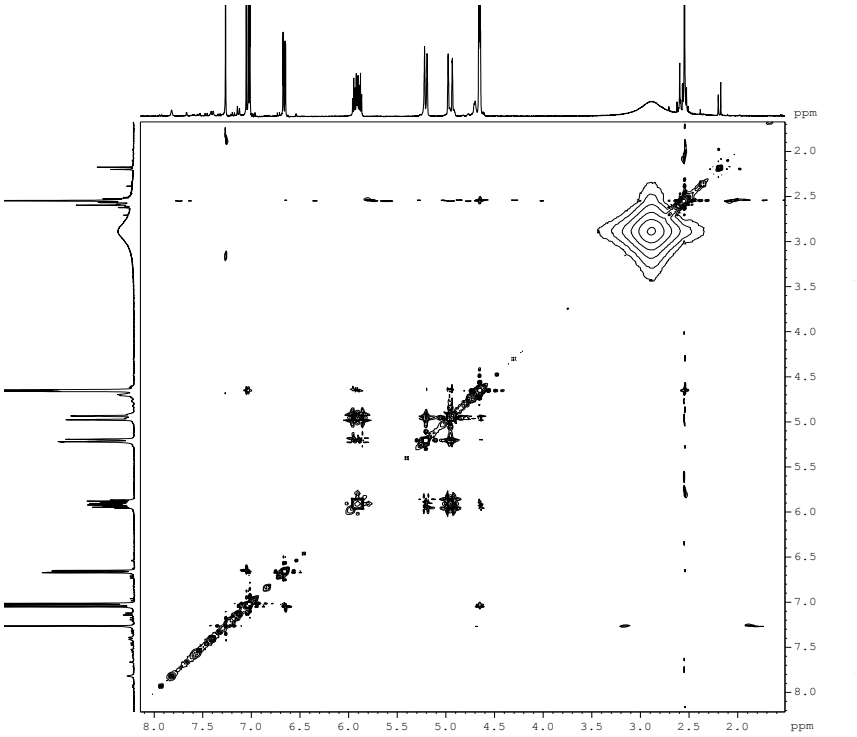

Figure 4. 2D NOE spectrum of 1-allyl-2-methyl-1*H*-benzimidazol-5-ylamine **(4b).**

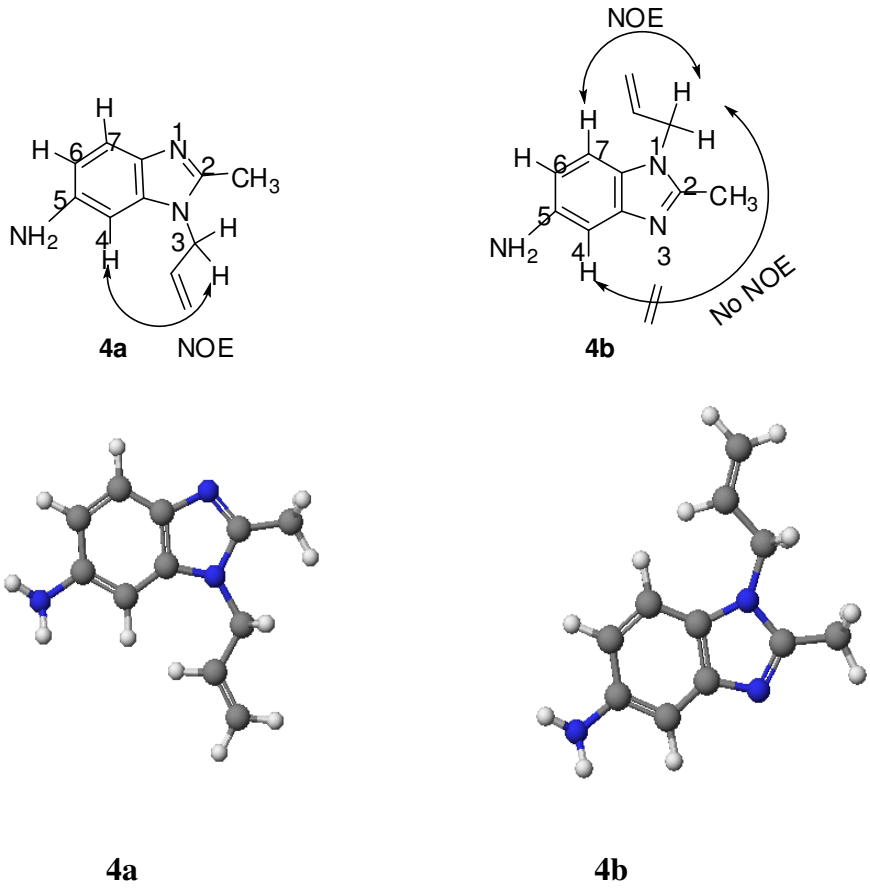

Figure 5. 2D NOEs ^{1}H, ^{1}H correlations used for structural assignment of compounds **4a** and **4b**, energy minimization of **4a** and **4b** compounds.

ring H7 of benzimidazole and negative NOE with singlet of H4 position as shown in **figure 4**. The energy minimized structures also corroborate NOE results as allyl group approaching towards the singlet of aromatic ring of benzimidazole in **4a** and allyl group is near to doublet of aromatic ring of benzimidazole in **4b** (**Figure 5**).

2.3.1.2. Synthesis of 1/3-allyl-2-methyl-1*H*/3*H*-benzimidazol-5-yl)-(2-amino-quinazolin-4-yl)-amine

Anthranilic acid (0.07 mol) was treated with urea (0.73 mol) with stirring at 160 °C for 6 h. Cooled the reaction mixture to 100 °C and water was added while stirring for 5 min. The white precipitate formed was filtered off and washed with cold water to yield solid cake that was suspended in a solution of 0.5N NaOH and heated to boil for 5-10 min. Cooled and adjusted the pH = 2 with concentrated HCl, and the solid was filtered off, washed with water : methanol (1:1) and dried to give white solid of 1*H*-quinazolin-2,4-dione **(5)** (mp. > 300 °C). 1*H*-Quinazolin-2,4-dione (0.03 mol) was then refluxed with phosphorous oxychloride (0.27 mol) and triethylamine (0.05 mol) for 7 h. Distilled off excess $POCl_3$ under vacuum, crushed ice was added to the reaction mixture and stirred the reaction mixture for 1 h at 0-5 °C. Filtered the solid product, washed with water and dried to give yellow solid of 2,4-dichoro-quinazoline **(6)**[34] (mp. 117-120 °C). Further, 2,4-dichloroquinazoline (0.011 mol) was treated with 3-allyl-2-methyl-3*H*-benzimidazol-5-ylamine (0.011 mol) **(4a)** in isopropyl alcohol (IPA) at room temperature for 12 h. After completion of the reaction, washed the solid product with IPA, dried to give white solid of compound **7a** (EIMS, m/z: 350.5 (M^++1)) with 92% yield (**Scheme 3**).

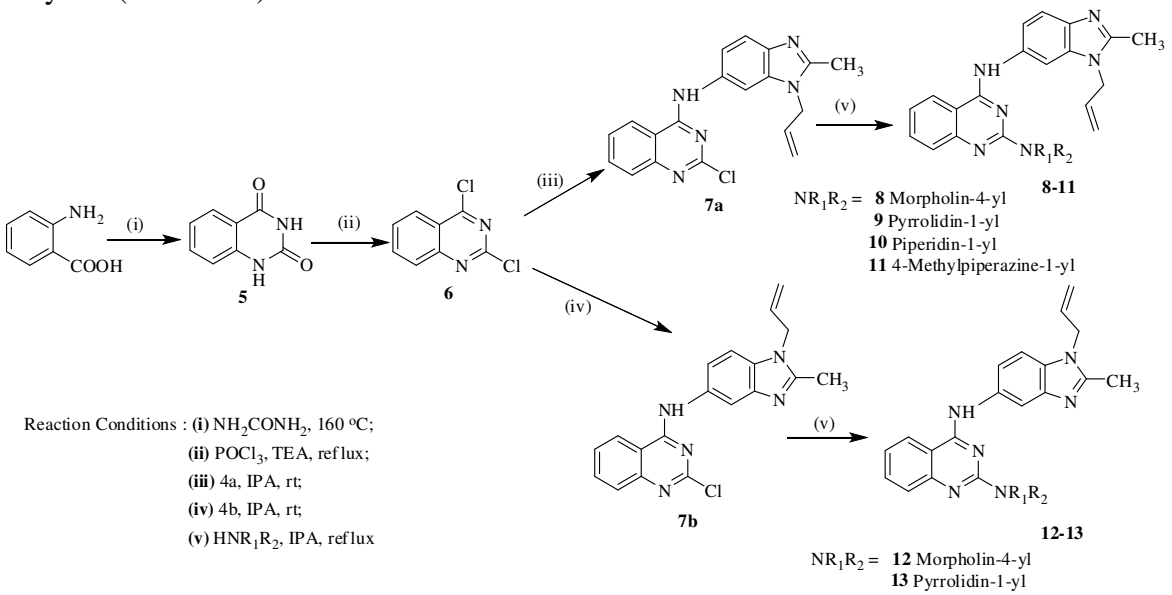

Scheme 3. Synthetic route for the preparation of target compounds **(8-13)**

^{1}H NMR spectrum of **7a** showed the 3H singlet at δ 2.55 of CH_3, 2H doublet at δ 5.12 of N-CH_2, 2H double doublet at δ 5.25 and 5.39 of allyl-CH_2, 1H multiplet at δ 6.06 of allyl-CH, 1H triplet at δ 7.61, three 1H doublets at δ 7.74, 8.57 and 8.76, 2H multiplet at δ 7.83 and 1H double doublet at δ 8.12 of aromatic-H and 1H broad singlet at δ 10.52 of NH (exchangeable with D_2O). ^{13}C NMR spectrum of this compound showed signals at δ 11.3 (CH_3), 46.7 (allyl-NCH_2), 106.9 (allyl-NCH_2-<u>CH</u>-CH_2), 111.6, 113.7, 114.2, 115.2, 119.0 (ArH), 121.2 (allyl-CH_2), 121.9, 123.7, 126.2, 126.5, 126.7, 127.7, 129.4, 129.7, 133.5, 134.3, 137.1, 140.6, 150.0, 150.4, 150.6, 155.8, 159.0, 162.9 (ArH). IR spectrum also showed the peaks at 3258 (NH), 3054 (CH), 1704, 1671, 1503, 1426 (C=C), 1289, 1141 (CN), 756 (CH) cm^{-1}. On the basis of these spectral data, this compound has been assigned the structure of [(3-allyl-2-methyl-3*H*-benzimidazol-5-yl)-(2-chloro-quinazolin-4-yl)-amine] **(7a).** Compound **7a** (0.2g, 0.57 mmol) was further refluxed with morpholine (0.62 mmol) in IPA for 7 h and after column chromatography gave pure light yellow coloured solid compound of **8** (EIMS, m/z: 401 (M^++1)) with 65% yield. ^{1}H NMR spectrum showed the 3H singlet at δ 2.59 of CH_3, 4H triplet at δ 3.76 of N-morCH_2, 4H singlet at δ 3.88 of O-morCH_2, three 2H doublets at δ 4.74 of allyl-NCH_2, 5.00 and 5.26 of allyl-CH_2, 1H multiplet at δ 5.96 of allyl-CH, 1H multiplet at δ 7.18, 3H multiplet at δ 7.26, two 1H doublets at δ 7.52 and 8.01, 1H triplet at δ 7.58 of aromatic-H and 1H broad singlet at δ 7.74 of NH (exchangeable with D_2O). ^{13}C NMR spectrum showed signals at δ 13.2 (CH_3), 46.0 (N-morCH_2), 46.5 (allyl-NCH_2), 65.7 (O-morCH_2), 108.2 (allyl-NCH_2-<u>CH</u>-CH_2), 110.2, 111.8, 116.6, 117.0, 119.9 (ArH), 121.9 (allyl-CH_2), 124.4, 131.1, 131.3, 131.9, 133.8, 142.0, 151.6, 151.7, 156.9, 157.3 (ArH). IR spectrum also showed the peaks at 3351 (NH), 3059, 2835 (CH), 1620, 1567, 1477, 1432 (C=C), 1398, 1232, 1106 (CN), 1003, 757 (CH) cm^{-1}. On the basis of these spectral data, this compound has been assigned the structure of (3-allyl-2-methyl-3*H*-benzimidazol-5-yl)-(2-morpholin-4-yl-quinazolin-4-yl)-amine (**8**). Similarly, compound **7a** was also treated with 1.2 equivalents of pyrrolidine, piperidine and 4-methylpiperazine at the same reaction conditions to obtain **9-11** with 55-89% yields **(Table 1)**.

Similarly, treatment of 2,4-dichloroquinazoline with **4b** in the presence of isopropyl alcohol at room temperature for 12 h gave white solid of compound **7b (**EIMS, m/z: 350.5 (M^++1)). The ^{1}H NMR spectrum of this compound showed the 3H singlet at δ 2.57 of CH_3, 2H doublet at δ 4.82 of allyl-NCH_2, two 2H double doublets at δ 5.04 and 5.25 of allyl-CH_2, 1H multiplet at δ 6.03 of allyl-CH, 1H double doublet at δ 7.48, 2H doublet at δ 7.57, three 1H doublets at δ 7.68, 7.99 and 8.59, 1H triplet at δ 7.81 of aromatic-H and 1H broad singlet at δ 10.17 due to NH (exchangeable with D_2O). ^{13}C NMR spectrum showed signals at δ 11.3

(CH_3), 46.6 (allyl-NCH_2), 106.9 (allyl-NCH_2-CH-CH_2), 111.9, 113.8, 114.2, 115.1, 118.9, 121.0 (ArH), 121.8 (allyl-CH_2), 123.5, 126.2, 126.6, 127.9, 129.7, 129.9, 133.6, 134.3, 136.9, 140.7, 150.3, 155.8, 159.1, 162.9 (ArH). IR spectrum also showed the peaks 3252 (NH), 3035, 2849 (CH), 1719, 1662, 1624, 1433 (C=C), 1299 (CN), 758 (CH) cm^{-1}. On the basis of these spectral data, this compound has been assigned the structure of [(1-allyl-2-methyl-1*H*-benzimidazol-5-yl)-(2-chloro-quinazolin-4-yl)-amine] (**7b)**.

Compound **7b** (0.2g, 0.57 mmol) was further refluxed with morpholine (0.62 mmol) in IPA for 7 h and after column chromatography gave pure light yellow coloured solid of compound **12** (EIMS, m/z: 401 (M^++1)). ^{1}H NMR spectrum of compound **12** showed the 3H singlet at δ 2.56 of CH_3, two 4H doublets at δ 3.72 and 3.82 of O/N-morCH_2, three 2H doublets at δ 4.79 of allyl-NCH_2, 4.87 and 5.22 of allyl-CH_2, two 1H multiplets at δ 6.03 of allyl-CH_2 and 7.15 (ArH), 1H singlet at δ 7.28, two 1H doublets at δ 7.44 and 8.42 and 3H multiplet at δ 7.64 of aromatic-H, 1H broad singlet at δ 10.06 due to NH (exchangeable with D_2O). ^{13}C NMR spectrum showed signals at δ 13.4 (CH_3), 44.2 (N-morCH_2), 45.4 (allyl-NCH_2), 66.3 (O-morCH_2), 108.5 (allyl-NCH_2-CH-CH_2), 110.9, 112.3, 116.5, 117.8 (ArH), 120.7 (allyl-CH_2), 122.8, 125.1, 131.6, 132.2, 133.4, 142.0, 151.8, 158.1, 158.3 (ArH). IR spectrum also showed peaks at 3457 (NH), 3123, 2931 (CH), 1637, 1593, 1577, 1409 (C=C), 1330, 1107 (CN), 1000 (CO), 760 (CH) cm^{-1}. On the basis of these spectral data, this compound has been assigned the structure of (1-allyl-2-methyl-1*H*-benzimidazol-5-yl)-(2-morpholin-4-yl-quinazolin-4-yl)-amine (**12**). This compound has also been confirmed by single X-ray crystallography (Section-2.3.1.3).

Under the same reaction conditions, compound **7b** was also treated with 1.2 equiv. of pyrrolidine in IPA for 8 h gave compound **13** in 52 % yields (EIMS, m/z: 385 (M^++1)). Structures of all the novel compounds have been confirmed by ^{1}H and ^{13}C NMR as well as mass spectrometry.

Table-1 Physicochemical properties of the newly synthesized compounds **7a-b** and **8-13**

Compound	Starting Material	NR_1R_2	% yields	M.pt. (°C)	Molecular formulae
7a	4a	--	92	210-215	$C_{19}H_{16}ClN_5$
7b	4b	--	82	217-220	$C_{19}H_{16}ClN_5$
8	7a	morpholin-4-yl	65	200-210	$C_{23}H_{24}N_6O$
9	7a	pyrrolidin-1-yl	89	150-155	$C_{23}H_{24}N_6$
10	7a	piperidin-1-yl	78	170-175	$C_{24}H_{26}N_6$
11	7a	4-methylpiperazin-1-yl	55	198-200	$C_{24}H_{27}N_7$
12	7b	morpholin-4-yl	70	200-210	$C_{23}H_{24}N_6O$
13	7b	pyrrolidin-1-yl	52	180-183	$C_{23}H_{24}N_6$

2.3.1.3. Single Crystal X-ray diffraction

Compound **12** was grown in ethanol to develop single crystal and the following data was obtained. Molecular formula = $C_{23}H_{24}N_6O$, M.wt. = 400.48, colourless crystals, 0.23×0.18×0.13 mm, monoclinic, space group $P2_1/c$, a = 6.3175 (2) Å, b = 23.8231 (6) Å, c = 14.1809 (4) Å, α= 90.0°, β = 98.004 (3)°, γ = 90.0°, V = 2113.47 (10) $Å^3$, Z = 4, D_{calcd} = 1.259 Mg/m^3, reflection collected = 16020, Unique: 3720 (R_{int} = 0.0278), Final R indices = R_1 = 0.0530, wR_2 = 0.1472, R indices = R_1 = 0.0635, wR_2 = 0.1577, T = 150K with Crystalispro diffractometer with graphite monochromated Mo Kα radiation (λ = 0.7107 Å) using SHELX-97, full-matrix least-square refinement method **(Table-2)**. The molecular solid state structure and numbering systems are indicated in **figure 6**. Molecule presents certain disorder in the terminal allyl group. Thus, there is some ambiguity in the atomic positions of the allyl group. These disorders are expected due to the conformational flexibility of the allyl fragment. The six-membered morpholine ring is positioned planar to the quinazoline ring that exists in chair conformation. Atom system C13–O1–C12 is in regular tetrahedron sp^3 angle of 109.5°. Atom system C14–N6–C11 having some angle strain, deviated by 4.1° from the ideal value (angle strain is calculated as the difference between internal angle and the ideal sp^3 angle of 109.5°). The structure of the compound **12** shown in **figure 6** is more likely on the basis of standard bond distances and angles. The benzimidazole ring is deviated from the planar quinazoline by 19.9°. The bond length of two C–N bonds linking between benzimidazole and quinazoline are differ, with the shorter C16–N3 [1.359 (4) Å] bond having a double-bond character compared with the longer N3–C8 [1.419 (4) Å] on benzimidazole side. It is indicated that the two carbon atoms (C16 and C8) in the molecule occupy anti-positions relative to the mean plane of the ring system. This anti-position of both carbon atoms in each molecule is one of the reason which makes the two rings are non planar. The crystal structure revealed that conformation morpholine is approaching towards the benzimidazole moiety. The bond length of N1–C1 [1.314 (5)] of benzimidazole ring is shorter having double bond character than that longer bond length of C1–N2 [1.369 (5)] indicates the presence of allyl group at N2 position and quinazoline attached at the 5-position of benzimidazole (C8).

Table 2. Summary of crystal data, data collection and structure refinement for compound **12**

A. Crystal data	
Empirical formula	$C_{23}H_{24}N_6O$
Formula weight	400.48

Crystal color, habit	Colourless, Crystals
Crystal dimensions	0.23×0.18×0.13 mm
Crystal system	Monoclinic
Lattice parameters	a = 6.3175 (2) Å
	b = 23.8231 (6) Å
	c = 14.1809 (4) Å
	α = 90.0°
	β = 98.004 (3)°
	γ = 90.0°, V = 2113.47 (10) $Å^3$
Space group	$P2_1/c$
Z value	4
Dcalcd	1.259 Mg/m^3
F (000)	848
μ (Mo Ka)	0.081 mm^{-1}
Mo Ka radiation, λ	0.7107 cm^{-1}
T	150 (2) K
B. Data collection and refinement	
Diffractometer	Crystalispro, Agilent Technology CCD
Structure solution	Direct methods
Radiation	MoKα (λ = 0.7107 A)
	Graphite monochromated
Radiation source	Fine-focus sealed tube
$2\theta_{max}$	32.267°
No. of reflections measured	Total: 16020
	Unique: 3720 (R_{int} = 0.0278)
Absorption corrections	Semi-empirical from equivalents
Max. and min. transmission	0.9895 and 0.9815
Refinement method	Full-matrix least-square on F2
Data/restraints/parameters	3720/29/292
Final R indices [I > 2sigma(I)]	R_1 = 0.0530, wR_2 = 0.1472
R indices (all data)	R_1 = 0.0635, wR_2 = 0.1577
Goodness of fit on F2	1.026
Extinction coefficient	0.011 (3)

Largest diff. peak and hole	0.302 and -0.345 eA^{-3}

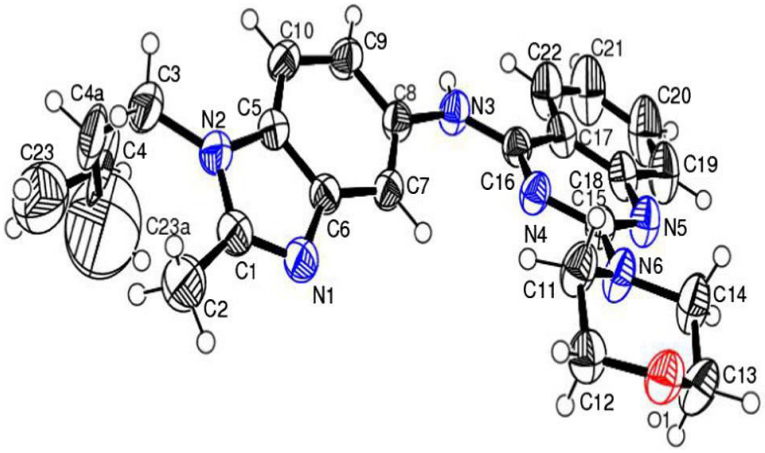

Figure 6. ORTEP diagram of compound **12** (CCDC No. 928250).

2.3.2. Synthesis of quinazoline-benzimidazole hybrids with primary amines

The synthetic methodology to prepare the target compounds **14-24** has been shown in **scheme 4**. Treatment of 2,4-dichloroquinazoline with **4a** and **4b** in isopropyl alcohol (IPA) at room temperature for 12 h gave **7a** (EIMS, m/z: 350.5 (M^++1)) and **7b** (EIMS, m/z: 350.5 (M^++1)) respectively. Compound **7a** (0.57 mmol) was further refluxed with ethanolamine (0.62 mmol) in IPA for 7 h and after work up gave compound **14** (EIMS, m/z: 375 (M^++1)) with 61% yield. ^{1}H NMR spectrum of compound **14** showed the 3H singlet at δ 2.55 of CH_3, 2H quartet at δ 3.45 of N-CH_2, 2H triplet at δ 3.63 of O-CH_2, three 2H doublets at δ 4.82 of allyl-NCH_2, 4.93 and 5.19 of allyl-CH_2, 1H multiplet at δ 6.00 of allyl–CH, 1H singlet due to NH at δ 6.51 (exchangeable with D_2O), 1H triplet at δ 7.16, two 2H multiplet at δ 7.36 and 7.56, two 1H doublets at δ 8.08 and 8.33 of aromatic-H and 1H broad singlet at δ 9.58 of NH (exchangeable with D_2O). ^{13}C NMR spectrum showed signals at δ 13.3 (CH_3), 44.0 (N-CH_2), 44.1 (allyl-NCH_2), 45.4 (O-CH_2), 108.4 (allyl-NCH_2-CH-CH_2), 113.0, 116.6, 118.3 (ArH), 120.9 (allyl-CH_2), 122.7, 131.5, 131.8, 132.4, 133.1, 141.9, 151.8, 158.4 (ArH). IR spectrum showed the peaks at 3285 (NH), 2933, 2854 (CH), 1631, 1573, 1522, 1483, 1400 (C=C), 1329, 1182, 1146, 1077 (CO), 759 (CH) cm^{-1}. On the basis of these spectral data, this compound has been assigned the structure of 2-(4-(3-allyl-2-methyl-3*H*-benzimidazol-5-ylamino)-quinazolin-2-ylamino)-ethanol (**14**). Similarly, compound **7a** was also treated with 1.2 equivalents of 4-aminophenol, *o*-phenylenediamine, 2-aminopyrimidine, 4-aminobenzenethiol, 3-allyl-2-methyl-3*H*-benzimidazol-5-ylamine, 1-allyl-2-methyl-1*H*-benzimidazole-5-ylamine, 4-

fluorophenylamine and 2,4-difluorophenylamine at the same reaction conditions to obtained compounds **15-22** with 60-83% yields.

Compound **7b** (0.57 mmol) was also refluxed with ethanolamine (0.62 mmol) in IPA for 7 h and after column chromatography gave pure white powder of **23 (**EIMS, m/z: 375 (M^++1)) with 65% yield. ^{1}H NMR spectrum of compound **23** showed the 3H singlet at δ 2.57 of CH_3, two 2H triplets at δ 3.66 and 4.02 of N/O-CH_2, 2H doublet at δ 4.82 of allyl-NCH_2, 1H double doublet at δ 5.08 of allyl-CH_2, 1H doublet at δ 5.26 of allyl-CH_2, 1H multiplet at δ 6.02 of allyl-CH, 1H triplet at δ 7.15, three 1H doublets at δ 7.28, 7.39 and 8.26, 2H multiplet at δ 7.56 and 1H singlet at δ 8.11 of aromatic-H, and two 1H broad singlets at δ 8.68 and 10.15 of NH (exchangeable with D_2O). ^{13}C NMR spectrum of this compound showed signals at δ 13.4 (CH_3), 28.9 (N-CH_2), 29.1 (allyl-NCH_2), 45.5 (O-CH_2), 100.9 (allyl-NCH_2-<u>CH</u>-CH_2), 114.5, 114.7, 116.7, 117.6, 118.0 (ArH), 121.4 (allyl-CH_2), 122.4, 125.1, 125.7, 132.1, 133.9, 135.0, 150.2, 151.1, 151.4 (ArH). IR spectrum showed the peaks at 3282 (NH), 2923, 2854 (CH), 1622, 1573, 1520, 1483, 1400 (C=C), 1329, 1186, 1146, 1061, 760 (CH) cm^{-1}. On the basis of these spectral data, this compound has been assigned the structure of 2-[4-(1-allyl-2-methyl-1*H*-benzimidazol-5-ylamino)-quinazolin-2-ylamino]-ethanol **(23).**

Under the same reaction conditions, compound **7b** was treated with 1.2 equiv. of 3-allyl-2-methyl-3*H*-benzimidazol-5-ylamine in IPA for 8 h gave compound **24** (EIMS, m/z: 501 (M^++1)) with 66% yield.

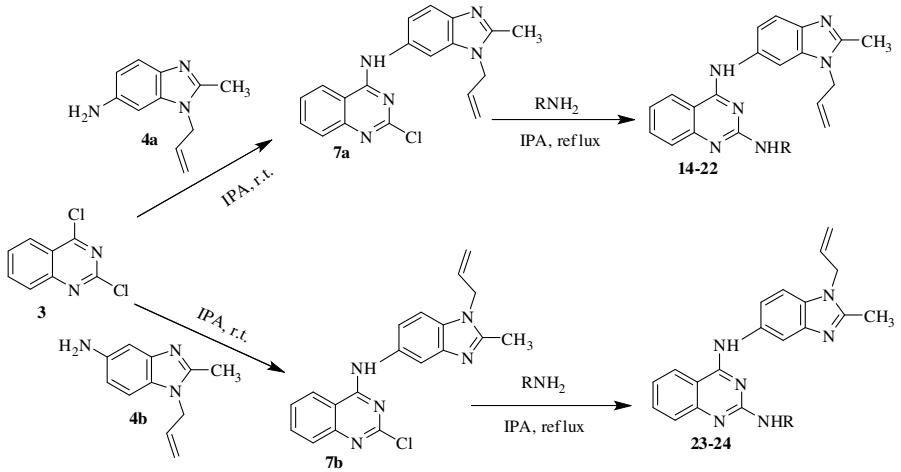

Scheme 4 Synthetic route for the preparation of target compounds (**14-24**)

Table-3 Physicochemical properties of the newly synthesized compounds **7a-b** and **14-24**

Compounds	Starting Material	NHR	% yields	M.pt. (°C)	Molecular formulae
7a	3a	--	92	210-215	$C_{19}H_{16}ClN_5$
7b	3b	--	82	217-220	$C_{19}H_{16}ClN_5$

14	7a	2-ethanolamine	61	190-195	$C_{21}H_{22}N_6O$
15	7a	4-aminophenol	76	260-265	$C_{25}H_{22}N_6O$
16	7a	*o*-phenlenediamine	83	110-115	$C_{25}H_{23}N_7$
17	7a	2-aminopyrimidine	70	170-175	$C_{24}H_{21}N_7$
18	7a	4-aminobenzenethiol	60	200-202(d)	$C_{25}H_{22}N_6S$
19	7a	3-allyl-2-methyl-3*H*-benzimidazol-5-yl amine	70	220-222 (d)	$C_{30}H_{28}N_8$
20	7a	1-allyl-2-methyl-*1H*-benzimidazole-5-ylamine	62	180-183	$C_{30}H_{28}N_8$
21	7a	4-fluorophenylamine	65	200-205 (d)	$C_{25}H_{21}FN_6$
22	7a	2,6-difluorophenylamine	70	215-220(d)	$C_{25}H_{20}F_2N_6$
23	7b	2-ethanolamine	65	100-105	$C_{21}H_{22}N_6O$
24	7b	3-allyl-2-methyl-3*H*-benzimidazol-5-yl-amine	66	200-205 (d)	$C_{30}H_{28}N_8$

2.4. BIOLOGY

2.4.1. *In vitro* evaluation of 60 human cancer cell line studies

2.4.1.1. Quinazoline-benzimidazole hybrids with secondary amines

All the selected compounds submitted to National Cancer Institute (NCI) for *in vitro* anticancer assay, were evaluated for their anticancer activities. Preliminary *in vitro* one dose anticancer assay was performed in full NCI 60 cell panel representing leukemia, melanoma and cancers of lung, colon, brain, breast, ovary, kidney and prostate in accordance with the protocol of the NCI, USA. The compounds were added at a single concentration (10^{-5} M) and the culture was incubated for 48 h. The data reported as mean-graph of the percent growth of the treated cells and presented as percentage growth inhibition (GI%). Seven out of eight synthesized compounds (**7a–b, 8–9, 11–13**) (**Table 4**) were subjected to the National Cancer Institute on the basis of degree of structure variation and computer modelling techniques for disease-oriented human cell lines screening assay for their *in vitro* antitumor activities.[35–37] Preliminary *in vitro* antitumor screening revealed that only compounds **8** and **9** showed significant growth inhibition (more than 60%) for most of the cancer cell lines. On the contrary, the percentage inhibition of compounds **7a–b** and **11–13** did not reach 50%. This showed that the presence of secondary amine (morpholine or pyrrolidine) is essential in place of chloro at 2-position of quinazoline for activity of compounds. Regarding the activity toward individual cell lines; all compounds showed selective potency toward renal cancer cells A498 with GI values of 44.5%, 31.5%, 41.1%, 28.5%, 20.7% and 27.6% of respective compounds **7a, 7b, 8, 9, 12** and **13**. Leukemia cancer cells HL-60 (TB) proved to be selective sensitive to **8** with GI value of 61.9%. Compound **9** showed selectivity toward leukemia cancer cells K-562, MOLT-4, RPMI-8226 and SR with GI values of 98.0%, 50.0%, 45.0%

and 94.2% respectively, colon cancer cells HCC-2998, HCT-116 and HT29 with GI values of 76.6%, 80.3% and 94.3% respectively, melanoma cancer cell LOX IMVI with GI value of 97.5% and breast cancer cell MDA-MB-231/ATCC with GI value of 58.0%. Compound **9** showed higher activity than 5-fluorouracil in leukemia cancer cells (K-562, MOLT-4, RPMI-8226 and SR), colon cancer cells (HCC-2998, HCT-116 and HT-29) and melanoma (LOX IMVI and SK-MEL-5). In addition, compound **11** showed sensitivity to leukemia cancer cell MOLT-4, non-small cell lung cancer cell HOP-92 and colon cancer cell HT29 having GI values of 43.1%, 42.4% and 42.6% respectively. From **table 4**, it is revealed that compound **9** is more active towards numerous cancer cell lines belonging to different tumor subpanels.

Table 4. The percentage growth inhibition (GI%) of the selected compounds over the full panel of tumor cell lines at 10 μM concentration.

Cell Line Type	Cell Line Name	7a	7b	8	9	11	12	13	5-FU
Leukemia	CCRF-CEM	Nt	Nt	Nt	Nt	31.5	Nt	Nt	57.1
	HL-60(TB)	15.9	--	**61.9**	11.5	--	13.5	--	47.9
	K-562	25.2	21.3	35.6	**98.0**	37.8	--	14.9	42.3
	MOLT-4	21.3	--	Nt	**50.0**	**43.1**	--	--	43.1
	RPMI-8226	24.7	22.3	Nt	**45.0**	28.5	13.4	12.2	41.4
	SR	--	--	--	**94.2**	Nt	-	11.0	24.8
Non-Small Cell Lung Cancer	A549/ATCC	18.5	--	11.8	25.4	--	--	10.1	34.2
	EKVX	--	17.2	--	--	Nt	--	--	58.4
	HOP-62	--	--	--	--	11.3	--	--	47.8
	HOP-92	--	--	--	18.6	**42.4**	-	15.5	50.6
	NCI-H226	--	17.8	--	--	13.6	--	22.0	69.5
	NCI-H23	--	--	--	11.3	19.2	--	--	39.0
	NCI-H322M	--	--	--	--	--	--	--	59.5
	NCI-H460	--	--	--	18.7	--	--	--	13.0
	NCI-H522	--	--	--	--	--	--	--	58.0
Colon Cancer	COLO 205	--	--	--	--	23.6	--	Nt	40.2
	HCC-2998	--	--	--	**76.6**	--	--	--	L
	HCT-116	--	--	--	**80.3**	33.0	--	--	17.8
	HCT-15	--	--	--	20.6	10.1	--	--	26.5
	HT29	--	--	34.7	**94.3**	**42.6**	--	--	27.1
	KM12	--	--	11.9	29.9	20.5	--	--	40.7
	SW-620	--	--	--	24.9	--	--	--	50.1
CNS Cancer	SF-268	10.1	--	--	13.1	--	--	--	59.0
	SF-295	15.2	10.3	--	16.3	--	--	--	69.1
	SF-539	--	--	--	--	23.5	--	--	L
	SNB-19	--	--	--	--	--	--	--	65.9
	SNB-75	--	--	12.6	16.3	17.6	--	--	65.9
	U251	--	--	--	--	10.2	--	--	50.3
Melanoma	LOX IMVI	--	--	--	**97.5**	18.0	--	--	30.4
	MALME-3M	--	Nt	--	--	--	Nt	--	58.2
	M14	--	--	--	10.3	--	--	--	Nt
	MDA-MB-435	--	--	--	--	--	--	--	36.6
	SK-MEL-2	--	--	--	--	--	--	--	95.5
	SK-MEL-28	--	--	--	19.8	--	--	--	Nt
	SK-MEL-5	--	--	--	37.6	18.3	--	--	33.7

	UACC-257	--	--	--	--	--	--	--	19.5
	UACC-62	--	10.2	--	--	--	--	--	39.7
Ovarian Cancer	IGROV1	--	--	--	--	--	--	--	51.2
	OVCAR-3	--	--	--	--	--	--	--	47.4
	OVCAR-4	--	--	--	--	20.7	--	--	59.4
	OVCAR-5	--	--	--	--	16.5	-	-	44.3
	OVCAR-8	--	--	20.1	15.9	23.4	--	--	Nt
	NCI/ADR-RES	--	10.5	23.6	16.7	--	--	--	47.6
	SK-OV-3	--	--	--	--	--	--	--	77.5
Renal Cancer	786-0	12.2	--	--	24.0	--	--	11.1	48.7
	A498	**44.5**	31.5	**41.2**	28.5	--	20.7	27.6	L
	ACHN	--	--	--	--	--	--	--	39.3
	CAKI-1	12.8	16.9	11.5	15.0	14.4	--	10.2	39.4
	RXF 393	12.5	--	--	**47.6**	--	--	--	34.3
	SN12C	--	--	--	--	--	--	--	54.0
	TK-10	--	--	--	--	--	--	--	66.9
	UO-31	--	10.3	14.7	31.9	34.2	--	10.1	41.3
Prostate Cancer	PC-3	18.0	19.5	11.4	--	25.9	11.9	18.2	58.2
	DU-145	--	--	--	26.2	--	--	--	35.5
Breast Cancer	MCF7	--	--	--	38.1	14.4	--	--	11.5
	MDA-MB-231/ATCC	10.1	14.5	--	**58.0**	22.8	--	--	78.1
	HS 578T	--	--	--	13.1	23.3	--	--	L
	BT-549	--	--	--	13.1	20.7	--	--	37.8
	T-47D	18.5	21.3	11.2	--	20.6	--	22.6	56.7
	MDA-MB-468	16.3	19.1	--	--	--	--	13.3	Nt

--, GI < 10%; nt, not tested.

2.4.1.2. Quinazoline-benzimidazole hybrids with primary amines

By using primary amines, the obtained results of the tested quinazoline-benzimidazole hybrids **14, 17-21** and **23-24 (Table 5)** showed distinctive potential pattern of selectivity, as well as broad-spectrum of antitumor activity. Compounds **19** and **20** were found to be broad spectrum against all nine subpanels of cancer cell lines at primary single high dose with mean growth percent of -54.60 and -77.59 respectively. On the other hand, compound **21** also showed remarkably lowest cell growth promotion against leukemia cancer MOLT-4 and non-small cell lung HOP-92 cancer cell line with cell growth promotion of -5.55 and -0.39 respectively. Close examination of the data presented in **table 5** indicated that compounds **19** and **20** were the most potent and **21** possess moderate antitumor activity; while compounds **14, 17-18** and **23-24** were the least active anti-tumors in the present investigation. Amongst the selected eight compounds, **19-21** were further screened for five dose concentration level as these have shown prominent cell growth inhibition at 10 μM concentration against variety of cell lines. Compound under investigation **19** exhibited remarkable anticancer activity against renal cancer A-498 cell line with GI_{50} value of 0.44 μM. Compound **21** showed anticancer activity against non-small cell lung cancer HOP-92 cell line with GI_{50} value of 0.58 μM. Obtained data revealed an obvious broad spectrum sensitivity profile of compound

20 toward all nine subpanels of cancer cell lines with GI_{50} values ranging from 2.27 µM to 0.78 µM, TGI values ranging from 5.16 µM to 0.90 µM. Compound **20** also showed highest potency against melanoma cancer cell line LOX IMVI and ovarian cancer cell line OVCAR-3 with LC_{50} values of 6.40 µM and 0.70 µM respectively. Anticancer activities of quinazoline-benzimidazole hybrids **(19-21)** were also compared with reported quinazoline and benzimidazole derivatives. Compound **19** was almost ten and eleven fold more active than respective quinazoline [(2-(2-thieno)-4-[4-sulfonamido benzylamino]-6-iodoquinazoline)][8] and benzimidazole [(6-amino-5-(5,6-dimethyl-1*H*-benzimidazol-2-yl)-4-(4-methoxy-phenyl)pyridine-3-carbonitrile)] analogue,[38] with full panel mean graph mid-point (MG MID); GI_{50}, TGI and LC_{50} values of 1.64 µM, 3.28 µM and 5.50 µM respectively.

Compound **20** showed twenty and twenty two fold more activity than respective quinazoline and benzimidazole derivative, with MG MID GI_{50}, TGI and LC_{50} values of 0.81 µM, 2.08 µM and 4.47 µM respectively while compound **21** showed four fold more active than quinazoline and benzimidazole analogue, with MG MID GI_{50}, TGI and LC_{50} values of 4.52 µM, 15.9 µM and 57.1 µM respectively **(Table 6, Fig. 7-8)**. Compounds **19**, **20** and **21** have also been showed thirteen fold, twenty fold and five fold more active than positive control **5-FU**.

Table 5. Percent growth promotion of *in-vitro* subpanel tumor cell lines at 10 µM concentration of compounds **14, 17-21** and **23-24**

Cell Line Type	Cell Line Name	14	17	18	19	20	21	23	24
Leukemia	CCRF-CEM	88.49	84.81	**65.48**	-20.80	-11.29	**22.48**	81.94	94.81
	HL-60(TB)	114.43	93.99	98.79	-63.18	-52.00	**51.60**	93.77	84.02
	K-562	92.21	83.00	92.53	-43.46	-27.00	**20.95**	**64.06**	101.89
	MOLT-4	96.68	97.19	88.20	-45.48	-26.83	-5.55	**56.70**	101.27
	RPMI-8226	95.74	**70.66**	**59.79**	-43.32	-23.97	NT	**63.44**	98.82
	SR	104.21	121.00	90.84	-57.22	-44.19	**22.43**	**68.83**	106.26
Non-Small Cell Lung Cancer	A549/ATCC	99.92	90.29	89.82	-83.06	-67.14	**52.12**	92.35	96.33
	EKVX	95.48	87.22	96.51	**2.58**	Nt	Nt	Nt	97.09
	HOP-62	97.62	84.79	104.07	-61.45	-99.54	75.91	83.32	100.65
	HOP-92	**73.86**	**70.50**	**61.09**	**43.21**	-79.03	-0.39	**57.86**	79.82
	NCI-H226	106.67	92.18	109.12	**67.36**	-47.06	85.42	78.80	99.77
	NCI-H23	92.74	82.84	100.72	**32.77**	-69.16	**56.03**	81.91	94.21
	NCI-H322M	99.96	100.26	102.47	-13.41	-92.17	85.42	91.31	108.79
	NCI-H460	102.84	97.83	103.80	-69.52	-84.21	**63.40**	95.98	117.38
	NCI-H522	100.53	98.09	89.53	-90.73	-94.80	**57.94**	88.09	99.13
Colon Cancer	COLO 205	105.53	101.72	121.32	-92.32	-100.0	**43.73**	**41.89**	107.88
	HCC-2998	109.68	106.44	103.01	-52.67	-96.13	80.62	89.03	103.53

	HCT-116	94.71	94.21	93.18	-97.80	-96.48	**26.89**	**64.04**	98.93
	HCT-15	112.68	110.79	96.49	-51.70	-76.21	**34.46**	105.16	106.86
	HT29	103.41	103.96	97.29	-96.68	-69.45	**18.71**	**64.48**	102.87
	KM12	102.16	105.94	96.78	-84.76	-93.21	**36.60**	**73.07**	108.75
	SW-620	97.73	100.33	107.97	-80.52	-76.19	**46.08**	**68.25**	105.83
CNS Cancer	SF-268	92.51	94.84	108.58	-32.41	-69.78	**66.04**	90.88	112.67
	SF-295	145.62	86.91	77.11	-67.46	-86.57	**31.44**	90.61	NT
	SF-539	103.87	102.82	108.24	-93.76	-95.76	72.97	94.81	98.59
	SNB-19	93.93	97.64	93.18	**30.64**	-66.14	96.47	90.22	99.97
	SNB-75	92.55	78.75	98.18	-95.23	-96.69	**54.57**	76.37	90.76
	U251	98.46	89.76	91.35	-94.19	-90.67	**59.59**	90.88	94.42
Melanoma	LOX IMVI	88.54	85.28	96.99	-88.62	-83.35	**45.27**	85.59	93.29
	MALME-3M	110.78	99.01	123.20	-78.94	-68.26	74.46	98.58	94.54
	M14	110.79	114.51	109.11	-88.35	-88.00	**45.20**	93.30	109.44
	MDA-MB-435	101.98	107.08	96.87	-78.02	-75.98	**57.11**	92.10	107.53
	SK-MEL-2	126.99	100.21	109.28	-83.85	-84.13	**58.11**	101.95	121.40
	SK-MEL-28	99.29	110.62	103.56	-95.95	-88.01	**72.01**	100.58	105.50
	SK-MEL-5	96.48	92.94	84.07	-94.16	-95.20	**33.34**	**75.43**	99.72
	UACC-257	100.00	101.19	110.36	-87.63	-79.76	92.58	97.73	101.62
	UACC-62	92.68	92.59	83.12	-86.95	-83.32	**63.17**	85.53	95.76
Ovarian Cancer	IGROV1	90.09	84.09	101.95	-47.54	-93.77	**51.15**	95.28	102.37
	OVCAR-3	98.33	99.27	106.44	-95.41	-99.79	**51.23**	94.84	108.38
	OVCAR-4	88.42	85.61	88.50	-93.30	-100.00	**48.25**	**65.19**	99.55
	OVCAR-5	106.82	114.41	118.45	**25.12**	-92.54	81.30	92.22	106.86
	OVCAR-8	98.95	94.29	**63.72**	-48.65	-40.90	**33.38**	**73.63**	98.87
	NCI/ADR-RES	105.57	102.80	97.84	**53.47**	-23.72	**38.40**	97.71	101.49
	SK-OV-3	109.04	104.20	123.73	-63.69	-95.70	98.61	102.91	104.03
Renal Cancer	786-0	95.65	106.28	102.39	-93.78	-70.60	76.74	89.12	113.02
	A498	78.32	76.76	**48.46**	99.49	-99.99	**59.90**	**55.39**	124.51
	ACHN	103.61	102.65	100.60	-80.03	-97.45	**67.55**	90.48	104.27
	CAKI-1	99.00	75.59	90.54	-24.14	-86.37	**58.20**	93.02	101.08
	RXF 393	116.45	114.17	143.88	-80.72	-97.36	**66.55**	97.46	124.35
	SN12C	87.58	97.64	93.93	-74.87	-69.64	**66.20**	84.67	96.49
	TK-10	124.13	117.98	107.16	-88.52	-97.20	82.29	118.34	130.13
	UO-31	92.56	82.11	89.50	-91.43	-94.43	**37.40**	**72.37**	89.29
Prostate Cancer	PC-3	93.81	`89.21	81.12	-47.79	-91.73	**42.14**	**69.16**	95.82
	DU-145	107.26	112.27	114.11	-67.62	-95.96	**74.08**	98.85	115.29
Breast Cancer	MCF7	93.67	82.38	93.19	-87.94	-89.35	**26.10**	**72.21**	92.43
	MDA-MB-231/ATCC	84.53	84.38	80.45	-78.76	-85.80	**73.75**	**72.87**	89.97
	HS 578T	91.48	87.66	98.12	-41.41	-48.06	**54.42**	77.45	100.04
	BT-549	96.46	82.76	87.89	**72.08**	-83.98	**59.15**	92.47	105.73
	T-47D	95.75	**55.84**	**71.73**	-91.01	-60.35	**35.01**	**69.01**	96.04
	MDA-MB-468	119.24	78.29	106.36	-92.76	-84.96	**49.30**	**53.51**	118.42

nt, not tested; 30-40% growth inhibition, 40-50% growth inhibition, 50-70% growth inhibition, 70-90% growth inhibition, 90-100% growth inhibition, highly potent compounds.

Table 6. Compounds **19-21**, quinazoline and benzimidazole analogue median growth inhibitory (GI_{50}, μM), total growth inhibitory (TGI, μM) and median lethal concentrations (LC_{50}, μM) of *in vitro* subpanel tumor cell lines

Compounds	Activity	I	II	III	IV	V	VI	VII	VIII	IX	MG MID[a]
19	**GI_{50}**	1.74	1.73	1.61	1.68	1.71	1.75	1.54	1.61	1.40	1.64
	TGI	3.85	3.27	3.13	3.28	3.23	3.55	3.06	3.09	3.07	3.28
	LC_{50}	B	6.15	5.56	5.71	5.38	5.59	5.48	5.79	5.12	5.50
20	**GI_{50}**	0.47	1.03	0.34	1.10	1.29	1.03	0.98	0.31	0.71	0.81
	TGI	2.44	2.53	0.81	2.72	2.86	2.44	2.31	0.95	1.69	2.08
	LC_{50}	[b]	6.14	4.61	6.04	5.43	3.38	4.90	3.62	1.63	4.47
21	**GI_{50}**	2.83	3.13	3.68	6.79	5.06	5.47	4.50	5.88	3.33	4.52
	TGI	10.6	14.0	12.2	19.3	16.0	18.9	17.7	18.8	15.6	15.9
	LC_{50}	[b]	62.7	49.7	50.4	47.0	68.7	52.8	52.2	73.1	57.1
Quinazoline	**GI_{50}**	23.9	14.7	16.7	18.2	16.0	15.7	13.6	17.1	12.3	16.9
Analogue	**TGI**	72.3	37.0	37.3	42.4	30.5	42.6	36.1	41.8	32.1	40.5
	LC_{50}	[b]	[b]	[b]	[b]	[b]	[b]	[b]	[b]	[b]	[b]
Benzimidazole	**GI_{50}**	17.4	62.0	6.32	6.80	17.5	21.8	11.2	7.90	12.1	18.1
Analogue	**TGI**	B	38.2	b	34.8	[b]	[b]	36.8	23.8	[b]	33.4
	LC_{50}	[b]	[b]	[b]	51.5	[b]	[b]	[b]	61.8	[b]	56.7
5-FU	**GI_{50}**	15.1	[b]	8.4	72.1	70.6	61.4	45.6	22.7	76.4	22.6
	TGI	[b]	[b]	[b]	[b]	[b]	[b]	[b]	[b]	[b]	[b]
	LC_{50}	[b]	[b]	[b]	[b]	[b]	[b]	[b]	[b]	[b]	[b]

I, leukemia cancer; II, non-small cell lung cancer; III, colon cancer; IV, CNS cancer; V, melanoma cancer; VI, ovarian cancer; VII, renal cancer; VIII, prostate cancer; IX, breast cancer.

[a] Full panel mean-graph midpoint (μM).

[b] Compounds showed values >100 μM.

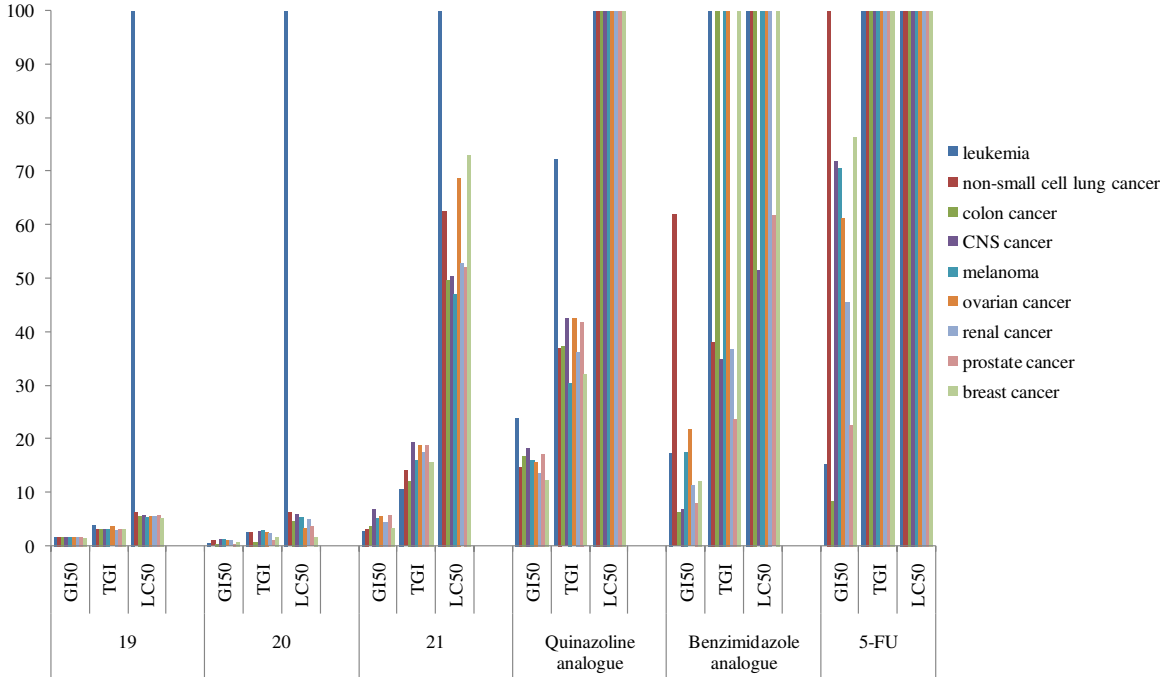

Figure 7. Compounds **19-21,** quinazoline, benzimidazole analogue median growth inhibitory (GI_{50}, μM), total growth inhibitory (TGI, μM) and median lethal concentrations (LC_{50}, μM) of *in vitro* subpanel tumor cell lines.

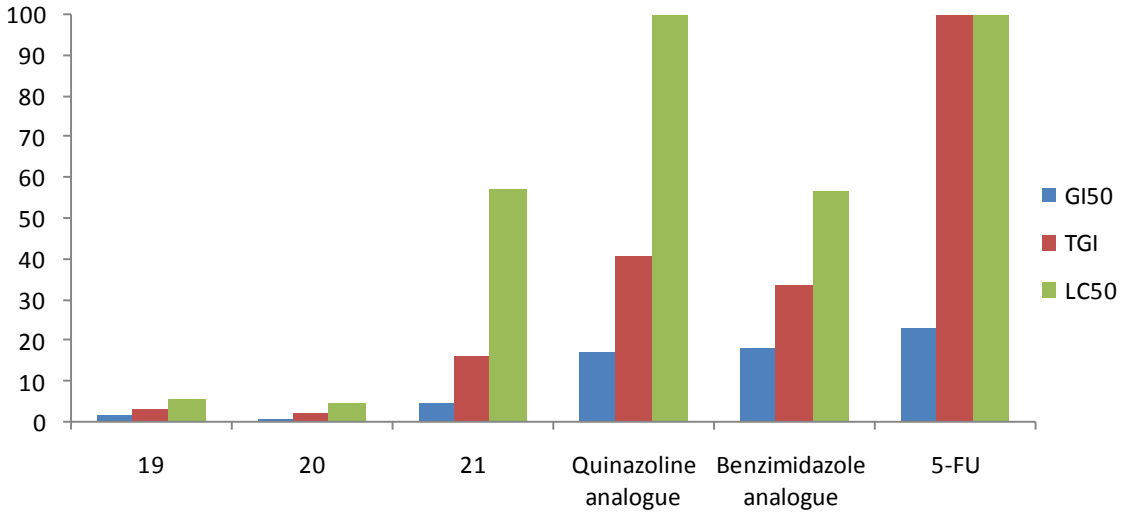

Figure 8. Comparison of full panel mean-graph midpoint (μM) of compounds **19-21** with quinazoline, benzimidazole analogue and 5-FU.

2.4.2. *In vitro* evaluation of Aurora kinase inhibitors with secondary and primary amine substituted quinazolines

To confirm the interaction of compounds with Aurora-A and probably the inhibition in enzymatic activity of Aurora-A in presence of quinazoline derivatives, enzyme immunoassay was performed using Aurora-A kinase assay screening kit. We began by exploring substitution at the C2–position of quinazoline in an attempt to improve enzyme inhibitory activity. In the series, compound **7a** with chloro substitution at C2 position of quinazoline showed moderate inhibitory activity with IC_{50} value of 0.45 μM. Substitution with primary and secondary amines has improved Aurora A inhibition except compounds **10** and **16** where they showed decrease in activity with IC_{50} values of 6.00 and 7.50 μM respectively. Substitution with 3-allyl-2-methyl-3*H*-benzimidazol-5-ylamine and 2,6-difluoroaniline resulted compounds **19** and **22** that showed increase the Aurora-A inhibitory activity with IC_{50} values of 0.1 and 0.308 μM respectively while substitution with 1-allyl-2-methyl-1*H*-benzimidazole-5-ylamine and 4-fluoroaniline resulted compounds **20** and **21** that further increased the Aurora-A inhibitory activity with IC_{50} values of 0.043 and 0.095 μM. Substitution with 4-aminophenol, 2-aminopyrimidine and 3-allyl-2-methyl-3*H*-benzimidazol-5-ylamine resulted compounds **15, 17** and **24** that also showed comparable inhibitory activity. But the substitution with 4-methylpiperazine (**11**) at C-2 position of quinazoline showed tremendous inhibitory activity towards Aurora-A with IC_{50} value of 0.035 μM (**Table 7**). Therefore, it seems that the compound **11** under present investigation probably target Aurora-

A for exhibiting best inhibitory activity. Ligand efficiency (LE) has also been determined for these compounds that are measurement of the binding energy per atom of a ligand to its binding partner, such as a receptor or enzyme. LE is a particularly important parameter in fragment drug design as it gives priorities to small molecules with relatively lower potency rather than larger, higher potency molecules. The LE also indicated that the higher efficiency of compounds **11** has comparable binding tendency to Aurora A kinase with ligand efficiency of 0.34**.**

Table 7. Aurora A kinase inhibitory activities of quinazoline derivatives

Compounds	IC_{50} (µM)	Ligand efficiency[a]
7a	0.450	0.35
9	0.532	0.31
10	6.000	0.24
11	**0.035**	**0.34**
15	0.080	0.31
16	7.500	0.22
17	0.080	0.32
19	0.100	0.25
20	0.043	0.27
21	0.095	0.30
22	0.308	0.39
24	0.083	0.26

[a] Calculated using the formula: LE = [$-1.4\times \log_{10}(IC_{50}\ (M))$]/(number of heavy atoms).

2.5. PHYSICO CHEMICAL PARAMETERS

Determination of log P (lipophilicity) value of drug candidates is an everyday routine in drug research. We have observed the compliance of compounds with secondary amines at C2 position of quinazoline by determining the experimental lipophilicity via 'Shake Flask' method.[39] Within the series of two regioisomeric precursors, **7a** showed higher log P value than **7b**. Introduction of secondary amines at 2-position of quinazoline moiety resulted in increase of log P value (lipophilicity). From **table 8**, it is clear that lipophilicity is a crucial factor for the activity amongst the synthesized compounds, as compound **9** (in the series of secondary amines) has higher log P value which corresponds to higher antitumor activity than

5-fluorouracil in leukemia cancer cells (K-562, MOLT-4, RPMI-8226 and SR), colon cancer cells (HCC-2998, HCT-116 and HT-29) and melanoma cancer cells (LOX IMVI and SK-MEL-5).

Table 8. Experimental determined lipophilicity

Compounds	P	Experimental log P
7a	125.9	2.10
7b	14.72	1.17
8	648.45	2.81
9	**797.24**	**2.90**
10	524.8	2.72
11	10.82	1.03
12	309.35	2.49
13	324.50	2.51

P—partition coefficient; log P—logarithm of the partition coefficient.

2.6. STRUCTURE-ACTIVITY RELATIONSHIPS

Structure-activity relationship, based on the number of cell lines proved sensitivity toward each of the synthesized individual compound revealed that the nature of the substituent at C2- and C4-positions (primary and secondary amines at C2 and benzimidazole at C4) of quinazoline effects biological functions. There is much difference in antitumor activity by orientations of benzimidazole present at C4-position which played a key role in the efficiency of the compound. On the basis of these activities, it has been proved that (3-allyl-2-methyl-3*H*-benzimidazol-5-yl)-(2-amino-quinazolin-4-yl)-amine **(8–9, 11, 14, 17-21)** are more active antitumor agents than their regioisomeric analogue (1-allyl-2-methyl-1*H*-benzimidazol-5-yl)-(2-aminoquinazolin-4-yl)-amine **(12–13, 23-24)**. Amongst the series of secondary amine substitution at 2-position of quinazoline, substitution of chloro **(7a)** with morpholin-4-yl **(8)** and 4-methylpiperzin-1-yl **(11)** did not improve their activity much. But substitution of chloro **(7a)** with pyrrolidin-1-yl **(9)** proved the remarkably activity as antitumor agents. On the other hand, compound **7b** showed activity in some of the tumor cell lines but substitution at 2-position of quinazoline with morpholin-4-yl **(12)** and pyrrolidin-1-yl **(13)** decreased its potency. Thus, position of allyl group is a crucial factor for the activity as allyl group of benzimidazole approached towards the secondary amine at 2-position of quinazoline **(9)** showed higher activity than on the opposite side **(13)**. Similarly, in the series of primary

amines, compound **21** with 4-fluoroaniline at 2-position of quinazoline was proved to be active member with antitumor activity against most of the cell lines. Furthermore, replacement of the 4-fluoroaniline with 3-allyl-2-methyl-3*H*-benzimidazol-5-ylamine **(19)** and 1-allyl-2-methyl-1*H*-benzimidazol-5-ylamine **(20)** resulted in a higher growth inhibitory effect. These results revealed the crucial role of these benzimidazoles at C2-position of quinazoline for their antitumor activity. In general, it is observed that the heteroaryl rings and electron rich aryl groups at C2-position of quinazoline showed better antitumor activity than the ones with an aliphatic chain.[10,38] The presence of 2-aminopyrimidine **(17)** and 4-aminobenzenethiol **(18)** at C2-position of quinazoline decreased the antitumor activity while introduction of aliphatic chain **(14** and **23)** exhibited a dramatic loss of activity against almost all screened cell lines. Amongst the most active compounds **19-21**, compound **20** showed almost two fold and five fold higher activities than compounds **19** and **21** respectively. Compound **20** proved to be higher antitumor activity to the colon and prostate cancer cell lines than other cell lines.

2.7. QUANTITATIVE STRUCTURE-ACTIVITY RELATIONSHIPS

Quantitative structure-activity relationship (QSAR) studies could provide correlations between toxicological properties and physico-chemical descriptors of compounds. Inhibitory concentrations (IC_{50}) of quinazoline-benzimidazole hybrid compounds were first calculated by using Aurora-A kinase assay kit. The geometries of these compounds have been further refined by means of semi empirical method PM3 (Parametric Method-3) and taken as theoretical descriptors being incorporated into QSARs by using QSARINS Software.[40] Quantitative structure-activity relationship describes how a given biological activity can vary as a function of molecular descriptors derived from the chemical structure of a set of molecules. Thus, a model containing those calculated descriptors can be used to predict responses of new compounds.[41,42] The structural descriptors employed in this work, such as log P, molar refractivity, ionization potential and heat of formation, are all obtained directly from the Scigress project leader data.[43]

In the present work, the QSAR equations were obtained by forward stepwise multiple linear regression technique. To determine the optimum number of components for the correlation models, the leave-one-out (LOO) cross-validation technique has been applied to validate the stability and predictive ability of constructed models. Based on the residuals, it is possible to calculate the cross validation coefficient Q^2, defines the goodness of prediction

which can assess external predictive ability of the model. The non-cross-validated conventional correlation coefficient (R^2) which can assess internal predictive ability of the model, used to characterize the fitness of the QSAR models. The root mean square error of cross-validated ($RMSE_{cv}$)were used to measure the robustness and predictive power. The results obtained in order to work out QSAR model for using a training set of 10 compounds (quinazoline-benzimidazoles) predicting log (IC_{50}) corresponds to different descriptors. The stepwise multiple linear regression analysis was performed for the training set. We have used these descriptor(s) for calculating Q^2, R^2, $RMSE_{cv}$, $RMSE_{tr}$ and F by using one, two, three and four descriptor(s) and optimal equations 1, 2, 3 and 4 were obtained as follows:

As shown previously in physicochemical parameters, lipophilicity (log P) seems to be an additional and independent predictive parameter for activity.[44] Thus, correlation of IC_{50} values of quinazoline-benzimidazole hybrids with log P has been expressed in equation 1.

$\log (IC_{50}) = 0.7365 - 0.1327 \log P$

$n = 10 \quad Q^2_{LOO} = -0.2948, \quad R^2 = 0.2916,$ .....Eq.(1)

$RMSE_{cv} = 0.198, RMSE_{tr} = 0.1464, F = 3.293$

Molar refractivity (MR) is an additive constitutive property of a compound and is connected with the molar volume. It is generally assumed that a positive coefficient with an MR term in a correlation equation suggests a binding action via dispersion forces. A negative coefficient with MR has been assumed to reflect steric hindrance. It has been found that MR and log P are highly correlated in a homologous series. But, if the series is designed to include different types of substituents, the MR and log P are not correlated and can give useful information. By introducing this additional parameter into a multiple linear regression analysis, we obtained an improved equation with good predictive power (eq 2):

$\log (IC_{50}) = 1.0697 - 0.0548 \log P - 0.0051$ molar refractivity

$n = 10 \quad Q^2_{LOO} = -0.3427, R^2 = 0.4463,$ .....Eq.(2)

$RMSE_{cv} = 0.2016, RMSE_{tr} = 0.1295, F = 2.8211$

The ionization potential of an element is a measure of its ability to enter into chemical reactions requiring ion formation or donation of electrons and is related to the nature of the chemical bonding in the compounds formed by elements. Addition of ionization potential into multiple linear regression analysis resulted in improvement of equation with good predictive power (eq 3):

$\log (IC_{50}) = 0.6137 - 0.0085 \log P + 0.0487$ ionization potential $- 0.0061$ molar refractivity

$n = 10 \quad Q^2_{LOO} = -3.9095, \quad R^2 = 0.542,$ .....Eq.(3)

$RMSE_{cv} = 0.3855$, $RMSE_{tr} = 0.1178$, $F = 2.3664$

Heat of formation is also an important parameter for determining the activity of compounds. So on using this parameters into a multiple linear regression analysis, we obtained much improved in the correlation coefficient (eq. 4):

$\log (IC_{50}) = 253.84 + 5.3960 \log P + 0.0414$ heat of formation $+ 30.1928$ ionization potential $- 0.1930$ molar refractivity

$n = 10 \quad Q^2_{LOO} = 0.6743, R^2 = 0.8457,$ .....Eq.(4)

$RMSE_{cv} = 1.965, RMSE_{tr} = 1.3527, F = 6.8492$ Here, n - number of data points, R^2 - correlation coefficient, Q^2 - crossvalidated, obtained by leave one out method and F - Fischer statistics.

By using single-descriptor model (lipophilicity) in equation 1, Q^2 and R^2 values come out to be -0.2948 and 0.2916 respectively. It is indicated that some other factors may also contributed for the activity of the compounds. Thus, by the addition of molar refractivity as another descriptor, the value of R^2 has been improved with 0.4463 as shown in equation 2. With the addition of ionization potential as another descriptor to molar refractivity and lipophilicity, R^2 have further been improved with increase in value of 0.542 (equation 3). It should be noted that addition of four descriptors most often improves, as a consequence of statistical effect, the robustness of the model. As it can be observed from equation 4, the cross-validated $Q^2 = 0.6743$, non-cross-validated $R^2 = 0.8457$ and degree of statistical confidence for test $F = 6.8492$ is usually considered significant. In general, a QSAR model is acceptable when it has an R^2 value greater than 0.6 and exhibits a good internal predictive power of the developed model. Equation 4 gives high value of $R^2 = 0.8457$, added to its usefulness as a predictive tool. **Figure 9** confirmed the best linear character of the equation 4 and its good fitting as compared to another figures.

A. Scatter plot by using one descriptor

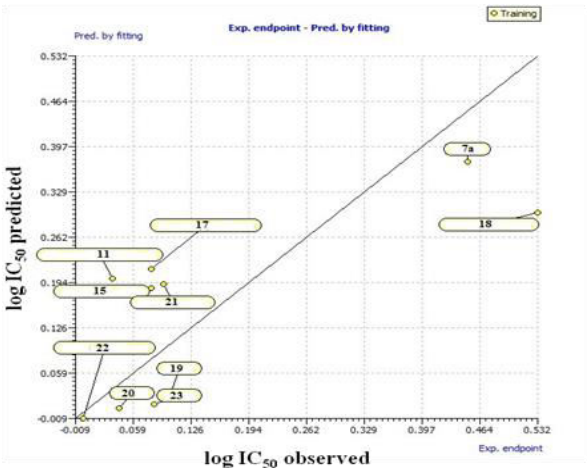

B. Scatter plot by using two descriptors

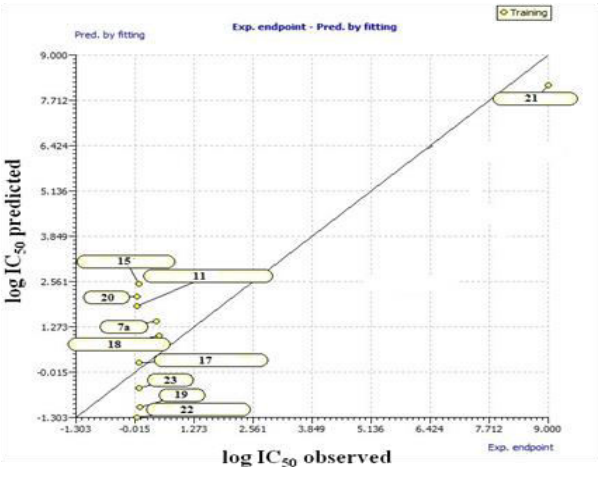

C. Scatter plot by using three descriptors **D. Scatter plot by using four descriptors**

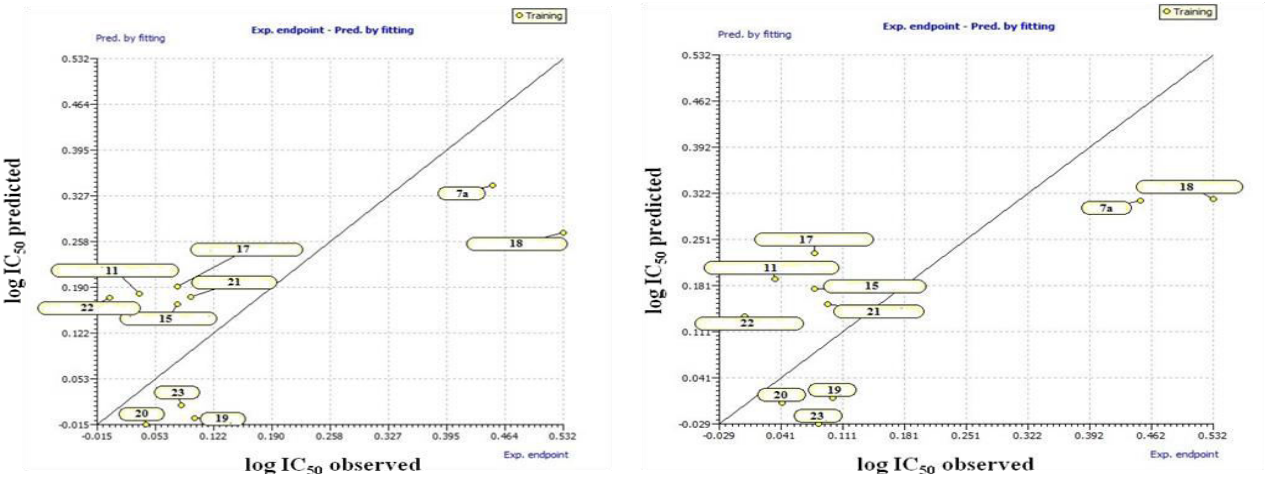

Figure 9. Scatter plots by using one, two, three and four descriptors

2.8. MOLCULAR MODELLING

2.8.1. Quinazoline-benzimidazole hybrids with secondary amines

Docking is frequently used to predict the binding orientation of small molecule drug candidate to their protein targets in order to predict the affinity and activity of the molecule. Hence, docking plays an important role in the rational design of drugs. We have performed docking experiments of these compounds with ribonucleotide reductase (RNR), topoisomerase I (Topo I) and topoisomerase II (Topo II) that possesses potent chemotherapeutic efficacy against leukemia.[45] We have carried out docking[46] of most active compound **9** in the active site of ribonucleotide reductase (pdb ID 4R1R), topoisomerase I (pdb ID 1A36) and topoisomerase II (pdb ID 1BJT). Ribonucleotide Reductase (RNR) is an enzyme responsible for the reduction of ribonucleotides to their corresponding deoxyribonucleotides (DNA), which is a building block for DNA replication and repair mechanisms. Topo I and Topo II, which are enzymes that control the changes in DNA structure by catalyzing the breaking and rejoining of the phosphodiester backbone of DNA strands during the normal cell cycle. Docking of compound **9** in the active site of RNR showed H-bond interactions between N atom of quinazoline moiety with F1023 (d = 2.73 Å) amino acid residue of active site, N atom of pyrrolidine moiety with F1023 and T1025 (d = 2.66 Å and d = 2.99 Å) amino acid residue, NH group with Q294 (d = 1.88 Å) amino acid

residue and N atom of benzimidazole moiety with G296 (d = 1.85 Å) amino acid residue (**Figure 10a**).

Similarly, compound **9** was also docked with active site of topoisomerase I and II (another enzyme involved in the propagation of cancer, synthesis of raw material for replication of DNA). Docking of compound **9** in the active site of Topo I showed H-bond interactions between N atom of quinazoline moiety with Q697 (d = 2.22 Å and d = 0.76 Å) amino acid residue, N atom of pyrrolidine moiety with Q697 (d = 1.74 Å) amino acid residue, NH group with Q696 and L694 (d = 2.91 Å and d = 1.66 Å) amino acid residue and N atom of benzimidazole moiety with R693 (d = 2.59 Å) amino acid residue (**Figure 10b**).

Docking of compound **9** in the active site of Topo II showed H-bond interactions between N atom of quinazoline moiety with active site of P701 (d = 2.38 Å) amino acid residue, N atom of pyrrolidine moiety with Y734 (d = 2.11 Å) amino acid residue, NH group with G702 (d = 0.88 Å) amino acid residue (**Figure 10c**). Here, also this compound interacted with the active site of amino acids through number of H-bonds. Therefore, docking of compound **9** in the active site of these enzymes indicated the probable mode of action of this compound for anticancer activities.

(a) **(b)**

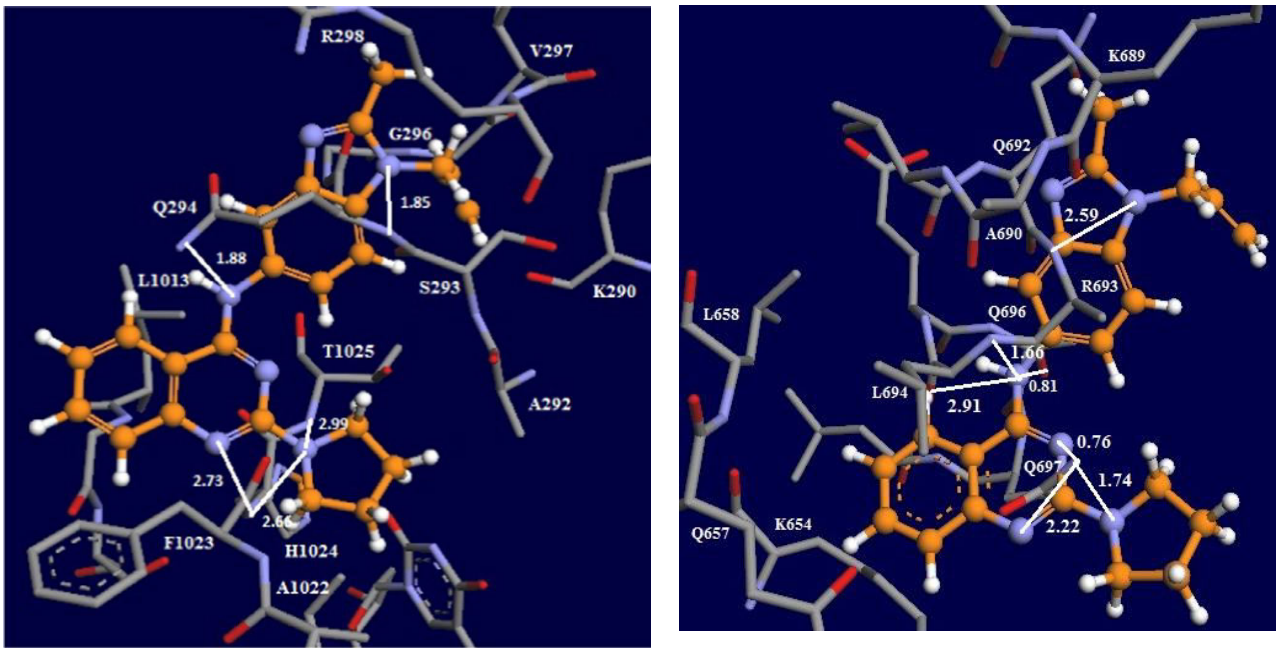

(c)

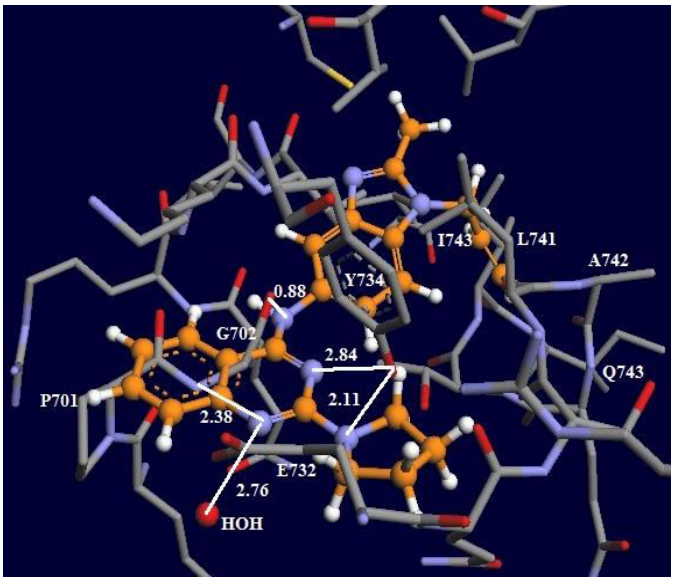

Figure 10. Compound **9** docked in the active site ofRNR (**10a**), Topo I (**10b**) and Topo II (**10c**), Hs' are omitted for clarity. Carbon atoms of compound **9** are given different colour.

2.8.2. Quinazoline-benzimidazole hybrids with primary amines

Molecular modeling studies were also carried out in primary amine series for most active compounds **19, 20** and **21** to gain insight into the probable nature of their respective binding interactions with ribonucleoside reductase (pdb ID 4R1R), topoisomerase I (pdb ID 1A36) and topoisomerase II (pdb ID 1BJT). One of the phenyl ring of benzimidazole (C4 position of quinazoline) of compound **19** showed π- π interaction with Y247 amino acid residue and secondbenzimidazole (C2 position of quinazoline) was tilted towards Y498 active site residue **(Figure 11a).** The allyl group of one benzimidazole (C2 position of quinazoline) was oriented towards S244 and R251 amino acid residues in the active site of 4R1R. Allyl group of another benzimidazole was bent towards Y498 and L504. The amino nitrogen atom showed hydrogen bonding with NH group of Y498 (d = 2.84 Å) and carbonyl oxygen group of N225 (d = 2.55 Å) amino acid residues. Quinazoline nitrogen atom showed hydrogen bond with hydroxyl oxygen group of residue Y247 (d = 2.81 Å). Another linker of quinazoline and benzimidazole i.e. NH group showed hydrogen bond with Q250 (d = 2.65 Å) amino acid residue. Moreover, the nitrogen atom of five membered ring of one benzimidazole (C4 position of quinazoline) showed hydrogen bonding interaction with NH of V226 (d = 1.91 Å) and nitrogen atom of five membered ring of another benzimidazole (C4 position of quinazoline) also showed hydrogen bonding with A503 (d = 2.71 Å) amino acid residue. The quinazoline ring of **19** has moved into the vicinity of Q221 amino acid residue.

A similar molecular docking simulation for compound **20** within 4R1R active site showed that compound **20** assume a position in a region similar to that described previously for compound **19**. However, the allyl group of one benzimidazole was oriented towards P1943 and L1942 amino acid residues and allyl group of another benzimidazole bent toward Q1933 and F1803 amino acid residues. Linker (NH) of quinazoline and benzimidazole formed hydrogen bonding with acid group of E1727 (d = 1.96 Å) and amino group of R1758

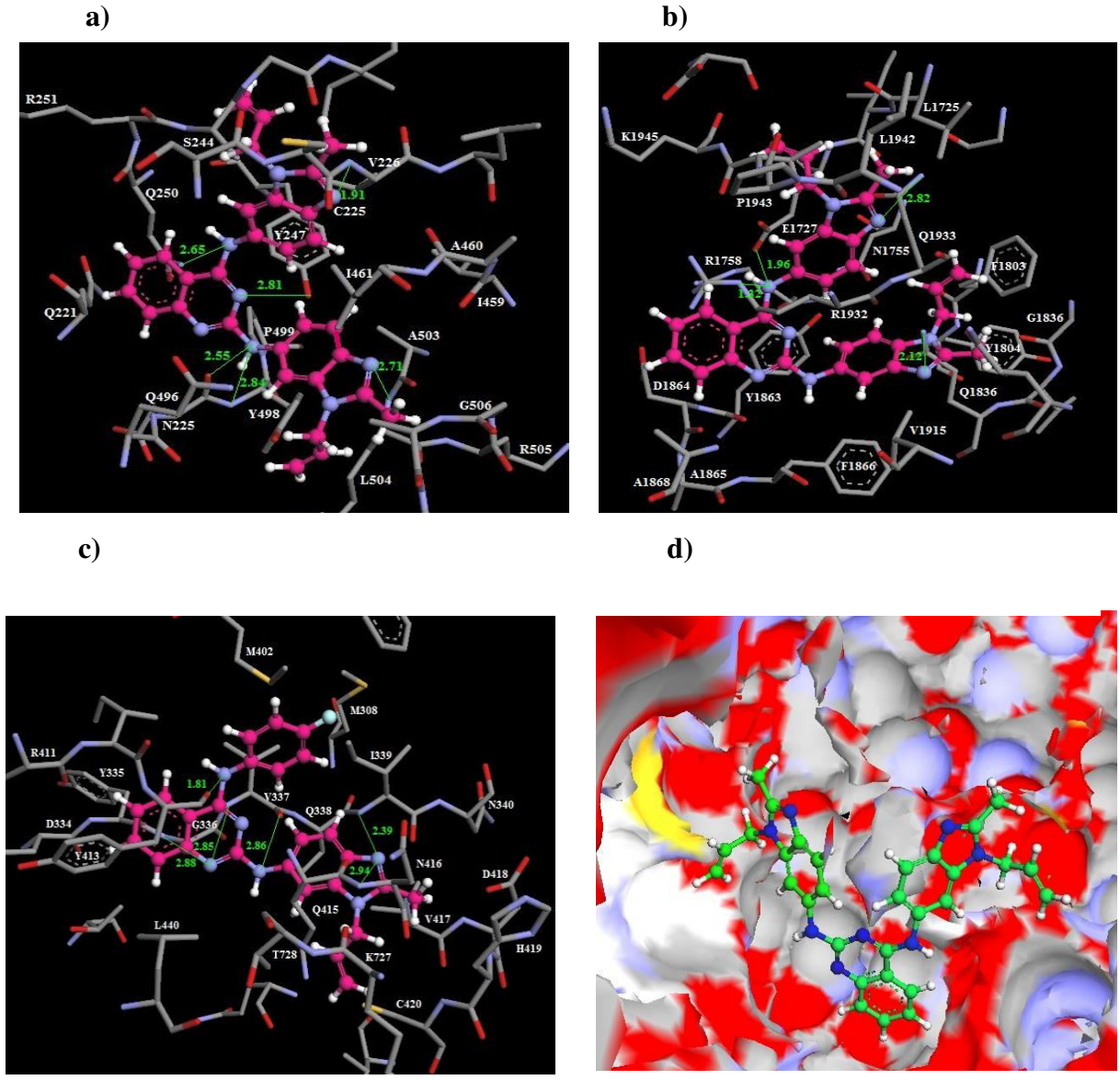

Figure 11. Molecular modelling (docking) of a) compound **19** ($E_{intermolecular}$ = -6.54 kcal mol^{-1}), b) compound **20** ($E_{intermolecular}$ = -7.18 kcal mol^{-1}) and c) compound **21** ($E_{intermolecular}$ = -7.25 kcal mol^{-1}) in the active site ribonucleotide reductase (pdb ID: 4R1R). H-bond distances are given in Å. H's are omitted for clarity. d) Comound **19** fits into the binding pocket of 4R1R (carbon atom shown in green color for clarity).

(*d* = 1.32 Å). The nitrogen atom of five membered ring of one benzimidazole showed hydrogen bond with amino group of Q1933 (*d* = 2.82 Å) amino acid residue and nitrogen atom of five membered ring of another benzimidazole forms hydrogen bond with Q1836 (*d* = 2.12 Å) amino acid residue **(Figure 11b)**

Molecular docking simulation for compound **21** within the 4R1R active site showed that 4-fluorophenyl ring of compound **21** was positioned near M308 whereas nitrogen of benzimidazole showed hydrogen bonding interactions with NH group of Q338 (*d* = 2.39 Å) and N416 (*d* = 2.94 Å) amino acid residues **(Figure 11c)**. The quinazoline ring was oriented towards the hydrophobic pocket of the 4R1R lined by two tyrosine amino acid residues Y413 and Y335. The docking of compound **21** within the 4R1R active site showed that benzimidazole component was positioned in the vicinity of the secondary pocket of the 4R1R isozyme, surrounded by residues Q415, K727, V417, N416, Q338 and I339, and allyl group of benzimidazole was bent towards K727 and C420 amino acid residues. The linker between benzimidazole and quinazoline showed hydrogen bonding interactions with carbonyl group of Y336 (*d* = 2.86 Å). Moreover, nitrogen atom of quinazoline ring formed hydrogen bond with V337 (*d* = 2.85 Å) and G336 (*d* = 2.88 Å) amino acid residues. Linker of 4-fluorophenyl and quinazoline i.e. NH showed hydrogen bonding interactions with hydroxyl oxygen group of Y413 (*d* = 1.81 Å) residue. The significant hydrogen bonding of the compounds **19, 20** and **21** in the active site of ribonucleotide reductase might play a key role in determining the selective inhibition of 4R1R.

Docking studies of compound **19, 20** and **21** were also performed with topoisomerase I enzyme (pdb ID 1A36). Docking of compound **19** in the active site of 1A36 showed H-bonding interactions between nitrogen atom of benzimidazole with L694 (*d* = 2.49 Å) amino acid residue. NH group (linker of quinazoline and benzimidazole) formed hydrogen bond interaction with K655 (*d* = 2.59 Å) amino acid residue **(Figure 12a)**. Nitrogen of benzimidazole of compound **20** also showed H-bonding interactions with residue Q697 (*d* = 2.33 Å) of topoisomerase I (1A36). Nitrogen of quinazoline formed H-bond with I694 (*d* = 1.19 Å) residue. One NH group linker also forms H-bonding interaction with Q697 (*d* = 2.74 Å) and other NH group linkers interact with E695 (*d* = 1.57 Å) amino acid residue. Nitrogen of one benzimidazole form hydrogen bonding interaction with Q697 (*d* = 2.33 Å) and nitrogen of another benzimidazole with Q692 (*d* = 1.90 Å) amino acid residue **(Figure 12b)**. Compound **21** was also docked into the active site of 1A36 isozymes. Nitrogen of quinazoline formed hydrogen bonding interactions with A653 and K654 (*d* = 2.94 Å and *d* = 2.75 Å) amino acid residues. NH linker of benzimidazole and quinazoline formed H-bonding

with K654 (d = 2.60 Å) residue. Nitrogen of benzimidazole also showed interactions with Q697 (d = 2.88 Å) amino acid residue **(Figure 12c)**.

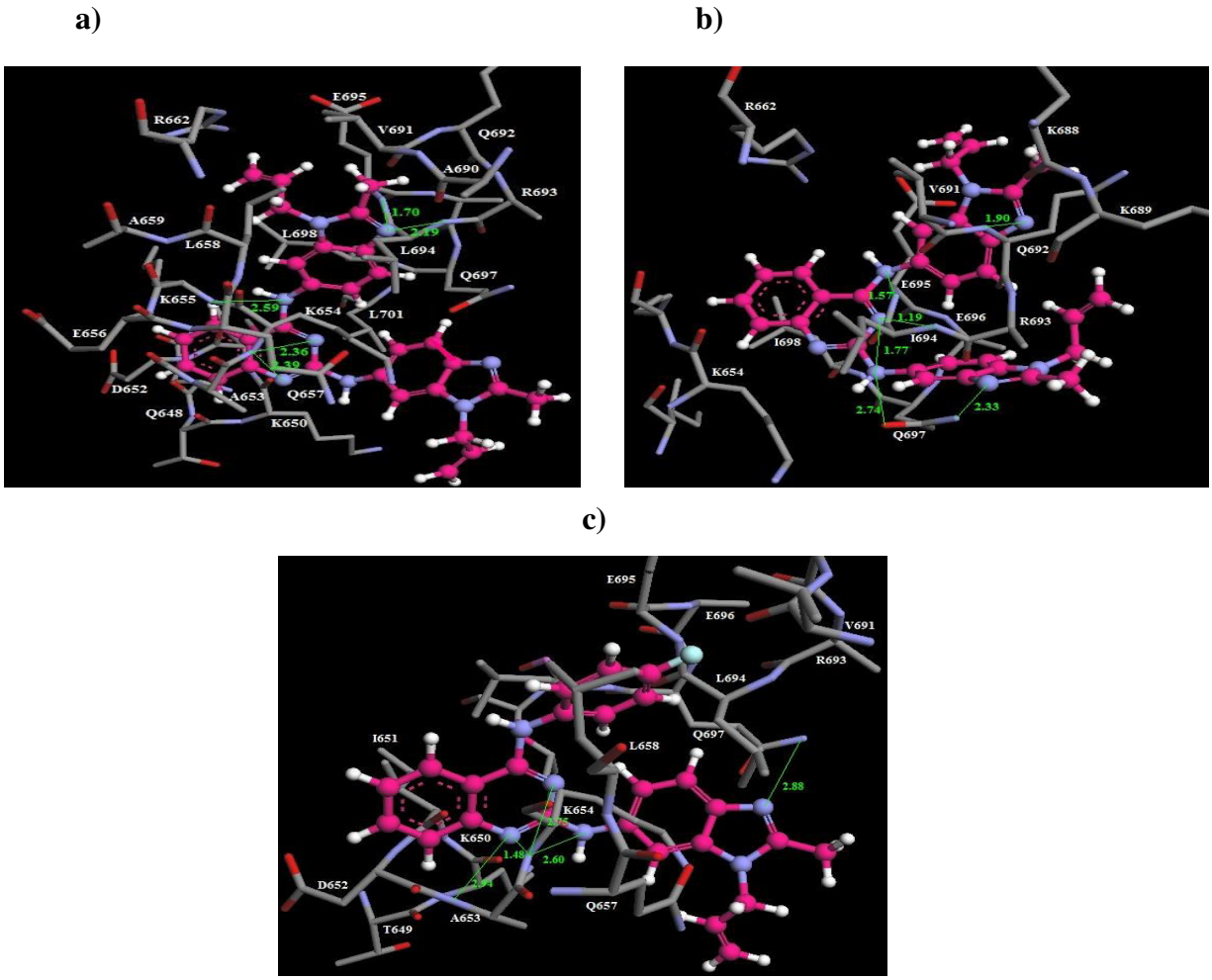

Figure 12. Molecular modelling (docking) of compounds **19**, **20** and **21** in the active site of Topo I (pdb ID : 1A36). H-bond distances are given in Å. H's are omitted for clarity.

Docking studies were also carried out between active compounds **19, 20** and **21** with topoisomerase II (pdb ID: 1BJT). Compound **19** was docked into the active site of 1BJT. Nitrogen group of quinazoline formed H-bonding interactions with C710 (d = 2.92 Å) amino acid residue. NH group showed interaction with L787 (d = 2.36 Å) and nitrogen of benzimidazole forms H-bond with K713 (d = 2.82 Å) and P726 (d = 2.97 Å) amino acid residue **(Figure 13a)**. Compound **20** also showed interaction with amino acid residue of 1BJT. Both linkers NH group between quinazoline and benzimidazole showed H-bonding interaction with A453 (d = 2.73 Å) residue. Nitrogen of benzimidazole showed interactions with C471, P473 and Y472 (d = 2.83 Å, d = 1.91 Å and d = 2.17 Å respectively) amino acid residues **(Figure 13b)**. NH group of compound **21** was also showed hydrogen bonding

interaction with G519 and L556 (d = 2.95 Å, d = 2.96 Å) amino acid residues. Nitrogen of benzimidazole formed interactions with L516 (d = 2.88 Å) amino acid residue (**Figure 13c**).

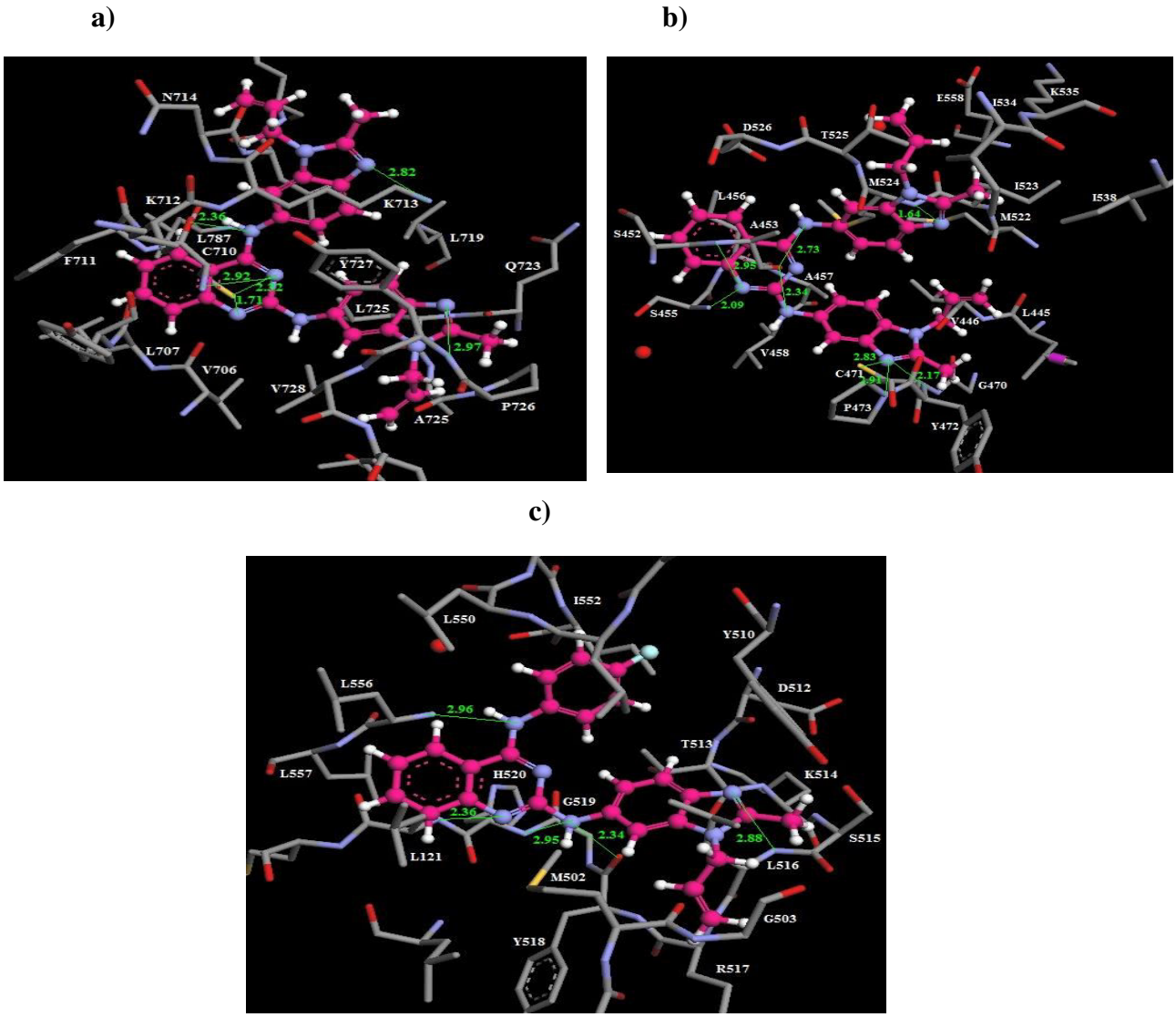

Figure 13. Molecular modelling (docking) of compounds **19**, **20** and **21** in the active site of Topo II (pdb ID : 1BJT). H-bond distances are given in Å. H's are omitted for clarity.

2.9. CONCLUSION

In conclusion, we have designed, synthesized the novel quinazoline and benzimidazole hybrids and their *in vitro* evaluations for antitumor agents. Here, we have synthesized and separated two regioisomeric benzimidazoles followed by molecular hybridization with substituted quinazolines. These novel molecules have been well characterized by ^{1}H and ^{13}C NMR as well as mass spectrometry and in case of compound **12**, by single X-ray crystallography. We have evaluated these compounds through 60 tumor cell lines for

anticancer activity. Some of these compounds have shown remarkable antitumor activity. In the secondary amine series, compound **9** showed broad spectrum antitumor agent by substituted pyrrolidine moiety showing effectiveness toward numerous cell lines belonging to different tumor subpanels. In the primary amine series, compounds **19, 20** and **21** with GI_{50} values of 1.64 μM, 0.81 μM and 4.52 μM respectively proved most active members as compared to quinazoline and benzimidazole analogue as well as 5-fluorouracil. It has also been clear that compounds with primary amines at 2-position of quinazoline showed more selectivity towards 60 human cancer cell line than secondary amines. As per the enzyme immunoassay, compound **11** exhibited significant activity for inhibition of Aurora-A enzyme with IC_{50} value of 0.035 μM. Subsequently, QSAR model for the affinity of this new series of Aurora A kinase inhibitors with physicochemical descriptors were developed with good predictive ability. Molecular modelling studies also indicating considerable interactions of these compounds in the active site of amino acids of RNR, Topo I and Topo II enzymes. Overall results revealed that: (i) quinazoline is a satisfactory backbone for antitumor activity, (ii) the presence of benzimidazole at 4-position is essential for activity, (iii) the presence of substituted secondary and primary amines at 2-position of quinazoline is necessary, and primary amine is more preferable than secondary amines, (iv) benzimidazole at C2 position of quinazoline is essential than other primary amines, (v) linker between quinazoline and benzimidazole is essential as H-bond region and (vi) regioisomerization of allyl groups at 1- or 3-position of benzimidazole increases the antitumor activity as indicated by comparing compounds **19** and **24**.

2.10. EXPERIMENTAL SECTION

2.10.1. Synthesis of compounds

General note

Melting points were determined in open capillaries and are uncorrected. For monitoring the progress of the reaction and for comparison with authentic samples, thin layer chromatography (TLC) was used. For this purpose, microslides were coated with silica gel 'G' containing calcium sulphate as binder or with silica gel HF-254 (Spectrochem, india), by dipping a pair of slides held back to back in slurry of adsorbent in chloroform : methanol (80:20). The chromatograms were developed in iodine chamber. Separation of various components was carried out by column chromatography using silica gel 60-120 mesh and 100-200 mesh (Spectrochem, india), as adsorbent and hexane : ethyl acetate, chloroform :

methanol or their mixtures as eluents. All the fractions collected from column chromatography were compared with chromatograms of reaction mixture (TLC) for checking their identity and purity.

The ^{1}H and ^{13}C NMR spectra were recorded on Bruker model No. FT-NMR Cryo-magnet Spectrometer 400 MHz and JEOL ECS 400 at 400 and 100 MHz NMR spectrometers respectively, using $CDCl_3$, DMSO-d_6 and trifluoroacetic acid (TFA) as solvents. The chemical shifts were expressed in parts per million with TMS as an internal reference and *J* values are given in hertz (Hz). The 2D–NOE studies were performed on the same instrument. Spectral patterns are designated as s = singlet; bs = broad singlet; d = doublet; t = triplet; dd = double doublet; q = quartet, m = multiplet. Mass Spectra of the synthesized compounds were recorded at MAT 120 in SAIF, Punjab University. Infrared Spectra were recorded on Jasco FTIR plus 460 Japan, and expressed in wave number (cm^{-1}), using potassium bromide discs. The crystal structure was collected on Agilent Technologies (Oxford Diffraction) Super Nova CCD System of Single Crystal X-ray Diffractrometer.

Materials: *o*-Phenylenediamine, sodium hydride, stannous chloride, anthranilic acid, urea, allyl bromide, phosphorous oxychloride, triethylamine, morpholine, piperidine, pyrrolidine, 4-methylpiperazine, 4-aminobenzenethiol, 4-aminophenol, 2-aminopyrimidine, 2-ethanolamine, 4-fluorophenylamine, 2,4-difluorophenylamine, acetic acid, sulphuric acid, nitric acid, tetrahydrofuran, hydrochloric acid, toluene, isopropyl alcohol, hexane, ethyl acetate, chloroform and methanol were purchased from S.D. fine chemicals, Loba chemicals,Spectrochemical and Sigma Aldrich. Absolute ethanol, isopropylalcohol, hexane, ethyl acetate, chloroform and methanol were of LR grade and were distilled before use.

General procedure for the preparation of 1/3-allyl-2-methyl-5-nitro-1*H*/3*H*-benzimidazole (3a, 3b)

o-Phenylenediamine (1 g, 0.009 mol) was treated with acetic acid (4 ml) at 100 $^{\circ}$C for 24 h. After completion of the reaction, work up was done with 10% NaOH to make the reaction mixture alkaline. Filtered the solid product, washed with water and dried over sodium sulphate to give brown solid of 2-methylbenzimidazole (**1**). Nitration has been done with equal amounts of nitric acid and concentrated sulfuric acid at 0 $^{\circ}$C for 5 h to give 80% yield. After completion of the reaction, crushed ice was added to the reaction mixture, filtered the solid product, washed with water several times and dried to give orange solid of 2-methyl-5-nitro-1*H*-benzimidazole **(2)** with 80% yield. To a suspension of 2-methyl-5-nitro-1*H*-benzimidazole **(2)** (9.0 g, 0.05 mol) in 60% NaH (3.03 g, 0.126 mol) and THF, allyl bromide

(9.17 g, 0.075 mol) was added dropwise at 0 °C and stirred at room temperature for 8 h. After the completion of the reaction (monitored by TLC), the reaction mixture was extracted with chloroform, dried over anhydrous Na_2SO_4, concentrated to give yellow solid. The residual mass was crystallized from ethanol.

1/3-allyl-2-methyl-5-nitro-1*H*/3*H*-benzimidazole (3a, 3b).

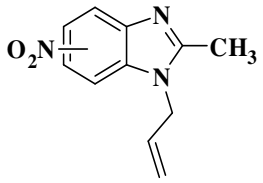

Greenish powder, yield: 80%; mp: 195-200 °C; IR (KBr, cm^{-1}) ν: 3073, 2932, 1517, 1410; ^{1}H NMR (DMSO-d_6): δ 8.42 (d, 1H, J = 2.16 Hz, ArH), 8.09 (m, 1H, ArH), 7.56 (d, 1H, J = 8.92 Hz, ArH), 6.01 (m, 1H, NCH_2-CH-CH_2), 5.22 (dd, 1H, ^2J = 10.44 Hz, ^3J = 0.88 Hz,=CH_2), 4.98 (dd, 1H, ^2J = 17.23 Hz, ^3J = 0.88 Hz, =CH_2), 4.93 (m, 2H, N-CH_2), δ 2.56 (s, 3H, CH_3); ^{13}C NMR (DMSO-d_6): δ 157.3, 155.9, 146.8, 142.5, 142.2, 141.4, 139.4, 134.3, 131.9, 131.7, 118.2, 117.3, 117.0, 116.8, 116.7, 114.3, 109.8, 106.5, 45.7, 45.6, 13.6, 13.5.

General procedure for the preparation of 1/3-allyl-2-methyl-1*H*/3*H*-benzimidazole-5-ylamine (4a, 4b)

To a suspension of $SnCl_2.2H_2O$ (30.9g, 0.135 mol) in 2N HCl (95.2 ml), 1/3-allyl-2-methyl-5-nitro-1*H*/3*H*-benzimidazole **(3)** (8.5g, 0.039 mol) was heated at 110 °C for 7 h. The reaction was monitored by TLC. After the completion of the reaction, the suspension was neutralized with 2N NaOH and diluted with ethanol. Filtered the solid product and extract the filtrate with chloroform, dried over Na_2SO_4, filtered and concentrated to get mixture of products which were separated through column chromatography using ethylacetate : methanol (9.5:0.5) to get pure solid compounds.

3-Allyl-2-methyl-3*H*-benzimidazol-5-ylamine (4a).

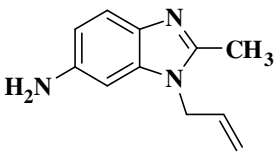

Brownish powder, yield: 65%; mp 137-139 °C; IR (KBr, cm^{-1}) ν: 3380, 3270, 3073, 1516, 1408, 1178; ^{1}H NMR ($CDCl_3$): δ 7.46 (d, 1H, J = 8.44 Hz, ArH), 6.60 (dd, 1H, ^2J = 8.40 Hz, ^3J = 2.08 Hz, ArH), 6.51 (d, 1H, J = 1.96 Hz, ArH), 5.89 (m, 1H, CH), 5.19 (d, 1H, J = 10.44 Hz, CH_2), 4.95 (d, 1H, J = 17.16 Hz, CH_2), 4.57 (d, 2H, J = 7.84 Hz, CH_2), 3.56 (bs, 2H, NH_2, exchangeable with D_2O), 2.50 (s, 3H, CH_3); ^{13}C NMR ($CDCl_3$): δ 149.9, 142.3, 136.1, 136.0, 131.7, 119.4, 117.1, 111.7, 94.9, 45.6, 13.6; EIMS, m/z: 188 (M^++1); Anal. calcd for $C_{11}H_{13}N_3$: C, 70.56; H, 7.00; N, 22.44 found: C, 70.58; H, 6.61; N, 22.54%.

1-Allyl-2-methyl-1*H*-benzimidazol-5-ylamine (4b).

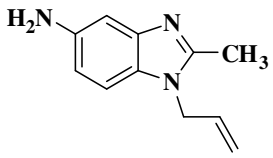

Brownish powder, yield: 25%; mp: 137-139 °C; IR (KBr, cm^{-1}) ν: 3380, 3272 , 2923, 1516, 1408, 1177 ; ^{1}H NMR ($CDCl_3$): δ 7.04 (d, 1H, *J* = 8.48 Hz, ArH), 7.02 (d, 1H, *J* = 1.96 Hz, ArH), 6.64 (dd, 1H, ^2J = 8.44 Hz, ^3J = 2.12 Hz, ArH), 5.91 (m, 1H, CH), 5.21 (dd, 1H, ^2J = 10.28 Hz, ^3J = 0.68 Hz, CH_2), 4.93 (dd, 1H, ^2J = 16.16 Hz, ^3J = 0.68 Hz, CH_2), 4.64 (m, 2H, CH_2), 3.74 (bs, 2H, NH_2), 2.53 (s, 3H, CH_3); ^{13}C NMR ($CDCl_3$): δ 151.6, 143.6, 141.8, 131.9, 129.1, 117.1, 111.9, 109.5, 104.4, 45.8, 13.7; EIMS, m/z: 188 (M^++1); Anal. calcd for $C_{11}H_{13}N_3$: C, 70.56; H, 7.00; N, 22.44 found: C, 70.61; H, 6.63; N, 22.51%.

General procedure for the preparation of (1/3-allyl-2-methyl-1*H*/3*H*-benzimidazol-5-yl)-2-chloro-quinazolin-4-yl)-amine (7a, 7b):

Anthranilic acid (10 g, 0.07 mol) and urea (43.79 g, 0.73 mol) were stirred at 160 °C for 6 h, cooled the reaction mixture to 100 °C and water was added while stirring for 5 min. The precipitate formed was filtered off and washed with water to yield a solid cake that was suspended in a solution of 0.5N NaOH and heated to boil for 5-10 min. Cooled and adjusted the pH = 2 with concentrated HCl, and the solid was filtered off. After washing with water : methanol (1:1), the product was dried, gave white solid of 1*H*-quinazolin-2,4-dione **(5)** (mp. > 300 °C). 1*H*-quinazolin-2,4-dione (5 g, 0.03 mol), triethylamine (6.43 ml, 0.05 mol) and $POCl_3$ (25 ml, 0.27 mol) were refluxed for 7 h. Distilled off excess $POCl_3$ under vacuum and crushed ice was added to the residue. Reaction mixture was then stirred for 1 h at 0-5 °C. Filtered the solid product, washed with water and dried to give yellow solid of 2,4-dichoroquinazoline **(6)** with 87% yield (mp. 117-120 °C) To a solution of 3-allyl-2-methyl-3*H*-benzimidazol-5-ylamine or 1-allyl-2-methyl-1*H*-benzimidazol-5-ylamine (**4a** or **4b**) (2.2 g, 0.011 mol) and isopropyl alcohol (40 ml), 2,4-dichoroquinazoline **(6)** (2.18 g, 0.011 mol) was added and stirred at room temperature for 8-12 h. After washing the crude solid with IPA, dried to give pure white solid of (3-allyl-2-methyl-3*H*-benzimidazol-5-yl)-(2-chloro-quinazolin-4-yl)-amine **(7a)** and (1-allyl-2-methyl-1*H*-benzimidazol-5-yl)-(2-chloro-quinazolin-4-yl)-amine **(7b).**

(3-Allyl-2-methyl-3*H*-benzimidazol-5-yl)-(2-chloro-quinazolin-4-yl)-amine (7a).

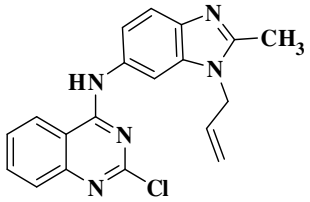

White powder, yield: 92%; mp. 210-215 °C; IR (KBr, cm^{-1}) ν: 3258, 3054, 1704, 1671, 1503, 1426, 1289, 1141, 756; ^{1}H NMR (DMSO-d_6): δ 10.52 (s, 1H, NH), 8.76 (d, 1H, *J* = 8.28 Hz, ArH), 8.57 (d, 1H, *J* = 1.08 Hz, ArH), 8.12 (dd, 1H, ^2J = 9.00 Hz, ^3J =

1.52 Hz, ArH), 7.83 (m, 2H, ArH), 7.74 (d, 1H, *J* = 8.16 Hz, ArH), 7.61 (t, 1H, *J* = 7.68 Hz, ArH), 6.06 (m, 1H, CH), 5.39 (d, 1H, *J* = 10.32 Hz, CH_2), 5.25 (d, 1H, *J* = 17.61 Hz, CH_2), 5.12 (d, 2H, *J* = 5.04 Hz, CH_2), 2.55 (s, 3H, CH_3); ^{13}C NMR (DMSO-d_6): δ 162.9, 159.0, 155.8, 150.6, 150.4, 150.0, 140.6, 137.1, 134.3, 133.5, 129.7, 129.4, 127.7, 126.7, 126.5, 126.2, 123.7, 121.9, 121.2, 119.0, 115.2, 114.2, 113.7, 111.6, 106.9, 46.7, 11.3; EIMS, m/z: 350.5 (M^++1); Anal. calcd for $C_{19}H_{16}ClN_5$: C, 65.24; H, 4.61; N, 20.02 found: C, 65.71; H, 4.63; N, 20.32%.

(1-Allyl-2-methyl-1*H*-benzimidazol-5-yl)-(2-chloro-quinazolin-4-yl)-amine (7b).

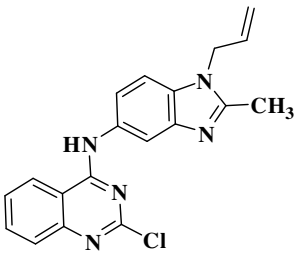

White powder, yield: 82%; mp. 217-220 °C; IR (KBr, cm^{-1}) ν: 3252 , 3035, 2849, 1719, 1662, 1624, 1433, 1299, 758; ^{1}H NMR (DMSO-d_6): δ 10.17 (s, 1H, NH), 8.59 (d, 1H, *J* = 8.04 Hz, ArH), 7.99 (d, 1H, *J* = 1.48 Hz, ArH), 7.81 (t, 1H, *J* = 6.88 Hz, ArH), 7.68 (d, 1H, *J* = 7.88 Hz, ArH), 7.57 (d, 2H, *J* = 8.24 Hz, ArH), 7.48 (dd, 1H, ^2J = 8.56 Hz, ^3J = 1.80 Hz, ArH), 6.03 (m, 1H, CH), 5.25 (dd, 1H, ^2J = 10.28 Hz, ^3J = 0.76 Hz, CH_2) 5.04 (dd, 1H, ^2J = 17.12 Hz, ^3J = 0.92 Hz, CH_2), 4.82 (d, 2H, *J* = 5.00 Hz, CH_2), 2.57 (s, 3H, CH_3); ^{13}C NMR (DMSO-d_6): δ 162.9, 159.1, 155.8, 150.3, 140.7, 136.9, 134.3, 133.6, 129.9, 129.7, 127.9, 126.6, 126.2, 123.5, 121.8, 121.0, 118.9, 115.1, 114.2, 113.8, 111.9, 106.9, 46.6, 11.3; EIMS, m/z: 350.5 (M^++1); Anal. calcd for $C_{19}H_{16}ClN_5$: C, 65.24; H, 4.61; N, 20.02 found: C, 65.68; H, 4.65; N, 20.36%.

General procedure for the preparation of (1/3-allyl-2-methyl-1*H*/3*H*-benzimidazol-5-yl)-(2-amino-quinazolin-4-yl)-amine:

(1/3-Allyl-2-methyl-1*H*/3*H*-benzimidazol-5-yl)-(2-chloro-quinazolin-4-yl)-amine (0.2 g, 0.57 mmol) was refluxed with amine (0.62 mmol) in IPA (20 ml) for 7-8 h. Reaction was monitored by TLC, crude solid obtained was filtered and washed with IPA gave solids of (1/3-allyl-2-methyl-1*H*/3*H*-benzimidazol-5-yl)-(2-amino-quinazolin-4-yl)-amine (**8-24**).

(3-Allyl-2-methyl-3*H*-benzimidazol-5-yl)-(2-morpholin-4-yl-quinazolin-4-yl)-amine (8).

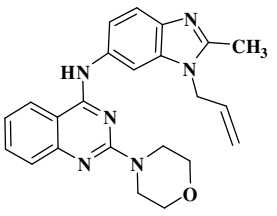

White crystals, yield: 65%; mp. 200-210 °C; IR (KBr, cm^{-1}) ν: 3351, 3059, 2835, 1620, 1567, 1477, 1432, 1398, 1232, 1106, 1003, 757; ^{1}H NMR ($CDCl_3$): δ 8.01 (d, 1H, *J* = 1.76 Hz, ArH), 7.74 (bs, 1H, NH), 7.58 (t, 1H, *J* = 7.52 Hz, ArH), 7.52 (d, 1H, *J* = 8.72 Hz, ArH), 7.26 (m, 3H, ArH), 7.18 (m, 1H, ArH), 5.96 (m, 1H, CH), 5.26 (d, 1H, *J* = 10.32 Hz,

CH_2), 5.00 (d, 1H, *J* = 17.00 Hz, CH_2), 4.74 (d, 2H, *J* = 4.60 Hz, CH_2), 3.88 (s, 4H, $_{mor}CH_2$), 3.76 (t, 4H, *J* = 4.48 Hz, $_{mor}CH_2$), 2.59 (s, 3H, CH_3); ^{13}C NMR (DMSO-d_6): δ 157.3, 156.9, 151.7, 151.6, 142.0, 133.8, 131.9, 131.3, 131.1, 124.4, 121.9, 119.9, 117.0, 116.6, 111.8, 110.2, 108.2, 65.7, 46.5, 46.0, 13.2; EIMS, m/z: 401 (M^++1); Anal. calcd for $C_{23}H_{24}N_6O$: C, 68.98; H, 6.04; N, 20.99 found: C, 68.58; H, 6.41; N, 20.54%.

(3-Allyl-2-methyl-3*H*-benzimidazol-5-yl)-(2-pyrrolidin-1-yl-quinazolin-4-yl)-amine (9).

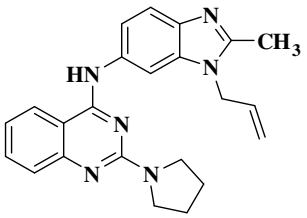

White crystals, yield: 89%; mp. 150-155 °C; IR (KBr, cm^{-1}) ν: 3224, 3063, 2922, 1691, 1623, 1512, 1478, 1328, 1278, 760; ^{1}H NMR (DMSO-d_6): δ 9.40 (bs, 1H, NH), 8.33 (d, 1H, *J* = 8.24 Hz, ArH), 8.27 (d, 1H, *J* = 1.48 Hz, ArH), 7.71 (dd, 1H, ^2J = 6.84 Hz, ^3J = 1.84 Hz, ArH), 7.55 (t, 1H, *J* = 7.44 Hz, ArH), 7.46 (d, 1H, *J* = 8.32 Hz, ArH), 7.32 (d, 1H, *J* = 8.68 Hz, ArH,), 7.14 (t, 1H, *J* = 7.32 Hz, ArH), 6.00 (m, 1H, CH), 5.23 (dd, 1H, ^2J = 10.32 Hz, ^3J = 1.00 Hz, CH_2), 4.99 (dd, 1H, ^2J = 17.12 Hz, ^3J = 0.96 Hz, CH_2), 4.80 (d, 2H, *J* = 4.88 Hz, CH_2), 3.64 (t, 4H, *J* = 6.52 Hz, N-$_{pyr}CH_2$), 2.56 (s, 3H, CH_3), 1.98 (t, 4H, *J* = 6.48 Hz, $_{pyr}CH_2$); ^{13}C NMR (DMSO-d_6): δ 157.3, 156.9, 151.7, 151.6, 142.0, 133.8, 131.9, 131.3, 131.1, 124.4, 121.9, 119.0, 117.0, 116.7, 111.6, 110.2, 108.2, 46.3, 45.3, 25.1, 13.3; EIMS, m/z: 385 (M^++1); Anal. calcd for $C_{23}H_{24}N_6$: C, 71.85; H, 6.29; N, 21.86 found: C, 72.08; H, 6.32; N, 21.52%.

(3-Allyl-2-methyl-3*H*-benzimidazol-5-yl)-(2-piperidin-1-yl-quinazolin-4-yl)-amine (10).

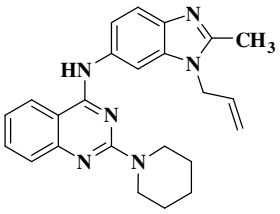

White crystals, yield: 78%; mp. 170-175 °C; IR (KBr, cm^{-1}) ν: 3413, 3093, 2929, 1624, 1569, 1508, 1433, 1239, 1150, 1019, 794, 756; ^{1}H NMR (DMSO-d_6): δ 9.48 (bs, 1H, NH), 8.29 (d, 1H, *J* = 8.08 Hz, ArH), 8.01 (d, 1H, *J* = 1.40 Hz, ArH), 7.60 (dd, 1H, ^2J = 7.00 Hz, ^3J = 1.64 Hz, ArH), 7.54 (t, 1H, *J* = 7.48 Hz, ArH), 7.37 (d, 1H, *J* = 8.36 Hz, ArH), 7.32 (d, 1H, *J* = 8.68 Hz, ArH), 7.12 (t, 1H, *J* = 7.52 Hz, ArH), 6.01 (m, 1H, CH), 5.22 (dd, 1H, ^2J = 9.56 Hz, ^3J = 0.76 Hz, CH_2), 4.95 (dd, 1H, ^2J = 16.2 Hz, ^3J = 0.84 Hz, CH_2), 4.82 (d, 2H, *J* = 4.92 Hz, CH_2), 3.80 (t, 4H, *J* = 4.84 Hz, $_{pip}CH_2$), 2.55 (s, 3H, CH_3), 1.65 (d, 2H, *J* = 4.36 Hz, $_{pip}CH_2$), 1.58 (d, 4H, *J* = 3.72 Hz, $_{pip}CH_2$); ^{13}C NMR ($CDCl_3$): δ 158.9, 157.8, 152.9, 152.3, 142.8, 133.7, 132.6, 131.9, 131.7, 126.0, 120.8, 120.7, 117.5, 117.3, 112.1, 110.4, 108.9, 45.9, 45.1, 26.0, 25.1, 13.8; EIMS, m/z: 399 (M^++1); Anal. calcd for $C_{24}H_{26}N_6$: C, 72.33; H, 6.58; N, 21.09 found: C, 72.21; H, 6.47; N, 21.00%.

(3-Allyl-2-methyl-3*H*-benzimidazol-5-yl)-[2-(4-methyl-piperazin-1-yl)-quinazolin-4-yl]-amine (11).

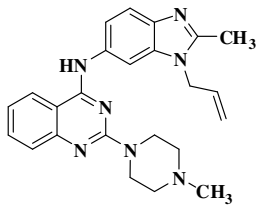

Yellow crystals, yield: 55%; mp. 198-200 °C; IR (KBr, cm^{-1}) ν: 3402, 3101, 2924, 1621, 1571, 1483, 1431, 1238, 1145, 768; ^{1}H NMR (DMSO-d_6): δ 9.53 (s, 1H, NH), 8.33 (d, 1H, *J* = 8.16 Hz, ArH), 7.99 (s, 1H, ArH), 7.60 (m, 2H, ArH), 7.40 (d, 1H, *J* = 8.64 Hz, ArH), 7.34 (d, 1H, *J* = 8.68 Hz, ArH), 7.17 (t, 1H, *J* = 7.64 Hz, ArH), 6.05 (m, 1H, CH), 5.22 (d, 1H, *J* = 10.32 Hz, CH_2), 4.95 (d, 1H, *J* = 17.04 Hz, CH_2), 4.83 (d, 2H, *J* = 4.84 Hz, CH_2), 3.89 (s, 4H, $_{piperazine}CH_2$), 2.60 (s, 3H, CH_3), 2.56 (s, 4H, $_{piperazine}CH_2$), 2.39 (s, 3H, CH_3); ^{13}C NMR (DMSO-d_6): δ 158.1, 151.9, 141.0, 133.3, 132.3, 132.2, 131.7, 122.9, 120.9, 117.9, 116.5, 112.4, 110.8, 108.6, 54.1, 45.4, 45.0, 42.9, 13.4; EIMS, m/z: 414 (M^++1); Anal. calcd for $C_{24}H_{27}N_7$: C, 69.71; H, 6.58; N, 23.71 found: C, 69.25; H, 6.51; N, 23.60%.

(1-Allyl-2-methyl-1*H*-benzimidazol-5-yl)-(2-morpholin-4-yl-quinazolin-4-yl)-amine (12).

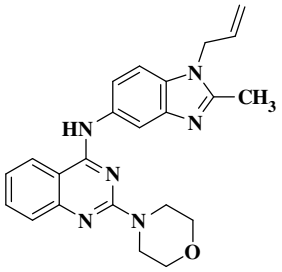

White crystals, yield: 70%; mp. 200-210 °C; IR (KBr, cm^{-1}) ν: 3457, 3123, 2931, 1637, 1593, 1577, 1409, 1330, 1107, 1000, 760; ^{1}H NMR (DMSO-d_6): δ 10.06 (bs, 1H, NH), 8.42 (d, 1H, *J* = 7.40 Hz, CH_2), 7.64 (m, 3H, ArH), 7.44 (d, 1H, *J* = 7.76 Hz, ArH), 7.28 (s, 1H, ArH), 7.15 (m, 1H, ArH), 6.03 (m, 1H, CH), 5.22 (d, 1H, *J* = 10.36 Hz, CH_2), 4.87 (d, 1H, *J* = 17.04 Hz, CH_2), 4.79 (d, 2H, *J* = 2.00 Hz, CH_2), 3.82 (d, 4H, *J* = 4.12 Hz, $_{mor}CH_2$), 3.72 (d, 4H, *J* = 4.56 Hz, $_{mor}CH_2$), 2.56 (s, 3H, CH_3); ^{13}C NMR (DMSO-d_6): δ 158.3, 158.1, 151.8, 142.0, 133.4, 132.2, 131.6, 125.1, 122.8, 120.7, 117.8, 116.5, 112.3, 110.9, 108.5, 66.3, 45.4, 44.2, 13.4; EIMS, m/z: 401 (M^++1); Anal. calcd for $C_{23}H_{24}N_6O$: C, 68.98; H, 6.04; N, 20.99 found: C, 68.58; H, 6.41; N, 20.54%.

(1-Allyl-2-methyl-1*H*-benzimidazol-5-yl)-(2-pyrrolidin-1-yl-quinazolin-4-yl)-amine (13).

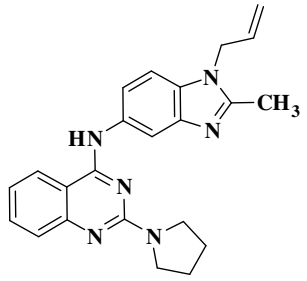

White crystals, yield: 52%; mp. 180-183 °C; IR (KBr, cm^{-1}) ν: 3224, 3063, 2923, 1691, 1623, 1577, 1478, 1128, 760; ^{1}H NMR (DMSO-d_6): δ 9.34 (bs, 1H, NH), 8.26 (d, 1H, J = 7.88 Hz, ArH), 8.11 (s, 1H, ArH), 7.56 (dd, 2H, ^2J = 17.84 Hz, ^3J = 8.92 Hz, ArH), 7.37 (d, 1H, J = 8.24 Hz, ArH), 7.25 (d, 1H, J = 8.56 Hz, ArH), 7.14 (t, 1H, J = 7.32 Hz, ArH), 5.99 (m, 1H, CH), 5.20 (d, 1H, J = 10.24 Hz, CH_2), 4.97 (d, 1H, J = 17.08 Hz, CH_2), 4.76 (d, 2H, J = 2.56 Hz, CH_2), 3.72 (s, 4H, N-$_{pyr}CH_2$), 2.57 (s, 3H, CH_3), 2.04 (s, 4H, $_{pyr}CH_2$); ^{13}C NMR (DMSO-d_6): δ 156.6, 151.4, 150.1, 138.9, 137.0, 135.9, 135.0, 134.8, 133.9, 133.5, 132.3, 132.2, 125.7, 125.3, 122.8, 122.4 , 121.2, 118.2, 118.0, 117.4, 116.7, 108.4, 45.4, 45.0, 29.0, 13.4; EIMS, m/z: 385 (M^++1); Anal. calcd for $C_{23}H_{24}N_6$: C, 71.85; H, 6.29; N, 21.86 found: C, 72.08; H, 6.32; N, 21.52%.

2-(4-(3-Allyl-2-methyl-3*H*-benzimidazol-5-ylamino)-quinazolin-2-ylamino)-ethanol (14).

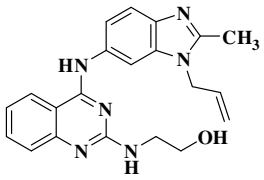

Brown crystalline solid, yield: 61%; mp 190-195 °C; IR (KBr, cm^{-1}) ν: 3285, 2933, 2854, 1631, 1573, 1522, 1483, 1400, 1329, 1182, 1146, 1077, 759; ^{1}H NMR (DMSO-d_6): δ 9.58 (s, 1H, NH), 8.33 (d, 1H, J = 8.08 Hz, ArH), 8.08 (d, 1H, J = 2.24 Hz, ArH), 7.56 (m, 2H, ArH), 7.36 (m, 2H, ArH), 7.16 (t, 1H, J = 7.5 Hz, ArH), 6.51 (s, 1H, NH), 6.00 (m, 1H, CH), 5.19 (dd, 1H, ^2J = 10.32 Hz, ^3J = 1.28 Hz, CH_2), 4.93 (dd, 1H, ^2J = 17.12 Hz, ^3J = 1.28 Hz, CH_2), 4.82 (d, 2H, J = 1.68 Hz, CH_2), 3.63 (t, 2H, J = 5.32 Hz, CH_2), 3.45 (q, 2H, J = 5.40 Hz, CH_2), 2.55 (s, 3H, CH_3); ^{13}C NMR (DMSO-d_6): δ 158.4, 151.8, 141.9, 133.1, 132.4, 131.8, 131.5, 122.7, 120.9, 118.3, 116.6, 113.0, 108.4, 45.4, 44.1, 44.0, 13.3; EIMS, m/z: 375 (M^++1); Anal. Calcd. for $C_{21}H_{22}N_6O$: C, 67.36; H, 5.92; N, 22.44. Found: C, 67.64; H, 6.14; N, 22.71%.

4-[4-(3-Allyl-2-methyl-3*H*-benzimidazol-5-ylamino)-quinazolin-2-ylamino]-phenol (15).

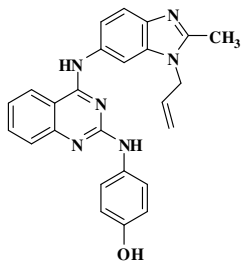

Brown crystalline solid**,** yield: 76%; mp. 260-265 °C; IR (KBr, cm^{-1}) : 3065, 2976, 2920, 2831, 1640, 1560, 1516, 1416, 1237, 826, 754; ^{1}H (TFA+$CDCl_3$): δ 12.49 (bs, 1H, NH), 8.75 (s, 1H, NH), 8.29 (s, 1H, 8.06 (s, 1H, ArH), 7.93 (t, 1H, J = 7.44 Hz, ArH), 7.85(s, 2H, s, 2H, 7.63 (m, 2H, ArH), 7.28 (s, 2H, ArH), 6.91 (s, 2H, ArH), 5.90 (m, 1H,

5.44 (d, 1H, J = 10.48 Hz, CH_2), 5.16 (d, 1H, J =16.96 Hz, CH_2), 4.78 (d, 2H, J = 4.12 Hz, CH_2), 2.99 (s, 3H, CH_3); ^{13}C NMR (DMSO-d_6): δ 164.2, 160.1, 152.5, 151.3, 139.7, 136.6, 134.9, 130.5, 130.2, 130.1, 125.8, 124.4, 123.6, 119.4, 115.9, 115.6, 112.8, 110.4, 47.1, 11.7; EIMS, m/z: 423 (M^++1); Anal. Calcd. for $C_{25}H_{22}N_6O$: C, 71.07; H, 5.25; N, 19.89. Found: C, 71.15; H, 5.53; N, 19.93%.

N^4-(3-allyl-2-methyl-3*H*-benzimidazol-5-yl)-N^2-(2-amino-phenyl)-quinazolin-2,4-diamine (16).

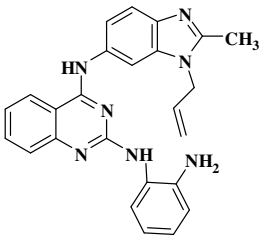

Brown crystalline solid**,** yield: 83%; mp. 110-115 °C; IR (KBr, cm^{-1}) ν: 3212, 3074, 2923, 2853, 1640, 1557, 1500, 1417, 1143, 755; ^{1}H NMR (DMSO-d_6): δ 10.99 (s, 1H, NH), 9.74 (bs, 1H, NH), 8.70 (d, 1H, J = 8.08 Hz, ArH), 7.96 (s, 1H, ArH), 7.78 (t, 1H, J = 7.68 Hz, ArH), 7.65 (dd, 2H, ^2J = 8.52 Hz, ^3J = 1.76 Hz, ArH), 7.46 (t, 1H, J = 8.00 Hz, ArH), 7.34 (d, 1H, J = 8.24 Hz, ArH), 7.18 (t, 1H, J = 5.92 Hz, ArH), 6.97 (d, 1H, J = 5.20 Hz, ArH), 6.84 (d, 1H, J = 7.88 Hz, ArH), 6.55 (s, 1H, ArH), 6.04 (m, 1H, CH), 5.26 (dd, 1H, ^2J = 10.32 Hz, ^3J = 0.80 Hz, CH_2), 4.95 (d, 1H, J = 17.16 Hz, CH_2), 4.87 (d, 2H, J = 4.92 Hz, CH_2), 2.64 (s, 3H, CH_3); ^{13}C NMR (DMSO-d_6): δ 158.8, 152.5, 152.2, 139.3, 134.8, 132.3, 131.7, 126.7, 124.6, 124.3, 119.7, 117.2, 116.9, 116.4, 115.8, 113.4, 110.5, 109.4, 45.6, 12.9; EIMS, m/z: 422 (M^++1); Anal. Calcd. for $C_{25}H_{23}N_7$: C, 71.24; H, 5.50; N, 23.26. Found: C, 71.56; H, 5.44; N, 23.12%.

N^4-(3-allyl-2-methyl-3*H*-benzimidazol-5-yl)-N^2-pyrimidin-2-yl-quinazolin-2,4-diamine (17).

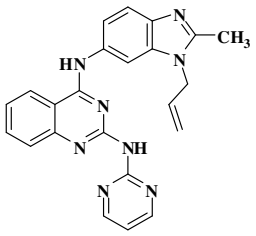

Brown crystalline solid, yield: 70%; mp. 170-175 °C; IR (KBr, cm^{-1}) ν: 3322, 3254, 3070, 2845, 1707, 1673, 1626, 1568, 1502, 1487, 1412, 1336, 1299, 1148, 759; ^{1}H NMR (DMSO-d_6): δ 11.07 (s, 1H, NH), 10.07 (s, 1H, NH), 8.55 (d, 1H, J = 7.80 Hz, ArH), 7.95 (d, 1H, J = 7.88 Hz, ArH), 7.89 (s, 1H, ArH), 7.79 (d, 1H, J = 1.20 Hz, ArH), 7.69 (d, 1H, J = 7.64 Hz, ArH), 7.66 (m, 2H, ArH), 7.36 (d, 1H, J = 4.64 Hz, ArH), 7.16 (m, 2H, ArH), 6.02 (m, 1H, CH), 5.26 (dd, 1H, ^2J = 10.32 Hz, ^3J = 0.88 Hz, CH_2), 5.00 (dd, 1H, ^2J = 16.08 Hz, ^3J = 1.20 Hz, CH_2), 4.82 (d, 2H, J = 5.52 Hz, CH_2), 2.57 (s, 3H, CH_3); ^{13}C NMR (TFA+$CDCl_3$): δ 160.2, 152.4, 152.0, 139.6, 138.4, 133.8, 131.7, 130.6, 128.6, 127.4, 124.1, 123.5, 120.7, 118.9, 116.1, 115.1, 111.6, 108.8, 47.7,

10.9; EIMS, m/z: 409 (M^++1); Anal. Calcd. for $C_{24}H_{21}N_7$: C, 70.74; H, 5.19; N, 24.06. Found: C, 70.77; H, 5.34; N, 24.41%.

(3-Allyl-2-methyl-3*H*-benzimidazol-5-yl)-[2-(4-amino-phenylsulfanyl)-quinazolin-4-yl]-amine (18).

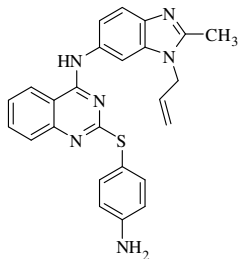

Yellow crystalline solid, yield: 60%; mp. 200-202 ^oC (decomp.); IR (KBr, cm^{-1}) ν: 3257, 3054, 2846, 1704, 1670, 1621, 1498, 1426, 1292, 1140, 757, 683; ^1H NMR (DMSO-d_6): δ 11.01 (bs, 2H, NH_2), 8.91 (s, 1H, NH), 7.98 (d, 2H, J = 8.60 Hz, ArH), 7.87 (d, 1H, ^2J = 13.0 Hz, ^3J = 8.40 Hz, ArH), 7.61 (t, 1H, J = 7.12 Hz, ArH), 7.54 (t, 1H, J = 7.12 Hz, ArH), 7.45 (d, 1H, J = 9.04 Hz, ArH), 7.24 (d, 1H, J = 7.68 Hz, ArH), 7.15 (m, 3H, ArH), 6.75 (d, 1H, J = 7.68 Hz, ArH), 6.08 (m, 1H, CH), 5.41 (d, 1H, J = 10.48 Hz, CH_2), 5.21 (d, 1H, J = 16.96 Hz, CH_2), 5.11 (d, 2H, J = 4.12 Hz, CH_2), 2.58 (s, 3H, CH_3); ^{13}C NMR (DMSO-d_6): δ 166.9, 157.5, 151.2, 136.6, 134.9, 131.5, 131.2, 129.7, 126.3, 124.5, 122.1, 120.9, 118.9, 118.3, 115.6, 113.8, 111.9, 107.0, 99.5, 46.5, 11.6; EIMS, m/z: 439 (M^++1); Anal. Calcd. for $C_{25}H_{22}N_6S$: C, 68.47; H, 5.06; N, 19.16; S, 7.31. Found: C, 68.62; H, 5.14; N, 19.71; S, 7.02%.

N^4-(3-Allyl-2-methyl-3*H*-benzimidazol-5-yl)-N^2-(3-allyl-2-methyl-3*H*-benzimidazol-5-yl)-quinazolin-2,4-diamine (19).

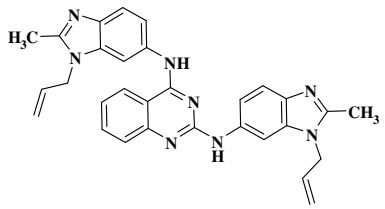

Pale green crystalline solid, yield: 70%; mp. 220-222 ^oC (decomp.); IR (KBr, cm^{-1}) ν: 3403, 3155, 2992, 2951, 1637, 1570, 1492, 1421, 1331, 1164, 998, 803, 763; ^1H NMR (DMSO-d_6): δ 11.20 (s, 1H, NH), 10.77 (s, 1H, NH), 8.74 (d, 1H, J = 8.08 Hz, ArH), 8.18 (s, 1H, ArH), 8.01 (s, 1H, ArH), 7.85 (t, 1H, J = 7.56 Hz, ArH), 7.74 (s, 1H, ArH), 7.65 (t, 1H, J = 10.72 Hz, ArH), 7.50 (d, 1H, J = 8.4 Hz, ArH), 6.04 (m, 1H, CH), 5.32 (d, 1H, J = 10.00 Hz, CH_2), 5.13 (dd, 1H, ^2J = 17.76 Hz, ^3J = 4.00 Hz, CH_2), 4.99 (dd, 2H, ^2J = 16.08 Hz, ^3J = 4.08 Hz, CH_2), 2.80 (s, 3H, CH_3), 2.58 (s, 3H, CH_3); ^{13}C NMR (TFA+$CDCl_3$): δ 160.4, 152.5, 152.0, 138.7, 137.6, 135.7, 130.4, 128.2, 128.1, 127.7, 123.6, 123.5, 121.2, 120.8, 118.5, 110.8, 48.4, 48.2, 11.4, 11.2; EIMS, m/z: 501 (M^++1); Anal. Calcd. for $C_{30}H_{28}N_8$: C, 71.98; H, 5.64; N, 22.38. Found: C, 72.15; H, 5.62; N, 22.64%.

N^4-(3-Allyl-2-methyl-3*H*-benzimidazol-5-yl)-N^2-(1-allyl-2-methyl-1*H*-benzimidazol-5-

yl)-quinazolin-2,4-diamine (20).

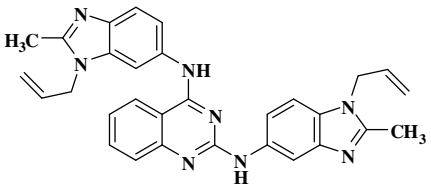

Brown powder, yield: 62%; mp. 180-183 °C; IR (KBr, cm^{-1}) ν: 3213, 3046, 1920, 1642, 1595, 1549, 1424, 1142, 761; ^{1}H NMR (DMSO-d_6): δ 11.19 (s, 1H, NH), 11.09 (s, 1H, NH), 7.92 (dd, 1H, ^2J = 7.80 Hz, ^3J = 1.24 Hz, ArH), 7.58 (m, 1H, ArH), 7.37 (d, 1H, J = 8.68 Hz, ArH), 7.19 (m, 2H, ArH), 6.82 (dd, 1H, ^2J = 8.68 Hz, ^3J = 2.00 Hz, ArH), 6.77 (d, 1H, J = 1.84 Hz, ArH), 6.00 (m, 1H, CH), 5.29 (dd, 1H, ^2J = 10.48 Hz, ^3J = 0.84 Hz, CH_2), 5.10 (dd, 1H, ^2J = 12.88 Hz, ^3J = 0.64 Hz, CH_2), 4.85 (d, 2H, J = 3.6 Hz, CH_2), 2.69 (s, 3H, CH_3), 2.56 (s, 3H, CH_3); ^{13}C NMR (TFA+$CDCl_3$): δ 160.6, 152.1, 138.9, 137.7, 135.7, 132.6, 130.3, 130.3, 128.2, 127.9, 127.5, 123.9, 123.4, 120.7, 118.8, 118.3, 112.9, 110.6, 110.4, 100.4, 48.1, 11.6, 11.5; EIMS, m/z: 501 (M^++1); Anal. Calcd. for $C_{30}H_{28}N_8$: C, 71.98; H, 5.64; N, 22.38. Found: C, 72.32; H, 5.23; N, 22.73%.

N^4-(3-Allyl-2-methyl-3*H*-benzimidazol-5-yl)-N^2-(4-fluoro-phenyl)-quinazolin-2,4-diamine (21).

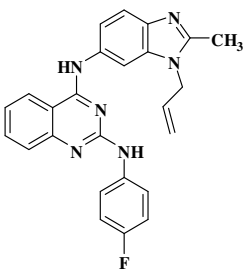

White powder, yield: 65%; mp. 200-205 °C (decomp.); IR (KBr, cm^{-1}) ν: 3402, 3212, 2932, 2840, 2732, 1612, 1565, 1421, 1342, 1238, 1150, 1000, 768; ^{1}H NMR (DMSO-d_6): δ 9.57 (s, 1H, NH), 8.89 (s, 1H, NH), 8.35 (d, 1H, J = 7.96 Hz, ArH), 7.97 (s, 1H, ArH), 7.85 (q, 2H, J = 5.00 Hz, ArH), 7.58 (m, 2H, ArH), 7.47 (d, 1H, J = 8.04 Hz, ArH), 7.39 (d, 1H, J = 6.36 Hz, ArH), 7.21 (t, 1H, J = 7.88 Hz, ArH), 6.87 (t, 2H, J = 8.76 Hz, ArH), 6.04 (m, 1H, CH), 5.24 (dd, 1H, ^2J = 10.32 Hz, ^3J = 1.04 Hz, CH_2), 4.99 (dd, 1H, ^2J = 17.08 Hz, ^3J = 1.08 Hz, CH_2), 4.86 (d, 2H, J = 4.88 Hz, CH_2), 2.58 (s, 3H, CH_3); ^{13}C NMR (TFA+$CDCl_3$): δ 160.4, 152.3, 151.8, 137.6, 130.3, 128.1, 127.8, 127.4, 124.1, 123.6, 121.1, 118.8, 118.1, 113.1, 110.5, 48.1, 11.5; EIMS, m/z: 425 (M^++1); Anal. Calcd. for $C_{25}H_{21}FN_6$: C, 70.74; H, 4.99; N, 19.80. Found: C, 70.46; H, 5.14; N, 19.81%.

N^4-(3-Allyl-2-methyl-3*H*-benzimidazol-5-yl)-N^2-(2,6-difluoro-phenyl)-quinazolin-2,4-diamine (22).

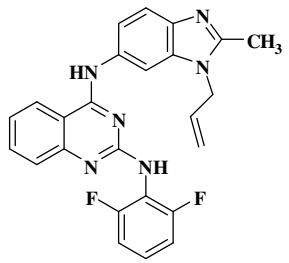

White powder, yield: 70%; mp. 215-220 °C (decomp.); IR (KBr, cm^{-1}) ν: 3402, 3201, 2924, 2847, 2795, 1621, 1571, 1483, 1431, 1394, 1238, 1145, 1005, 768; ^{1}H NMR (DMSO-d_6): δ 11.64 (s, 1H, NH), 10.31 (s, 1H, NH), 8.87 (d, 1H, *J* = 7.80 Hz, ArH), 8.05 (s, 1H, ArH),7.93 (t, 1H, *J* = 7.88 Hz, ArH), 7.76 (d, 2H, *J* = 8.24 Hz, ArH), 7.59 (m, 2H, ArH), 7.40 (t, 1H, *J* = 6.40 Hz, ArH), 7.20 (t, 2H, *J* = 8.28 Hz, ArH), 6.00 (m, 1H, CH), 5.29 (d, 1H, *J* = 10.56 Hz, CH_2), 4.99 (d, 1H, *J* = 17.40 Hz, CH_2), 4.98 (s, 2H, CH_2), 2.83 (s, 3H, CH_3); ^{13}C NMR (DMSO-d_6): δ 160.1, 159.8, 152.9, 152.8, 136.4, 134.9, 132.0, 131.2, 128.6, 125.8, 125.6, 123.2, 119.5, 114.1, 112.6, 111.1, 108.7, 100.0, 48.5, 12.2; EIMS, m/z: 443 (M^++1); Anal. Calcd. for $C_{25}H_{20}F_2N_6$: C, 67.86; H, 4.56; N, 18.99. Found: C, 67.43; H, 4.44; N, 19.11%.

2-[4-(1-Allyl-2-methyl-1*H*-benzimidazol-5-ylamino)-quinazolin-2-ylamino]-ethanol (23).

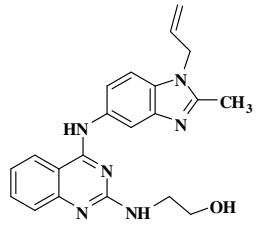

White powder, yield: 65%; mp. 100-105 °C; IR (KBr, cm^{-1}) ν: 3282, 2923, 2854, 1622, 1573, 1520, 1483, 1400, 1329, 1186, 1146, 1061, 760; ^{1}H NMR (DMSO-d_6): δ 10.15 (s, 1H, NH), 8.68 (s, 1H, NH), 8.26 (d, 1H, *J* = 7.88 Hz, ArH), 8.11 (s, 1H, ArH), 7.56 (m, 2H, ArH), 7.39 (d, 1H, *J* = 8.24 Hz, ArH), 7.28 (d, 1H, *J* = 8.56 Hz, ArH), 7.15 (t, 1H, *J* = 7.32 Hz, ArH), 6.02 (m, 1H, CH), 5.26 (d, 1H, *J* = 10.24 Hz, CH_2), 5.08 (dd, 1H, ^2J = 17.12 Hz, ^3J = 1.28 Hz, CH_2), 4.82 (d, 2H, *J* = 4.80 Hz, CH_2), 4.02 (t, 2H, *J* = 8.40 Hz, CH_2), 3.66 (t, 2H, *J* = 5.20 Hz, CH_2), 2.57 (s, 3H, CH_3); ^{13}C NMR (DMSO-d_6): δ 151.4, 151.1, 150.2, 135.0, 133.9, 132.1, 125.7, 125.1, 122.4, 121.4, 118.0, 117.6, 116.7, 114.7, 114.5, 100.9, 45.5, 29.1, 28.9, 13.4; EIMS, m/z: 375 (M^++1); Anal. Calcd. For $C_{21}H_{22}N_6O$: C, 67.36; H, 5.92; N, 22.44. Found: C, 67.55; H, 5.44; N, 22.19%.

N^4-(1-Allyl-2-methyl-1*H*-benzimidazol-5-yl)-N^2-(3-allyl-2-methyl-3*H*-benzimidazol-5-yl)-quinazolin-2,4-diamine (24).

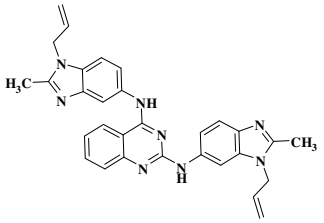

Brown powder, yield: 66%; mp. 200-205 °C (decomp.); IR (KBr, cm^{-1}) ν: 3203, 3023, 2905, 1637, 1613, 1587, 1510, 1472, 1253, 1109, 802, 759; ^{1}H NMR (DMSO-d_6): δ 11.02 (s, 1H, NH), 8.77 (s, 1H, ArH), 8.08 (d, 1H, *J* = 7.24 Hz, ArH), 7.66 (d, 1H, *J* = 7.67 Hz, ArH), 7.45 (d, 2H, *J* = 7.47 Hz, ArH), 7.24 (t, 1H, *J* = 7.26 Hz, ArH), 6.93 (m, 1H, ArH), 6.04 (m, 1H, CH), 5.46 (d, 1H, *J* = 11.44 Hz, CH_2), 5.34 (d, 1H,

J = 15.12 Hz, CH_2), 5.04 (s, 2H, CH_2), 2.79 (s, 3H, CH_3), 2.89 (s, 3H, CH_3); ^{13}C NMR (TFA+$CDCl_3$): δ 165.6, 154.1, 153.4, 139.3, 137.9, 132.3, 130.2, 128.4, 127.5, 127.2, 126.1, 123.5, 121.2, 116.6, 114.1, 108.8, 48.1, 12.1. EIMS, m/z: 501 (M^++1); Anal. Calcd. for $C_{30}H_{28}N_8$: C, 71.98; H, 5.64; N, 22.38. Found: C, 72.33; H, 5.31; N, 22.45%.

2.10.2. *In Vitro* studies (60 human cancer cell lines)

All the synthesized compounds were submitted to National Cancer Institute (NCI) disease-oriented human cell lines for screening assay to be evaluated for their *in-vitro* antitumor activities against 60 cell lines which included nine tumour subpanels namely; leukemia, non-small lung, colon, CNS, melanoma, ovarian renal, prostate and breast cancer cells. The human tumour cell lines of the cancer screening panel were grown in RPMI 1640 medium containing 5% fetal bovine serum and 2 mM L-glutamine. Cells were inoculated into 96 well microtiter plates in 100 ml at plating densities ranging from 5,000 to 40,000 cells/well depending on the doubling time of individual cell lines. The microtiter plates were then incubated at 37 °C, 5% CO_2, 95% air and 100% relative humidity for 24 h.

After 24 h, two plates of each cell line were fixed in situ with TCA, to represent a measurement of the cell population for each cell line. Experimental drugs were solubilized in DMSO at 400-fold the desired final maximum test concentration and stored frozen prior to use. At the time of drug addition, an aliquot of frozen concentrate was thawed and diluted to twice the desired final maximum test concentration with complete medium containing 50 µg/ml gentamicin. Additional four, 10-fold or ½ log serial dilutions were made to provide a total of five drug concentrations plus control. Aliquots of 100 µL of these different drug dilutions were added to the appropriate microtiter wells, resulting in the required final drug concentrations. Following drug addition, the plates were incubated for an additional 48 h at 37 °C, 5% CO_2, 95% air, and 100% relative humidity. For adherent cells, the assay was terminated by the addition of cold TCA. Cells were fixed in situ by the gentle addition of 50 µL of cold 50% (w/v) TCA and incubated for 60 min at 4 °C. The supernatant was discarded, and the plates were washed five times with tap water and air dried. Sulforhodamine B (SRB) solution (100 µL) at 0.4% (w/v) in 1% acetic acid is added to each well, and plates were incubated for 10 min at room temperature. After staining, unbound dye was removed by washing five times with 1% acetic acid and the plates are air dried and then subsequently solubilized with 10 mM trizma base, and the absorbance was read on an automated plate reader at a wavelength of 515 nm. Using the seven absorbance measurements [time zero (T_z),

control growth (C), and test growth in the presence of drug at the five concentration levels (T_i)], the percentage growth was calculated at each of the drug concentrations levels. Percentage growth inhibition is calculated as:

[(Ti -Tz)/(C - Tz)] × 100 for concentrations for which $T_i \geq Tz$; [(Ti -Tz)/Tz] × 100 for concentrations for which Ti < Tz.

Three dose response parameters was calculated for each experimental agent. Growth inhibition of 50% (GI_{50}) was calculated from [(Ti -Tz)/(C - Tz)] × 100 = 50. The drug concentration resulting in total growth inhibition (TGI) is calculated from $T_i = Tz$. The LC_{50} was calculated from [(Ti-Tz)/Tz]×100 = 50.[35,37,47]

2.10.3. *In Vitro* studies (Aurora kinase inhibitors)

UV-Vis spectral studies:

UV-visible spectral studies were performed on Biotek powerwave XS spectrophotometer. The stock solution for both the compounds and the enzyme were prepared in HPLC grade DMSO. The conc. of the compound stock solution was kept at 10^{-3} M and was diluted accordingly to get the final conc. of 10^{-5} M to 10^{-8} M. 50 µL of the enzyme was diluted to 950 µL in a kinase pure for further titration with compound solution.

Procedure for Aurora-A kinase assay

The Aurora-A kinase Assay/Inhibitor Screening Kit was a single-site, non-quantitative immunoassay for Aurora-A activity. Plates were pre-coated with a substrate corresponding to recombinant Lats2, which contains serine83 residues that can be phosphorylated by Aurora-A. First of all, removed the appropriate number of microtiter 96 wells from the foil pouch and placed them into the well holder. The stock solutions of the entire compounds were prepared in dimethylsulfoxide (spectroscopy grade) at concentration of 10^{-3} M. 30 µL of compound was added into a substrate coated plate. Begin the kinase reaction by addition of 80 µL Kinase Reaction Buffer per well, covered with plate sealer or lid, and incubated at 30 °C for 30-60 minutes. Wells was washed five times with Wash Buffer making to sure each well was filled completely. Residual Wash Buffer was removed by gentle tapping or aspiration. Pipetted 100 µL of Anti-Phospho-Lats2-S83 Monoclonal Antibody ST-3B11 into each well, cover with plate sealer or lid, and incubate at room temperature for 1 h. Wells was washed wells five times with Wash Buffer making sure each well is filled completely. Then, pipette 100 µL of HRP-conjugated Anti-mouse IgG into each well, covered with plate sealer or lid, and incubated at room temperature for 1 h. Any unused conjugate was discarded after use.

Wells was washed five times with Wash Buffer making sure each well was filled completely. Added 100 µL of Substrate Reagent to each well and incubate at room temperature for 5–15 minutes. At last, 100 µL of Stop Solution was added to each well in the same order as the previously added Substrate Reagent. Absorbance was measured in each well using a spectrophotometric plate reader at wavelengths of 450 nm. Wells was read within 30 minutes of adding the Stop Solution.

2.10.4. Shake flask method for lipophilicity determination

Partition coefficient for the target compounds were determined at room temperature using n-octanol–phosphate buffer (0.15 M, pH = 7.4). The experiments were performed in the system phosphate buffer : n-octanol at different volumes (10 : 1, 50 : 1). The stock solutions of the entire compounds were prepared in dimethylsulfoxide (spectroscopy grade) at concentration of 5×10^{-4} M. All solutions were pipette into glass vials; phosphate buffer and stock solutions (125µL, 250µL) were added with a micropipette. The wavelength chosen according to the λ_{max} of the compounds i.e., 350, 310, 349, 325, 335, 310, 392, and 370 for **7a**, **7b**, **8**, **9**, **10**, **11**, **12**, and **13** respectively. Initial absorbance (A_i) of stock solution in the buffer phase was recorded for each compound. Followed this, n-octanol was added into each vial. The phases were shaken together on a mechanical shaker (METREX, Cat No. MRS-50H) for 45 minutes, centrifuged (REMI R-24) at 2500 rpm for 30 min to afford complete phase separation, and n-octanol phase was removed. Absorbance of the buffer phase was measured spectrophotometrically using a CHAMPION UV-500 spectrophotometer.

P values were calculated from the following equation:-

$$P = \frac{A_i - A_f}{A_f} \times \frac{V_w}{V_o}$$

Where A_i and A_f represent the absorbance of compounds in the aqueous phase before and after partitioning, respectively. V_w and V_o represent the volume of the aqueous and organic phases used in the octanol/buffer system.

REFERENCES

1. Eckhardt, S. *Curr. Med. Chem. Anti-Cancer Agents* **2002**, *2*, 419.
2. Medina, J. C.; Shan, B.; Beckmann, H.; Farrell, R. P.; Clark, D. L.; Learned, R. M.; Roche, D.; Baichwal, A.; Li, V.; Case, C.; Baeuerle, P. A.; Rosen, T.; Jaen, J. C. *Bioorg. Med. Chem. Lett.* **1998**, *8*, 2653.

3. Abdel-Aziz, A. A. M. *Eur. J. Med. Chem.* **2007**, *42*, 614.
4. Medina, J. C.; Roche, D.; Shan, B.; Learned, R. M.; Frankmoelle, W. P.; Clark, D. L.; Rosen, T.; Jaen, J. C. *Bioorg. Med. Chem. Lett.* **1999**, *9*, 1843.
5. Hwang, H. S.; Moon, E. Y.; Seong, S. K.; Choi, C. H.; Chung, C. H.; Jung, S. H.; Yoon, S. J. *Anticancer Res.* **1999**, *19*, 5087.
6. Choo, H. Y. P.; Kim, M.; Lee, S. K.; Kim, S. W.; Chung, S. W. *Bioorg. Med. Chem.* **2002**, *10*, 517.
7. Al-Rashood, S. T.; Aboldahab, I. A.; Nagi, M. N.; Abouzeid, L. A.; Abdel-Aziz, A. A. M.; Abdel-Hamide, S. G.; Youssef, K. M.; Al-Obaid, A. M.; El-Subbagh, H. I. *Bioorg. Med. Chem.* **2006**, *14*, 8608.
8. Al-Obaid, A. M.; Abdel-Hamide, S. G.; El-Kashef, H. A.; Abdel-Aziz, A. A. M.; El-Azab, A. S.; Al-Khamees, H. A.; El-Subbagh, H. I. *Eur. J. Med. Chem.* **2009**, *44*, 2379.
9. Al-Omary, F. A. M.; Abouzeid, L. A.; Nagi, M. N.; Habib, E. E.; Abdel-Aziz, A. A. M.; El-Azab, A. S.; Abdel-Hamide, S. G.; Al-Omar, M. A.; Al-Obaid, A. M.; El-Subbagh, H. I. *Bioorg. Med. Chem.* **2010**, *18*, 2849.
10. (a) Baselga, J.; Swain, S. M. *Nat. Rev. Cancer* **2009**, *9*, 463; (b) Brown, C. H. J.; Lain, S.; Verma, C. H. S.; Fersht, A. R.; Lane, D. P. *Nat. Rev. Cancer* **2009**, *9*, 862.
11. Landquist, J. K. In *Comprehensive Heterocyclic Chemistry*; Katritzky, A. R., Rees, C. W., Eds.; Pergamon: Oxford, **1984**, *1*, 166.
12. (a) Bansal, Y.; Silakari, O. *Bioorg. Med. Chem.* **2012**, *20*, 6208; (b) Michael, J. P. *Nat. Prod. Rep.* **2008**, *25*, 166; (c) Marzaro, G.; Guiotto, A.; Chilin, A. *Expert Opin. Ther. Pat.* **2012**, *22*, 223.
13. Raghavendra, N. M.; Thampi, P.; Gurubasavarajaswamy, P. M.; Sriram, D. *Chem. Pharm. Bull.* **2007**, *55*, 1615.
14. Verhaeghe, P.; Azas, N.; Gasquet, M.; Hutter, S.; Ducros, C.; Laget, M.; Rault, S.; Rathelot, P.; Vanelle, P. *Bioorg. Med. Chem. Lett.* **2008**, *18*, 396.
15. (a) Alagarsamy, V.; Solomon, V. R.; Sheorey, R. V.; Jayakumar, R. *Chem. Biol. Drug Des.* **2009**, *73*, 471; (b) Smits, R. A.; Adami, M.; Istyastono, E. P.; Zuiderveld, O. P.; van Dam, C. M. E.; de Kanter, F. J. J.; Jongejan, A.; Coruzzi, G.; Leurs, R.; de Esch, I. J. P. *J. Med. Chem.* **2010**, *53*, 2390.
16. Georgey, H.; Abdel-Gawad, N.; Abbas, S. *Molecules* **2008**, *13*, 2557.
17. Panneerselvam, P.; Rather, B. A.; Reddy, D. R. S.; Kumar, N. R. *Eur. J. Med. Chem.* **2009**, *44*, 2328.

18. Ismail, M. A. H.; Barker, S.; Abau El Ella, D. A.; Abouzid, K. A. M.; Toubar, R. A.; Todd, M. H. *J. Med. Chem.* **2006**, *49*, 1526.
19. (a) Kasibhatla, S.; Baichwal, V.; Cai, S. X.; Roth, B.; Skvortsva, I.; Skvortsov, S.; Lucas, P.; English, N. M.; Sirisoma, N.; Drewe, J.; Pervin, A.; Tseng, B.; Carlson, R. O.; Pleiman, C. M. *Cancer Res.* **2007**, *67*, 5865; (b) Font, M.; Gonzalez, A.; Palop, J. A.; Sanmartin, C. *Eur. J. Med. Chem.* **2011**, *46*, 3887; (c) Liu, F.; Lovejoy, D. B.; Hassani, A. A.; He, Y.; Herold, J. M.; Chen, X.; Yates, C. M.; Frye, S. V.; Brown, P. J.; Huang, J.; Vedadi, M.; Arrowsmith, C. H.; Jin, J. *J. Med. Chem.* **2011**, *54*, 6139; (d) EI-Azab, A. S.; Al-Omar, M. A.; Abdel-Aziz, A. A. M.; Abdel-Aziz, N. I.; EI-Sayed, M. A. -A.; Aleisa, A. M.; Sayad-Ahmed, M. M.; Abdel-Hamide, S. G. *Eur. J. Med. Chem.* **2010**, *45*, 4188; (e) Noolvi, M. N.; Patel, H. M.; Bhardwaj, V.; Chauhan, A. *Eur. J. Med. Chem.* **2011**, *46*, 2327.
20. (a) Chandrika, P. M.; Yakaiah, T.; Rao, A. R. R.; Narsaiah, B.; Reddy, N. C.; Srindar, V.; Rao, J. V. *Eur. J. Med. Chem.* **2008**, *43*, 846; (b) Al-Obaid, A. M.; Abdel-Hamide, S. G. A.; El-Kashef, H. A.; Abdel-Aziz, A. A.-M.; El-Azad, A. S.; Al-Khamees, H. A.; El-Subbagh, H. I. *Eur. J. Med. Chem.* **2009**, *44*, 2379; (c) Li, M.; Jung, A.; Ganswindt, U.; Marini, P.; Friedl, A.; Daniel, P. T.; Lauber, K.; Jendrossek, V.; Belka, C. *Biochem. Pharmacol.* **2010**, *79*, 122; (d) Sirisoma, N.; Pervin, A.; Zhang, H.; Jiang, S.; Willardsen, J. A.; Anderson, M. B.; Mather, G.; Pleiman, C. M.; Kasibhatla, S.; Tseng, B.; Drewe, J.; Cai, S. X. *J. Med. Chem.* **2009**, *52*, 2341; (e) Sirisoma, N.; Pervin, A.; Zhang, H.; Jiang, S.; Adam, W. J.; Anderson, M. B.; Mather, G.; Pleiman, C. M.; Kasibhatla, S.; Tseng, B.; Drewe, J.; Cai, S. X. *Bioorg. Med. Chem. Lett.* **2010**, *20*, 2330.
21. (a) Garofalo, A.; Goossens, L.; Lemoine, A.; Ravez, S.; Six, P.; Howsam, M.; Farce, A.; Depreux, P. *Med. Chem. Commun.* **2011**, *2*, 65; (b) Nakamura, H.; Horikoshi, R.; Usui, T.; Ban, H. S. *Med. Chem. Commun.* **2010**, *1*, 282; (c) Li, R. D.; Zhang, X.; Li, Q. Y.; Ge, Z. M.; Li, R. T. *Bioorg. Med. Chem. Lett.* **2011**, *21*, 3637; (d) Cruz-Lopez, O.; Conejo-Garcia, A.; Nunez, M. C.; Kimatrai, M.; Garcia-Rubino, M. E.; Morales, F.; Gomez-Perez, V.; Campos, J. M. *Curr. Med. Chem.* **2011**, *18*, 943.
22. Chinigo, G. M.; Paige, M.; Grindrod, S.; Hamel, E.; Dakshanamurthy, S.; Chruszcz, M.; Minor, W.; Brown, M. L. *J. Med. Chem.* **2008**, *51*, 4620.
23. (a) Sardon, T.; Cottin, T.; Xu, J.; Giannis, A.; Vernos, I. *Chem. Biol. Chem.* **2009**, *10*, 464; (b) Bebbington, D.; Binch, H.; Charrier, J.-D.; Everitt, S.; Fraysse, D.; Golec, J.; Kay, D.; Knegtel, R.; Mak, C.; Mazzei, F.; Miller, A.; Mortimore, M.; O'Donnell, M.;

Patel, S.; Pierard, F.; Pinder, J.; Pollard, J.; Ramaya, S.; Robinson, D.; Rutherford, A.; Studley, J.; Westcott, J. *Bioorg. Med. Chem. Lett.* **2009**, *19*, 3586.

24. Cao, S. L.; Wang, Y.; Zhu, L.; Liao, J.; Guo, Y. W.; Chen, L. L.; Liu, H. Q.; Xu, X. *Eur. J. Med. Chem.* **2010**, *45*, 3850.
25. (a) Sirisoma, N.; Kasibhatla, S.; Pervin, A.; Zhang, H.; Jiang, S.; Willardsen, J. A.; Anderson, M. B.; Baichwal, V.; Mather, G. G.; Jessing, K.; Hussain, R.; Hoang, K.; Pleiman, C. M.; Tseng, B.; Drewe, J.; Cai, S. X. *J. Med. Chem.* **2008**, *51*, 4771; (b) Olaussen, K. A.; Commo, F.; Tailler, M.; Lacroix, L.; Vitale, I.; Raza, S. Q.; Richon, C.; Dessen, P.; Lazar, V.; Soria, J. C.; Kroemer, G. *Oncogene* **2009**, *28*, 4249.
26. (a) Hong, S. Y.; Kwak, K. W.; Ryu, C. K.; Kang, S. J.; Chung, K. H. *Bioorg. Med. Chem.* **2008**, *16*, 644; (b) Boiani, M.; Gonzalez, M. *Mini-Rev. Med. Chem.* **2005**, *5*, 409.
27. (a) Krim, J.; Grunewald, C.; Taourirte, M.; Engels, J. W. *Bioorg. Med. Chem.* **2012**, *20*, 480; (b) Goker, H.; Ozden, S.; Yıldız, S.; Boykin, D. W. *Eur. J. Med. Chem.* **2005**, *40*, 1062; (c) Bandyopadhyay, P.; Sathe, M.; Ponmariappan, S.; Sharma, A.; Sharma, P.; Srivastava, A. K.; Kaushik, M. P. *Bioorg. Med. Chem. Lett.* **2011**, *21*, 7306.
28. Xu, J. Y.; Zeng, Y.; Ran, Q.; Wei, Z.; Bi, Y.; He, Q. H.; Wang, Q. J.; Hu, S.; Zhang, J.; Tang, M. Y.; Hua, W. Y.; Wu, X. M. *Bioorg. Med. Chem. Lett.* **2007**, *17*, 2921.
29. Taniguchi, K.; Shigenaga, S.; Ogahara, T.; Fujitsu, T.; Matsuo, M. *Chem. Pharm. Bull.* **1993**, *41*, 301.
30. Soto, S. E.; Molina, R. V.; Crespo, F. A.; Galicia, J. V.; Dıaz, H. O.; Piedra, M. T.; Vazquez, G. N. *Life Sci.* **2006**, *79*, 430.
31. (a) Starcevic, K.; Kralj, M.; Ester, K.; Sabol, I.; Grce, M.; Pavelic, K.; Zamola, G. K. *Bioorg. Med. Chem.* **2007**, *15*, 4419; (b) Fonseca, T.; Gigante, B.; Marques, M. M.; Gilchrist, L. T.; Clercq, E. D. *Bioorg. Med. Chem.* **2004**, *12*, 103.
32. (a) Snow, R. J.; Abeywardane, A.; Campbell, S.; Lord, J.; Kashem, M. A.; Khine, H. H.; King, J.; Kowalski, J. A.; Pullen, S. S.; Roma, T.; Roth, G. P.; Sarko, C. R.; Wilson, N. S.; Winters, M. S.; Wolak, J. P.; Cywin, C. L. *Bioorg. Med. Chem. Lett.* **2007**, *17*, 3660; (b) Lewaire, G.; Delescluse, C.; Pralavorio, M.; Ledirac, N.; Lesca, P.; Rahmani, R. *Life Sci.* **2004**, *74*, 2265.
33. (a) Duan, Y. C.; Ma, Y. C.; Zhang, E.; Shi, X. J.; Wang, M. M.; Ye, X. W.; Liu, H. M. *Eur. J. Med. Chem.* **2013**, *62*, 11; (b) Jeankumar, V. U.; Renuka, J.; Santosh, P.; Soni, V.; Sridevi, J. P.; Suryadevara, P.; Yogeeswari, P.; Sriram, D. *Eur. J. Med.*

Chem. **2013**, *70*, 143; (c) Malika, S.; Bahare, R. S.; Khana, S. A. *Eur. J. Med. Chem.* **2013**, *67*, 1. (d) Singh, P.; Kaur, M.; Verma, P. *Bioorg. Med. Chem. Lett.*, **2009***, 19,* 3054. (e) Hans, R. H.; Wiid, I. J. F.; van Helden, P. D.; Wanc, B.; Franzblau, S. G.; Gut, J.; Rosenthal, P. J.; Chibale, K. *Bioorg, Med. Chem. Lett.* **2011**, *21*, 2055.

34. Sun, Z.; Wang, H.; Wen, K.; Li, Y.; Fan, E. *J. Org. Chem.* **2011**, *76*, 4149.
35. Grever, M. R.; Sehepartz, S. A.; Chabners, B. A. *Semin. Oncol.* **1992**, *19*, 622.
36. Monks, A.; Schudiero, D.; Skehan, P.; Shoemaker, R.; Paull, K.; Vistica, D.; Hose, C.; Langley, J.; Cronise, P.; Vaigro-Wolff, A.; Gray-Goodrich, M.; Campbell, H.; Mayo, J.; Boyd, M. *J. Natl. Cancer Inst.* **1991**, *83*, 757.
37. Boyd, M. R.; Paull, K. D. *Drug Dev. Res.* **1995**, *34*, 91.
38. Elzahabi, H. S. A. *Eur. J. Med. Chem.*, **2011**, *46*, 4025.
39. Caco, A. I.; Tome, L. C.; Dohrn, R.; Marrucho, I. M. *J. Chem. Eng. Data* **2010**, *55*, 3160.
40. QSARINS(QSAR-INSubria): QSARINS, software for QSAR MLR model Development and validation, version 2.1- 2014, QSAR Research Unit in Environmental Chemistry and Ecotoxicology, Department of theoretical and applied sciences (DiSTA), University of Insubria, Via J.H. Dunant 3, Varese, Italy. http://www.qsar.it.
41. Ribeiro, F. A. L.; Ferreira, M. M. C. *J. Mol. Struct. (Theochem.)* **2003**, *663*, 109.
42. Molfetta, F. A.; Bruni, A. T.; Rosseli, F. P.; da Silva, A. B. F. *Struct. Chem.* **2007**, *18*, 49.
43. SciGress Ultra: Molecular Modeling System 7.7.0.47, FujitsuKyushu Systems, Fukuoka-Shi, Japan, 1981.
44. Neaz, M. M.; Muddassar, M.; Pasha, F. A.; Cho, S. J. *Acta Pharmacol. Sin.* **2010**, *31* 244.
45. (a) Fernandes, P. A.; Maria, J. R. *J. Am. Chem. Soc.* **2003**, *125*, 6311; (b) Bailly, C. *Chem. Rev.* **2012**, *112*, 3611; (c) Pommier, Y. *Chem. Rev.* **2009**, *109*, 2894.
46. Compounds were constructed and docked with builder toolkit of the software package ArgusLab 4.0.1 (www.arguslab.com).
47. Alley, M. C.; Scudiero, D. A.; Monks, P. P.; Hursey, M. L.; Czerwinski, M. J.; Fine, D. L.; Abbott, B. J.; Mayo, J. G;. Shoemaker, R. H.; Boyd, M. R. *Cancer Res*. **1988**, *48*, 589.

CHAPTER-3

Purine-Benzimidazole Hybridization

3.1. INTRODUCTION

Cancer is a complex manifestation of genomic instability in cells that leads to disruption of basic biological functions, such as cell division, differentiation, angiogenesis and migration, which promote cancer.[1] Cancer represents one of the most pressing health challenges of 21st century. The American Cancer Society estimated that only year, 2014 over 16,65,540 cases of cancer were diagnosed in the United States alone and that over 5,85,720 people died from this disease.[2] In the course of identifying various chemical substances which may serve as leads for designing novel antitumor agents, we were particularly interested in the molecular hybridization of purine and benzimidazole derivatives as these two moieties have been identified as a new class of cancer chemotherapeutic agents with significant therapeutic efficacy against solid tumors.[3] It is well known that purine derivatives are potent inhibitors of Aurora kinase,[4] cyclin dependent kinase (CDK),[5] epidermal growth factor receptor (EGFR) and vascular endothelial growth factor receptor (VEGFR).[6] Consequently, various approaches have been adopted to enhance the potency and selectivity of these inhibitors. These efforts led to discovery of many drugs such as Olomoucine, Roscovitine, R-CR8 and Dinaciclib (**Figure 1**) that have also maintained selectivity towards various kinases. Olomoucine and Roscovitine are first discovered CDK inhibitors while the optically pure R-enantiomer of Roscovitine (Seliciclib) is currently being evaluated as an oncology drug candidate in patient diagnosed with non small cell lung cancer and nasopharyngeal cancer or other malignancies.[7] The anti-HIV/HBV drugs *abacavir* and *penciclovir* are some of the purine drugs, also available presently in the market.[8]

Similarly, benzimidazole and its derivatives are categorized as the important pharmacophores and privileged sub-structures in medicinal chemistry owing to their involvement as a key component for various biological activities.[9] Benzimidazole derivatives are among the important heterocyclic compounds that found in natural and non-natural products such as vitamin B12, marine alkaloid kealiiquinone[10] etc. Some of their derivatives are marketed as anti-fungal agent such as Carbendazim,[11] anti-helmintic agents such as Mebendazole and Thiabendazole[12] and anti-psychotic drug such as Pimozide.[13]

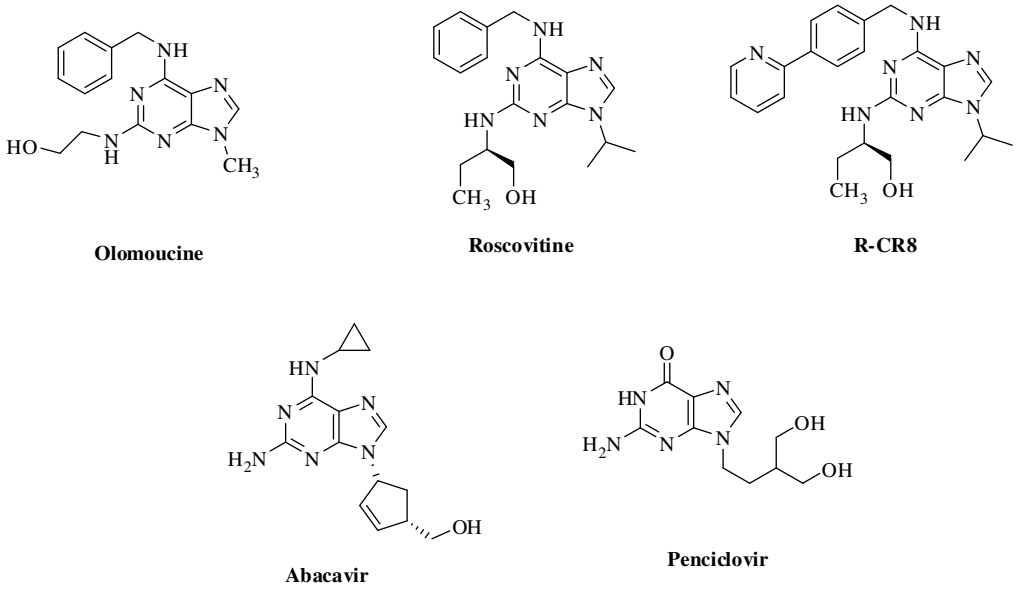

Figure 1. Purine related drugs

Objective:

Various methods for the synthesis of purine with different substitution have been documented in the literature. It has been found that most of the study was done with amine derivatives like pyrazole, morpholine, piperidine, piperazine etc at 6-position of purine as anticancer drugs but no report has been given about the synthesis and evaluation of benzimidazole linked with purine (at 6-position). Regioisomeric alkylation of benzimidazole moiety has not been reported for different electronic environment towards the purine ring. As a part of our research programme aimed at developing amino benzimidazole moiety at 6-position of purine with secondary amines at 2-position became interesting to develop a new and highly potent hybrids as anticancer agents.

3.2. DESGINING

Knowledge from other purine-based kinase inhibitors, such as Roscovitine, served as inspiration and lead structure for this chapter. Roscovitine has also been found to produce apoptosis in treated cancerous cells of non-small cell lung cancer (NSCLC) and other cancers. Based on the structure of Roscovitine, we planned to synthesize several series of analogs of purine-benzimidazole hybrids and indicated that the extended benzimidazole group should occupy the selectivity pocket, play an important role in its activity and selectivity. Thus, a new series of purine-benzimidazole molecular hybrids using some of the common features of purine and benzimidazole drugs have been designed (**Figure 2**). These compounds have been synthesized and evaluated through 60

human cancer cell lines for *in vitro* antitumor activities as well as Aurora A kinase inhibitors. Aurora-A which belongs to the Aurora kinase family, was first discovered in the screening for Drosophila mutations affecting the poles of the mitotic spindle function.[14,15] Human Aurora-A is located on the chromosome 20q13 and found overexpressed in several human cancers. Many research groups have proved that the overexpression of Aurora-A induces several cancer-associated phenotypes, including enhanced cell proliferation and colony formation, and inhibition of apoptosis.[16-18] The substitution pattern at the 2,6-disubstituted purine and benzimidazole pharmacophore were selected so as to confer different electronic environment that would affect the activity of target molecules. These hybrid molecules consisted of heterocyclic ring (purine) as central core that can act as a scaffold to carry two functionalized branches at positions 2 and 6, in such a way to accommodate a benzimidazole ring at 6-position and secondary amines at 2-position of purine. Introduction of butyl and allyl groups at 1- or 3-position of benzimidazole has also increase lipid solubility of polar compounds, a character very much needed for the activity. Meanwhile, in current drug research field, substituted purines have attracted considerable attention from the medicinal chemists in recent years, owing to the high number of positive hits encountered with this heterocycle. The physical properties can be modulated by further substitution of hydrophilic/hydrophobic part to the purine or benzimidazole ring. SAR and QSAR studies were used to identify the structural features, required for the antitumor properties of these new hybrid series. In order to have an insight into the molecular interaction of compounds with Aurora kinase, their docking was also planned to scrutinize the mode of interactions of compound with amino acids in the active site of the enzyme.

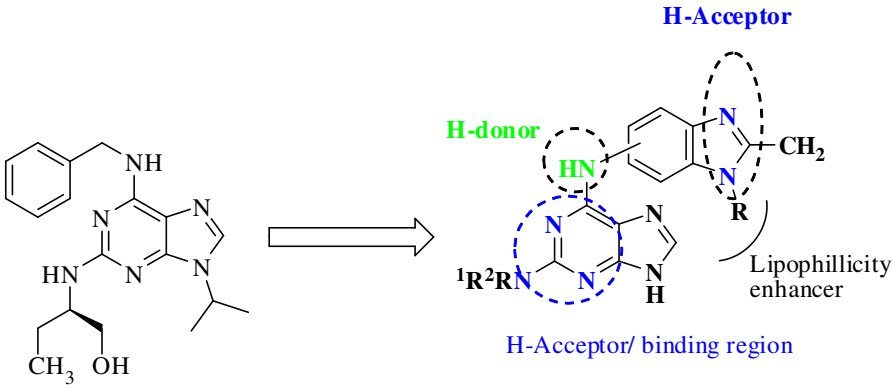

Figure 2. Designing of Purine-benzimidazole hybrids

3.3. CHEMISTRY

3.3.1. Synthesis of purine-benzimidazole hybrids

The synthetic strategy to prepare the purine-benzimidazole hybrids **(3-19)** has been depicted in **scheme 1**. The target compounds were achieved in three steps using 3,4-dihydro-1*H*-purin-2,6-(5*H*,9*H*)-dione as starting material. Refluxing of 3,4-dihydro-1*H*-purin-2,6-(5*H*,9*H*)-dione with phosphorus oxychloride in the presence of triethylamine for 5 h afforded 2,6-dichloropurine **(1)** (mp. 117-120 °C). *N*-1-Allyl-2-methyl-1*H*-benzo[*d*]imidazol-5-ylamine **(2a)** and *N*-3-allyl-2-methyl-3*H*-benzo[*d*]imidazol-5-ylamine **(2c)** have been synthesized and characterized as given in chapter 2. *N*-1/3-Butyl-2-methyl-1*H/3H*-benzo[*d*]imidazole-5-ylamine has been synthesized by the alkylation of 2-methyl-5-nitro-benzimidazole (0.05 mol) with butyl bromide (0.075 mol) in the presence of NaH (0.126 mol) in THF at room temperature for 8 h followed by treatment with suspension of $SnCl_2.2H_2O$ (135 mmol) in 2N HCl (95.2 ml) at 110 $^{\circ}$C for 7 h. After the completion of the reaction, the suspension was neutralized with 2N NaOH and diluted with ethanol. Filtered and extracted the filtrate, dried over Na_2SO_4, concentrated to get mixture of products which were separated through column chromatography using ethylacetate : methanol (9.5:0.5) to get pure solid compounds of **2b** (EIMS, m/z; 203.4 (M^++1)) and **2d** (EIMS, m/z; 203.4 (M^+ + 1)). ^{1}H NMR spectrum of compound **2b** showed the 3H triplet at δ 0.97 of butyl-CH_3, two 2H multiplets at δ 1.39 and 1.77 of butyl-CH_2, 3H singlet at δ 2.55 of CH_3, 2H multiplet at δ 4.04 of butyl-NCH_2, 1H multiplet at δ 6.67 of aromatic-H, two 1H doublets at δ 7.08 and 7.46 of aromatic-H. IR spectrum also showed the peaks at 3314, 3184 (NH_2), 2955 2921 (CH), 1624, 1465, 1401 (C=C), 1211 cm^{-1}. On the basis of these spectral data, this compound has been assigned the structure of *N*-1-butyl-2-methyl-1*H*-benzo[*d*]imidazol-5-ylamine **(2b)**. Similarly, ^{1}H NMR spectrum of **2d** showed 3H triplet at δ 0.96 of butyl-CH_3, two 2H multiplets at δ 1.41 and 1.76 of butyl-CH_2, 3H singlet at δ 2.52 of CH_3, 2H triplet at δ 3.98 of butyl-NCH_2, 1H doublet at δ 6.56 and 7.44 and 1H double doublet at δ 6.62 of aromatic-H. IR spectrum also showed the peaks at 3349, 3198 (NH_2), 2956, 2926 (CH), 1624, 1454, 1406 (C=C), 1213 cm^{-1}. On the basis of these spectral data, this compound has been confirmed the structure of *N*-3-butyl-2-methyl-3*H*-benzo[*d*]imidazol-5-ylamine **(2d).**

2,6-Dichloropurine **(1)** was treated with **2a** and **2b** in the presence of isopropyl alcohol (IPA) at room temperature for 24 h gave **3a** (EIMS, m/z; 340.1 (M^+ + 1)) and **3b** (EIMS, m/z; 356.1 (M^+ + 1)) with 79% and 47% yields respectively. ^{1}H NMR spectrum of **3a** showed the

appearance of 3H singlet at δ 2.56 of CH_3, 2H doublet at δ 5.11 of allyl-NCH_2, two 1H doublets at δ 5.29 and 5.36 of allyl-CH_2, 1H multiplet at δ 6.08 of allyl-CH, two 1H doublets at δ 7.80 and 7.97, 1H singlet at δ 8.60 of aromatic-H, 1H singlet at δ 8.66 of CH and two 1H broad singlets at δ 10.58 and 13.36 of NH (exchangeable with D_2O). ^{13}C NMR spectrum showed the signals at δ 12.2 (CH_3), 46.9 (allyl-NCH_2), 112.6 (allyl-NCH_2-<u>CH</u>-CH_2), 119.0 (allyl-CH_2), 128.3, 131.2 (ArH), 132.1, 137.6, 151.2, 151.5, 152.5 (ArH). IR spectrum also showed the peaks at 3354, 3305 (NH), 3199 (CH), 1637, 1596, 1496, 1302, 1250, 1166 cm^{-1}. On the basis of these spectral data, this compound has been assigned the structure of *N*-(1-allyl-2-methyl-1*H*-benzo[*d*]imidazol-5-yl)-2-chloro-9*H*-purin-6-amine **(3a)**. Similarly, ^1H NMR spectrum of compound **3b** showed the appearance of 3H triplet at δ 1.01 of butyl-CH_3, two 2H multiplets at δ 1.51 and 1.92 of butyl-CH_2, 3H singlet at δ 2.82 of CH_3, 2H triplet at δ 4.36 of butyl-NCH_2, two 1H doublets at δ 7.75 and 7.87 of aromatic-H, 1H singlet at δ 8.32 of aromatic-H, 1H singlet at δ 8.59 of CH, two 1H broad singlets at δ 8.72 and 10.62 of NH (exchangeable with D_2O). ^{13}C NMR spectrum showed the signals at δ 12.2 (butyl-CH_3), 13.6 (CH_3), 19.5, 25.1 (butyl-CH_2), 46.8 (butyl-NCH_2), 101.0, 115.2, 117.3, 132.9, 136.7, 137.4, 150.3, 151.1, 152.6 (ArH). IR spectrum also showed the peaks at 3380 (NH), 2958 (CH), 1648, 1498, 1433, 1232, 1109 cm^{-1}. On the basis of these spectral data, this compound has been assigned the structure of *N*-(1-butyl-2-methyl-1*H*-benzo[*d*]imidazol-5-yl)-2-chloro-9*H*-purin-6-amine **(3b)**.

Refluxing of compounds **3a** and **3b** with morpholine in ethanol for 48 h and after purification with column chromatography gave white powder of **4** (EIMS, m/z; 391.0 (M^+ + 1)) and **8 (**EIMS, m/z; 407.5 (M^+ + 1)) with 75% and 63% yields respectively. ^1H NMR spectrum of compound **4** showed appearance of 3H singlet at δ 2.59 of CH_3, 8H singlet at δ 3.80 of morCH_2, 2H doublet at δ 4.72 of allyl-NCH_2, two 1H doublets at δ 4.99 and 5.24 of allyl-NCH_2, 1H multiplet at δ 5.96 of allyl-CH, 1H doublet at δ 7.46, two 1H singlets at δ 7.66 and 7.83 of aromatic-H, 1H singlet at δ 8.20 of CH and 1H broad singlet at δ 10.03 of NH (exchangeable with D_2O). ^{13}C NMR spectrum of this compound showed signals at δ 13.6 CH_3, 29.4, 45.1 (N-morCH_2), 45.6 (allyl-NCH_2), 66.7 (O-morCH_2), 108.9 (allyl-NCH_2-<u>CH</u>-CH_2), 110.1, 115.9 (ArH), 116.9 (allyl-CH_2), 131.1, 131.7, 133.4, 134.1, 142.5, 151.9, 159.2 (ArH). IR spectrum also showed the peaks at 3322 (NH), 3066, 2975 (CH), 1626, 1588, 1478, 1424, 1293, 1168, 1110 cm^{-1}. On the basis of these spectral data, this compound has been assigned the structure of *N*-(1-allyl-2-methyl-1*H*-benzo[*d*]imidazol-5-yl)-2-morpholino-9*H*-purin-6-amine **(4)**. Similarly, ^1H NMR spectrum of **8** showed appearance of 3H triplet at δ 1.01 of butyl-CH_3, two 2H multiplets at δ 1.45 and 1.85 of butyl-CH_2, 3H singlet at δ 2.62 of

CH_3 group, two 4H triplets at δ 2.61 and 3.90 of morCH$_2$, 2H triplet at δ 4.17 of butyl-NCH$_2$, two 1H doublets at δ 7.62 and 7.83, 1H singlet at δ 7.69 of aromatic-H, 1H singlet at δ 8.17 of CH and two 1H broad singlets at δ 8.76 and 12.23 of NH (exchangeable with D_2O). ^{13}C NMR spectrum of this compound showed the signals at δ 13.3 (butyl-CH_3), 19.5, 31.2 (butyl-CH_2), 42.9 (butyl-NCH$_2$), 43.1 (N-morCH$_2$), 44.7 (N-morCH$_2$), 48.9, 63.3 (O-morCH$_2$), 66.2 (O-morCH$_2$), 108.6, 109.5, 115.6, 130.5, 133.9, 141.7, 151.2, 158.7 (ArH). IR spectrum also showed the peaks at 3317 (NH), 3060, 2962 (CH), 1589, 1480, 1428, 1292, 1261, 1170, 1107 cm^{-1}. On the basis of these spectral data, this compound has been assigned the structure of *N*-(1-butyl-2-methyl-1*H*-benzo[*d*]imidazol-5-yl)-2-morpholino-9*H*-purin-6-amine **(8)**. Similarly, treatment of compounds **3a** and **3b** with piperidine, pyrrolidine and N-methylpiperazine at the same reaction conditions to obtained **5-7** and **9-11** with 53-74% and 55-80% yields respectively.

Similarly, compounds **2c** and **2d** were also treated with 2,4-dichloropurine at the same reaction conditions to obtain **3c** (EIMS, m/z; 340.1 (M^+ + 1)) and **3d** (EIMS, m/z; 356.1 (M^+ + 1)) with 94% and 86% yields respectively. ^1H NMR spectrum of **3c** showed the appearance of 3H singlet at δ 2.77 of CH_3, 2H doublet at δ 4.97 of allyl-NCH$_2$, 2H triplet at δ 5.40 of allyl-CH$_2$, 1H multiplet at δ 6.05 of allyl-CH, two 1H doublets at δ 7.71 and 8.27, 1H singlet at δ 7.82 of aromatic-H, 1H singlet at δ 8.48 of CH and two 1H broad singlets at δ 8.69 and 10.54 of NH (exchangeable with D_2O). ^{13}C NMR spectrum showed the signals at δ 12.0 (CH_3), 46.9 (allyl-NCH$_2$), 103.8 (allyl-NCH$_2$-<u>CH</u>-CH$_2$), 114.9, 115.1 (allyl-CH$_2$), 119.4, 119.8, 119.9 (ArH), 130.8, 136.6, 151.4, 152.4 (ArH). IR spectrum also showed the peaks at 3341 (NH), 3122, 2964 (CH), 1646, 1559, 1422, 1230, 1128 cm^{-1}. On the basis of these spectral data, this compound has been assigned the structure of *N*-(3-allyl-2-methyl-3*H*-benzo[*d*]imidazol-5-yl)-2-chloro-9*H*-purin-6-amine **(3c)**. Similarly, ^1H NMR spectrum of **3d** showed appearance of 3H doublet at δ 0.96 of butyl-CH_3, two 2H multiplets at δ 1.46 and 1.89 of butyl-CH$_2$, 3H singlet at δ 2.79 of CH_3, 2H triplet at δ 4.34 of butyl-NCH$_2$, two 1H doublets at δ 7.75 and 7.82, 1H singlet at δ 8.35 of aromatic-H, 1H singlet at δ 8.53 of CH and two 1H broad singlets at δ 8.78 and 10.65 of NH (exchangeable with D_2O). ^{13}C NMR spectrum showed the signals at δ 10.7 (butyl-CH_3), 12.4 (CH_3), 19.6, 30.4 (butyl-CH$_2$), 45.5 (butyl-NCH$_2$), 105.4, 109.3, 121.5, 127.1, 131.7, 135.2, 139.5, 147.8, 149.3, 150.6, 156.5 (ArH). IR spectrum also showed the peaks at 3350 (NH), 2959 (CH), 1649, 1500, 1432, 1235, 1112 cm^{-1}. On the basis of these spectral data, this compound has been assigned the structure of *N*-(3-butyl-2-methyl-3*H*-benzo[*d*]imidazol-5-yl)-2-chloro-9*H*-purin-6-amine **(3d)**.

Refluxing of compounds **3c** and **3d** with morpholine in ethanol for 48 h and after purification with column chromatography gave solid of compounds **12** (EIMS, m/z; 391.4 (M^+ + 1)) and **16** (EIMS, m/z; 407.5 (M^+ + 1)) with 96% and 65% yields respectively. ^{1}H NMR spectrum of compound **12** showed appearance of 3H singlet at δ 2.53 of CH_3, two 4H singlets at δ 2.57 and 3.73 of morCH$_2$, 2H singlet at δ 4.75 of allyl-NCH$_2$, two 1H doublets at δ 4.86 and 5.20 of allyl-CH$_2$, 1H multiplet at δ 6.03 of allyl-CH, 1H doublet at δ 7.49, two 1H singlets at δ 7.69 and 8.01 of aromatic-H, 1H singlet at δ 8.28 of CH and two 1H broad singlets at δ 9.19 and 12.29 of NH (exchangeable with D_2O). ^{13}C NMR spectrum showed the signals at δ 13.1 CH_3, 30.4, 44.7 (N-morCH$_2$), 44.9 (allyl-NCH$_2$), 66.2 (O-morCH$_2$), 100.6, 113.4 (allyl-NCH$_2$-CH-CH$_2$), 114.9, 116.0 (allyl-CH$_2$), 117.8, 131.4, 134.5, 134.7, 135.9, 137.5, 150.8, 151.2, 151.7, 158.6 (ArH). IR spectrum also showed the peaks at 3394 (NH), 2958 (CH), 1626, 1583, 1458, 1309, 1101 cm^{-1}. On the basis of these spectral data, this compound has been assigned the structure of *N*-(3-allyl-2-methyl-3*H*-benzo[*d*]imidazol-5-yl)-2-morpholino-9*H*-purin-6-amine **(12)**. Similarly, ^{1}H NMR spectrum of **16** showed appearance of 3H triplet at δ 0.99 of butyl-CH$_3$, two 2H multiplets at δ 1.39 and 1.77 of butyl-CH$_2$, 3H singlet at δ 2.53 of CH_3, 4H doublet at δ 2.54 of N-morCH$_2$, 4H singlet at δ 3.73 of O-morCH$_2$, 2H triplet at δ 4.12 of butyl-NCH$_2$, two 1H doublets at δ 7.43 and 7.50, 1H singlet at δ 7.80 of aromatic-H, 1H singlet at δ 8.25 of CH and two 1H broad singlets at δ 9.42 and 12.46 of NH (exchangeable with D_2O). ^{13}C NMR spectrum showed the signals at δ 13.6 (butyl-CH$_3$), 19.6 (CH_3), 25.3, 30.6 (butyl-CH$_2$), 31.2 (butyl-NCH$_2$), 44.9 (N-morCH$_2$), 48.6, 66.1 (O-morCH$_2$), 99.4, 101.0, 115.2, 117.6, 134.6, 134.7, 136.5, 137.7, 158.6 (ArH). IR

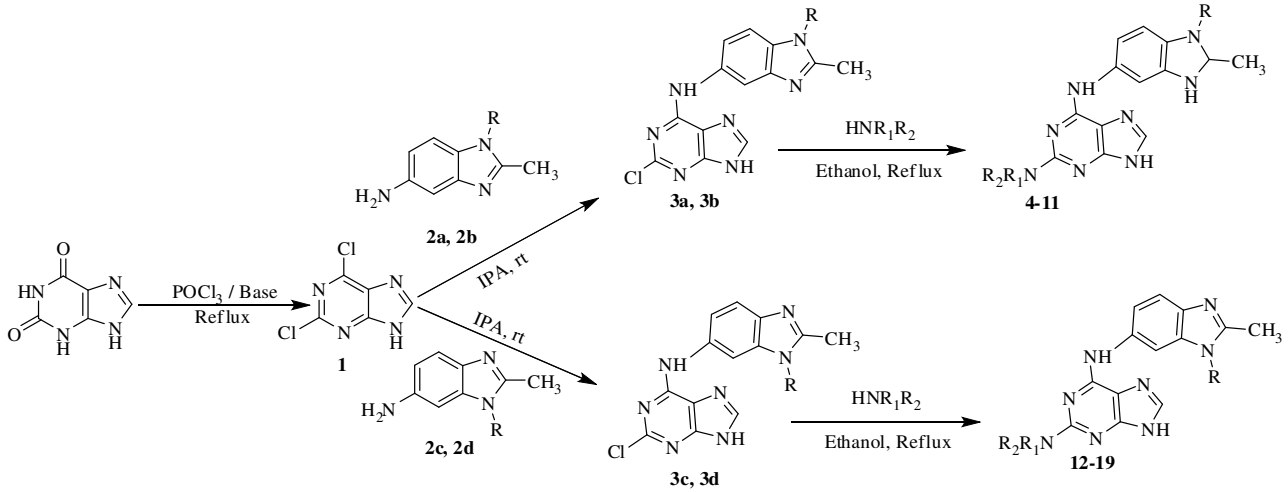

Scheme 1. Synthetic route for the preparation of target compounds **4-19**

spectrum also showed the peaks at 3353 (NH), 2931 (CH), 1600, 1585, 1471, 1431, 1382, 1254, 1124 cm^{-1}. On the basis of these spectral data, this compound has been assigned the structure of *N*-(3-butyl-2-methyl-3*H*-benzo[*d*]imidazol-5-yl)-2-morpholino-9*H*-purin-6-amine (**16**). Similarly, treatment of compounds **3c** and **3d** with piperidine, pyrrolidine and N-methylpiperazine at the same reaction conditions to obtain **13-15** and **17-19** with 55-85% and 70-82% yields respectively.

We have also tried the reaction with primary amines like aniline, 4-fluoroaniline, 2,6-difluoroaniline, 4-aminothiophenol, 4-aminophenol etc. as well as Suzuki coupling with various boronic acids at different reaction conditions, but in all the cases only starting material was recovered.

Table 1. Physicochemical properties of the newly synthesized compounds **3a-d** and **4-19**

Compds	Starting Material	NHR_1R_2	% yields	M.pt. (°C)	Molecular formulae
3a	2a	--	79	270 (d)	$C_{16}H_{14}N_7Cl$
3b	2b	--	47	260 (d)	$C_{17}H_{18}N_7Cl$
3c	2c	--	94	285(d)	$C_{16}H_{14}N_7Cl$
3d	2d	--	86	280 (d)	$C_{17}H_{18}N_7Cl$
4	3a	morpholin-4-yl	75	239-240	$C_{20}H_{22}N_8O$
5	3a	piperidin-1-yl	53	242-244	$C_{21}H_{24}N_8$
6	3a	pyrrolidin-1-yl	60	260(d)	$C_{20}H_{22}N_8$
7	3a	4-methylpiperazin-1-yl	74	70-72	$C_{21}H_{25}N_9$
8	3b	morpholin-4-yl	63	228-232	$C_{21}H_{26}N_8O$
9	3b	piperidin-1-yl	72	218-220	$C_{22}H_{28}N_8$
10	3b	pyrrolidin-1-yl	80	280 (d)	$C_{21}H_{26}N_8$
11	3b	4-methylpiperazin-1-yl	55	225-228	$C_{22}H_{29}N_9$
12	3c	morpholin-4-yl	96	260(d)	$C_{20}H_{22}N_8O$
13	3c	piperidin-1-yl	85	243-245	$C_{21}H_{24}N_8$
14	3c	pyrrolidin-1-yl	55	240(d)	$C_{20}H_{22}N_8$
15	3c	4-methylpiperazin-1-yl	62	159-162	$C_{21}H_{25}N_9$
16	3d	morpholin-4-yl	65	218 (d)	$C_{21}H_{26}N_8O$
17	3d	piperidin-1-yl	72	278 (d)	$C_{22}H_{28}N_8$
18	3d	pyrrolidin-1-yl	70	260 (d)	$C_{21}H_{26}N_8$
19	3d	4-methylpiperazin-1-yl	82	238-240	$C_{22}H_{29}N_9$

3.3.2. Single Crystal X-ray diffraction

N-(3-Butyl-2-methyl-3*H*-benzo[*d*]imidazol-5-yl)-2-(4-methylpiperazin-1-yl)-9*H*-purin-6-amine (**19**) was grown in ethanol to develop single crystal and the following data was obtained. Molecular formula = $C_{22}H_{29}N_9.H_2O$, M.wt. = 437.56, colourless crystal, monoclinic, space group $P2_1/c$, a = 8.6730 (9) Å, b = 12.6408 (14) Å, c = 21.721 (3) Å, α = 90.0°, β = 101.007 (6)°, γ = 90.0°, V = 2337.5 (4) $Å^3$, Z = 4, D_{calcd} = 1.243 Mg/m^3,

Absorption coefficient = 0.082 mm^{-1}, reflection collected = 11271, Unique: 3545 (R_{int} = 0.0897), Final R indices = R_1 = 0.0668, wR_2 = 0.1396, R indices = R_1 = 0.1473, wR_2 = 0.1643, Extinction coefficient = 0.0043(7) with Crystalispro diffractometer with graphite monochromated Mo Kα radiation (λ = 0.71073 Å) using SHELX-97, full-matrix least-square refinement method (**Table-2**). The molecular solid state structure and numbering system is indicated in **figure 3**.[19] The six-membered 4-methylpiperazine ring is positioned planar to the purine ring that exists in chair conformation. Atom system C13-N1-C2 is in regular tetrahedron sp^3 angle of 109.5°. Atom system C3–N2–C14 having some angle strain, deviated by 2.7° from the ideal value (angle strain is calculated as the difference between internal angle and the ideal sp^3 angle of 109.5°).

The benzimidazole ring C7–C6–N4 is deviated from the planar purine ring N4–C5–C15 by 2.2°. The bond lengths of two C–N bonds linking between benzimidazole and purine rings are differ, with the short N4-C5 [1.364 (4) Å] bond having a double-bond character compared with the longer N4–C6 [1.401 (4) Å] on benzimidazole side. It is indicated that the two carbon atoms (C5 and C6) in the molecule occupy anti-positions relative to the mean plane of the ring system. This anti-position of both carbon atoms in each molecule is one of the reason which makes the two rings are non planar. The bond length of N9‑C21 [1.337 (5)] of benzimidazole ring is shorter having double bond character than that longer bond length of C21‑N5 [1.365 (4)] indicate the presence of butyl group at N5 position. Comparing the bond distances of N6-C16 (1.307(4)Å) and N7-C16 (1.372(4)Å) of five membered purine ring, it has been clear that former has double bond character than later. Four water molecules have been encapsulated in a unit cell, stabilised by hydrogen bonds. The water molecule has been found to be two kinds of hydrogen bond interactions (a) NH···O or N···HO (b) CH···O. The NH···O interactions are with linker NH [N4H4···O1S(H_2O); *d* = 2.09Å], with purine N-atom N···OH [N6(purine)···H5C O1S(H_2O); *d* = 2.10Å] and with substituted piperazine ring N···HO [N1···H4C O1S; *d* = 1.92 Å]. The CH···O interactions are with the hydrogen atom of benzene of benzimidazole moiety [C19H19···O1S; *d* = 2.70Å], and with hydrogen atom of base moiety purine ring [C16H16···O1S; *d* = 2.59Å]. All these parameters have been examined graphically using Mercury 3.3.

Table 2. Summary of crystal data, data collection and structure refinement for compound **19**

A. Crystal data	
Chemical formula	$C_{22}H_{29}N_{9,}H_2O$
Formula weight	437.56

Temperature	296(2) K
Wavelength	0.71073 Å
Crystal habit	Colourless
Crystal system	Monoclinic
Space group	$P2_1/c$
Unit cell dimensions	a = 8.6730(9) Å α = 90°
	b = 12.6408(14) Å β = 01.007(6)°
	c = 21.721(3) γ = 90°
Volume	2337.5(4) $Å^3$
Z	4
Density (calculated)	1.243 Mg/cm^3
Absorption coefficient	0.082 mm^{-1}
F(000)	936

B. Data collection and structure refinement

Theta range for data collection	1.87 to 25.05°
Index ranges	-10<=h<=10, -15<=k<=14, 25<=l<=25
Reflections collected	11271
Independent reflections	3545 [R(int) = 0.0897]
Coverage of independent reflections	85.8%
Absorption correction	Multi-scan
Structure solution technique	Direct methods
Structure solution program	SHELXS-97 (Sheldrick, 2008)
Refinement method	Full-matrix least-squares on F^2
Function minimized	Σ w(Fo2 - Fc2)2
Data / restraints / parameters	3545 / 0 / 301
Goodness-of-fit on F2	0.820
Δ/σmax	0.001
Final R indices	1511 data; I > 2σ(I) R1 = 0.0668, wR2 = 0.1396
	R1 = 0.1473, wR2 = 01643
Weighting scheme	$w=1/[\sigma^2(F_o^2)+(0.0623P)^2+0.0000P]$ where, $P=(F_o^2+2F_c^2)/3$
Extinction coefficient	0.0043(7)

Largest diff. peak and hole	0.279 and -0.306 eÅ^{-3}
R.M.S. deviation from mean	0.104 eÅ^{-3}

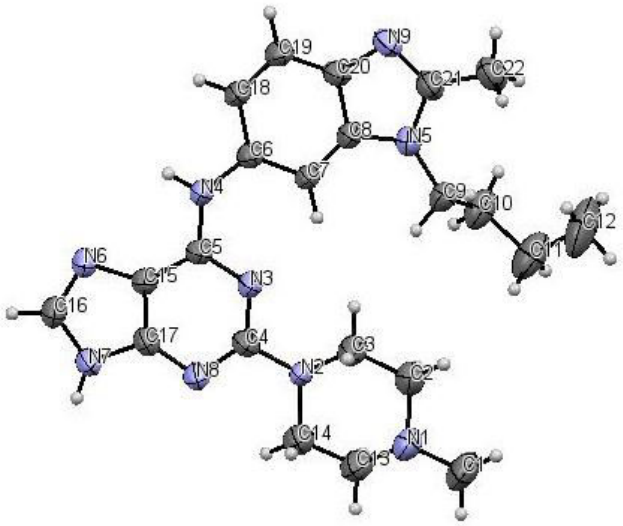

Figure 3. ORTEP diagram of compound **19** (CCDC No. 1022534)

3.4. BIOLOGY

3.4.1. *In vitro* evaluation of 60 human cancer cell line studies

All the synthesized compounds were submitted to National Cancer Institute (NCI) disease-oriented human cell lines for screening assay, to be evaluated for their *in-vitro* antitumor activities (**Table 3-4**). Fourteen compounds (**3a-d, 4, 6-11, 16, 18-19**) were evaluated against 60 human cancer cell lines at single dose of 10 µM which included nine tumor subpanels namely; leukemia, non-small lung, colon, CNS, melanoma, ovarian, renal, prostate and breast cancer cells.[20-23] Their outputs were reported as a mean graph of the percent growth of treated cells, and presented as percentage growth inhibition (GI%). Compound **6** exhibited significant growth inhibition and was evaluated for further 60 cell panel at five dose concentration levels.

Preliminary *in vitro* antitumor screening was revealed that only compounds belonging to the series **4-11** showed significant inhibition for most of cancer cell lines. The percentage of growth inhibition for cancer cells were more than 50% in a number of the tested derivatives. On the contrary, compounds **18** and **19** showed weak activities compared with other compounds and percentage of inhibition did not reach 30% except one or two cell lines. These variations could be correlated to the difference in positions of allyl or butyl group on

the benzimidazole moiety in which the distance between the core purine moiety and allyl or butyl chain of benzimidazole are important factor for affecting antitumor activity. In this series of compounds, a significant inhibition was observed for non-small cell lung cancer cell (HOP-92; 22.50-95.83%), renal cancer (A498; 21.32-98.65%) and breast cancer cells (HS 578T; 31.72-93.87% and T-47D; 21.94-93.22%).

Regarding the activity towards individual cell lines; compounds **3a**, **3c**, **4**, **8**, **10** and **16** showed selective potency against lung cancer cell HOP-92 with GI values of 74.56%, 70.48%, 95.83%, 81.36%, 76.97% and 72.25% respectively. Compound **6** proved to be active towards leukemia cell RPMI-8226 with GI value of 70.09%, lung cell NCI-H60 with GI value of 99.63%, colon cells HT29 and KM12 with GI values of 87.58% and 86.91%, CNS cells SF-268 and U251 with GI values of 70.69% and 78.76%, melanoma cells M14 and MDA-MB-435 with GI values of 71.21% and 90.84%, renal cells A498, ACHN and TK-10 with GI values of 98.65%, 82.19% and 88.17% respectively. Meanwhile, compound **9** showed selectivity towards leukemia cells K-562 and MOLT-4 with GI values of 71.25% and 90.95%; colon cell COLO 205 with GI value of 71.08%, CNS cell SNB-75 with GI value of 88.56%; ovarian cell OVCAR-4 with GI value of 80.98%, renal cell RXF 393 with GI value of 77.90%, prostate cell PC-3 with GI value of 74.35% and breast cancer cell lines BT-549 and T-47D with GI values of 82.04% and 93.22% respectively. In addition, compounds **3b** and **16** showed activity toward the renal cancer cell line A498 with GI values of 74.03% and 77.40% respectively.

Table 3. The Percentage growth inhibition (GI%) of compounds **3a-d**, **4** and **6-7** over the full panel of tumor cell lines at 10 μM concentration

Cell Line Type	Cell Line Name	3a	3b	3c	3d	4	6	7
Leukemia	CCRF-CEM	-	21.97	-	47.02	-	-	-
	HL-60(TB)	NT	NT	NT	NT	NT	NT	NT
	K-562	-	-	-	30.16	28.99	L	-
	MOLT-4	-	35.99	-	62.09	25.57	-	-
	RPMI-8226	-	34.63	-	56.32	-	**70.09**	-
	SR	L	33.33	-	57.49	-	L	-
Non-Small Cell Lung Cancer	A549/ATCC	-	-	-	-	-	53.68	-
	EKVX	NT	NT	NT	NT	NT	NT	NT
	HOP-62	-	34.02	20.18	33.85	32.23	49.42	-
	HOP-92	**74.56**	L	**70.48**	L	**95.83**	L	22.50
	NCI-H226	-	24.96	-	37.58	-	41.13	-
	NCI-H23	-	22.09	-	24.69	-	47.62	-
	NCI-H322M	-	23.19	-	-	-	49.13	
	NCI-H460	-	-	-	29.08	-	**99.63**	-
	NCI-H522	-	-	-	26.84	-	43.72	-
Colon Cancer	COLO 205	-	-	-	-	-	26.58	-
	HCC-2998	-	-	-	-	-	23.60	-
	HCT-116	-	-	-	32.25	-	L	-

	HCT-15	-	-	-	-	-	-	-
	HT29	-	-	-	20.10	-	**87.58**	-
	KM12	-	-	-	22.49	-	**86.91**	-
	SW-620	-	-	-	21.42	-	59.17	-
CNS Cancer	SF-268	-	-	-	23.96	-	**70.69**	-
	SF-295	-	25.52	-	23.65	-	68.80	-
	SF-539	-	23.73	-	20.14	-	L	-
	SNB-19	-	-	-	-	-	55.06	-
	SNB-75	-	21.64	-	37.21	-	L	-
	U251	-	22.83	-	25.50	-	**78.76**	-
Melanoma	LOX IMVI	-	-	-	-	-	44.20	-
	MALME-3M	-	20.18	-	21.86	-	L	-
	M14	-	-	-	31.66	-	**71.21**	-
	MDA-MB-435	-	-	-	22.76	-	**90.84**	-
	SK-MEL-28	-	-	-	-	-	69.75	-
	SK-MEL-5	-	26.37	-	36.37	-	50.51	-
	UACC-257	-	-	-	-	-	39.10	-
	UACC-62	-	26.99	-	30.22	-	68.30	-
Ovarian Cancer	IGROV1	-	29.29	-	31.76	27.15	44.20	-
	OVCAR-3	-	-	-	37.31	-	L	-
	OVCAR-4	-	21.09	-	31.65	-	L	-
	OVCAR-5	-	-	-	25.50	25.87	69.4	-
	OVCAR-8	-	-	-	21.80	-	25.26	-
	NCI/ADR-RES	-	-	-	-	-	-	-
	SK-OV-3	-	-	-	22.97	-	41.04	-
Renal Cancer	786-0	-	23.64	-	44.61	36.94	L	-
	A498	21.32	**74.03**	41.89	L	62.54	**98.65**	25.02
	ACHN	-	-	-	21.01		**82.19**	-
	CAKI-1	-	23.91	-	39.46		-	-
	RXF 393	-	-	-	37.14		45.58	-
	SN12C	-	21.08	-	25.40		63.21	-
	TK-10	-	26.48	-	32.74		**88.17**	-
	UO-31	-	35.43	21.76	42.24		38.76	-
Prostate Cancer	PC-3	21.08	40.30	27.66	63.69	20.08	57.43	-
	DU-145	-	-	-	-	-	51.75	-
Breast Cancer	MCF7	-	24.59	-	23.50		26.45	-
	MDA-MB-231/ATCC	20.88	25.00	33.88	35.15	22.28	L	-
	HS 578T	-	47.32	34.75	**93.87**	42.68	L	-
	BT-549	-	27.72	-	52.21	-	L	-
	T-47D	-	60.70	21.94	66.07	24.63	54.96	-
	MDA-MB-468	-	55.72	18.57	65.36	-	48.94	-

Prominent GI values are bolded.

- GI < 20%; L, compounds proved lethal to the cancer cell line; NT, not tested.

Table 4. Percentage growth inhibition (GI%) of *in vitro* subpanel tumour cell lines at 10 μM concentration of compounds **8-11, 16** and **18, 19**

Cell Line Type	Cell Line Name	8	9	10	11	16	18	19
Leukemia	CCRF-CEM	30.34	53.43	-	-	50.66	-	-
	HL-60(TB)	-	21.58	NT	-	-	-	-
	K-562	42.33	**71.25**	-	-	37.24	-	-
	MOLT-4	30.68	**90.95**	-	-	45.85	-	-
	RPMI-8226	37.88	59.66	21.39	-	47.17	-	-
	SR	-	68.80	27.71	-	36.40	29.22	-
Non-Small	A549/ATCC	-	51.55	-	-	22.58	-	-

Cell Lung Cancer								
	EKVX	-	47.46	NT	-	-	-	-
	HOP-62	24.32	37.91	21.93	-	27.81	-	-
	HOP-92	**81.36**	L	**76.97**	24.45	**72.25**	50.20	35.15
	NCI-H226	28.20	55.57	-	-	43.41	28.95	-
	NCI-H23	21.98	48.63	-	-	21.25	-	-
	NCI-H322M	-	-	-	-	-	-	-
	NCI-H460	-	34.46	-	-	-	-	-
	NCI-H522	23.35	47.36	-	-	25.42	-	-
Colon Cancer	COLO 205	-	**71.08**	-	-	20.45	-	-
	HCC-2998	-	33.80	-		L	-	-
	HCT-116	25.14	51.22	-	-	-	-	24.21
	HCT-15	-	47.13	-	-	-	-	-
	HT29	-	40.24	-	-	-	-	-
	KM12	-	61.91	-	-	23.46	-	-
	SW-620	-	21.00	-	-	-	-	-
CNS Cancer	SF-268	26.38	39.58	-	-	30.84	-	26.76
	SF-295	20.41	52.91	-	-	-	-	-
	SF-539	-	28.82	-	-	-	-	-
	SNB-19	-	26.75	-	-	-	-	-
	SNB-75	67.69	**88.56**	-	-	46.88	28.36	36.53
	U251	-	41.46	-	-	22.51	-	-
Melanoma	LOX IMVI	44.20	66.30	-	-	34.86	-	-
	MALME-3M	-	38.45	-	-	-	-	-
	M14	-	67.16	-	-	-	-	-
	MDA-MB-435	-	62.64	-	-	-	-	-
	SK-MEL-28	-	23.99	-	-	-	-	-
	SK-MEL-5	23.53	L	-	-	35.93	31.68	-
	UACC-257	-	37.86	-	-	-	-	-
	UACC-62	33.96	54.55	-	-	53.72	-	-
Ovarian Cancer	IGROV1	52.86	**70.00**	-	-	-	-	-
	OVCAR-3	27.08	62.30	-	-	23.24	-	-
	OVCAR-4	-	**80.98**	-	-	29.23	-	-
	OVCAR-5	25.97	49.85	-	-	-	-	-
	OVCAR-8	38.60	**70.00**	-	-	50.47	-	-
	NCI/ADR-RES	-	64.96	-	-	-	-	-
	SK-OV-3	-	33.55	-	-	-	-	-
Renal Cancer	786-0	28.37	50.87	-	-	27.68	-	-
	A498	51.31	65.66	40.69	-	**77.40**	53.97	28.29
	ACHN	45.91	63.17	-	-	21.42	-	-
	CAKI-1	-	68.85	40.14	-	-	30.60	-
	RXF 393	54.76	**77.90**	24.46	-	69.03	-	-
	SN12C	28.97	50.44	-	-	28.00	-	-
	TK-10	23.90	42.83	-	-	28.88	21.14	-
	UO-31	51.53	**71.94**	32.52	-	63.63	44.13	-
Prostate Cancer	PC-3	27.52	**74.35**	-	-	26.56	-	-
	DU-145	22.05	39.83	-	-	24.32	-	-
Breast Cancer	MCF7	-	67.53	-	-	-	-	-
	MDA-MB-231/ATCC	26.93	60.75	26.78	-	34.49	-	-
	HS 578T	33.98	56.25	-	-	31.72	-	-
	BT-549	-	**82.04**	-	-	30.83	-	-
	T-47D	48.08	**93.22**	-	-	55.08	41.88	-
	MDA-MB-468	-	63.90	21.94	-	32.57	28.37	-

Prominent GI values are bolded.

- GI < 20%; L, compounds proved lethal to the cancer cell line; NT, not tested.

Table 5. Compound **6** and **5-FU** median growth inhibitory (GI_{50}, μM), total growth inhibitory (TGI, μM) and median lethal concentrations (LC_{50}, μM) of *in vitro* subpanel tumour cell lines.

Compounds	Activity	I	II	III	IV	V	VI	VII	VIII	IX	MG-MID[a]
6	GI_{50}	54.5	b	3.16	2.00	29.6	1.34	b	b	b	18.12
	TGI	b	b	b	b	b	b	b	b	b	b
	LC_{50}	b	b	b	b	b	b	b	b	b	b
5-FU	GI_{50}	15.1	b	8.4	72.1	70.6	61.4	45.6	22.7	76.4	22.60
	TGI	b	b	b	b	b	b	b	b	b	b
	LC_{50}	b	b	b	b	b	b	b	b	b	b

I, Leukemia; II, non-small cell lung cancer; III, colon cancer; IV, CNS cancer; V, melanoma; VI, ovarian cancer; VII, renal cancer; VIII, prostate cancer; IX, breast cancer.

[a] Full panel mean-graph midpoint (μM).

[b] Compounds showed values >100 μM.

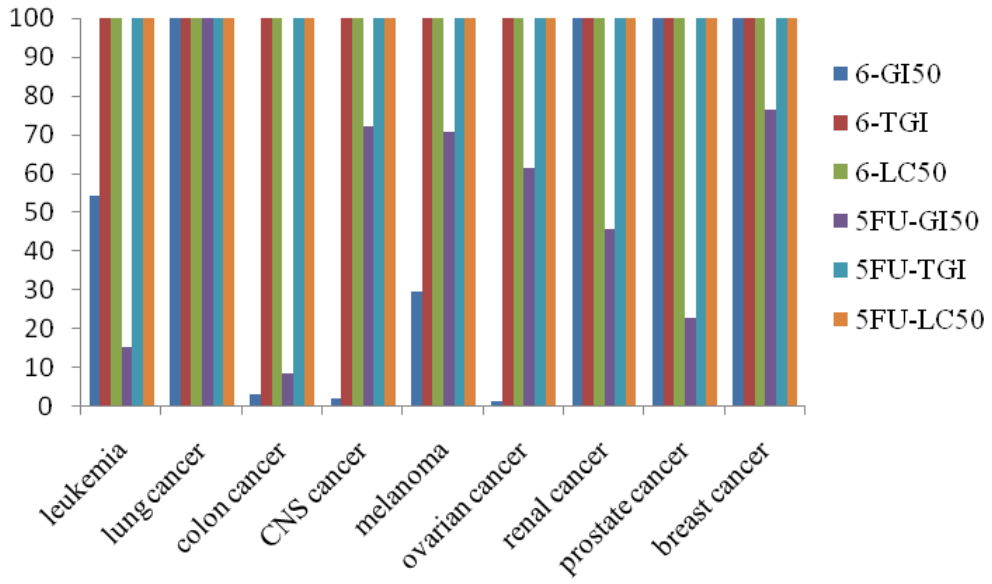

Figure 4. Compound **6** and **5-FU** median growth inhibitory (GI_{50}, μM), total growth inhibitory (TGI, μM) and median lethal concentrations (LC_{50}, μM) of *in vitro* subpanel tumor cell lines.

From the above data, it is clear that compound **6** is the most active member of the series. Consequently, this active compound was carried over and tested against a panel of different tumor cell lines at 5-dose concentration range. Three response parameters, GI_{50}, TGI and LC_{50} were monitored for each cell line, using the known drug 5-fluorouracil (5-FU) as a positive control. Compound **6** showed specificity towards colon, CNS and ovarian cancer cell lines with GI_{50} values of 3.16, 2.00 and 1.34 μM respectively. MG-MID revealed that

compound **6** is 1.25 fold more active than 5-FU, with GI_{50} value of 18.12 µM (**Table-5**, **Figure 4-5**).

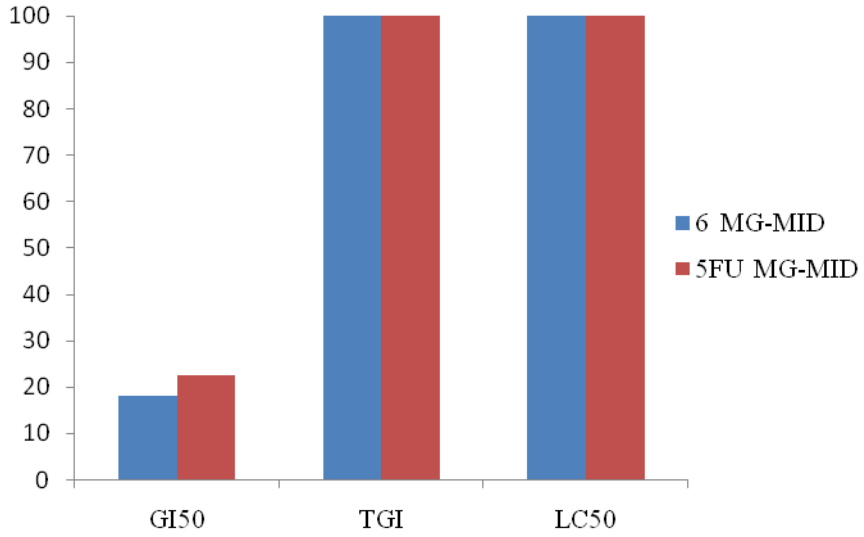

Figure 5. Comparison of full panel mean-graph midpoint (µM) of compound **6** with **5-FU**.

3.4.2. *In vitro* evaluation of Aurora kinase inhibitors

Based on the anticancer activities of the synthesized compounds, it was desirable to investigate some of the compounds for probable cellular targets. Interactions of the compounds with Aurora-A enzyme involved in the process of propagation of cancer, has been investigated with the help of enzyme immunoassay using Aurora-A kinase inhibitor screening kit.[24] It has been shown that compounds **3a** and **5** displayed least activity towards Aurora A with IC_{50} values of 8.00 and 8.50 µM respectively. Amines substitution at C2 position of purine with morpholine and pyrrolidine resulted compounds **4** and **6** respectively that showed excellent inhibitory activity towards Aurora-A with IC_{50} values of 0.02 and 0.01 µM (**Table-6**). Substitution of **3a** with piperidine (compound **5**) decreased the inhibitory activity while substitution with 4-methylpiperazine(compound **7**) increased the Aurora A inhibitory activity with IC_{50} value of 0.07 µM. Replacement of N-allyl group with N-butyl group (compound **3b**) of benzimidazole resulted in increase in potency with IC_{50} value of 0.07 µM. Substitution of **3b** at C2 position of purine with pyrrolidine resulted in almost 10 fold decrease in inhibitory activity. Therefore, it seems that the compound **6** under present investigation probably target Aurora-A for exhibiting best anticancer activity. Ligand

efficiency (LE) has also been determined for these compounds that indicated the higher efficiency of compound **6** with LE = 0.39 for binding to the enzyme.

Table 6. Aurora A kinase inhibitory activities of purine derivatives

Compounds	IC_{50} (µM)	Ligand efficieny[a]
3a	8.00	0.29
3b	0.07	0.38
4	0.02	0.24
5	8.50	0.35
6	**0.01**	**0.39**
7	0.07	0.29
10	0.70	0.33

[a] Calculated using the formula: LE = [-1.4× $\log_{10}$ (IC_{50} (M))]/(number of non hydrogen atoms).

3.5. PHYSICO CHEMICAL PARAMETERS

The partition of the molecules was studied in octanol/water systems for determining the log P values by shake-flask method.[25]Lipophilicity is a crucial factor for the activity amongst the synthesized compounds. The lipophilic aptitude of a compound increased with increasing log P. It has been indicated that compound **6** (**Table 7**) showed higher log P value that supported the dependency of lipophilicity with higher activity of this compound towards Aurora A inhibition and cancer cell lines.

Table 7. Experimental determined lipophilicity

Compounds	P	Experimental log P
3a	305	2.48
3b	19	1.28
3c	16	1.21
3d	18.16	1.25
4	39	1.59
5	36	1.55
6	**335**	**2.53**
7	18	1.25
8	101	2.00

9	10	1.01
10	23	1.36
11	14	1.15
12	210	2.32
13	48	1.68
14	125	2.09
15	243	2.38
16	50	1.69
17	24	1.38
18	30.46	1.48
19	25	1.39

P—partition coefficient; log P—logarithm of the partition coefficient.

3.6. STRUCTURE-ACTIVITY RELATIONSHIP

Structure-activity correlation, based on the number of cancer cell lines and Aurora A kinase inhibitors revealed that the nature of the substituents at C2- and C6-positions of purine affected the biological functions. Regarding 60 human tumor cell line studies, compounds **4**, **6-11** showed comparatively higher activity than their isomers **16**, **18-19** suggested that there is much difference in antitumor activity with orientations of alkyl chain of benzimidazole. In the first series of compounds, when the allyl group is replaced with butyl group, a comparable affinity is found (compare **3a** and **3b**), but when chloro of **3a** is constrained in a cyclic morpholine system (compound **4**), some activity is increased although other rings are well tolerated as illustrated by pyrrolidine (**6)** and 4-methylpiperazine (**7**) analogues and former showed higher activity than later. Similarly, substitution at C2-position of **3b** with piperidine leading to compound **9** that has increased the activity while decrease in activity was observed with morpholine (**8**), pyrrolidine (**10**) and 4-methylpiperazine (**11**). Another series of compounds **16**, **18-19**, substitution of **3d** with morpholine (**16**) increases the activity while pyrrolidine (**18**) and 4-methylpiperazine (**19**) decreases the activity. The SAR study of Aurora A kinase inhibitory activity was also demonstrated that substitution of **3a** with morpholine (compound **4**), and pyrrolidine (compound **6**) showed almost 400-fold and 800-fold increase in activity while replacement of these cyclic substituent with 4-methylpiperazine decreases the affinity slightly (compound **7**). These studies indicated that

substitution of the purine heterocycle with various cyclic secondary amines led to highly potency towards 60 human cancer cell line activities as well as Aurora A kinase inhibitions.

3.7. QUANTITATIVE STRUCTURE-ACTIVITY RELATIONSHIP

Quantitative structure-activity relationship studies could provide correlations between inhibitory activities and physico-chemical descriptors of compounds. Inhibitory concentration (IC_{50}) of purine-benzimidazole hybrid compounds was first calculated by Aurora-A kinase assay kit. Geometries of these compounds were refined by means of semi empirical method PM3 that were used for theoretical descriptors being incorporated into QSARs by using QSARINS Software.[26] The results obtained in order to work out QSAR model for using a training set of 7 compounds (purine-benzimidazoles) predicting log(IC_{50}) corresponds to different descriptors. The structural descriptors employed in this work, such as log P, heat of formation, molar refractivity and steric energy are all obtained directly from the SciGress project leader data.[27] We have used these descriptor(s) for calculating Q^2, R^2, $RMSE_{cv}$, $RMSE_{tr}$ and F by using one, two, three and four descriptor(s) and optimal equations 1, 2, 3 and 4 were obtained as follows:

log (IC_{50}) = - 5.4958 + 0.0856 heat of formation

n = 7 Q^2_{LOO} = - 0.5191, R^2 = 0.1635, ...eq.(1)

$RMSE_{cv}$ = 4.6807, $RMSE_{tr}$ = 3.4734, F = 0.7819

As shown previously for Aurora kinase inhibitors, lipophilicity (log P) seems to be an additional and independent predictive parameter for activity.[28] By introducing this additional parameter into a multiple linear regression analysis, we obtained an improved equation with good predictive power (eq 2):

log (IC_{50}) = - 36.1356 + 6.6367 log P + 0.1801 heat of formation

n = 7 Q^2_{LOO} = - 0.9868, R^2 = 0.3781, ...eq.(2)

$RMSE_{cv}$ = 5.3531, $RMSE_{tr}$ = 2.9948, F = 0.9121

Addition of molar refractivity into multiple linear regression analysis resulted in improvement of equation with good predictive power.

log (IC_{50}) = - 25.7340 + 9.7839 log P + 0.0079 heat of formation + 0.2306 molar refractvity

n = 7 Q^2_{LOO} = - 5.8523, R^2 = 0.6452, ...eq.(3)

$RMSE_{cv}$ = 9.9413, $RMSE_{tr}$ = 2.2621, F = 1.2124

Steric hindrance is also an important parameter for determination of activity of compounds. So on using this parameters into multiple linear regression analysis, we obtained much improved in the correlation coefficient (eq. 4)

log (IC_{50}) = 25.4623 + 14.2235 log P + 0.1660 heat of formation - 0.3082 molar refractivity + 1.1124 steric energy

n = 7 Q^2_{LOO} = 0.9185, R^2 = 0.994, ...eq.(4)

$RMSE_{cv}$ = 1.0444, $RMSE_{tr}$ = 0.2825, F = 83.3054

Here, n - number of data points, R^2 - correlation coefficient, Q^2 - crossvalidated, obtained by leave one out method and F - Fischer statistics.

As it can be observed from eq. 4, the cross-validated Q^2 = 0.9185, correlation coefficient R^2 =

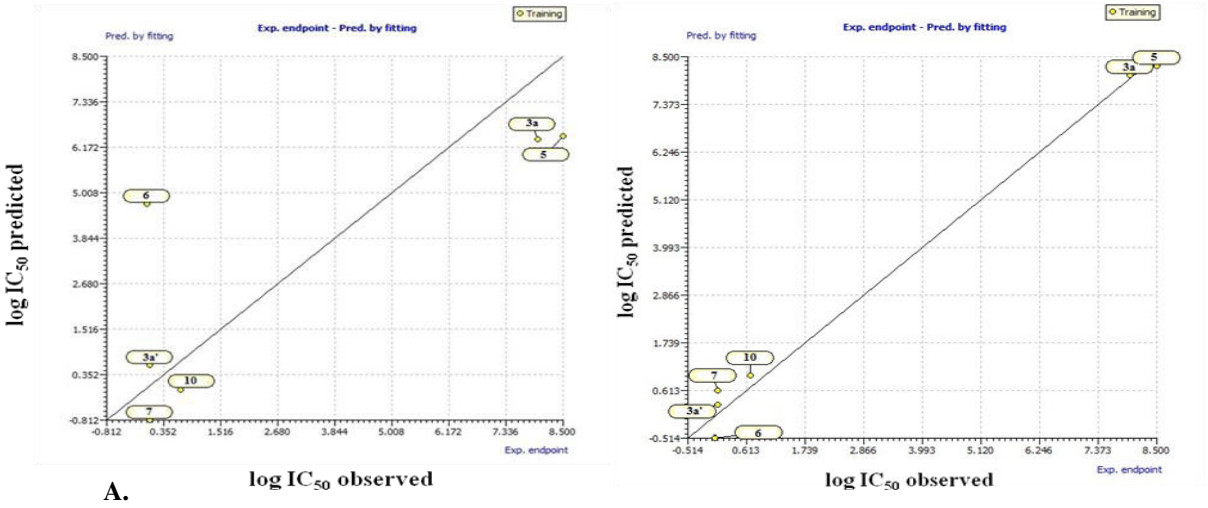

A. **Scatter plot by using three descriptor** **B. Scatter plot by using four descriptor**

Figure 6. Plot of observed vs predicted Aurora A kinase inhibitory activity (expressed as log (IC_{50}) values for compounds **3a-3b**, **4-7** and **10** using (A) eq. 3 and (B) eq. 4). Predicted values were obtained with a leave-one-out cross-validation procedure.

0.994 and degree of statistical confidence for test F = 83.3054 is usually considered significant for the activity. Eq. 4 appears to be the best QSAR model obtained by the multiple linear regression analysis. Eq. 4 showed the positive contribution of log P and steric energy as well as molar refractivity indicating the importance of lipophilicity and steric hindrance of purine towards the benzimidazole rings. **Figure 6** confirmed the best linear character of the equation 4 and its good fitting as compared to another figures.

3.8. MOLCULAR MODELLING

Molecular docking studies were also carried out for compound **6**, which has been proved to be most active compound. Although the cellular targets were not defined in the experimental anticancer investigation of these molecules, to look into the possible interactions at the enzymatic level, we have carried out the docking studies[29] of compound **6** in the active site of Aurora-A kinase (pdb ID 2WTV and pdb ID 2XNE).

Docking of compound **6** in the active site of Aurora-A (2WTV) showed hydrogen bonding interaction of N atom of five membered purine moiety in the active site of His644 (d = 2.48 Å, d = 2.09 Å and d = 2.79 Å) amino acid residue. Linker NH group of purine and benzimidazole showed H-bonding interaction with Asp622 (d = 2.39 Å) amino acid residue and nitrogen atom of benzimidazole moiety showed H-bonding interaction with Ser625 (d = 2.59 Å) amino acid residue. Pyrrolidine moiety also showed hydrogen bonding of N atom with active site of Arg626 (d = 1.87 Å) amino acid residue (**Figure 7**). Therefore, docking of compound **6** in the active site of these enzymes indicated the probable mode of action for anticancer activities. CPK model of Aurora-A kinase (2WTV) also clearly showed the compatibility of compound **6** in the active site of the enzyme (**Figure 8**).

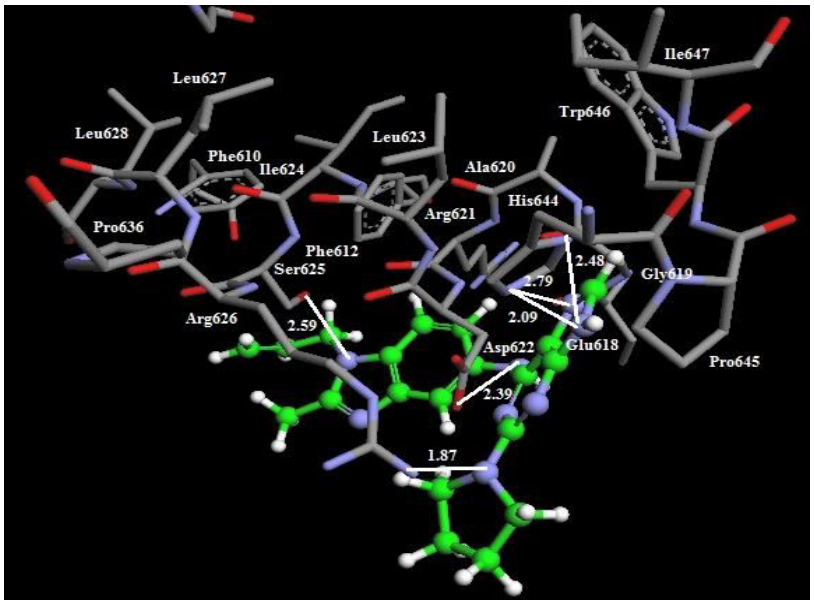

Figure 7. Compound **6** docked in active site of Aurora-A enzyme. H-bonds of compound **6** with different amino acids residues are visible. Carbon atoms are given in green colour.

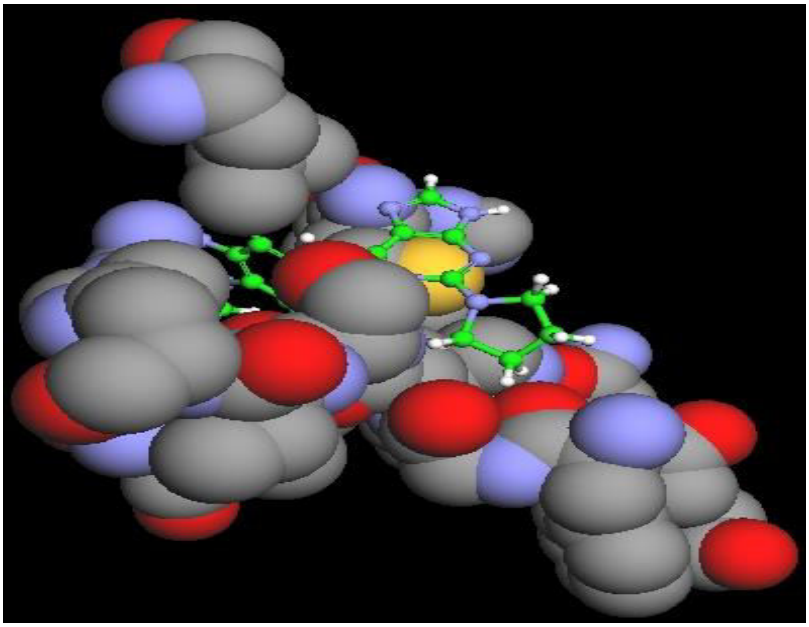

Figure 8. CPK model of active site of Aurora-A enzyme with docking of compound **6**.

The binding mode of purine-benzimidazole-based kinase inhibitors were also elucidated by co-crystallisation of Aurora-A (2XNE) and compared with isoform Aurora B/C. The N9 of purine in compound **6** showed hydrogen bonding with carbonyl group of Leu215 (d = 2.60 Å), amino groups of Leu 264 (d = 2.81 Å) and Gly216 (d = 1.91 Å) in the hinge region of the kinase. Purine N7 is hydrogen bonded to the amino group of Gly216 (d = 2.36 Å) and the nitrogen atom of pyrrolidine to the carbonyl and amino groups of Thr217 (d = 2.39 Å and d = 2.32 Å) as shown in **figure 9**. N1 atom of purine also showed hydrogen bonding with carbonyl group Thr217 (d = 2.66 Å). Linker NH group of benzimidazole and purine showed hydrogen bonding interaction with amino group of Thr217 (d = 2.91 Å). The benzimidazole with allyl chain of the inhibitor sits in a hydrophobic pocket formed the gatekeeper residues Val147, Glu211, Lys162 and Ala160. Importantly, the C2 pyrrolidine moiety substituent resides in close proximity to Val218 of Aurora-A (3.3 Å closest contact), whereas the equivalent residue in Aurora-B/C is a leucine. This is one of the three active site sequence differences between Aurora-A and Aurora-B/C. The Arg220 side chain in Aurora-A (lysine in Aurora-B/C) points away from the active site. We exploited this observation in the design of compounds with substantially enhanced selectivity in inhibiting Aurora-A over isoforms -B and -C. It was envisaged that isoform selectivity for Aurora-A could be achieved by the introduction of a C2 purine and pyrrolidine moieties bearing an electron rich substituent capable of interacting with Leu215, Thr217 and Arg220 in Aurora-A, which would sterically clash with the equivalent residue in Aurora-B/C. It should be noted that Bavetsias et. al. and

Coumar et al. recently reported a pyrazole-based Aurora-A selective inhibitor, and rationalised the selectivity for inhibition of Aurora-A over Aurora-B/C by proposing a similar argument, that is, hydrogen bonding interaction with the backbone NH of Thr217 in Aurora-A and steric clash with the equivalent residue (Glu) in Aurora B/C. [30]

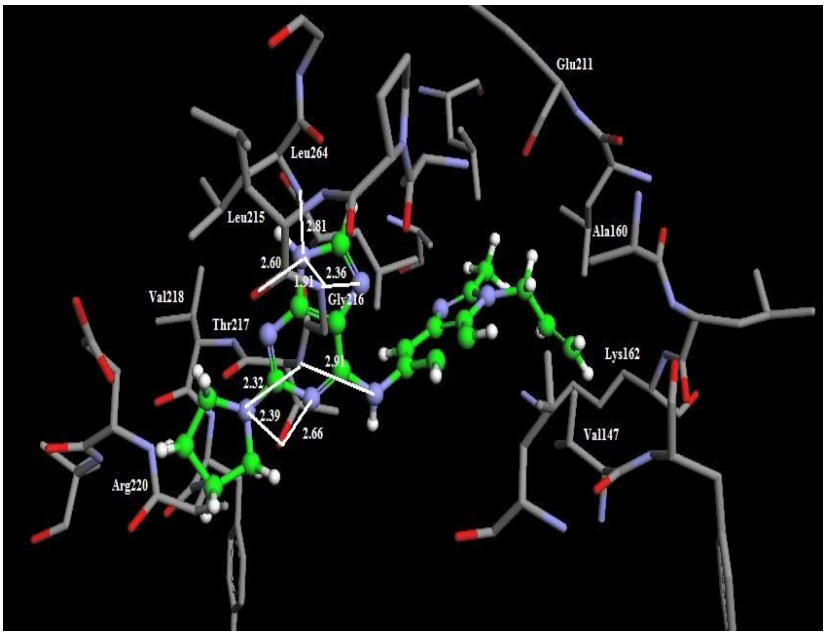

Figure 9. Compound **6** docked in active site of Aurora-A (2XNE). H-bonds of compound **6** with different amino acids residues are visible. Carbon atoms are given in green colour.

3.9. CONCLUSION

This work has led to the development of novel hybrids of purine-benzimidazole molecules and some of which shown promising antitumor activities. These novel molecules have been well characterized by ^{1}H and ^{13}C NMR as well as mass spectrometry, and in case of compound **19**, by X-ray crystallography. At one dose concentration level, compound **6** showed more active in most of the cancer cell lines. It showed sensitivity towards colon cancer, CNS cancer and ovarian cancer with GI_{50} values of 3.16, 2.00 and 1.36 µM respectively with MG-MID GI_{50} value of 18.12 µM, 1.25 fold more active than 5-fluorouracil As per the results of enzyme immunoassays towards Aurora A kinase, compound **6** exhibited significant activity for inhibition of Aurora-A enzyme with IC_{50} value of 0.01 µM. Subsequently, physicochemical studies (Log P) and QSAR model (Log p, steric energy, heat of formation and molar refractivity) for the affinity of this new series of Aurora A kinase inhibitors were developed with good predictive ability. Molecular modelling studies indicating considerable interactions of these compounds in the active site of amino acids of Aurora-A kinase enzyme that also favor the enzyme immunoassay results. The experimental

(60 human cancer cell lines and Aurora A kinase enzyme) as well as theoretical studies (QSAR and molecular modelling) clearly predicted activity of purine-benzimidazole hybrids.

3.10. EXPERIMENTAL SECTION

3.10.1. Synthesis of compounds

General note

Melting points were determined in open capillaries and are uncorrected. For monitoring the progress of the reaction and for comparison with authentic samples, thin layer chromatography (TLC) was used. For this purpose, microslides were coated with silica gel 'G' containing calcium sulphate as binder or with silica gel HF-254 (Spectrochem, india), by dipping a pair of slides held back to back in slurry of adsorbent in chloroform : methanol (80:20). The chromatograms were developed in iodine chamber. Separation of various components was carried out by column chromatography using silica gel 60-120 mesh (Spectrochem, india), as adsorbent and hexane : ethyl acetate, chloroform : methanol or their mixture as eluents. All the fractions collected from column chromatography were compared with chromatograms of reaction mixture (TLC) for checking their identity and purity.

The ^{1}H and ^{13}C NMR spectra were recorded on Jeol ECS-400 at 400 and 100 MHz NMR spectrometer (Tokyo, Japan) respectively, using $CDCl_3$, DMSO-d_6 and trifluoroacetic acid (TFA) as solvents. The chemical shifts were expressed in parts per million with TMS as internal reference and *J* values are given in hertz (Hz). 2D–NOE studies was performed on the same instrument. Spectral patterns are designated as s = singlet; bs = broad singlet; d = doublet; t = triplet; dd = doudle doublet; q = quartet, m = multiplet. Mass Spectra of the synthesized compounds were recorded at Waters Micromass Q-Tof Micro (Milford, MA). Infrared Spectra were recorded on Agilent Technology Cary 630 USA and expressed in wave number (cm^{-1}). The crystal structure was collected on Bruker AXS KAPPA APEX II CCD diffractometer (Billerica, Massachusttes).

Materials: *o*-phenylenediamine, sodium hydride, stannous chloride, allyl bromide, butyl bromide, morpholine, piperidine, pyrrolidine, 4-methylpiperazine, acetic acid, sulphuric acid, nitric acid, tetrahydrofuran, hydrochloric acid, hexane, ethyl acetate, chloroform and methanol were purchased from S.D. fine chemicals, Loba chemicals, Spectrochemical and Sigma Aldrich. Absolute ethanol, hexane, ethyl acetate, chloroform and methanol were of LR grade and were distilled before use.

General procedure for the preparation of *N*-1/3-butyl-2-methyl-1*H*/3*H*-benzo[*d*]imidazole-5-ylamine (2b and 2d).

N-1/3-Butyl-2-methyl-5-nitro-1*H*/3*H*-benzimidazole was synthesized by previous reported method by the alkylation of 2-methyl-5-nitro-1*H*-benzimidazole (0.05 mol) with butyl bromide (0.075 mol) in the presence of NaH (0.126 mol) in THF at room temperature for 8 h. To a suspension of $SnCl_2.2H_2O$ (135 mmol) in 2N HCl (95.2 ml), 1/3-butyl-2-methyl-5-nitro-1*H*/3*H*-benzimidazole (36.4 mmol) was heated at 110 °C for 7 h. After the completion of the reaction (monitored by TLC), the suspension was neutralized with 2N NaOH and diluted with ethanol. Filtered the solid product and extracted the filtrate with chloroform, dried over Na_2SO_4, filtered and concentrated to get mixture of products which were separated through column chromatography using ethylacetate : methanol (9.5:0.5) to get pure solid compounds **2b** and **2d**.

***N*-1-Butyl-2-methyl-1*H*-benzo[*d*]imidazol-5-ylamine (2b).**

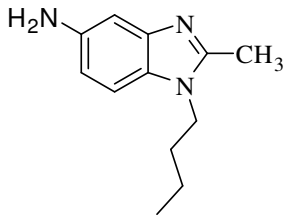

Brownish powder, yield: 52%; mp. 138-140 °C; IR (KBr, cm^{-1}) υ: 3314, 3184, 2955, 2921, 1624, 1465, 1401, 1211; ^{1}H NMR ($CDCl_3$): δ 7.46 (d, 1H, *J* = 8.72 Hz, CH), 7.08 (d, 1H, *J* = 8.24 Hz, ArH), 6.67-6.61 (m, 1H, ArH), 4.04-3.96 (m, 2H, N-CH_2), 2.55 (s, 3H, CH_3), 1.77-1.72 (m, 2H, CH_2), 1.39-1.34 (m, 2H, CH_2), 0.97 (t, 3H, *J* = 3.66 Hz, CH_3); EIMS, m/z: 203.4 (M^+ + 1).

***N*-3-Butyl-2-methyl-3*H*-benzo[*d*]imidazol-5-ylamine (2d).**

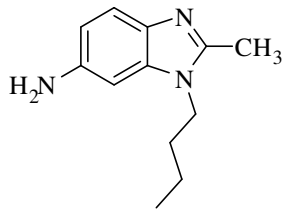

Brownish powder, yield: 86%; mp. 138-140 °C; IR (KBr, cm^{-1}) υ: 3349, 3198, 2956, 2926, 1624, 1454, 1406, 1213; ^{1}H NMR ($CDCl_3$): δ 7.44 (d, 1H, *J* = 8.24 Hz, CH), 6.62 (dd, 1H, ^2J = 8.64 Hz, ^3J = 2.28 Hz, ArH), 6.56 (d, 1H, *J* = 2.28 Hz, ArH), 3.98 (t, 2H, *J* = 7.32 Hz, N-CH_2), 2.52 (s, 3H, CH_3), 1.76-1.69 (m, 2H, CH_2), 1.41-1.32 (m, 2H, CH_2), 0.96 (t, 3H, *J* = 7.36 Hz, CH_3); EIMS, m/z: 203.4 (M^+ + 1).

General procedure for the preparation of 3a-d

To a solution of **2a-d** (5.34 mmol) and isopropyl alcohol (25 ml), 2,6-dichoropurine (5.29 mmol) was added and stirred at room temperature for 24 h. After washing the crude solid with IPA, dried under vacuum to obtain pure white solid of compounds **3a-d**.

***N*-(1-Allyl-2-methyl-1*H*-benzo[*d*]imidazol-5-yl)-2-chloro-9*H*-purin-6-amine (3a).**

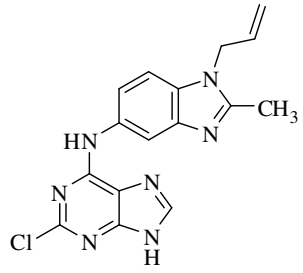

White powder, yield: 79%; mp. 270 °C (d); IR (KBr, cm^{-1}) υ: 3354, 3305, 3199, 1637, 1596, 1496, 1302, 1250, 1166; ^{1}H NMR (DMSO-d_6): δ 13.36 (bs, 1H, NH), 10.58 (bs, 1H, NH), 8.66 (s, 1H, CH), 8.60 (s, 1H, ArH), 7.97 (d, 1H, *J* = 9.16 Hz, ArH), 7.80 (d, 1H, *J* = 8.68 Hz, ArH), 6.08-6.04 (m, 1H, CH), 5.36 (d, 1H, *J* = 10.52 Hz, CH_2), 5.29 (d, 1H, *J* = 16.96 Hz, CH_2), 5.11 (d, 2H, *J* = 5.04 Hz, N-CH_2), 2.56 (s, 3H, CH_3); ^{13}C NMR (DMSO-d_6): δ 152.5, 151.5, 151.2, 137.6, 132.1, 131.2, 128.3, 119.0, 112.6, 46.9, 12.2; EIMS, m/z: 340.1 (M^+ + 1).

***N*-(1-Butyl-2-methyl-1*H*-benzo[*d*]imidazol-5-yl)-2-chloro-9*H*-purin-6-amine (3b).**

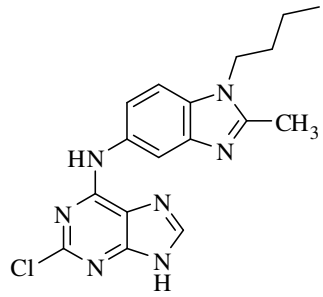

White powder, yield: 47%; mp. 260 °C (d); IR (KBr, cm^{-1}) υ: 3380, 2958, 1648, 1498, 1433, 1232, 1109; ^{1}H NMR (DMSO-d_6): δ 10.62 (bs, 1H, NH), 8.72 (bs, 1H, NH), 8.59 (s, 1H, CH), 8.32 (s, 1H, ArH), 7.87 (d, 1H, *J* = 1.46 Hz, ArH), 7.75 (d, 1H, *J* = 9.16 Hz, ArH), 4.36 (t, 2H, *J* = 7.32 Hz, N-CH_2), 2.82 (s, 3H, CH_3), 3H CH_3), 1.92-1.85 (m, 2H, CH_2), 1.51-1.41 (m, 2H, CH_2), 1.01 (t, 3H, *J* = 7.36 Hz, CH_3); ^{13}C NMR (DMSO-d_6): δ 152.6, 151.1, 150.3, 137.4, 136.7, 132.9, 117.3, 115.2, 101.0, 46.8, 25.1, 19.5, 13.6, 12.2; EIMS, m/z: 356.1 (M^+ + 1).

***N*-(3-Allyl-2-methyl-3*H*-benzo[*d*]imidazol-5-yl)-2-chloro-9*H*-purin-6-amine (3c).**

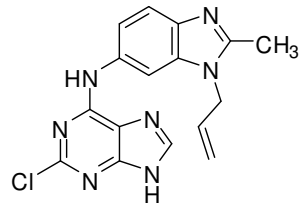

White powder, yield: 94%; mp. 285 °C (d); IR (KBr, cm^{-1}) υ: 3341, 3122, 2964, 1646, 1559, 1422, 1230, 1128; ^{1}H NMR (DMSO-d_6): δ 10.54 (bs, 1H, NH), 8.69 (bs, 1H, NH), 8.48 (s, 1H, CH), 8.27 (d, 1H, *J* = 11.92 Hz, ArH), 7.82 (s, 1H, ArH), 7.71 (d, 1H, *J* = 9.16 Hz, ArH), 6.05-5.98 (m, 1H, CH), 5.40 (t, 2H, *J* = 16.52 Hz, CH_2), 4.97 (d, 2H, *J* = 6.40 Hz, N-CH_2), 2.77 (s, 3H, CH_3); ^{13}C NMR (DMSO-d_6): δ 152.4, 151.4, 136.6, 130.8, 119.9, 119.8, 119.4, 115.1, 114.9, 103.8, 46.9, 12.0; EIMS, m/z: 340.1 (M^+ + 1).

***N*-(3-Butyl-2-methyl-3*H*-benzo[*d*]imidazol-5-yl)-2-chloro-9*H*-purin-6-amine (3d).**

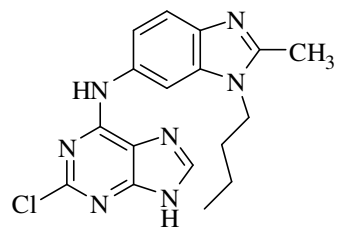

White powder, yield: 86%; mp. 280 °C (d); IR (KBr, cm^{-1}) υ: 3350, 2959, 1649, 1500, 1432, 1235, 1112; ^{1}H NMR (DMSO-d_6): δ 10.65 (bs, 1H, NH), 8.78 (bs, 1H, NH), 8.53 (s, 1H, CH), 8.35 (s, 1H, ArH), 7.82 (d, 1H, *J* = 8.72 Hz, ArH), 7.75 (d, 1H, *J* = 8.68 Hz, ArH), 4.34 (t, 2H, *J* = 7.36 Hz, N-CH_2), 2.79 (s, 3H, CH_3), 1.89-1.80 (m, 2H, CH_2), 1.46-1.37 (m, 2H, CH_2), 0.96 (d, 3H, *J* = 7.32 Hz, CH_3); ^{13}C NMR (TFA+$CDCl_3$): δ 156.5, 150.6, 149.3, 147.8, 139.5, 135.2, 131.7, 127.1, 121.5, 109.3, 105.4, 45.5, 30.4, 19.6, 12.4, 10.7; EIMS, m/z: 356.4 (M^+ + 1).

General procedure for the preparation of compounds 4-19

(1/3-Allyl/butyl-2-methyl-1*H*/3*H*-benzo[*d*]imidazol-5-yl)-2-chloro-9*H*-purin-6-amine (**3a-d**) (0.29 mmol) was refluxed with amines (0.73 mmol) in ethanol (20 ml) for 2-3 days. Reaction was monitored by TLC, crude solid obtained with evaporation of the solvent under vacuum that was purified by column chromatography using chloroform : methanol as eluents to give pure compounds **4-19**.

***N*-(1-Allyl-2-methyl-1*H*-benzo[*d*]imidazol-5-yl)-2-morpholino-9*H*-purin-6-amine (4).**

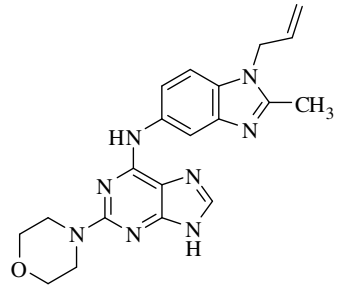

White powder, yield: 75%; mp. 239-240 °C; IR (KBr, cm^{-1}) υ: 3322, 3066, 2975, 1626, 1588, 1478, 1424, 1293, 1168, 1110; ^{1}H NMR (DMSO-d_6): δ 10.03 (bs, 1H, NH), 8.20 (s, 1H, CH), 7.83 (s, 1H, ArH), 7.66 (s, 1H, ArH), 7.46 (d, 1H, *J* = 8.28 Hz, ArH), 5.96-5.93 (m, 1H, CH), 5.24 (d, 1H, *J* = 10.56 Hz, CH_2), 4.99 (d, 1H, *J* = 17.44 Hz, CH_2), 4.72 (d, 2H, *J* = 2.76 Hz, N-CH_2), 3.80 (s, 8H, $_{mor}CH_2$), 2.59 (s, 3H, CH_3); ^{13}C NMR (DMSO-d_6): δ 159.2, 151.9, 142.5, 134.1, 133.4, 131.7, 131.1, 116.9, 115.9, 110.1, 108.9, 66.7, 45.6, 45.1, 29.4, 13.6; EIMS, m/z: 391.0 (M^+ + 1).

***N*-(1-Allyl-2-methyl-1*H*-benzo[*d*]imidazol-5-yl)-2-(piperidin-1-yl)-9*H*-purin-6-amine (5).**

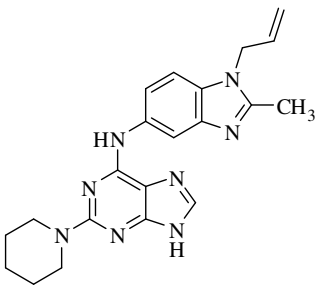

White powder, yield: 53%; mp. 242-244 °C; IR (KBr, cm^{-1}) υ: 3312, 2929, 1604, 1581, 1475, 1302, 1255, 1174; ^{1}H NMR ($CDCl_3$): δ 10.10 (bs, 1H, NH), 8.22 (d, 1H, *J* = 1.96 Hz, CH), 7.97 (s, 1H, ArH), 7.53 (dd, 1H, ^2J = 8.68 Hz, ^3J = 2.28 Hz, ArH), 7.22 (d, 1H, *J* = 8.68 Hz, ArH), 5.98-5.91 (m, 1H, CH), 5.24 (d, 1H, *J* =10.52 Hz, CH_2), 4.99 (d, 1H, *J* = 16.92 Hz, CH_2), 4.72 (d, 2H, *J* = 5.04 Hz, N-CH_2),

3.80 (s, 4H, $_{pip}CH_2$), 2.58 (s, 3H, CH_3), 1.82 (s, 2H, $_{pip}CH_2$), 1.67 (s, 4H, $_{pip}CH_2$); ^{13}C NMR ($CDCl_3$): δ 159.4, 152.2, 152.1, 142.8, 135.0, 134.2, 131.7, 131.5, 117.4, 116.1, 110.6, 109.0, 50.9, 46.0, 45.9, 25.9, 25.0, 13.8; EIMS, m/z: 389.0 (M^+ + 1).

_N_-(1-Allyl-2-methyl-1_H_-benzo[_d_]imidazol-5-yl)-2-(pyrrolidin-1-yl)-9_H_-purin-6-amine (6).

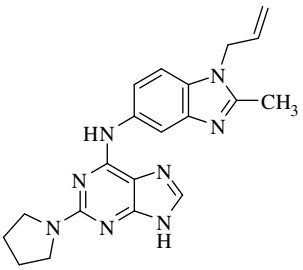

White powder, yield: 60%; mp. 260 °C (d); IR (KBr, cm^{-1}) υ: 3388, 2969, 1642, 1589, 1478, 1344, 1282, 1172; ^1H NMR (DMSO-d_6): δ 10.21 (bs, 1H, NH), 9.05 (s, 1H, CH), 8.47 (d, 1H, J = 1.84 Hz, ArH), 7.66 (t, 1H, J = 4.60 Hz, ArH), 7.28 (d, 1H, J = 8.68 Hz, ArH), 6.02-5.95 (m, 1H, CH), 5.21 (d, 1H, J = 11.00 Hz, CH_2),4.95 (d, 1H, J = 16.96 Hz, CH_2), 4.79 (d, 2H, J = 4.84 Hz, N-CH_2), 3.61 (s, 4H, N-$_{pyr}CH_2$), 2.55 (s, 3H, CH_3), 2.00 (t, 4H, J = 6.40 Hz, $_{pyr}CH_2$); ^{13}C NMR (DMSO-d_6): δ 157.9, 152.0, 142.5, 135.4, 132.6, 130.8, 116.9, 115.7, 109.6, 109.3, 47.1, 45.8, 25.7, 13.7; EIMS, m/z: 375.0 (M^++1).

_N_-(1-Allyl-2-methyl-1_H_-benzo[_d_]imidazol-5-yl)-2-(4-methylpiperazin-1-yl)-9_H_-purin-6-amine (7).

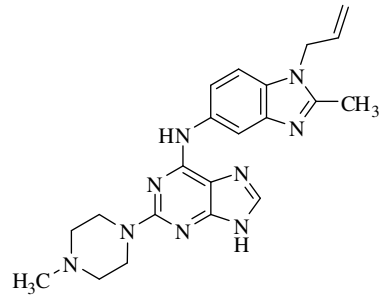

White powder, yield: 74%; mp. 70-72 °C; IR (KBr, cm^{-1}) υ: 3412, 2971, 1638, 1598, 1461, 1307, 1263, 1101; ^1H NMR ($CDCl_3$): δ 10.01 (bs, 1H, NH), 8.16 (d, J = 1.84 Hz, 1H, CH), 7.78 (s, 1H, ArH), 7.65 (s, 1H, ArH), 7.50 (dd, 1H, ^2J = 8.72 Hz, ^3J =1.84 Hz, ArH), 5.95-5.92 (m, 1H, CH), 5.25 (d, 1H, J = 11.00 Hz, N-CH_2), 5.00 (d, 1H, J = 16.96 Hz, CH_2), 4.73 (d, 2H, J = 4.60 Hz, N-CH_2), 3.90 (s, $_{piperazine}CH_2$, 4H), 2.59 (s, 3H, CH_3), 2.38 (s, 3H, CH_3), 1.25 (s, $_{piperazine}CH_2$, 4H); ^{13}C NMR ($CDCl_3$): δ 153.7, 152.2, 134.9, 131.3, 117.4, 116.3, 116.2, 110.7, 108.9, 54.8, 46.6, 45.8, 29.6, 13.7; EIMS, m/z: 404.3 (M^++ 1).

_N_-(1-Butyl-2-methyl-1_H_-benzo[_d_]imidazol-5-yl)-2-morpholino-9_H_-purin-6-amine (8).

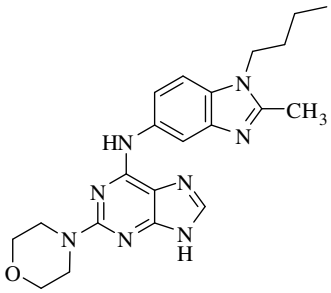

White powder, yield: 63%; mp. 228-232 °C; IR (KBr, cm^{-1}) υ: 3317, 3060, 2962, 1589, 1480, 1428, 1292, 1261, 1170, 1107; ^{1}H NMR (DMSO-d_6): δ 12.23 (bs, 1H, NH), 8.76 (s, 1H, NH), 8.17 (s, 1H, CH), 7.83 (d, 1H, *J* = 2.72 Hz, ArH), 7.69 (s, 1H, ArH), 7.62 (d, 1H, *J* = 7.36 Hz, ArH), 4.17 (t, 2H, *J* = 7.32 Hz, N-CH_2), 3.90 (t, 4H, *J* = 4.82 Hz, $_{mor}CH_2$), 2.62 (s, 3H, CH_3), 2.61 (t, 4H, *J* = 1.84 Hz, $_{mor}CH_2$), 1.85-1.77 (m, 2H, CH_2), 1.45-1.37 (m, 2H, CH_2), 1.01 (t, 3H, *J* = 7.32 Hz, CH_3); ^{13}C NMR (DMSO-d_6): δ 158.7, 151.2, 141.7, 133.9, 130.5, 115.6, 109.5, 108.6, 66.2, 63.3, 48.9, 44.7, 43.1, 42.9, 31.2, 19.5, 13.3; EIMS, m/z: 407.5 (M^+ + 1).

_N_-(1-Butyl-2-methyl-1_H_-benzo[_d_]imidazol-5-yl)-2-(piperidin-1-yl)-9_H_-purin-6-amine (9).

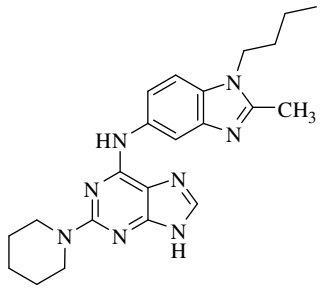

White powder, yield: 72%; mp. 218-220 °C; IR (KBr, cm^{-1}) υ: 3206, 2979, 1643, 1558, 1500, 1421, 1230, 1113; ^{1}H NMR (DMSO-d_6): δ 12.00 (bs, 1H, NH), 8.11 (s, 1H, CH), 7.59 (d, 2H, *J* = 11.92 Hz, ArH), 7.25 (d, 1H, *J* = 8.72 Hz, ArH), 4.11 (t, 2H, *J* = 7.32 Hz, N-CH_2), 3.78 (s, 4H, $_{pip}CH_2$), 2.58 (s, 3H, CH_3), 1.80 -1.73 (m, 2H, CH_2), 1.61 (s, 6H, $_{pip}CH_2$), 1.40-1.35 (m, 2H, CH_2), 0.96 (t, 3H, *J* = 7.32 Hz, CH_3); ^{13}C NMR (DMSO-d_6): δ 158.7, 151.2, 142.1, 133.8, 130.6, 115.2, 109.4, 108.4, 45.3, 43.1, 31.2, 25.1, 24.4, 19.5, 13.4, 13.2; EIMS, m/z: 405.5 (M^+ + 1).

_N_-(1-Butyl-2-methyl-1_H_-benzo[_d_]imidazol-5-yl)-2-(pyrrolidin-1-yl)-9_H_-purin-6-amine (10).

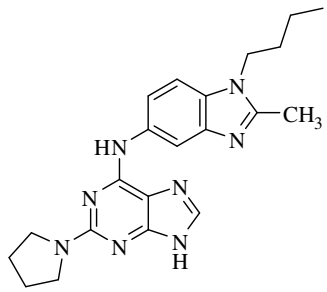

White powder, yield: 80%; mp. 280 °C (d); IR (KBr, cm^{-1}) υ: 3340, 2957, 1626, 1580, 1450, 1339, 1277, 1112; ^{1}H NMR (DMSO-d_6): δ 12.42 (bs, 1H, NH), 9.32 (s, 1H, NH), 8.70 (s, 1H, CH), 8.24 (s, 1H, ArH), 7.75 (s, 1H, ArH), 7.50 (d, 1H, *J* = 8.72 Hz, ArH), 4.12 (t, 2H, *J* = 7.32 Hz, N-CH_2), 3.61 (s, 4H, $_{pyr}CH_2$), 2.56 (s, 3H, CH_3), 2.01 (t, 4H, *J* = 6.44 Hz, $_{pyr}CH_2$), 1.77-1.73 (m, 2H, CH_2), 1.41-1.35 (m, 2H, CH_2), 0.97 (t, 3H, *J* = 7.32 Hz, CH_3); ^{13}C NMR (TFA+$CDCl_3$): δ 151.1, 150.9, 149.6, 149.4, 140.6, 138.3, 135.0, 134.7, 131.7, 127.9, 122.9, 105.8, 49.6, 47.4, 30.8, 19.6, 13.1, 12.4, 11.5; EIMS, m/z: 391.2 (M^+ + 1).

***N*-(1-Butyl-2-methyl-1*H*-benzo[*d*]imidazol-5-yl)-2-(4-methylpiperazine-1-yl)-9*H*-purin-6-amine (11).**

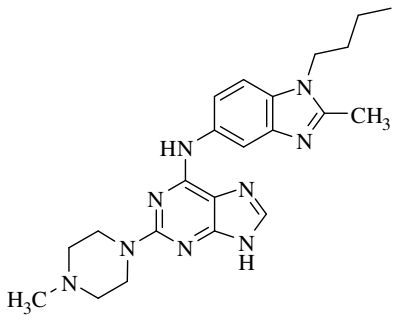

White powder, yield: 55%; mp. 225-228 °C; IR (KBr, cm^{-1}) υ: 3350, 2935, 1583, 1470, 1426, 1366, 1253, 1147; ^1H NMR (DMSO-d_6): δ 12.45 (bs, 1H, NH), 9.47 (bs, 1H, NH), 8.21 (s, 1H, CH), 8.05 (s, 1H, ArH), 7.83 (s, 1H, ArH), 7.43 (d, 1H, *J* = 8.72 Hz, ArH), 4.08-4.02 (m, 2H, N-CH_2), 3.68 (s, 4H, $_{piperazine}CH_2$), 2.47 (s, 3H, CH_3), 2.45 (s, 4H, $_{piperazine}CH_2$), 2.36 (s, 3H, CH_3), 1.69-1.63 (m, 2H, CH_2), 1.28-1.22 (m, 2H, CH_2), 0.87 (t, 3H, *J* = 7.36 Hz, CH_3); ^{13}C NMR (DMSO-d_6): δ 158.7, 152.4, 152.3, 151.9, 151.7, 151.3, 138.8, 137.8, 137.0, 134.9, 133.2, 117.9, 116.2, 115.4, 113.5, 103.2, 101.2, 54.5, 45.9, 44.3, 43.1, 31.3, 19.8, 13.6, 13.6; EIMS, m/z: 420.5 (M^+ + 1).

***N*-(3-Allyl-2-methyl-3*H*-benzo[*d*]imidazol-5-yl)-2-morpholino-9*H*-purin-6-amine (12).**

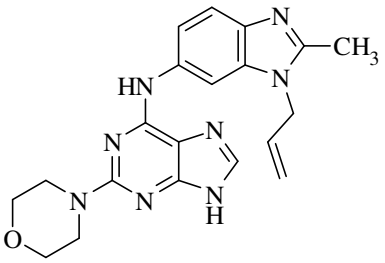

White powder, yield: 96%; mp. 260 °C (d); IR (KBr, cm^{-1}) υ: 3394, 2958, 1626, 1583, 1458, 1309, 1101; ^1H NMR (DMSO-d_6): δ 12.29 (bs, 1H, NH), 9.19 (bs, 1H, NH), 8.28 (s, 1H, CH), 8.01 (s, 1H, ArH), 7.69 (s, 1H, ArH), 7.49 (d, 1H, *J* = 8.72 Hz, ArH), 6.03-5.97 (m, 1H, CH), 5.20 (d, 1H, *J* = 10.52 Hz, CH_2), 4.86 (d, 1H, *J* = 16.96 Hz, CH_2), 4.75 (s, 2H, N-CH_2), 3.73 (s, 4H, $_{mor}CH_2$), 2.57 (s, 4H, $_{mor}CH_2$), 2.53 (s, 3H, CH_3); ^{13}C NMR (DMSO-d_6): δ 158.6, 151.7, 151.2, 150.8, 137.5, 135.9, 134.7, 134.5, 131.4, 117.8, 116.0, 114.9, 113.4, 100.6, 66.2, 44.9, 44.7, 30.4, 13.1; EIMS, m/z: 391.4 (M^+ + 1).

***N*-(3-Allyl-2-methyl-3*H*-benzo[*d*]imidazol-5-yl)-2-(piperidin-1-yl)-9*H*-purin-6-amine (13).**

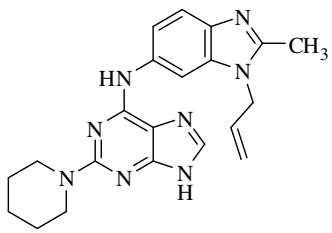

White powder, yield: 85%; mp. 243-245 °C; IR (KBr, cm^{-1}) υ: 3275, 2925, 1623, 1583, 1437, 1425, 1305, 1255, 1191; ^1H NMR (DMSO-d_6): δ 12.21 (bs, 1H, NH), 9.02 (bs, 1H, NH), 8.40 (s, 1H, CH), 7.93 (s, 1H, ArH), 7.64 (s, 1H, ArH), 7.49 (d, 1H, *J* = 8.72 Hz, ArH), 6.01-5.97 (m, 1H, CH), 5.20 (d, 1H, *J* = 10.52 Hz, CH_2), 4.88 (d, 1H, *J* = 16.96 Hz, CH_2), 4.74 (s, 2H, N-CH_2), 3.80 (t, 4H, *J* = 5.52 Hz, $_{pip}CH_2$), 2.54 (s, 3H, CH_3), 1.67 (s, 2H, $_{pip}CH_2$), 1.61 (s, 4H, $_{pip}CH_2$); ^{13}C NMR (DMSO-d_6): δ 158.5, 150.9, 150.7, 137.2,

135.8, 134.8, 134.7, 131.4, 117.7, 116.0, 114.7, 100.2, 45.2, 44.9, 25.2, 24.4, 13.2; EIMS, m/z: 389.5 (M^+ + 1).

_N_-(3-Allyl-2-methyl-3_H_-benzo[_d_]imidazol-5-yl)-2-(pyrrolidin-1-yl)-9_H_-purin-6-amine (14).

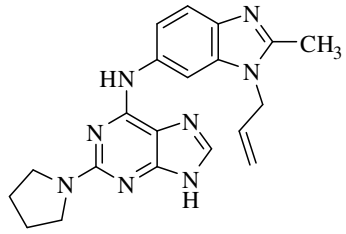

White powder, yield: 55%; mp. 240 °C (d); IR (KBr, cm^{-1}) υ: 3320, 2964, 1633, 1578, 1460, 1337, 1275, 1204, 1113; ^{1}H NMR (DMSO-d_6): δ 12.36 (bs, 1H, NH), 9.26 (bs, 1H, NH), 8.63 (s, 1H, CH), 8.15 (s, 1H, ArH), 7.68 (s, 1H, ArH), 7.47 (d, 1H, J = 5.28 Hz, ArH), 6.04-5.96 (m, 1H, CH), 5.16 (d, 1H, J = 10.08 Hz, CH_2), 4.82 (s, 1H, CH_2), 4.78 (d, 2H, J = 9.16 Hz, N-CH_2), 3.57 (s, 4H, N-$_{pyr}CH_2$), 2.52 (s, 3H, CH_3), 1.99 (t, 4H, J = 6.44 Hz, $_{pyr}CH_2$); ^{13}C NMR (DMSO-d_6): δ 156.8, 150.8, 150.4, 136.2, 135.1, 134.3, 131.8, 131.7, 117.1, 116.9, 115.4, 114.4, 102.2, 100.2, 46.3, 44.6, 24.7, 12.7; EIMS, m/z: 375.5 (M^+ + 1).

_N_-(3-Allyl-2-methyl-3_H_-benzo[_d_]imidazol-5-yl)-2-(4-methylpiperazin-1-yl)-9_H_-purin-6-amine (15).

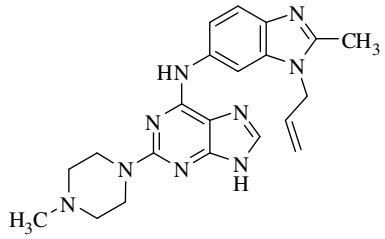

White powder, yield: 62%; mp. 159-162 °C; IR (KBr, cm^{-1}) υ: 3313, 2936, 1629, 1601, 1583, 1476, 1440, 1364, 1257, 1139; ^{1}H NMR (DMSO-d_6): δ 12.38 (bs, 1H, NH), 9.38 (bs, 1H, NH), 8.30 (s, 1H, CH), 8.14 (s, 1H, ArH), 7.75 (s, 1H, ArH), 7.45 (d, 1H, J = 8.68 Hz, ArH), 6.05-5.98 (m, 1H, CH), 5.17 (d, 1H, J = 10.52 Hz, CH_2), 4.80 (s, 1H, CH_2), 4.75 (s, 2H, N-CH_2), 3.73 (s, 4H, $_{piperazine}CH_2$), 2.52 (s, 3H, CH_3), 2.49 (s, 3H, CH_3), 2.27 (s, 4H, $_{piperazine}CH_2$); ^{13}C NMR (DMSO-d_6): δ 158.5, 152.0, 151.4, 150.9, 137.5, 136.3, 134.4, 132.2, 117.7, 115.8, 115.1, 100.9, 54.5, 45.8, 45.0, 44.2, 13.2; EIMS, m/z: 404.5 (M^+ + 1).

_N_-(3-Butyl-2-methyl-3_H_-benzo[_d_]imidazol-5-yl)-2-morpholino-9_H_-purin-6-amine (16).

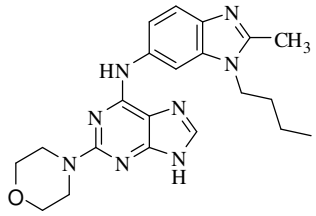

White powder, yield: 65%; mp. 218 °C (d); IR (KBr, cm^{-1}) υ: 3353, 2931, 1600, 1585, 1471, 1431, 1382, 1254, 1124; ^{1}H NMR (DMSO-d_6): δ 12.46 (s, 1H, NH), 9.42 (s, 1H, NH), 8.25 (s, 1H, CH), 7.80 (s, 1H, ArH), 7.50 (d, 1H, J = 8.72 Hz, ArH), 7.43 (d,

1H, *J* = 9.04 Hz, ArH), 4.12 (t, 2H, *J* = 7.32 Hz, N-CH_2), 3.73 (s, 4H, $_{mor}CH_2$), 2.54 (d, 4H, *J* = 2.28 Hz, $_{mor}CH_2$), 2.53 (s, 3H, CH_3), 1.77-1.72 (m, 2H, CH_2), 1.39-1.32 (m, 2H, CH_2), 0.99 (t, 3H, *J* = 7.32 Hz, CH_3); ^{13}C NMR (DMSO-d_6): δ 158.6, 137.7, 136.5, 134.7, 134.6, 117.6, 115.2, 101.0, 99.4, 66.1, 48.6, 44.9, 31.2, 30.6, 25.3, 19.6, 13.6; EIMS, m/z: 407.5 (M^+ + 1).

_N_-(3-Butyl-2-methyl-3_H_-benzo[_d_]imidazol-5-yl)-2-(piperidin-1-yl)-9_H_-purin-6-amine (17).

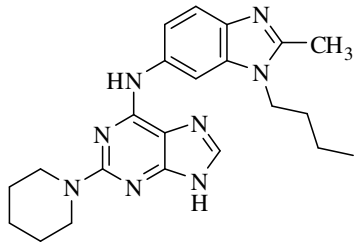

Light brown, yield: 72%; mp. 278 °C (d); IR (KBr, cm^{-1}) υ: 3328, 2924, 1627, 1603, 1583, 1480, 1307, 1252, 1126; ^{1}H NMR (DMSO-d_6): δ 12.37 (bs, 1H, NH), 9.38 (bs, 1H, NH), 8.27 (s, 1H, CH), 7.80 (s, 1H, ArH), 7.40 (d, 1H, *J* = 8.72 Hz, ArH), 7.36 (d, 1H, *J* = 8.24 Hz, ArH), 4.04 (t, 2H, *J* = 7.36 Hz, N-CH_2), 3.71 (t, 4H, *J* = 5.04 Hz, $_{pip}CH_2$), 2.45 (s, 3H, CH_3), 1.69-1.61 (m, 2H, CH_2), 1.56 (s, 2H, $_{pip}CH_2$), 1.49 (s, 4H, $_{pip}CH_2$), 1.29-1.21 (m, 2H, CH_2), 0.89 (t, 3H, *J* = 7.36 Hz, CH_3); ^{13}C NMR (DMSO-d_6): δ 158.5, 152.4, 151.6, 150.9, 137.8, 136.5, 134.8, 117.8, 115.2, 113.1, 100.9, 45.2, 42.9, 31.3, 25.3, 24.5, 19.6, 13.7, 13.6; EIMS, m/z: 405.5 (M^+ + 1).

_N_-(3-Butyl-2-methyl-3_H_-benzo[_d_]imidazol-5-yl)-2-(pyrrolidin-1-yl)-9_H_-purin-6-amine (18).

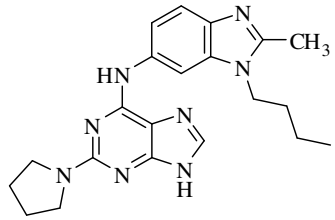

White powder, yield: 70%; mp. 260 °C (d); IR (KBr, cm^{-1}) υ: 3321, 2956, 1581, 1521, 1467, 1382, 1274, 1198, 1115; ^{1}H NMR (DMSO-d_6): δ 12.39 (bs, 1H, NH), 9.27 (bs, 1H, NH), 8.67 (s, 1H, CH), 8.22 (s, 1H, ArH), 7.48 (d, 1H, *J* = 7.80 Hz, ArH), 7.37 (d, 1H, *J* = 8.68 Hz, ArH), 4.09 (t, 2H, *J* = 10.08 Hz, N-CH_2), 3.59 (s, 4H, $_{pyr}CH_2$), 2.52 (s, 3H, CH_3), 1.98 (t, 4H, *J* = 5.96 Hz, $_{pyr}CH_2$), 1.78-1.68 (m, 2H, CH_2), 1.40-1.31 (m, 2H, CH_2), 0.94 (t, 3H, *J* = 7.32 Hz, CH_3); ^{13}C NMR (DMSO-d_6): δ 157.2, 152.2, 150.3, 137.2, 135.3, 134.7, 131.6, 121.9, 119.0, 117.5, 114.5, 100.1, 62.0, 48.6, 46.6, 43.0, 31.4, 25.3, 19.6, 13.6, 13.4; EIMS, m/z: 391.5 (M^+ + 1).

_N_-(3-Butyl-2-methyl-3_H_-benzo[_d_]imidazol-5-yl)-2-(4-methylpiperazin-1-yl)-9_H_-purin-6-amine (19).

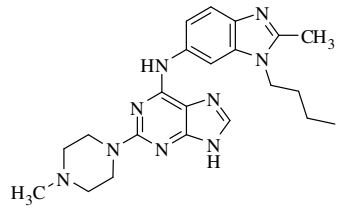

White powder, yield: 82%; mp. 238-240 °C; IR (KBr, cm^{-1}) υ: 3393, 2955, 1624, 1583, 1442, 1355, 1252, 1136; ^{1}H NMR (DMSO-d_6): δ 12.29 (bs, 1H, NH), 9.08 (bs, 1H, NH), 8.30 (s, 1H, CH), 7.96 (d, 1H, J = 3.20 Hz, ArH), 7.48 (d, 1H, J = 5.88 Hz, ArH), 7.46 (s, 1H, ArH), 4.12-4.08 (m, 2H, N-CH_2), 3.82 (s, 4H, $_{piperazine}CH_2$), 2.58 (s, 3H, CH_3), 2.49 (t, 4H, J = 4.6 Hz, $_{piperazine}CH_2$), 2.32 (s, 3H, CH_3), 1.85-1.75 (m, 2H, CH_2), 1.40-1.36 (m, 2H, CH_2), 0.96 (t, 3H, J = 6.84 Hz, CH_3); ^{13}C NMR (DMSO-d_6): δ 158.5, 150.5, 137.5, 134.6, 134.5, 117.7, 114.9, 100.5, 56.3, 54.4, 45.7, 44.1, 43.0, 31.2, 25.0, 19.6, 18.1, 13.4; EIMS, m/z: 420.5 (M^+ + 1).

3.10.2. *In vitro* studies (60 human cancer cell lines)

All the synthesized compounds were submitted to National Cancer Institute (NCI) disease-oriented human cell lines for screening assay to be evaluated for their *in-vitro* antitumor activities against 60 cell lines which included nine tumour subpanels namely; leukemia, non-small lung, colon, CNS, melanoma, ovarian renal, prostate and breast cancer cells. The human tumour cell lines of the cancer screening panel were grown in RPMI 1640 medium containing 5% fetal bovine serum and 2 mM L-glutamine. Cells were inoculated into 96 well microtiter plates in 100 ml at plating densities ranging from 5,000 to 40,000 cells/well depending on the doubling time of individual cell lines. The microtiter plates were then incubated at 37 °C, 5% CO_2, 95% air and 100% relative humidity for 24 h.

After 24 h, two plates of each cell line were fixed in situ with TCA, to represent a measurement of the cell population for each cell line. Experimental drugs were solubilized in DMSO at 400-fold the desired final maximum test concentration and stored frozen prior to use. At the time of drug addition, an aliquot of frozen concentrate was thawed and diluted to twice the desired final maximum test concentration with complete medium containing 50 µg/ml gentamicin. Additional four, 10-fold or ½ log serial dilutions were made to provide a total of five drug concentrations plus control. Aliquots of 100 µL of these different drug dilutions were added to the appropriate microtiter wells, resulting in the required final drug concentrations. Following drug addition, the plates were incubated for an additional 48 h at 37 °C, 5% CO_2, 95% air, and 100% relative humidity. For adherent cells, the assay was terminated by the addition of cold TCA. Cells were fixed in situ by the gentle addition of 50 µL of cold 50% (w/v) TCA and incubated for 60 min at 4 °C. The supernatant was discarded, and the plates were washed five times with tap water and air dried. Sulforhodamine B (SRB) solution (100 µL) at 0.4% (w/v) in 1% acetic acid is added to each well, and plates are

incubated for 10 min at room temperature. After staining, unbound dye was removed by washing five times with 1% acetic acid and the plates were air dried and then subsequently solubilized with 10 mM trizma base, and the absorbance was read on an automated plate reader at a wavelength of 515 nm. Using the seven absorbance measurements [time zero (T_z), control growth (C), and test growth in the presence of drug at the five concentration levels (T_i)], the percentage growth was calculated at each of the drug concentrations levels. Percentage growth inhibition is calculated as:

[(Ti -Tz)/(C - Tz)] × 100 for concentrations for which $T_i \geq Tz$; [(Ti -Tz)/Tz] × 100 for concentrations for which Ti < Tz.

Three dose response parameters were calculated for each experimental agent. Growth inhibition of 50% (GI_{50}) was calculated from [(Ti -Tz)/(C - Tz)] × 100 = 50. The drug concentration resulting in total growth inhibition (TGI) is calculated from $T_i = Tz$. The LC_{50} was calculated from [(Ti-Tz)/Tz]×100 = 50.[20,23,31]

3.10.3. *In vitro* studies (Aurora kinase inhibitors)

UV-Vis spectral studies:

UV-visible spectral studies were performed on Biotek powerwave XS spectrophotometer. The stock solution for both the compounds and the enzyme were prepared in HPLC grade DMSO. The conc. of the compound stock solution was kept at 10^{-3} M and was diluted accordingly to get the final conc. of 10^{-5} M to 10^{-8} M. 50 µL of the enzyme was diluted to 950 µL in a kinase pure for further titration with compound solution.

Procedure for Aurora-A kinase assay

The Aurora-A kinase Assay/Inhibitor Screening Kit was a single-site, non-quantitative immunoassay for Aurora-A activity. Plates were pre-coated with a substrate corresponding to recombinant Lats2, which contains serine83 residues that can be phosphorylated by Aurora-A. First of all, removed the appropriate number of microtiter 96 wells from the foil pouch and placed them into the well holder. The stock solutions of the entire compounds were prepared in dimethylsulfoxide (spectroscopy grade) at concentration of 10^{-3} M. 30 µL of compound was added into a substrate coated plate. Begin the kinase reaction by addition of 80 µL Kinase Reaction Buffer per well, covered with plate sealer or lid, and incubated at 30 °C for 30-60 minutes. Wells was washed five times with Wash Buffer making to sure each well was

filled completely. Residual Wash Buffer was removed by gentle tapping or aspiration. Pipetted 100 µL of Anti-Phospho-Lats2-S83 Monoclonal Antibody ST-3B11 into each well, cover with plate sealer or lid, and incubate at room temperature for 1 h. Wells was washed wells five times with Wash Buffer making sure each well is filled completely. Then, pipette 100 µL of HRP-conjugated Anti-mouse IgG into each well, covered with plate sealer or lid, and incubated at room temperature for 1 h. Any unused conjugate was discarded after use. Wells was washed five times with Wash Buffer making sure each well was filled completely. Added 100 µL of Substrate Reagent to each well and incubate at room temperature for 5–15 minutes. At last, 100 µL of Stop Solution was added to each well in the same order as the previously added Substrate Reagent. Absorbance was measured in each well using a spectrophotometric plate reader at wavelengths of 450 nm. Wells was read within 30 minutes of adding the Stop Solution.

3.10.4. Shake flask method for lipophilicity determination

Partition coefficient for the target compounds were determined at room temperature using n-octanol–phosphate buffer (0.15 M, pH = 7.4). The experiments were performed in the system phosphate buffer : n-octanol at different volumes (10: 1, 50: 1). The stock solutions of the entire compounds were prepared in dimethylsulfoxide (spectroscopy grade) at concentration of 5×10^{-4} M. All solutions were pipette into glass vials; phosphate buffer and stock solution (125µL, 250µL) were added with a micropipette. The wavelength chosen according to the λ_{max} of the compounds i.e., 225, 226, 227, 229, 307, 309, 310, 311, 315, 316, 317, 318, 335 and 336 for **3a-d, 4-19** respectively. Initial absorbance (A_i) of stock solution in the buffer phase was recorded for each compound. Followed this, n-Octanol was added into each vial. The phases were shaken together on a mechanical shaker (METREX, Cat No. MRS-50H) for 45 minutes, centrifuged (REMI R-24) at 2500 rpm for 30 min to afford complete phase separation, and n-octanol phase was removed. Absorbance of the buffer phase was measured spectrophotometrically using a CHAMPION UV-500 spectrophotometer.

P values were calculated from the following equation:-

$$P = \frac{A_i - A_f}{A_f} \times \frac{V_w}{V_o}$$

Where A_i and A_f represent the absorbance of compounds in the aqueous phase before and after partitioning, respectively. V_w and V_o represent the volume of the aqueous and organic phases used in the octanol/buffer system.

3.11. Docking Studies

Compounds were built using the builder tool kit of the software package Argus Lab 4.0.1.23 and energy minimized with semi-empirical quantum mechanical method PM3. Crystal coordinates of Aurora-A kinase in complexation with an anti-cancer agent (pdb ID 2WTV and 2XNE) were downloaded from protein data bank (www.rcsb.org) and in the molecule tree view of the software, the monomeric structures of the crystal co-ordinate was selected and the active site was defined as 15 Å around the ligand. Validation of the docking programme was checked by docking the known inhibitors of the respective enzymes in their binding sites. The molecule to be docked in the active site of the enzyme was pasted in the work space carrying the structure of the enzyme. The docking programme implements an efficient grid based docking algorithm which approximates an exhaustive search within the free volume of the S19 binding site cavity. The conformational space was explored by the geometry optimization of the flexible ligand (rings were treated as rigid) in combination with the incremental construction of the ligand torsions. Thus, docking occurs between the flexible ligand parts of the compound and enzyme. The docking was repeated several times (approx. 10000 iterations) until no change in the position of the ligand and a constant value of the binding energy was observed. The ligand orientation was determined by a shape scoring function based on Ascore and the final positions were ranked by lowest interaction energy values. H-bond and hydrophobic interactions between the respective compound and enzyme were explored.

REFERENCES

1. Hanahan, D.; Weinberg, R. A. *Cell* **2000**, *100*, 57.
2. American Cancer Society. Cancer Facts & Figures **2014**, 1-68.
3. Parker, W. B. *Chem. Rev.* **2009**, *109*, 2880.
4. D'Alise, A. M.; Amabile, G.; Iovino, M.; Giorgio, F. P. D.; Bartiromo, M.; Sessa, F.; Villa, F.; Musacchio, A.; Cortese, R. *Mol. Cancer Ther.* **2008**, *7*, 1140.
5. Legraverend, M.; Tunnah, P.; Noble, M.; Ducrot, P.; Ludwig, O.; Grierson, D. S.; Leost, M.; Meijer, L.; Endicott, J. *J. Med. Chem.* **2000**, *43*, 1282.
6. (a) Peifer, C.; Buhler, S.; Hauser, D.; Kinkel, K.; Totzke, F.; Schachtele, C.; Laufer, S. *Eur. J. Med. Chem.* **2009**, *44,* 1788; (b) Hsieh, W. S.; Soo, R.; Peh, B. K.; Loh, T.; Dong, D.; Soh, D.; Wong, L. S.; Green, S.; Chiao, J.; Cui, C. Y.; Lai, Y. F.; Lee, S.

C.; Mow, B.; Soong, R.; Salto-Tellez, M.; Goh, B. C. *Clin. Cancer Res.* **2009**, *15*, 1435.

7. Tourneau, C. L.; Faivre, S.; Laurence, V.; Delbaldo, C.; Vera, K.; Girre, V.; Chiao, J.; Armour, S.; Frame, S.; Green, S. R.; Gianella-Borradori, A.; Dieras, V.; Raymond, E. *Eur. J. Cancer* **2010**, *46*, 3243.
8. Ferrero, M.; Gotor, V. *Chem. Rev.* **2000**, *100,* 4319.
9. (a) Singh, G.; Kaur, M.; Mohan, C. *Int. J. Pharm.* **2013,** *4,* 82; (b) Bansal, Y.; Silakari, O. *Bioorg. Med. Chem.* **2012,** *20*, 6208; (c) Singla, P.; Luxami, V.; Paul, K. *RSC Adv*. **2014**, *41*, 2422; (d) Toro, P.; Klahn, A. H.; Pradines, B.; Lahoz, F.; Pascual, A.; Biot, C.; Arancibia, R. *Inorg. Chem. Commun.* **2013**, *35*, 126.
10. Nakamura, S.; Tsuno, N.; Yamashita, M.; Kawasaki, I.; Ohta, S.; Ohishi, Y. *J. Chem. Soc. Perkin Trans.* **2001,** *1*, 429.
11. Park, E. S.; Lee, H. J.; Park, H.; Kim, M. N.; Chung, K. H.; Yoon, J. S. *J. Appl. Poly. Sci.* **2001**, *80*, 728.
12. (a) Hazelton, J. C.; Iddon, B.; Suschitzky, H.; Woolley, L. H. *Tetrahedron* **1995**, *51,* 10771; (b) Labaw, C. S.; Webb, R. L. U.S 4285878, **1981**; Chem. Abstr. **1981**, *95*, 168837; (c) Kohler, P. *Int. J. Parasitol.* **2001**, *31*, 336.
13. Meisel, P.; Heidrich, H. J.; Jaensch, H. J.; Kretzschmar, E.; Henker, S.; Laban, G.; DD 243284, **1987**; Chem. Abstr. **1987,** *107*, 217629; (b) Kyle, D.; Goehring, R. R.; Shao, B. WO 001,039775; Chem. Abstr. **2001,** *135,* 33477.
14. Glover, D. M.; Leibowitz, M. H.; McLean, D. A.; Parry, H. *Cell* **1995**, *81*, 95.
15. Pan, J.; Wang, Q.; Snell, W. J. *Cell* **2004**, *6*, 445.
16. Bischoff, J. R.; Anderson, L.; Zhu, Y.; Mossie, K.; Ng, L.; Souza, B.; Schryver, B.; Flanagan, F.; Clairvoyant, F.; Ginther, C.; Chan, C. S.; Novotny, M.; Slamon, D. J.; Plowman, G. D. *EMBO J.* **1998,** *17*, 3052.
17. Tong, T.; Zhong, Y.; Kong, J.; Dong, L.; Song, Y.; Fu, M.; Liu, Z.; Wang, M.; Guo, L.; Lu, S.; Wu, M.; Zhan, Q. *Clin. Cancer Res.* **2004**, *10*, 7304.
18. Wang, X. X.; Liu, R.; Jin, S. Q.; Fan, F. Y.; Zhan, Q. M. *Cell Res.* **2006**, *16*, 356.
19. Crystallographic data for the structural analysis have been deposited at the Cambridge Crystallographic Data Centre, CCDC No. 1022534 (E-mail: deposit@ccdc.cam.ac.uk).
20. Grever, M. R.; Sehepartz, S. A.; Chabners, B. A. *Semin. Oncol.* **1992,** *19*, 622.

21. Monks, A.; Schudiero, D.; Skehan, P.; Shoemaker, R.; Paull, K.; Vistica, D.; Hose, C.; Langley, J.; Cronise, P.; Vaigro-Wolff, A.; Gray-Goodrich, M.; Campbell, H.; Mayo, J.; Boyd, M. *J. Natl. Cancer Inst.* **1991**, *83*, 757.
22. Boyd, M. R.; Paull, K. D. *Drug Dev. Res.* **1995**, *34*, 91.
23. Skehan, P.; Storeng, R.; Scudiero, D.; Monks, A.; McMahon, J.; Vistica, D.; Warren, J. T.; Bokesch, H.; Kenney, S.; Boyd, M. R. *J. Natl. Cancer Inst.* **1990**, *82*, 1107.
24. CycLex Aurora-A kinase Assay/Inhibitor Screening kit Cat# CY-1165.
25. Caco, A. I.; Tome, L. C.; Dohrn, R.; Marrucho, I. M. *J. Chem. Eng. Data* **2010**, *55*, 3160 and references therein.
26. QSARINS (QSAR-INSubria): QSARINS, software for QSAR MLR model Development and validation, version 2.1- 2014, QSAR Research Unit in Environmental Chemistry and Ecotoxicology, Department of theoretical and applied sciences (DiSTA), University of Insubria, Via J.H. Dunant 3, Varese, Italy. http://www.qsar.it.
27. SciGress Ultra: Molecular Modeling System 7.7.0.47, FujitsuKyushu Systems, Fukuoka-Shi, Japan, 1981.
28. Neaz, M. M.; Muddassar, M.; Pasha, F. A.; Cho, S. J. *Acta Pharmacol. Sin.* **2010**, *31* 244.
29. Compounds were constructed and docked with builder tool kit of software package ArgusLab 4.0.1 (www.arguslab.com).
30. (a) Bouloc, N.; Large, J. M.; Kosmopoulou, M.; Sun, C.; Faisal, A.; Matteucci, M.; Reynisson, J.; Brown, N.; Atrash, B.; Blagg, J.; McDonald, E.; Linardopoulos, S.; Bayliss, R.; Bavetsias, V. *Bioorg. Med. Chem. Lett.* **2010**, *20*, 5988; (b) Coumar, M. S.; Leou, J. S.; Shukla, P.; Wu, J. S.; Dixit, A. K.; Lin, W. H.; Chang, C. Y.; Lien, T. W.; Tan, U. K.; Chen, C. H.; Hsu, J. T. A.; Chao, Y. S.; Wu, S. Y.; Hsieh, H. P. *J. Med. Chem.* **2009,** *52*, 1050.
31. Alley, M. C.; Scudiero, D. A.; Monks, A.; Hursey, M. L.; Czerwinski, M. J.; Fine, D. L.; Abbott, B. J.; Mayo, J. G.; Shoemaker, R. H.; Boyd, M. R. *Cancer Res.* **1988***, 48,* 589.

CHAPTER-4

Pd-Catalyzed Coupling Reaction of 2, 4-Dichloroquinazoline

4.1. INTRODUCTION

Palladium-catalyzed cross-coupling reaction of aromatic halides with organoboronic acids, known as the Suzuki cross-coupling, is a versatile and highly utilized reaction for the selective formation of carbon–carbon bond, in particular for the synthesis of biaryls.[1-4] The key advantage of the Suzuki reaction is to observed the high tolerance to most functional groups, the mild conditions under which the reaction is conducted, the relative stability of boronic acids/esters to heat, oxygen, and water, the ease of handling and separation of boron-containing byproducts, and their abundant commercial availability. These are all desirable features for the construction of diverse aryl and heteroaryl species needed in medicinal chemistry.

Hydroxylation is also one of the fundamental transformations for the formation of C-O bond in organic synthesis. Although more limited in scope, hydroxylation reactions incorporating primary, secondary and tertiary alcohols, phenols, and silanols have all been described. Recently, several research groups reported palladium- and copper catalyzed hydroxylation of aryl halides under relatively mild conditions.[5-9] Efforts have also been focused on the development of efficient and selective catalytic systems for these reactions, but many such reactions are limited to the couplings of aromatic iodides and bromides because of the much higher energy is required for the oxidative insertion of palladium catalysts into the C-Cl bond of aryl chlorides.[10-17] Thus, only aryl bromides and iodides can be used, as the chlorides only react slowly. In recent years, the use of readily available aryl chlorides in these transformations has received increasing attention, and a number of effective catalytic systems have been developed for this purpose.[14,15,18] The use of the catalytic cross-coupling reaction for the preparation of aryl-functionalised heterocycles with multiple applications is increasing at an accelerating phase. Unlike the aryl chlorides, heteroaryl chlorides undergo the standard Suzuki-Miyaura cross-coupling reaction with commonly used tetrakis(triphenylphosphine)palladium(0) [$Pd(PPh_3)_4$] catalyst. Incorporation of the nitrogen atom into the benzene ring decreases the energy required for the oxidative addition. When this energy is sufficiently decreased, Pd catalysts having less electron-donating ligands are able to insert into the C–Cl bond. Moreover, these reactions are typically

carried out in the presence of an additive or ligand, the role of which is to form a higher valent, more reactive complex.[16]

The different functionalizations of halogenated heteroaromatics in palladium catalyzed reactions has been extensively studied and provide a versatile means for the synthesis of libraries containing functionalized substituents in specific positions of the heterocyclic scaffold.[19] For example, Suzuki, Heck, Negishi reactions in the presence of traditionally palladium catalysts including imidazopyridines,[20] pyridines,[21,22] pyrazines,[23-25] triazines,[26,27] quinazolines,[28,29] cinnolines,[30] difluoroalkene analogous,[31] imidazopyridazines,[32-34] pyrazolopyrimidines,[35-38] triazolopyrimidines,[39] pyrrolopyrimidines,[40] purines[41] and uridines[42] are all well known. These processes have reached a level of sophistication that permits a wide range of coupling partners to be combined efficiently.

Quinazoline scaffold is present in a great number of biologically active drugs including potent kinase inhibitors,[43,44] anti-inflammatory,[45] antiviral,[46] anticancer,[47,48] antitubercular agents[49] and also components of several approved drugs, such as erlotinib, gefitinib, canertinib, vandetanib and lapatinib[50] (As discussed in Chapter-2). Hence, the functionalization at 2-position of quinazolin-4(3*H*)-one and diarylation at C2 and C4 positions of quinazoline moiety provide an interesting challenge in organic and medicinal chemistry. As a result, various synthetic efforts have been made for their synthesis.[51-54] Herein, we have reported the first one pot palladium catalysed hydroxylation at non activated C4 position and subsequent arylation at C2 position of 2,4-dichloroquinazoline with variety of boronic acids. Of interest is the fact that palladium catalyzed diarylation at C2 and C4 positions with boronic acids in the presence of water and base has also been performed. Use of water is suitable in this coupling reaction as boronic acids are stable in aqueous conditions. Its ability to dissolve various bases helps in activation of boronic acids and enhancing the rate of reaction.

The most widely used method for the synthesis of 2-substituted-quinazolin-4(3*H*)-one is probably with 2-aminobenzamide or their derivatives under acidic or basic conditions or in the presence of copper catalyst (**Scheme 1**).[55,56] Recently, Fu and co-authors developed novel cascade methods starting from 2-halobenzoic acids or 2-halobenzamides.[57-61] Zhu and co-authors reported alternative approaches via intramolecular C(sp^2)-H carboxamidation reaction of N-arylamidines involving palladium-catalyst.[62] We speculated that the quinazolin-4(3*H*)-one motif could also be constructed by palladium-catalyzed oxidation C(sp^2)-O bond formation of simple chloroquinazoline, which are derived readily from anthranilic acid and

urea followed by chlorination with $POCl_3$.[63] This strategy delivers palladium catalyzed single step for quinazolin-4(3*H*)-ones along with monoarylation at C2 position with different aryl boronic acids (**Scheme 1**). Of interest is the fact that palladium catalyzed diarylation at C2 and C4 positions of quinazoline with boronic acids in the presence of water and base has also been performed. These synthesized molecules were then evaluated for 60 human cancer cell line studies.

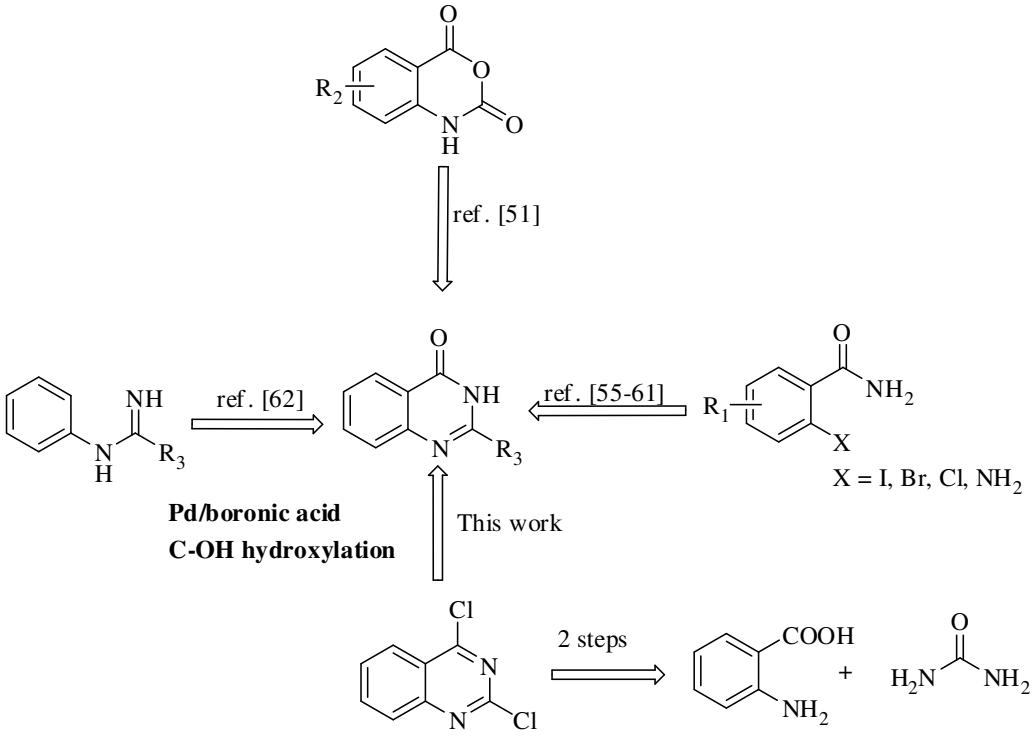

Scheme 1. Major approaches to quinazolin-4(3*H*)-one

Objective:

Various methods for the coupling reactions at C2 and C4 positions of quinazoline have been documented in the literature. It has been found that most of the research groups reported the substitution of quinazoline with various reagents and catalysts such as iodine, copper, iridium, gallium(III)triflate, bmim[$FeCl_4$], $InCl_3$ and palladium catalyst but no one has reported the Suzuki-Miyaura coupling reaction for simultaneously C-C and C-O (hydroxylation) bond formation at C2 and C4 positions respectively. As part of our research programme aimed at developing C-C and C-O coupling reaction of 2,4-dichloroquinazoline by substituting with different boronic acids, catalysts and bases and evaluated for *in-vitro* 60 human cancer cell line for one dose studies.

4.2. CHEMISTRY

4.2.1. Synthesis of monoarylated and diarylated products

The synthetic strategy for the synthesis of monoarylated and diarylated quinazolines **(1-9)** has been shown in **scheme 2**. Compounds **1-9** have been synthesized by the easily available starting material quinazolin-2,4-dione. Refluxing of quinazolin-2,4-dione with phosphorous oxychloride in the presence of toluene for 7 h to obtain 2,4-dichlorquinazoline which was then treated with different aryl boronic acids through Suzuki-Miyaura cross coupling reaction gave compounds **1-9**.

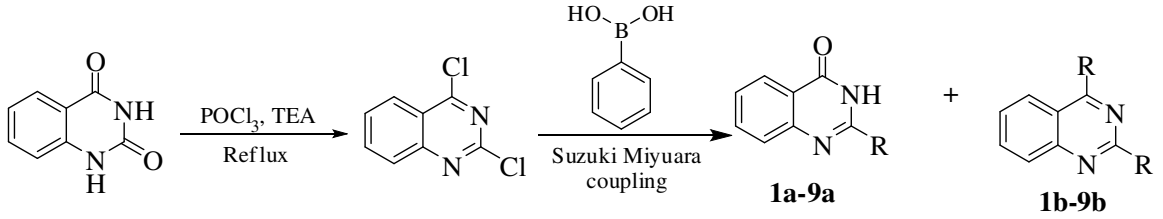

R = *p*- ClC_6H_5, *p*- BrC_6H_5, *p*- FC_6H_5, *m*- $CH_3C_6H_5$, *p*- $OCH_3C_6H_5$, thiophene, furan, naphthalene

Scheme 2

A variety of conditions and combinations of catalyst systems, bases and solvents were adopted for optimal reaction conditions for monosubstitution and disubstitution of 2,4-dichloroquinazolines (**Table 1**). Interestingly, under most of the reaction conditions, C4 hydroxylated/C2 monoarylated were the major products, with varying amounts of C2 and C4 diarylated products resulting from different aryl/heteroaryl boronic acids. Csp^2-O and C-C coupling reactions between 2,4-dichloroquinazoline and phenylboronic acid with palladium based catalysts like $Pd(PPh_3)_4$, $Pd(PPh_3)_2Cl_2$ and $Pd_2(dba)_3$; $Pd(PPh_3)_4$ proved as an effective catalyst for monoarylation (hydroxylated) and diarylation (**Table 1, entries 1-3**). Among the variation of bases such as K_2CO_3, Na_2CO_3, Cs_2CO_3 and NaO^tBu with $Pd(PPh_3)_4$ catalyst (**Table 1, entries 3-6**) revealed that K_2CO_3 turned out to be the most effective base to give desired product (**Table 1, entry 3**). Further, catalytic reactions using $Pd(PPh_3)_2Cl_2$, better yield of product was obtained with Na_2CO_3 (**Table 1, entry 7**) than K_2CO_3, Cs_2CO_3 or NaO^tBu (**Table 1, entries 1, 8-9**) but with $Pd_2(dba)_3$ and different bases viz., K_2CO_3, Na_2CO_3, NaO^tBu or Cs_2CO_3, a significant decrease in yields were observed (**Table 1, entries 2, 10-12**). The effect of different solvents like toluene, acetonitrile, dioxane and tetrahydrofuran (THF) along with water as a co-solvent were also studied and observed that

better yield of products were obtained in toluene : H_2O (9:1) mixture (**Table 1, entries 3, 13-15**). The arylation and hydroxylation failed completely when the reaction was carried out in the absence of palladium catalyst or base (**Table 1 entries 16-17**). Thus, base and palladium catalyst have major role for the formation of C-C bond at C4 position as well as hydroxylation at C2 position.

Table 1. Optimization of Pd-catalyzed monoarylation and diarylation of 2,4-dichloroquinazoline

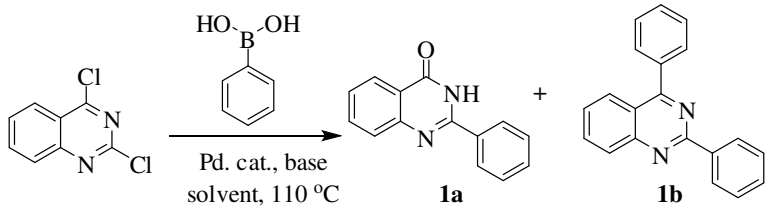

Entry	Catalyst	Base	Solvent (9:1)	Time (h)	Yield (%)[a] 1a	1b
1	$Pd(PPh_3)_2Cl_2$	K_2CO_3	Toluene:H_2O	10	42	10
2	$Pd_2(dba)_3$	K_2CO_3	Toluene:H_2O	14	40	11
3	**$Pd(PPh_3)_4$**	**K_2CO_3**	**Toluene:H_2O**	**12**	**75**	**16**
4	$Pd(PPh_3)_4$	Na_2CO_3	Toluene:H_2O	8	60	12
5	$Pd(PPh_3)_4$	Cs_2CO_3	Toluene:H_2O	8	65	10
6	$Pd(PPh_3)_4$	NaO^tBu	Toluene:H_2O	8	62	10
7	$Pd(PPh_3)_2Cl_2$	Na_2CO_3	Toluene:H_2O	10	44	11
8	$Pd(PPh_3)_2Cl_2$	Cs_2CO_3	Toluene:H_2O	10	42	9
9	$Pd(PPh_3)_2Cl_2$	NaO^tBu	Toluene:H_2O	10	40	5
10	$Pd_2(dba)_3$	Na_2CO_3	Toluene:H_2O	14	40	10
11	$Pd_2(dba)_3$	Cs_2CO_3	Toluene:H_2O	14	35	5
12	$Pd_2(dba)_3$	NaO^tBu	Toluene:H_2O	14	38	8
13	$Pd(PPh_3)_4$	K_2CO_3	CH_3CN: H_2O	8	68	13
14	$Pd(PPh_3)_4$	K_2CO_3	THF:H_2O	10	65	15
15	$Pd(PPh_3)_4$	K_2CO_3	Dioxane:H_2O	10	68	10
16	-	K_2CO_3	Toluene:H_2O	9	-	-
17	$Pd(PPh_3)_4$	-	Toluene:H_2O	14	-	-

[a]isolated yields,- indicates <5%.

Having optimized the reaction conditions, we have performed the palladium catalyzed reaction of 2,4-dichloroquinazoline (0.001 mol) with 2.0 equivalents of phenylboronic acid (0.002 mol), 10 mol% of $Pd(PPh_3)_4$ and 2.0 equivalents of K_2CO_3 (0.002 mol) in 9:1 mixture of toluene and water (**Table 1, entry 3**) in a sealed tube at 110 $^{\circ}$C for 10 h. After the completion of the reaction, the reaction mixture was cooled, extracted with water and chloroform. Organic layer was separated, dried over sodium sulphate, filtered and concentrated under *vacuo* to get crude product. The residue was purified by column chromatography using chloroform : methanol (8:2) as eluents to give pure solid compound of **1a** (EIMS, m/z: 223.1 (M^++1) and **1b** (EIMS, m/z: 283.1 (M^++1) in 75% and 16% yields respectively. ^{1}H NMR spectrum of **1a** showed the 1H triplet at δ 7.52, 3H triplet at δ 7.59, 2H multiplet at δ 7.88, 2H triplet at δ 8.21, 1H doublet at δ 8.33 of aromatic-H and 1H broad singlet due to NH (exchangeable with D_2O) at downfield region of δ 11.20. ^{13}C NMR spectrum of **1a** showed the signals at δ 120.8, 126.5, 126.9, 127.4, 128.1, 129.2, 131.8, 132.9, 135.0, 149.5, 151.7, 163.7 (ArH). IR spectrum also showed the peaks at 3359 (NH), 3060, 1658, 1334, 1289 cm^{-1}. On the basis of these spectral data, this compound has been assigned the structure of 2-phenyl-3*H*-quinazolin-4-one (**1a**). The presence of NH signal at δ 11.20 ppm in ^{1}H NMR and 3359 in IR spectrum confirmed the keto form (more stability of the keto form than enol form) at C4 position and appearance of aromatic signals in NMR indicated the Suzuki coupling at C2 position of quinazoline.

^{1}H NMR spectrum of **1b** showed the 7H multiplet at δ 7.60, 3H triplet at δ 7.90, 2H triplet at δ 8.17, 2H doublet at δ 8.70 of aromatic-H. ^{13}C NMR spectrum showed the signals at δ 121.8, 127.1, 128.7, 128.8, 129.3, 130.0, 130.3, 130.6, 133.7, 137.8, 138.3, 152.1, 160.3 and 168.4 (ArH). IR spectrum also showed the peaks at 3061, 1336, 1289 cm^{-1}. On the basis of these spectral data, this compound has been assigned the structure of 2,4-diphenyl-quinazoline (**1b**). Absence of NH singlet and appearance of fourteen protons in the aromatic region in proton NMR confirmed the diarylation of 2,4-dichloroquinazoline.

Thus, number of 2-aryl-3*H*-quinazolin-4-ones (**1a-9a**) and 2,4-diarylquinazolines (**1b-9b**) were prepared via coupling of 2,4-dichloroquinazoline with variety of aryl boronic acids under the same reaction conditions as shown in **table 2**. Both monosubstitution at C2 position along with hydroxylation at C4 position and disubstitution at C2 and C4 positions of quinazoline participated well in C–O and C-C bond forming reaction to afford the desired products.

We also examined the reactions of activated and non-activated substituted hetero (aryl) boronic acids including electron-withdrawing and electron-donating groups. Phenyl boronic acids with electron withdrawing para-substituent such as fluoro, chloro and bromo produced the corresponding hydroxylated monoaryl (64-70% yields) and diaryl (19-25% yields) products (**Table 2, entries 2-4**). Compared with reaction of 4-bromophenyl boronic acids, the yields in the case of corresponding 4-fluorophenyl and 4-chlorophenyl boronic acids were slightly lower demonstrating that electron withdrawing halogen substitution on the phenyl boronic acid ring has a role for the reactivity. 4-Methoxyphenyl boronic acids with an electron donating methoxy group underwent smooth conversion for monoarylation/hydroxylation and diarylation of quinazoline to afford 75% and 20% yields respectively (**Table 2, entry 5**). Selectively monoarylated products were obtained with 3-methylphenyl boronic acids, thiophen-2-boronic acids and furan-2-boronic acids with 65%, 60% and 60% yields respectively (**Table 2, entries 6-8**). Finally, Suzuki-Miyaura reaction of 2,4-dichloroquinazoline with naphthalene-1-boronic acid, monoarylated product was predominant with 55% yield and only 17% of diarylated product obtained (**Table 2, entry 9 and Fig. 1**). These compounds have been well characterized by ^{1}H and ^{13}C NMR as well as mass spectrometry and in case of compound **9b**, single X-ray crystallography has been used. We have also tried the reactions of 2,4-dichloroquinazoline with other boronic acids like 2-hydroxyphenylboronic acid, 4-ethylphenylboronic acid and 4-formylphenylboronic acid but in all the cases, only starting material has been recovered.

Table 2. Monoarylation and diarylation products with different arylboronic acids

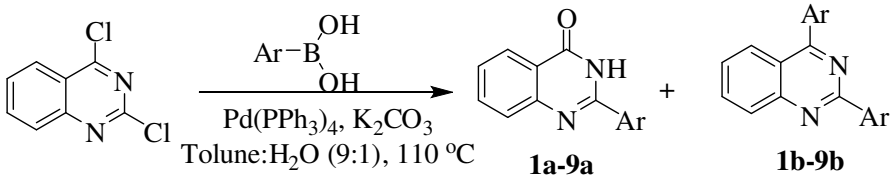

1a-9a **1b-9b**

Entry	$ArB(OH)_2$	Products		M.pt. (°C)		Time (h)	Products (%)	
		monoarylated	diarylated	mono	di			
1	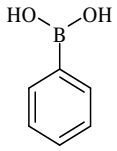	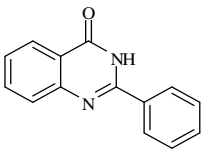	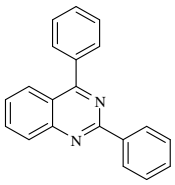	238-240	118-119	12	**1a** (75)	**1b** (16)

2	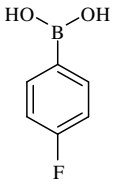	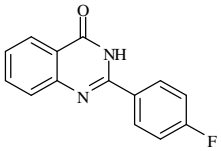	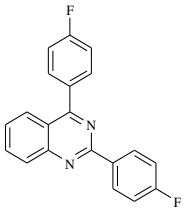	238-240	170-172	8	**2a** (64)	**2b** (25)
3	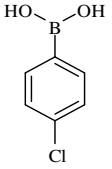	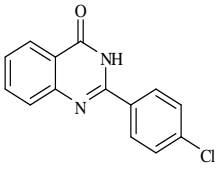	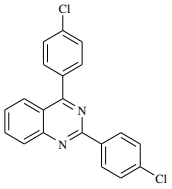	298-300	198-200	8	**3a** (68)	**3b** (19)
4	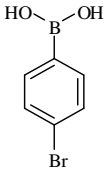	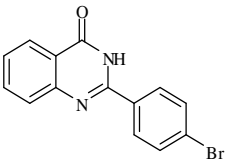	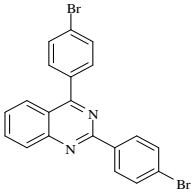	291-294	(trace)	8	**4a** (70)	**4b** (trace)
5	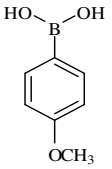	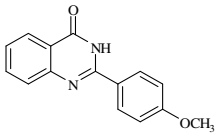	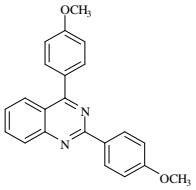	245-247	115-117	8	**5a** (75)	**5b** (20)
6	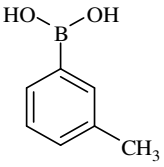	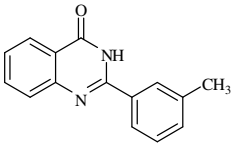	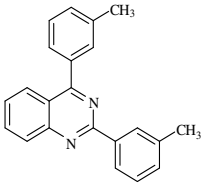	210-212	(trace)	8	**6a** (65)	**6b** (trace)
7	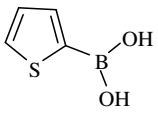	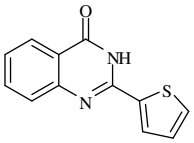	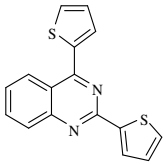	277-280	(trace)	8	**7a** (60)	**7b** (trace)
8	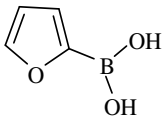	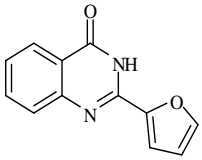	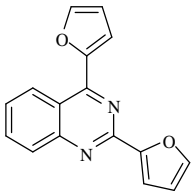	217-219	(trace)	7	**8a** (60)	**8b** (trace)
9	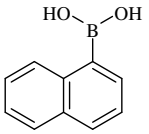	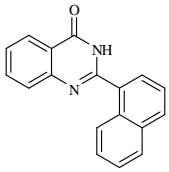	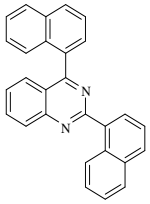	291-293	160-163	8	**9a** (55)	**9b** (17)

4.2.2. Proposed mechanism for the formation of monoarylation (hydroxylation)

The catalytic cycle of the palladium-catalyzed arylation of quinazoline for C-C bond is thought to proceed via. Suzuki-Miyaura cross-coupling reactions. The reaction of monoarylation (hydroxylation) begins with the oxidative addition of an aryl halide to Pd(0) (**1**) complex to form an aryl palladium(II)halide intermediate (**2**). Reaction with base gives intermediate (**3**) which via transmetalation with the boronate complex forms the organopalladium species (**4**). The co-solvent H_2O has subsequently participated for the oxidation at C4 position for hydroxylation product, form an intermediate (**5**). The reductive elimination of the desired product (**6**) restores the original palladium catalyst (**1**) which completes the catalytic cycle to form C4 hydroxylation along with monoarylation at C2

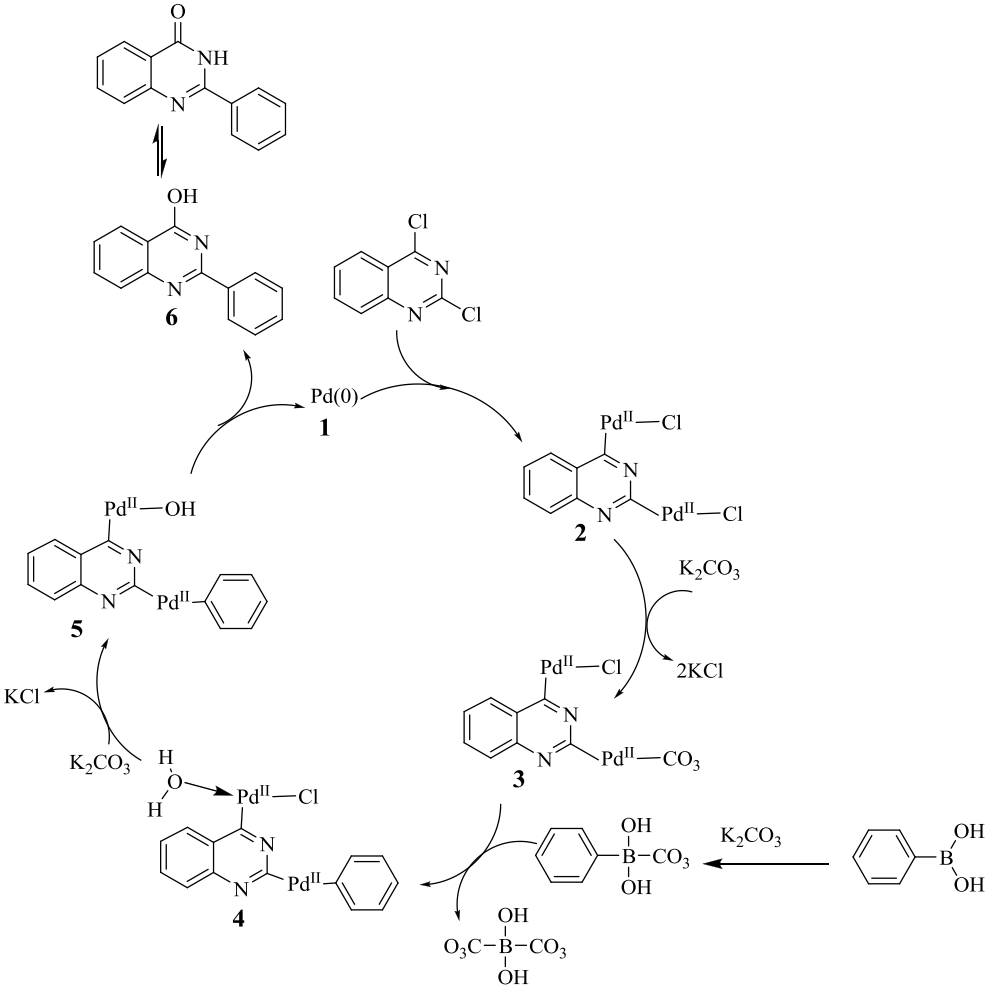

Scheme 3. Proposed reaction mechanism for hydroxylated monoarylation.

position of quinazoline that subsequently converted into the stable keto form (**Scheme 3**). The use of base is obligatory for the Suzuki-Miyaura cross coupling reaction in order to

critically increase reactivity of the transmetallation step. Thus, base is involved in the coordination sphere of the palladium and the formation of Ar-Pd–OH from Ar-Pd–X has been accelerated the transmetalation step for hydroxylation. Base also involved in the arylation at C2 position of quinazoline with arylboronic acids.

4.2.3. Single Crystal X-ray diffraction

2,4-Di-naphthalen-1-yl-quinazoline **(9b)** was grown in ethanol to develop single crystal and the following data was obtained. Molecular formula = $C_{28}H_{18}N_2$, M.wt. = 382.44, colourless rectangular crystals, 0.30×0.30×0.40 mm, monoclinic, space group $P2_1/c$, a = 18.6473 (14) Å, b = 12.4471 (7) Å, c = 8.3228 (6) Å, α = 90.0°, β = 97.850 (5)°, γ = 90.0°, V = 1913.7 (2) $Å^3$, Z = 4, D_{calcd} = 1.327 Mg/m^3, reflection collected = 15314, Unique: 3300 (R_{int} = 0.0319), Final R indices = R_1 = 0.0473, wR_2 = 0.1018, R indices = R_1 = 0.0957, wR_2 = 0.1213, T = 250K with Bruker AXS KAPPA APEX II diffractometer with graphite monochromated Mo Kα radiation (λ = 0.7107 Å) using SHELX-97, full-matrix least-square refinement method (**Table-3**). The molecular solid state structure and numbering system is indicated in **figure 1**.[64] Molecule has intermolecular CH-π interactions where quinazoline π cloud interacts with hydrogen atom of napthalene ring (C23···H17C17, *d* = 2.79Å). Naphthalene hydrogen atom has also showed interactions with π cloud of intermolecular naphthalene moiety (C26···H26C4, *d* = 2.76Å). The aryl rings were inclined at a dihedral angle of 138.94° between N2C6-C5C4 and 54° between N1C7-C8C9, indicating that the two naphthelene rings are not in planer with quinazoline ring and two rings are approaching towards each other.The bond length of N2-C6 [1.322 (2)] of quinazoline ring is shorter having double bond character than that longer bond length of C6–N1 [1.371 (2)] having single bond character. The bond length of C5 and C6 (1.48 Å), and C7 and C8 (1.49 Å) have also revealed that the two naphthathene rings are attached to the quinazoline with single bond character.

Table 3. Summary of crystal data, data collection and structure refinement for compound **9b**

A. Crystal data	
Empirical formula	$C_{28}H_{18}N_2$
Formula weight	382.44
Temperature	250(2) K
Wavelength	0.71073 Å

Crystal size	0.30 x 0.30 x 0.40 mm	
Crystal habit	colorless rectangular	
Crystal system	monoclinic	
Space group	$P2_1/c$	
Unit cell dimensions	a = 18.6473(14)Å	α = 90°
	b = 12.4471(7) Å	β = 97.850(5)°
	c = 8.3228(6) Å	γ = 90°
Volume	1913.7(2) $Å^3$	
Z	4	
Density (calculated)	1.327 Mg/cm^3	
Absorption coefficient	0.078 mm^{-1}	
F(000)	800	

B. Data collection and refinement

Theta range for data collection	1.97 to 25.04°
Index ranges	-22<=h<=22, -12<=k<=14, -9<=l<=9
Reflections collected	15314
Independent reflections	3300 [R(int) = 0.0319]
Coverage of independent reflections	97.5%
Absorption correction	multi-scan
Structure solution technique	direct methods
Structure solution program	SHELXS-97 (Sheldrick, 2008)
Refinement method	Full-matrix least-squares on F^2
Refinement program	SHELXL-97 (Sheldrick, 2008)
Function minimized	$\Sigma\, w(F_o^2 - F_c^2)^2$
Data / restraints / parameters	3300 / 0 / 271
Goodness-of-fit on F^2	1.006
Δ/σ_{max}	0.001

Final R indices	2035 data; I>2σ(I)	$R_1 = 0.0473$, $wR_2 = 0.1018$
		$R_1 = 0.0957$, $wR_2 = 0.1213$
Weighting scheme	$w=1/[\sigma^2(F_o^2)+(0.0614P)^2+0.0000P]$ where $P=(F_o^2+2F_c^2)/3$	
Largest diff. peak and hole	0.151 and -0.179 eÅ^{-3}	
R.M.S. deviation from mean	0.041 eÅ^{-3}	

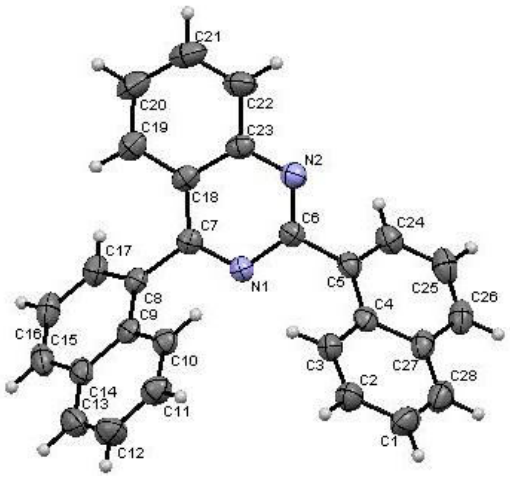

Figure 1. X-ray structure of compound **9b** (CCDC No. 974588)

4.3. BIOLOGY

In vitro evaluation of 60 human cancer cell line studies

Out of fourteen synthesized compounds, three compounds **2b, 3b** and **9b** have been selected for the investigation on 60 cell lines panel of human cancer cells at a single dose of 10 μM at National Cancer Institute (NCI), Bethesda, MD, USA which included nine tumor subpanels namely; leukemia, non-small lung, colon, CNS, melanoma, ovarian, renal, prostate and breast cancer cells[65-68] and their output was reported as mean graph of the percent growth of treated cells and presented as percentage growth inhibition (GI %). These compounds were found to be selective for some of the cell lines and anti-cancer data of compounds with activity over cancer cell lines are given in **table-4**.

Preliminary *in vitro* antitumor screening revealed that compounds **2a, 3b** and **9b** showed moderate growth inhibition (20-70%) for some of the cancer cell lines. On the contrary, compound **3b** showed weak activities compared with other compounds and percentage of

growth inhibition did not reach 40%. Regarding the activity towards individual cell lines; compounds **2b, 3b** and **9b** showed selective potency against breast cancer cell T-47D with GI values of 30.13%, 20.80% and 50.00% respectively. Compound **9b** was identified as the most potent in this series and proved to be active towards leukemia cell line K-562 with GI value of 65.76%, breast cancer cell line MCF7 with GI value of 41.37% and renal cancer cell line UO-31 with GI value of 40.00%. Compound **2b** showed most sensitivity to non-small cell lung cancer cell HOP-92 with GI value of 45.81% than other cancer cell lines. Compound **3b** showed sensitivity to non-small cell lung cancer cell line NCI-H460 with GI value of 40.58%.

Table 4. The percentage growth inhibition (GI%) of the selected compounds over the full panel of tumor cell lines at 10 μM concentration

Cell Line Type	Cell Line Name	2b	3b	9b
Leukemia	CCRF-CEM	-	-	-
	HL-60(TB)	-	-	-
	K-562	-	24.13	**65.36**
	MOLT-4	-	-	37.12
	RPMI-8226	-	-	-
	SR	-	18.41	14.82
Non-Small Cell Lung Cancer	A549/ATCC	-	24.89	14.39
	EKVX	-	17.80	-
	HOP-62	12.79	12.53	-
	HOP-92	45.81	-	21.04
	NCI-H226	19.26	-	19.43
	NCI-H23	18.82	13.21	23.61
	NCI-H322M	-	-	15.00
	NCI-H460	-	40.58	-
	NCI-H522	12.84	12.24	19.20
Colon Cancer	COLO 205	-	10.21	19.42
	HCC-2998	-	-	-
	HCT-116	-	24.92	29.53
	HCT-15	-	-	16.00
	HT29	-	-	33.02
	KM12	-	-	14.88
	SW-620	-	-	-
CNS Cancer	SF-268	10.20	-	10.20
	SF-295	-	11.00	-
	SF-539	-	-	-
	SNB-19	-	-	-
	SNB-75	19.41	15.00	21.80
	U251	30.31	25.32	17.75
Melanoma	LOX IMVI	10.44	18.41	17.30
	MALME-3M	13.76	11.72	15.99
	M14	-	-	21.32
	MDA-MB-435	-	-	-
	SK-MEL-2	-	-	-
	SK-MEL-28	-	-	-
	SK-MEL-5	14.67	-	11.75
	UACC-257	-	-	-

	UACC-62	11.04	10.25	-
Ovarian Cancer	IGROV1	13.60	-	14.61
	OVCAR-3	13.23	-	-
	OVCAR-4	30.95	36.89	15.37
	OVCAR-5	-	-	17.06
	OVCAR-8	11.57	32.37	13.36
	NCI/ADR-RES	13.24	15.12	10.00
	SK-OV-3	14.24	15.72	-
Renal Cancer	786-0	-	12.81	11.93
	A498	-	-	-
	ACHN	-	39.68	-
	CAKI-1	26.42	-	24.23
	RXF 393	-	-	-
	SN12C	10.32	14.36	21.45
	TK-10	-	11.32	-
	UO-31	34.36	20.00	40.00
Prostate Cancer	PC-3	20.00	-	24.40
	DU-145	-	-	-
Breast Cancer	MCF7	17.96	17.01	41.37
	MDA-MB-231/ATCC	12.70	10.84	20.00
	HS 578T	-	-	-
	BT-549	-	-	-
	T-47D	30.13	20.80	**50.00**
	MDA-MB-468	-	-	-

- GI < 10 %, Prominent GI values are bolded.

4.4. CONCLUSION

We have developed an efficient, economical, and practical method for the synthesis of palladium catalyzed cross coupling reaction and subsequent hydroxylation of 2,4-dichloroquinazoline. A variety of monoarylated and diarylated quinazoline products have been prepared from activated and non-activated heteroaryl substrates. Key to the success is the use of water and boronic acids for unique simultaneous C-O and C-C bond formation in the presence of palladium catalyst. The anticancer activities of compounds **2b**, **3b** and **9b** towards 60 human cancer cell lines indicated that these compounds inhibited tumor growth for some of the cancer cell lines with most active to leukemia K562 cancer cell line with percentage growth inhibition of 65.36%.

4.5. EXPERIMENTAL SECTION

4.5.1. Synthesis of compounds

General note

Melting points were determined in open capillaries and are uncorrected. For monitoring the progress of the reaction and for comparison with authentic samples, thin layer

chromatography (TLC) was used. For this purpose, microslides were coated with silica gel 'G' containing calcium sulphate as binder or with silica gel HF-254 (Spectrochem, india), by dipping a pair of slides held back to back in slurry of adsorbent in chloroform : methanol (80:20). The chromatograms were developed in iodine chamber. Separation of various components was carried out by column chromatography using silica gel 60-120 mesh (Spectrochem, india), as adsorbent and chloroform: methanol or their mixture as eluents. All the fractions collected from column chromatography were compared with chromatograms of reaction mixture (TLC) for checking their identity and purity.

The ^{1}H and ^{13}C NMR spectra were recorded on Jeol ECS-400 (^{1}H, 400 MHz; ^{13}C, 100 MHz) spectrometer (Tokyo, Japan) at ambient temperature, using $CDCl_3$ and DMSO-d_6 as solvents. The chemical shifts were expressed in parts per million with TMS as internal reference and *J* values are given in hertz (Hz). Spectral patterns are designated as s = singlet; bs = broad singlet; d = doublet; t = triplet; dd = double doublet; q = quartet and m = multiplet. Mass Spectra of the synthesized compounds were recorded at Waters Micromass Q-Tof Micro (Milford, MA). Infrared Spectra were recorded on Agilent technology cary 630 USA. The crystal structure was collected on Bruker AXS KAPPA APEX II CCD diffractometer (Billerica, Massachusttes).

Materials: Anthranilic acid, urea, phosphorous oxychloride, triethylamine, potassium carbonate, sodium carbonate, cesium carbonate, sodium *tert*-butoxide, tetrakis(triphenylphosphine)palladium(0), tris(dibenzylideneacetone)dipalladium(0), bis(triphenylphosphine)palladium(II)dichloride, phenylboronic acid, 4-fluorophenyl boronic acid, 4-chlorophenyl boronic acid, 4-bromophenyl boronic acid, 3-methylphenyl boronic acid, 4-methoxyphenylboronic acid, thiophen-2-ylboronic acid, furan-2-ylboronic acid, naphthalen-1-ylboronic acid, toluene, chloroform and methanol were purchased from S.D. fine chemicals, Loba chemicals, Spectrochemical and Sigma Aldrich. Absolute ethanol chloroform and methanol were of LR grade and were distilled before use.

General procedure for the synthesis of compounds 1-9

A vial equipped with stirring bar was charged with 2,4-dichloroquinazoline (0.2 g, 1.0 mmol), K_2CO_3 (0.28 g, 2.0 mmol) and boronic acids (2.0 mmol), dissolved in toluene : water (9:1) at 110 ^{0}C under inert atmosphere. Then, 10 mol% of $Pd(PPh_3)_4$ was added and vial was capped and sealed. The reaction mixture was refluxed for 7-12 h. After the completion of the reaction (monitored by TLC), cooled the reaction mixture, and then extract with water and

chloroform. Organic layer was dried over sodium sulphate, filtered and concentrated under *vacuo* to get crude product. The residue was purified by silica gel (60-120 mesh) column chromatography using hexane : ethyl acetate (3:2) as eluents to give pure solid.

2-Phenyl-3*H*-quinazolin-4-one (1a).

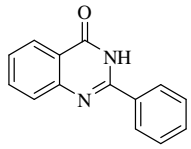

Light yellow solid, yield: 75%; mp. 238-240 °C (Lit.[61] mp. 235-237 °C); IR (KBr, cm^{-1}) ν: 3359, 3060, 1658, 1334, 1289 ; ^{1}H NMR (400 MHz, $CDCl_3$): δ 11.20 (s, 1H, NH), 8.33-8.31 (d, 1H, *J* = 7.8 Hz, ArH), 8.21-8.19 (t, 2H, *J* = 6.0 Hz, ArH), 7.88-7.78 (m, 2H, ArH), 7.59-7.57 (t, 3H, *J* = 2.28 Hz, ArH), 7.52-7.48 (t, 1H, *J* = 6.64 Hz, ArH); ^{13}C NMR (100 MHz, $CDCl_3$): δ 163.7, 151.7, 149.5, 135.0, 132.9, 131.8, 129.2, 128.1, 127.4, 126.9, 126.5, 120.8; EIMS, m/z: 223.1 (M^++1).

2,4-Diphenyl-quinazoline (1b).

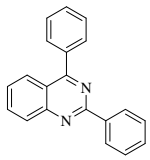

White solid, yield: 16%; mp. 118-119 °C (Lit. [69] mp. 116-117 °C); IR (KBr, cm^{-1}) ν: 3061, 1336, 1289; ^{1}H NMR (400 MHz, $CDCl_3$): δ 8.70-8.68 (d, 2H, *J* = 7.76 Hz, ArH), 8.17-8.12 (t, 2H, *J* = 8.72 Hz, ArH), 7.90-7.89 (t, 3H, *J* = 4.60 Hz, ArH), 7.60-7.51 (m, 7H, ArH); ^{13}C NMR (100 MHz, $CDCl_3$): δ 168.4, 160.3, 152.1, 138.3, 137.8, 133.7, 130.6, 130.3, 130.0, 129.3, 128.8, 128.7, 127.1, 121.8; EIMS, m/z: 283.1 (M^++1).

2-(4-Fluoro-phenyl)-3*H*-quinazolin-4-one (2a).

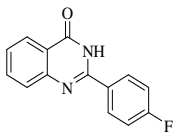

Light yellow solid, yield: 64%; mp. 238-240 °C (Lit.[70] mp. 251-253 °C); IR (KBr, cm^{-1}) ν: 3350, 3044, 1660, 1286, 1164; ^{1}H NMR (400 MHz, $CDCl_3$): δ 10.62 (s, 1H, NH), 8.33-8.31 (d, 1H, *J* = 7.76 Hz, ArH), 8.20-8.16 (m, 2H, ArH), 7.83-7.82 (d, 2H, *J* = 3.28 Hz, ArH), 7.54-7.50 (m, 1H, ArH), 7.27-7.26 (d, 2H, *J* = 5.04 Hz, ArH); ^{13}C NMR (100 MHz, $CDCl_3$): δ 163.3, 150.5, 149.4, 135.1, 129.5, 129.4, 128.1, 127.1, 126.5, 120.8, 116.5, 116.3; EIMS, m/z: 241.1 (M^++1).

2,4-bis(4-Fluoro-phenyl)-quinazoline (2b).

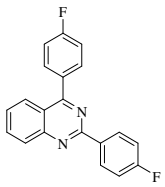

White solid, yield: 25%; mp. 170-172 °C; IR (KBr, cm^{-1}) ν: 3047, 1336, 1219, 1146; ^{1}H NMR (400 MHz, $CDCl_3$): δ 8.70-8.67 (dd, 2H, ^2J = 5.48 Hz, ^3J = 3.10 Hz, ArH), 8.15-8.08 (dd, 2H, ^2J =8.28 Hz, ^3J = 3.01 Hz, ArH), 7.91-7.87 (m, 3H, ArH), 7.59-7.55 (t, 1H, *J* = 7.32 Hz, ArH), 7.32-7.27 (t, 2H, *J* = 10.08 Hz, ArH), 7.22-7.18 (t, 2H, *J* = 8.72 Hz, ArH); ^{13}C NMR (100 MHz, $CDCl_3$): δ 162.6, 161.2, 160.5, 158.7, 158.1, 154.6, 147.3, 129.6, 129.1, 129.0, 127.5, 127.4, 126.1, 126.0, 124.5, 122.5, 122.1, 116.8, 111.2, 110.9, 110.7; EIMS, m/z: 319.1 (M^++1).

2-(4-Chloro-phenyl)-3*H*-quinazolin-4-one (3a).

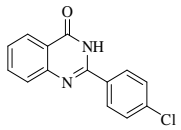

Light yellow solid, yield: 68%; mp. 298-300 °C (Lit.[56] mp. 299-300 °C); IR (KBr, cm^{-1}) ν: 3341, 3046, 1671, 1342, 1281, 938; ^{1}H NMR (400 MHz, DMSO-d_6): δ 12.55 (s, 1H, NH), 8.17-8.15 (d, 2H, *J* = 8.24 Hz, ArH), 8.11-8.09 (d, 1H, *J* = 7.80 Hz, ArH), 7.79-7.75 (t, 1H, *J* = 7.56 Hz, ArH), 7.69-7.67 (d, 1H, *J* = 8.28 Hz, ArH), 7.54-7.52 (d, 2H, *J* = 8.24 Hz, ArH), 7.48-7.44 (t,1H, *J* = 7.32 Hz, ArH); ^{13}C NMR (100 MHz, DMSO-d_6): δ 162.8, 151.7, 149.1, 136.9, 134.9, 132.0, 130.0, 129.1, 127.9, 127.0, 126.3, 121.5; EIMS, m/z: 257.5 (M^++1).

2,4-bis(4-Chloro-phenyl)-quinazoline (3b).

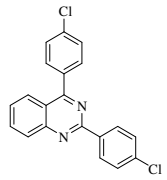

White solid, yield: 19%; mp. 198-200 °C; IR (KBr, cm^{-1}) ν: 3048, 1336, 1219, 1014; ^{1}H NMR (400 MHz, DMSO-d_6): δ 8.57-8.55 (d, 2H, *J* = 8.68 Hz, ArH), 8.19 (s, 1H, ArH), 8.09-8.04 (q, 2H, *J* = 8.28 Hz, ArH), 8.00-7.96 (t, 1H, *J* = 7.80 Hz, ArH), 7.87-7.85 (d, 2H, *J* = 8.72 Hz, ArH), 7.67-7.63 (t, 2H, *J* = 8.72 Hz, ArH), 7.55-7.53 (d, 2H, *J* = 8.72 Hz, ArH); ^{13}C NMR (100 MHz, DMSO-d_6): δ 167.4, 158.6, 151.7, 136.7, 136.4, 136.1, 135.8, 134.9, 132.2, 130.3, 129.2, 128.6, 127.1, 121.5; EIMS, m/z: 352.1 (M^++1).

2-(4-Bromo-phenyl)-3*H*-quinazolin-4-one (4a).

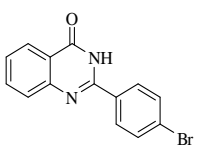

Grey solid, yield: 70%; mp. 291-294 °C (Lit.[56] mp. 295-296 °C); IR (KBr, cm^{-1}) ν: 3375, 3034, 1656, 1384, 1340, 504; ^{1}H NMR (400 MHz, DMSO-d_6): δ 11.18 (s, 1H, NH), 7.93-7.89 (t, 2H, *J* = 8.24 Hz, ArH), 7.86 (s, 1H,

ArH), 7.73-7.71 (dd, 2H, ^{2}J = 8.24 Hz, ^{3}J = 1.36 Hz, ArH), 7.60 (s, 2H, ArH), 7.57-7.56 (d, 1H, J = 4.60 Hz, ArH); ^{13}C NMR (100 MHz, DMSO-d_6): δ 163.9, 161.8, 160.7, 135.8, 134.6, 134.5, 131.5, 131.4, 128.3, 128.2, 127.0, 126.8, 125.3, 120.9; EIMS, m/z: 302.1 (M^++1).

2-(4-Methoxy-phenyl)-3*H*-quinazolin-4-one (5a).

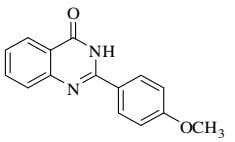

Yellow solid, yield: 75%; mp. 245-247 °C (Lit.[56] mp. 247-248 °C); IR (KBr, cm^{-1}) ν: 3350, 3061, 1672, 1242, 1026; ^{1}H NMR (400 MHz, $CDCl_3$): δ 11.02 (s, 1H, NH), 8.32-8.31 (d, 1H, J = 6.88 Hz, ArH), 8.19-8.16 (t, 2H, J = 6.88 Hz, ArH), 7.80-7.79 (t, 2H, J = 3.24 Hz, ArH), 7.50-7.48 (m, 1H, ArH), 7.13-7.07 (m, 2H, ArH), 3.92 (s, 3H, OCH_3); ^{13}C NMR (100 MHz, $CDCl_3$): δ 163.2, 162.5, 151.1, 149.6, 134.8, 131.8, 130.2, 128.8, 127.8, 126.4, 126.4, 125.0, 114.5, 113.9, 113.8, 55.5; GC-MS: 252.2 $(M)^+$.

2,4-bis(4-Methoxy-phenyl)-quinazoline (5b).

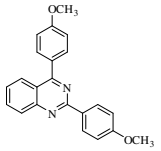

White solid, yield: 20%; mp. 115-117 °C; (Lit.[69]); IR (KBr, cm^{-1}) ν: 3100, 1291, 1254, 1137; ^{1}H NMR (400 MHz, $CDCl_3$): δ 8.17-8.15 (d,1H, J = 8.24 Hz, ArH), 8.02-8.00 (d, 2H, J = 8.28 Hz, ArH), 7.92-7.83 (m, 2H, ArH), 7.80-7.77 (d, 2H, J = 8.68 Hz, ArH), 7.61-7.58 (t, 2H, J = 7.32 Hz, ArH), 7.11-7.06 (t, 3H, J = 8.20 Hz, ArH), 3.90 (s, 6H, OCH_3); ^{13}C NMR (100 MHz, $CDCl_3$): δ 171.1, 161.9, 157.1, 153.1, 134.8, 132.1, 128.4, 128.1, 127.9, 127.6, 121.6, 114.3, 55.6, 31.0; EIMS, m/z: 343.2 (M^++1).

2-*m*-Tolyl-3*H*-quinazolin-4-one (6a).

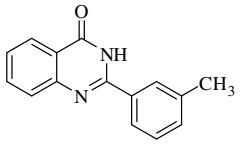

Light yellow solid, yield: 65%; mp. 210-212 °C (Lit.[56] mp. 210-211 °C); IR (KBr, cm^{-1}) ν: 3290, 3044, 1675, 1305, 1248; ^{1}H NMR (400 MHz, $CDCl_3$): δ 10.96 (s,1H, NH), 8.34-8.32 (d,1H, J = 7.32 Hz, ArH), 8.03 (s, 1H, ArH), 7.97-7.95 (d,1H, J = 7.80 Hz, ArH), 7.84-7.81 (m, 2H, ArH), 7.53-7.39 (m, 3H, ArH), 2.51 (s, 1H, CH_3); ^{13}C NMR (100 MHz, $CDCl_3$): δ 163.5, 151.7, 149.4, 138.8, 134.7, 132.6, 132.4, 128.9, 127.8, 126.6, 126.2, 124.2, 120.7, 21.4; EIMS, m/z: 237.3 (M^++1).

2-(Thiophen-2-yl)-3*H*-quinazolin-4-one (7a).

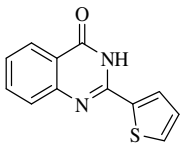

Yellow solid, yield: 60%; mp. 277-280 °C (Lit.[61] mp. 275-276 °C); IR (KBr, cm^{-1}) ν: 3365, 2991, 1681, 1375, 1252, 1057; ^{1}H NMR (400 MHz, DMSO- d_6): δ 10.96 (s, 1H, NH), 7.71-7.70 (dd, 2H, ^2J = 7.36 Hz, ^3J = 2.76 Hz, ArH), 7.56-7.38 (m, 3H, ArH), 7.09-7.01 (m, 2H, ArH); ^{13}C NMR (100 MHz, DMSO-d_6): δ 162.9, 150.4, 140.7, 134.3, 131.4, 131.3, 128.3, 128.2, 126.7, 126.7, 121.9, 115.2, 114.3; EIMS, m/z: 229.2 (M^++1).

2-(Furan-2-yl)-3*H*-quinazolin-4-one (8a).

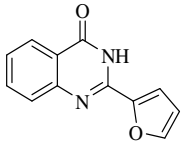

Light yellow solid, yield: 60%; mp. 217-219 °C (Lit.[55] mp. 219-220 °C); IR (KBr, cm^{-1}) ν: 3325, 3116, 1609, 1337, 1280, 1106; ^{1}H NMR (400 MHz, $CDCl_3$): δ 11.43 (s, 1H, NH), 8.95 (d, 1H, J = 8.68 Hz, ArH),

7.99-7.90 (m, 2H, ArH), 7.83 (s, 1H, ArH), 7.69 (d, 2H, J = 3.68 Hz, ArH), 6.72-6.70 (m, 1H, ArH); ^{13}C NMR (100 MHz, $CDCl_3$); δ 157.8, 157.0, 153.8, 152.5, 147.0, 139.4, 134.9, 128.3, 128.2, 127.2, 119.5, 118.3, 114.2, 112.9; GC-MS: 212.3 $(M)^+$.

2-Naphthalen-1-yl–3*H*-quinazolin-4-one (9a).

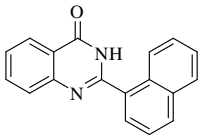

Light yellow solid, yield: 55%; mp. 291-293 °C (Lit.[57] mp. 289-292 °C); IR (KBr, cm^{-1}) ν: 3433, 2981, 1669, 1284, 1252; ^{1}H NMR (400 MHz, DMSO-d_6): δ 12.59 (s, 1H, NH), 8.27-8.21 (m, 2H, ArH), 8.06-8.04

(d, 1H, J = 8.24 Hz, ArH), 7.98-7.90 (dd, 2H, ^2J = 5.48 Hz, ^3J = 1.84 Hz, ArH), 7.83-7.74 (m, 1H, ArH), 7.64-7.55 (m, 4H, ArH); ^{13}C NMR (100 MHz, DMSO-d_6): δ 162.5, 154.1, 149.2, 134.8, 133.6, 132.2, 130.8, 130.8, 128.7, 128.1, 127.9, 127.4, 127.1, 126.7, 126.3, 125.7, 125.4, 121.8; EIMS, m/z: 273.1 (M^++1).

2,4-Di-naphthalen-1-yl-quinazoline (9b).

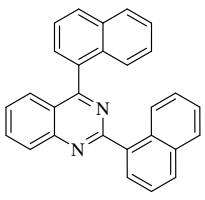

White solid, yield: 17%; mp. 160-163 °C; (Lit.[69]); IR (KBr, cm^{-1}) ν: 2977, 1335, 1249; ^{1}H NMR (400 MHz, $CDCl_3$): δ 8.84-8.82 (d, 1H, J = 8.24 Hz, ArH), 8.28-8.23 (q, 2H, ^2J = 7.32 Hz, ^3J = 2.80 Hz, ArH), 8.05-8.03 (d, 1H, J = 8.24 Hz, ArH), 7.98-7.90 (m, 4H, ArH), 7.71-7.49

(m, 10H, ArH); ^{13}C NMR (100 MHz, $CDCl_3$): δ 169.4, 163.0, 151.3, 134.8, 134.3, 133.8, 131.7, 131.4, 130.4, 130.0, 129.9, 129.1, 128.6, 128.0, 127.6, 127.5, 126.9, 126.9, 126.4, 126.1, 125.9, 125.8, 125.4, 125.2, 123.0; EIMS, m/z: 383.2 (M^++1).

4.5.2. *In Vitro* studies (60 human cancer cell lines)

All the synthesized compounds were submitted to National Cancer Institute (NCI) disease-oriented human cell lines for screening assay to be evaluated for their *in-vitro* antitumor activities against 60 cell lines which included nine tumour subpanels namely; leukemia, non-small lung, colon, CNS, melanoma, ovarian renal, prostate and breast cancer cells. The human tumour cell lines of the cancer screening panel were grown in RPMI 1640 medium containing 5% fetal bovine serum and 2 mM L-glutamine. Cells were inoculated into 96 well microtiter plates in 100 ml at plating densities ranging from 5,000 to 40,000 cells/well depending on the doubling time of individual cell lines. The microtiter plates were then incubated at 37 °C, 5% CO_2, 95% air and 100% relative humidity for 24 h.

After 24 h, two plates of each cell line were fixed in situ with TCA, to represent a measurement of the cell population for each cell line. Experimental drugs were solubilized in DMSO at 400-fold the desired final maximum test concentration and stored frozen prior to use. At the time of drug addition, an aliquot of frozen concentrate was thawed and diluted to twice the desired final maximum test concentration with complete medium containing 50 µg/ml gentamicin. Additional four, 10-fold or ½ log serial dilutions were made to provide a total of five drug concentrations plus control. Aliquots of 100 µL of these different drug dilutions were added to the appropriate microtiter wells, resulting in the required final drug concentrations. Following drug addition, the plates were incubated for an additional 48 h at 37 °C, 5% CO_2, 95% air, and 100% relative humidity. For adherent cells, the assay was terminated by the addition of cold TCA. Cells were fixed in situ by the gentle addition of 50 µL of cold 50% (w/v) TCA and incubated for 60 min at 4 °C. The supernatant was discarded, and the plates were washed five times with tap water and air dried. Sulforhodamine B (SRB) solution (100 µL) at 0.4% (w/v) in 1% acetic acid is added to each well, and plates are incubated for 10 min at room temperature. After staining, unbound dye was removed by washing five times with 1% acetic acid and the plates were air dried and then subsequently solubilized with 10 mM trizma base, and the absorbance was read on an automated plate reader at a wavelength of 515 nm. Using the seven absorbance measurements [time zero (T_z), control growth (C), and test growth in the presence of drug at the five concentration levels

(T_i)], the percentage growth was calculated at each of the drug concentrations levels. Percentage growth inhibition is calculated as:

[(Ti -Tz)/(C - Tz)] × 100 for concentrations for which $T_i \geq Tz$; [(Ti -Tz)/Tz] × 100 for concentrations for which Ti < Tz.

Three dose response parameters were calculated for each experimental agent. Growth inhibition of 50% (GI_{50}) was calculated from [(Ti -Tz)/(C - Tz)] × 100 = 50. The drug concentration resulting in total growth inhibition (TGI) is calculated from $T_i = Tz$. The LC_{50} was calculated from [(Ti-Tz)/Tz]×100 = 50.[65,67,71]

REFERENCES

1. Gravett, E. C.; Hilton, P. J.; Jones, K.; Peron, J. M. *Synlett* **2003**, 253.
2. Arterburn, J. B.; Bryant, B. K.; Chen, D. J. *Chem. Commun.* **2003**, 1890.
3. Cossy, J.; Belotti, D.; Magner, A. *Synlett* **2003**, 1515.
4. Li, J. H.; Deng, C. L.; Xie, Y. X. *Synth. Commun.* **2007**, *37*, 2433.
5. Yu, C. W.; Chen, G. S.; Huang, C. W.; Chern, J. W. *Org. Lett.* **2012**, *14*, 3688.
6. Xiao, Y.; Xu, Y.; Cheon, H. S.; Chae, J. *J. Org. Chem.* **2013**, *78*, 5804.
7. (a) Sergeev, A. G.; Schulz, T.; Torborg, C.; Spannenberg, A.; Neumann, H.; Beller, M. *Angew. Chem. Int. Ed.* **2009**, *48*, 7595; (b) Schulz, T.; Torborg, C.; Schaffner, B.; Huang, J.; Zapf, A.; Kadyrov, R.; Borner, A.; Beller, M. *Angew. Chem. Int. Ed.* **2009**, *48*, 918.
8. Lavery, C. B.; Rotta-Loria, N. L.; McDonald, R.; Stradiotto, M. *Adv. Synth. Catal.* **2013**, *355*, 981.
9. Chen, G.; Chan, A. S. C.; Kwong, F. Y. *Tetrahedron Lett.* **2007**, *48*, 473.
10. Khanapure, S. P.; Garvey, D. S. *Tetrahedron Lett.* **2004**, *45*, 5283.
11. Miyaura, N.; Suzuki, A. *Chem. Rev.* **1995**, *95*, 2457.
12. Ohta, H.; Tokunaga, M.; Obora, Y.; Iwai, T.; Iwasawa, T.; Fujihara, T.; Tsuji, Y. *Org. Lett.* **2007**, *9*, 89.
13. Han, F. S. *Chem. Soc. Rev.* **2013**, *42*, 5270.
14. Kotha, S.; Lahiri, K.; Kashinath, D. *Tetrahedron* **2002**, *58*, 9633.

15. Alonso, F.; Beletskaya, I. P.; Yus, M. *Tetrahedron* **2008**, *64*, 3047.
16. Littke, A. F.; Fu, G. C. *Angew. Chem. Int. Ed.* **2002**, *41*, 4176.
17. Roy, D.; Mom, S.; Beauperin, M.; Doucet, H.; Hierso, J. C. *Angew. Chem. Int. Ed.* **2010**, *49*, 6650.
18. Hassan, J.; Sevignon, M.; Schulz, E.; Lemaire, M. *Chem. Rev.* **2002**, *102*, 1359.
19. Schroter, S.; Stock, C.; Bach, T. *Tetrahedron* **2005**, *61*, 2245.
20. Ducray, R; Boutron, P; Didelot, M; Germain, H; Lach, F; Lamorlette, M; Legriffon, A; Maudet, M; Ménard, M; Pasquet, G; Renaud, F; Simpson, I; Young, G. L. *Tetrahedron Lett.* **2010**, *51*, 4755.
21. Guram, A. S.; Wang, X.; Bunel, E. E.; Faul, M. M.; Larsen, R. D.; Martinelli, M. J. *J. Org. Chem.* **2007***, 72*, 5104.
22. Bianchini, C.; Giambastiani, G.; Luconi, L.; Meli, A. *Coord. Chem. Rev.* **2010**, *254*, 431.
23. Fauber, B. P.; Dragovich, P. S.; Chen, J.; Corson, L. B.; Ding, C. Z.; Eigenbrot,C.; Giannetti, A. M.; Hunsaker, T.; Labadie, S.; Liu, Y.; Liu, Y.; Malek, S.; Peterson, D.; Pitts, K.; Sideris, S.; Ultsch, M.; VanderPorten, E.; Wang, J.; Wei, B.; Yen, I.; Yue, Q. *Bioorg. Med. Chem. Lett.* **2013**, *23*, 5533.
24. Mishra, N. M.; Vachhani, D. D.; Modha, S. G.; Van der Eycken, E. V. *Eur. J. Org. Chem.* **2013***, 693.*
25. Nikishkin, N. I.; Huskens, J.; Verboom, W. *Org. Biomol. Chem.* **2013**, *11*, 3583.
26. Courme, C.; Gresh, N.; Vidal, M.; Lenoir, C.; Garbay, C.; Florent, J. C.; Bertounesque, E. *Eur. J. Med. Chem. **2010**, 45, 244.*
27. Wagner, D.; Hoffmann, S. T.; Heinemeyer, U.; Munster, I; Kohler, A.; Strohriegl, P. *Chem. Mater.* **2013**, *25*, 3758.
28. Bursavich, M. G.; Dastrup, D.; Shenderovich, M.; Yager, K. M.; Cimbora, D. M.; Williams, B.; Kumar, D. V. *Bioorg. Med. Chem. Lett.* **2013**, *23*, 6829.
29. Parhi, A. K.; Zhang, Y.; Saionz, K. W.; Pradhan, P.; Kaul, M.; Trivedi, K.; Pilch, D. S.; LaVoie, E. J. *Bioorg. Med. Chem. Lett.* **2013**, *23*, 4968.
30. Scott, D. A.; Dakin, L. A.; Daly, K.; Del Valle, D. J.; Diebold, R. B.; Drew, L.; Ezhuthachan, J.; Gero, T. W.; Ogoe, C. A.; Omer, C. A.; Redmond, S. P.; Repik, G.; Thakur, K.; Ye, Q.; Zheng, X. *Bioorg. Med. Chem. Lett.* **2013**, *23*, 4591.
31. Jeon, J. H.; Kim, J. H.; Jeong, Y. J.; Jeong, I. H. *Tetraheron Lett*. **2014**, *55*, 1292.
32. Chapman, T. M.; Osborne, S. A.; Bouloc, N.; Large, J. M; Wallace, C.; Birchall, K.;

Ansell, K. H; Jones, H. M.; Taylor, D.; Clough, B.; Green, J. L.; Holder, A. A. *Bioorg. Med. Chem. Lett.* **2013**, *23*, 3064.

33. Enguehard-Gueiffier, C.; Musiu, S.; Henry, N.; Véron, J. B.; Mavel, S.; Neyts, J.; Leyssen, P.; Paeshuyse, J.; Gueiffier, A. *Eur. J. Med. Chem.* **2013**, *64*, 448.
34. Akkaoui, A. E.; Berteina-Raboin, S.; Mouaddib, A.; Guillaumet, G. *Eur. J. Org. Chem*. **2010**, 862.
35. Dwyer, M. P.; Paruch, K.; Labroli, M.; Alvarez, C.; Keertikar, K. M.; Poker, C.; Rossman, R.; Fischmann, T. O.; Duca, J. S.; Madison, V.; Parry, D.; Davis, N.; Seghezzi, W.; Wiswell, D.; Guzi, T. J. *Bioorg. Med. Chem. Lett.* **2011**, *21*, 467.
36. Engers, D. W.; Frist, A. Y.; Lindsley, C. W.; Hong, C. C.; Hopkins, C. R. *Bioorg. Med. Chem. Lett.* **2013**, *23*, 3248.
37. Lee, W.; Ortwine, D. F.; Bergeron, P.; Lau, K.; Lin, L.; Malek, S.; Nonomiya, J.; Pei, Z.; Robarge, K. D.; Schmidt, S.; Sideris, S.; Lyssikatos, J. P. *Bioorg. Med. Chem. Lett.* **2013**, *23*, 5097.
38. Kumar, P. M.; Kumar, K. S.; Meda, C. L. T.; Reddy, G. R.; Mohakhud, P. K.; Mukkanti, K.; Krishna, G. R.; Reddy, C. M.; Rambabu, D.; Kumar, K. S.; Priya, K. K.; Chennubhotla, K. S.; Banote, R. K.; Kulkarni, P.; Parsa, K. V. L.; Pal, M. *Med. Chem. Commun.* **2012**, *3*, 667.
39. Gillespie, R. J.; Bamford, S. J.; Botting, R.; Comer, M.; Denny, S.; Gaur, S.; Griffin, M.; Jordan, A. M.; Knight, A. R.; Lerpiniere, J.; Leonardi, S.; Lightowler, S.; McAteer, S.; Merrett, A.; Misra, A.; Padfield, A.; Reece, M.; Saadi, M.; Selwood, D. L.; Stratton, G. C.; Surry, D.; Todd, R.; Tong, X.; Ruston, V.; Upton, R.; Weiss, S. M. *J. Med. Chem.* **2009**, *52*, 33.
40. Tumkevicius, S.; Dodonova, J. *Chem. Heterocyc. Compd.* **2012**, *48*, 258.
41. Manvar, A.; Shah, A. *Tetrahedron* **2013**, *69*, 8105.
42. Gallagher-Duval, S.; Herve, G.; Sartori, G.; Enderlin, G.; Len, C. *New J. Chem.* **2013**, *37*, 1989.
43. Bebbington, D.; Binch, H.; Charrier, J. D.; Everitt, S.; Fraysse, D.; Golec, J.; Kay, D.; Knegtel, R.; Mak, C.; Mazzei, F.; Miller, A.; Mortimore, M.; O'Donnell, M.; Patel, S.; Pierard, F.; Pinder, J.; Pollard, J.; Ramaya, S.; Robinson, D.; Rutherford, A.; Studley, J.; Westcott, J. *Bioorg. Med. Chem. Lett.* **2009**, *19*, 3586.
44. Jung, F. H.; Pasquet, G.; Lambert-van der Brempt, C. A.; Heron, N.; Wilkinson, R. W.; Wedge, S. R.; Heaton, S. P.; Odedra, R.; Keen, N. J.; Green, S.; Brown, E.;

Thompson, K.; Brightwell, S. *J. Med. Chem.* **2006**, *49*, 955.

45. Smits, R. A.; Adami, M.; Istyastono, E. P.; Zuiderveld, O. P.; van Dam, C. M. E.; de Kanter, F. J. J.; Jongejan, A.; Coruzzi, G.; Leurs, R.; de Esch, I. J. P. *J. Med. Chem.* **2010,** *53*, 2390.
46. Herget, T.; Freitag, M.; Morbitzer, M.; Kupfer, R.; Stamminger, T.; Marschall, M. *Antimicrob. Agents Chemother.* **2004**, *48*, 4154.
47. Sharma, A.; Luxami, V.; Paul, K. *Bioorg. Med. Chem. Lett.* **2013**, *23*, 3288.
48. Paul, K.; Sharma, A.; Luxami, V. *Bioorg. Med. Chem. Lett.* **2014**, *24*, 624.
49. Waisser, K.; Gregor, J.; Dostal, H.; Kunes, J.; Kubicova, L.; Klimesova, V.; Kaustova, J. *Farmaco* **2001**, *56*, 803.
50. Bikker, J. A.; Brooijmans, N.; Wisser, A.; Mansour, T. S. *J. Med. Chem.* **2009**, *52*, 1493.
51. Chen, J.; Wu, D.; He, F.; Liu, M.; Wu, H.; Ding, J.; Su, W. *Tetrahedron Lett.* **2008**, *49*, 3814.
52. Connolly, D. J.; Cusack, D.; O'Sullivan, T. P.; Guiry, P. J. *Tetrahedron* **2005**, *61*, 10153.
53. Zhang, X. D.; Ye, D. J.; Sun, H. F.; Guo, D. L.; Wang, J.; Huang, H.; Zhang, X.; Jiang, H. L.; Liu, H. *Green Chem.* **2009**, *11*, 1881.
54. Gupta, S.; Agarwal, P. K.; Kundu, K. B. *Tetrahedron Lett.* **2010**, *51*, 1887.
55. Ge, W.; Zhu, X.; Wei, Y. *RSC Adv.* **2013**, *3*, 10817.
56. Zhou, J.; Fang, J. *J. Org. Chem.* **2011**, *76*, 7730.
57. Xu, W.; Jin, Y.; Liu, H.; Jiang, H.; Fu, H. *Org. Lett.* **2011**, *13*, 1274.
58. Yang, D.; Fu, H.; Hu, L.; Jiang, Y.; Zhao, Y. *J. Comb. Chem.* **2009**, *11*, 653.
59. Liu, X.; Fu, H.; Jiang, Y.; Zhao, Y. *Angew. Chem. Int. Ed.* **2009**, *48*, 348.
60. Huang, C.; Fu, H.; Jiang, Y.; Zhao, Y. *Chem. Commun*. **2008**, *47*, 6333.
61. Xu, W.; Fu, H. *J. Org. Chem.* **2011**, *76*, 3846.
62. Ma, B.; Wang, Y.; Peng, J.; Zhu, Q. *J. Org. Chem.* **2011**, *76*, 6362.
63. Sun, Z.; Wang, H.; Wen, K.; Li, Y.; Fan, E. *J. Org. Chem.* **2011**, *76,* 4149.
64. Crystallographic data for the structural analysis have been deposited at the Cambridge Crystallographic Data Centre. (E-mail: deposit@ccdc.cam.ac.uk).
65. Grever, M. R.; Sehepartz, S. A.; Chabners, B. A. *Semin. Oncol.* **1992**, *19*, 622.
66. Monks, A.; Schudiero, D.; Skehan, P.; Shoemaker, R.; Paull, K.; Vistica, D.; Hose, C.; Langley, J.; Cronise, P.; Vaigro-Wolff, A.; Gray- Goodrich, M.; Campbell, H.;

Mayo, J.; Boyd, M. *J. Natl. Cancer Inst.* **1991**, *83*, 757.

67. Boyd, M. R.; Paull, K. D. *Drug Dev. Res.* **1995**, *34*, 91.
68. Sketan, P.; Storeng, R.; Scudiero, D.; Monks, A.; McMahon, J.; Vistica, D.; Warren, J. R.; Bokesch, H.; Kenney, S.; Boyd, M. R. *J. Natl. Cancer Inst.* **1990**, *82*, 1107.
69. Panja, S. S.; Saha, S. *RSC Adv.* **2013**, *3*, 14495.
70. Montazeri, N.; Pourshamsian, K.; Yosefiyan, S.; Samaneh Momeni, S. *J. Chem. Sci.* **2012**, *124*, 883.
71. Alley, M. C.; Scudiero, D. A.; Monks, P. P.; Hursey, M. L.; Czerwinski, M. J.; Fine, D. L.; Abbott, B. J.; Mayo, J. G;. Shoemaker, R. H.; Boyd, M. R. *Cancer Res*. **1988**, *48*, 589.

SUMMARY

Cancer is a group of diseases that leads to disruption of basic biological functions, such as cell division, differentiation, angiogenesis and migration, thus promote cancer.[1] Cancer has afflicted our ancestors throughout the history of mankind, but it has become a major cause of mortality only in the last century.[2] The American Cancer Society estimated that only year (2014), over 16,65,540 cases of cancer were diagnosed in the United States alone and that over 5,85,720 people died from this disease. The increase in cancer incidence led to the search for latest, safer and efficient anticancer agents, aiming the prevention or the cure of this deadly disease. In the past decade, the development of new anti-cancer therapeutic tools had achieved enormous advancement. Thus approach for the treatment of cancer that has moved towards targeting the molecular modifications that occur in tumor cells. This modification has been concentrated on the development of both small molecules and biological agents that have shown significant activity without toxicity associated with conventional chemotherapy.[3] Most of chemotherapeutics presently used in cancer therapy are agents that inhibit tumor growth by inhibiting the replication or transcription of DNA. Protein kinases also play a key role in variety of pathways that mediate essential physiological processes such as transcription, metabolism, cell cycle progression, apoptosis and development. Selective inhibition of kinases is a well-accepted therapeutic approach for treatment of various diseases.[4,5] The protein kinases including serine-threonine kinases, known as mitotic kinases, include cyclin dependent kinase 1 (CDK1), polo kinases, NIMA kinases, WARTS/LATS1 kinases, and Aurora kinases that play an important role in different stages of cell division. Aurora-A is a key member of a closely related subgroup of serine/threonine kinases which belongs to the Aurora kinase family, was first discovered in the screening for Drosophila mutations affecting the poles of the mitotic spindle function.[6,7] Many research groups have proved that the overexpression of Aurora-A induces several cancer-associated phenotypes, including enhanced cell proliferation and colony formation, and inhibition of apoptosis.[8,9] In the path of identifying new chemical substances which may lead to the designing of novel antitumor agents, nitrogen-containing heterocycles are of particular interest.[10] Among these, quinazoline, purine and benzimidazole are important classes of heterocyclic compounds and are the most common motifs present in drugs and bioactive compounds with a broad spectrum of pharmacological activities.[11]

Keeping in view the above points, the following objectives have been designed.

(1) Different fragments of amino benzimidazole linked quinazoline /purine will be designed with the help of molecular modelling software.

(2) To synthesize of designed compounds of amino benzimidazole linked to central core substituted quinazoline/purine.

(3) Characterization of these compounds with different spectroscopy techniques.

(4) To evaluate in vitro studies of these compounds as anticancer drugs, predict the structure –activity relationship (SAR) studies and correlate with various physico-chemical parameters to each fragment.

In the present investigation, we have combined the structural artifacts of benzimidazole with quinazoline and purine moieties to make a hybrid and substituted them with different secondary and primary amines in order to observe the effect of electron-donor and acceptor nitrogen groups within the moieties. Introduction of allyl and butyl groups at 1- or 3-position of benzimidazole are also known to increase lipid solubility of polar compounds, a character very much needed for the activity. Characterizations of these molecules were done with different spectroscopic techniques such as NMR, IR, mass and X-ray crystallography. These synthesized molecules were evaluated *in vitro* over 60 human cancer cell lines and Aurora A kinase inhibition. SAR and QSAR studies were used to identify the structural features required for the antitumor properties of these new hybrid series. In order to have an insight into the molecular interaction of compounds, their docking were also planned to scrutinize the mode of interactions of compound with amino acids in the active site of the enzyme. We have also reported the first one pot palladium catalysed hydroxylation at C4 position and subsequent arylation at C2 position of 2,4-dichloroquinazoline with variety of boronic acids.

RESULTS

Chapter 2: covers quinazoline-benzimidazole hybridization, their characterization, *in-vitro* evaluation and molecular modelling

2.1. Synthesis of (1/3-allyl-2-methyl-1H/3H-benzimidazol-5-yl)-(2-amino-quinazolin-4-yl)-amine (8-24):

The present research work is based on the synthesis of benzimidazole linked quinazoline hybrid molecules. Treatment of *o*-phenylenediamine with acetic acid at 100 $^{\circ}$C for 24 h to give brown solid of 2-methylbenzimidazole (**1**). Nitration has been done with equal amounts of nitric acid and concentrated sulphuric acid at 0 $^{\circ}$C for 5 h to give orange solid of 2-methyl-

5-nitro-1*H*-benzimidazole **(2).** Treatment of 2-methyl-5-nitro-1*H*-benzimidazole with allyl bromide in the presence of sodium hydride and THF at room temperature for 8 h to give yellow solid of mixture of 1-allyl-2-methyl-5-nitro-1*H*-benzimidazole **(3a)** and 3-allyl-2-methyl-5-nitro-3*H*-benzimidazole **(3b)**. Reduction of 1/3-allyl-2-methyl-5-nitro-1/3*H*-benzimidazole with stannous chloride and 2 N HCl at 110 °C for 7 h gave mixture of products which were separated through column chromatography using ethylacetate: methanol (9.5:0.5) afforded pure solid regioisomeric 1/3-allyl-2-methyl-1/3*H*-benzimidazol-5-ylamine **(4a)/(4b)** (Scheme 1).

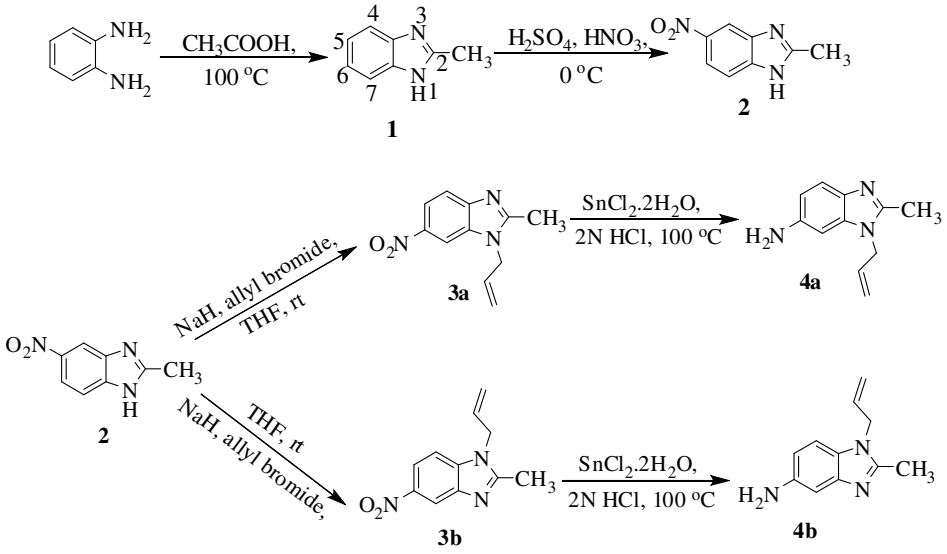

Scheme 1

Anthranilic acid was treated with urea with stirring at 160 °C for 6h to give white solid of 1*H*-quinazolin-2,4-dione **(5)** followed by treatment with phosphorous oxychloride and triethylamine for 7h to give yellow solid of 2,4-dichoro-quinazoline **(6).** Then, 2,4-dichloroquinazoline was treated with 1/3-allyl-2-methyl-1/3*H*-benzimidazol-5-ylamine **(4a)** and **(4b)** in isopropyl alcohol (IPA) at room temperature for 12 h to give white solid of **7a** and **7b**. Compounds **7a** and **7b** were further refluxed with secondary and primary amines in IPA gave compounds **8-24** in moderate to good yields (Scheme 2).

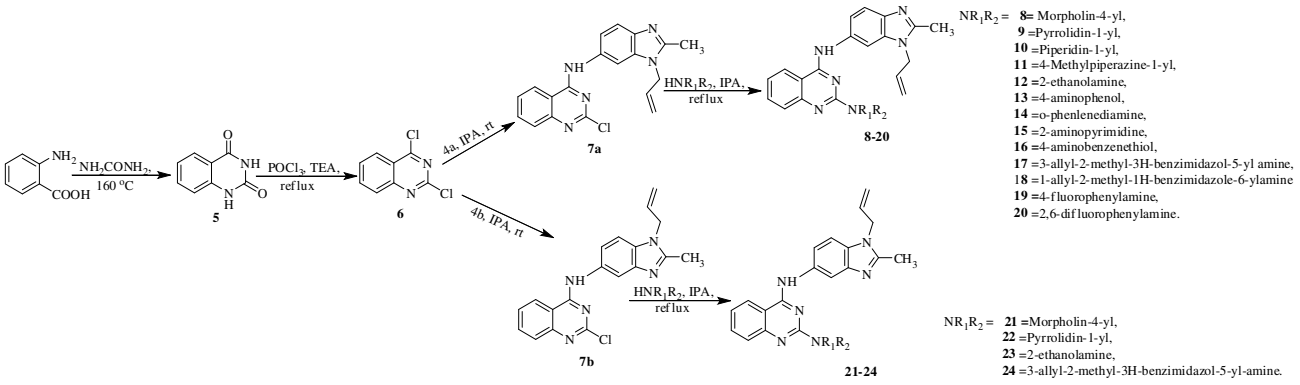

Scheme 2

2.2. Characterization :

(a) All the synthesized compounds were characterized by ^{1}H and ^{13}C NMR spectra (Bruker FT-NMR 400 MHz and JEOL ECS-400 MHz spectrometers), Mass Spectra (Waters Micromass Q-Tof Micro, Milford, MA) and Infrared Spectra (Jasco FTIR plus 460 Japan).

(b) Single crystal X-ray crystallography of compound **21** was grown in ethanol to develop single crystal with Crystalispro diffractometer with graphite monochromated Mo Kα radiation (λ = 0.7107 Å) using SHELX-97, full-matrix least-square refinement method.

2.3. Biological Evaluation:

(a) Compounds **7a-b**, **8-9**, **11-12**, **15-19** and **21-24,** submitted to National Cancer Institute (NCI) for *in vitro* anticancer assay were evaluated for their anticancer activities. Preliminary *in vitro* one dose anticancer assay was performed in full NCI 60 cell panel representing leukaemia, melanoma and cancers of lung, colon, brain, breast, ovary, kidney and prostate in accordance with the protocol of the NCI, USA. The data reported as mean-graph of the percent growth of the treated cells and presented as percentage growth inhibition (GI%). Among the selected compounds, **17-19** were further screened for 5-log dose molar range as these have shown prominent cell growth inhibition at 10 μM concentration against variety of cell lines. Compound **17** was almost ten and eleven fold more active than respective quinazoline and benzimidazole derivative, with MG MID GI_{50}, TGI and LC_{50} values of 1.64 μM, 3.28 μM and 5.50 μM respectively. Compound **18** showed twenty and twenty two fold more activity than respective quinazoline and benzimidazole derivative, with MG MID GI_{50}, TGI and LC_{50} values of 0.81 μM, 2.08 μM and 4.47 μM respectively while compound **19** showed four fold more active than quinazoline and benzimidazole analogue, with MG MID GI_{50}, TGI and LC_{50} values of 4.52 μM, 15.9 μM and 57.1 μM respectively

(c) Interaction of compounds **7a**, **9-11**, **13-15** and **17-19** with Aurora-A has also been studied using Aurora-A kinase assay/inhibitor screening kit. The compound **11** under present

investigation targeted Aurora-A for exhibiting best anti-cancer activity. Ligand efficiency indicated that the higher activity of compounds **7a, 11** and **22** have comparable binding tendency to enzyme with ligand efficiency of 0.35, 0.34 and 0.39 respectively**.**

2.4. Physicochemical Parameters

(a) Log P (lipophilicity) value of hybrid compounds (secondary amines) were determined with the help of 'Shake Flask' method. Compound **9** has higher log P value (2.90) which corresponds to higher antitumor activity.

(b) Quantitative structure-activity relationship provided correlations between pharmacological and physico-chemical descriptors of hybrid compounds. Four descriptors(log P, molar refractivity, ionization potential and heat of formation) have improved the robustness of the model with cross-validated $q^2 = 0.6743$, non-cross-validated $r^2 = 0.8457$ and degree of statistical confidence for test F = 6.8492, considered significant.

2.5. Molcular Modelling

We have carried out docking of most active compounds **9, 17-19** in the active site of ribonucleotide reductase (enzyme responsible for DNA replication), topoisomerase I, topoisomerase II and Aurora A kinase. Docking of compounds **9, 17-19** in the active site of these enzymes indicated the probable mode of action of these compounds for anticancer activities.

Chapter 3: covers purine-benzimidazole hybridization, their characterization, *in-vitro* evaluation and molecular modelling

3.1. Synthesis of purine-benzimidazole hybrids

The synthetic strategy to prepare the purine-benzimidazole hybrids **(3-19)** has been depicted in **scheme 3**. Treatment of 3,4-dihydro-1*H*-purin-2,6-(5*H*,9*H*)-dione with phosphorus oxychloride in the presence of triethylamine for 5h afforded 2,6-dichloropurine **(1)**. *N*-1-Allyl-2-methyl-1*H*-benzo[*d*]imidazol-5-ylamine **(2a)** and *N*-3-allyl-2-methyl-3*H*-benzo[*d*]imidazol-5-ylamine **(2c)** have been synthesized and characterized as given in section-2.1. *N*-1/3-Butyl-2-methyl-1*H*/3*H*-benzo[*d*]imidazole-5-ylamine has been synthesized by the alkylation of 2-methyl-5-nitro-benzimidazole with butyl bromide in the presence of NaH in THF at room temperature for 8 h to followed by treated with suspension of $SnCl_2.2H_2O$ in 2N HCl at 110 $^{\circ}$C for 7 h to give pure solid compounds of **2b** and **2d.** 2,6-Dichloropurine **(1)** was then treated with **2a-d** in the presence of isopropyl alcohol (IPA) at room temperature for 24 h gave **3a-d.** Refluxing of compounds **3a-d** with morpholine, piperidine, pyrrolidine and N-methylpiperazine in ethanol and after purification with column chromatography gave compounds **4-19** in good yields.

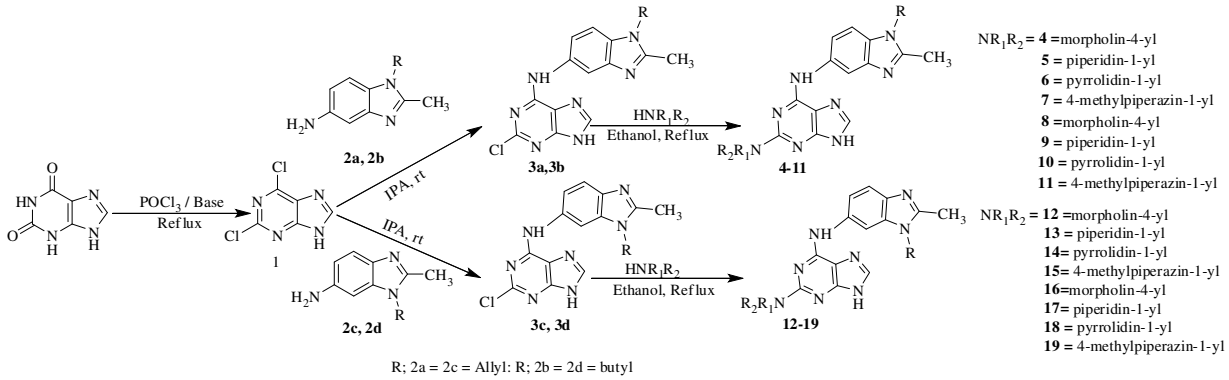

Scheme 3

3.2. Characterization :

(a) All the synthesized compounds were characterized by ^{1}H and ^{13}C NMR spectra (JEOL ECS -400 at 400 and 100 MHz NMR spectrometers), Mass Spectra (Waters Micromass Q-Tof Micro, Milford, MA) and Infrared Spectra (Agilent technology cary 630 USA).

(b) Single crystal X-ray crystallography of compound **19** was grown in ethanol to develop single crystal with Crystalispro diffractometer with graphite monochromated Mo Kα radiation (λ = 0.71073 Å) using SHELX-97, full-matrix least-square refinement method.

3.3. Biological Evaluation:

(a) Compounds **3a-d, 4, 6-11, 16** and **18-19** submitted to National Cancer Institute (NCI) for *in vitro* anticancer assay were evaluated for their anticancer activities. Compound **6** exhibited significant growth inhibition and was evaluated for further 60 cell panel at five dose concentration level. MG-MID revealed that compound **6** is 1.25 fold more active than 5-fluorouracil, with GI_{50} value of 18.12 µM

(b) Interaction of compounds **3a-b**, **4-7** and **10** were also studied with Aurora-A enzyme using Aurora-A kinase inhibitor screening kit. The compound **6** under present investigation probably target Aurora-A for exhibiting best anti-cancer activities with IC_{50} value of 0.01 µM. Ligand efficiency (LE) has also been determined for these compounds that indicated the higher efficiency of compound **6** with LE = 0.39 for binding to the enzyme.

3.4. Physicochemical Parameters

(a) The partition of all the compounds **3a-d** and **4-19** were studied in octanol/water systems determining the log P values with shake-flask method. It has been indicated that compound **6** showed higher log P value (2.53) that supported the dependency of lipophilicity with higher activity of this compound towards Aurora A inhibition and cancer cell lines.

(b) Quantitative structure-activity relationship has been provided correlations between inhibitory activities and physico-chemical descriptors of compounds. Four descriptorshave improved the robustness of the model with cross-validated q^2 = 0.9185, correlation coefficient r^2 = 0.994 and degree of statistical confidence for test F = 83.3054 that considered significant for the activity.

3.5. Molecular Modelling

Docking has been done with most active compound **6** in the active site of Aurora-A kinase (pdb ID 2WTV). Docking of compound **6** in the active site of this enzyme indicated the probable mode of action for anticancer activity. CPK model of Aurora-A kinase (2WTV) also clearly showed the compatibility of compound **6** in the active site of the enzyme.

Chapter 4: covers Pd-catalyzed coupling reaction of 2,4-dichloroquinazoline

4.1. Synthesis of monoarylated and diarylated quinazolines:

The synthetic strategy for the synthesis of monoarylated and diarylated quinazolines **(1-9)** has been shown in **scheme 4**. Refluxing of quinazolin-2,4-dione with phosphorous oxychloride in the presence of triethylamine for 7 h to obtain 2,4-dichlorquinazoline which was then treated with different aryl boronic acids, catalysts and bases through Suzuki-Miyaura cross coupling reaction gave compounds **1-9**.

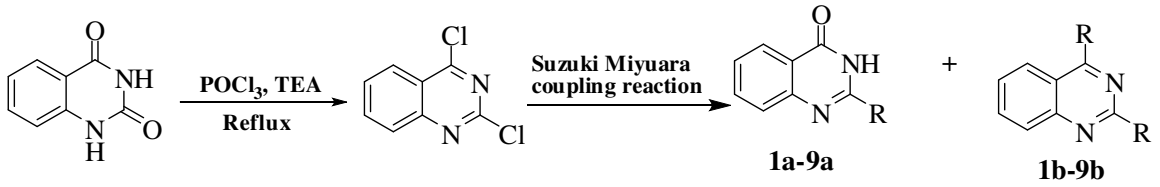

R = p-ClC_6H_5, p-BrC_6H_5, p-FC_6H_5, m-$CH_3C_6H_5$, p-$OCH_3C_6H_5$, thiophene, furan, naphthalene

Scheme 4

A variety of conditions and combinations of catalyst systems, bases and solvents were screened and adopted for optimal reaction conditions for monosubstitution and disubstitution of 2,4-dichloroquinazoline with phenyl boronic acid. Interestingly, under most of the reaction conditions, C2 monoarylated was the major product, with varying amounts of C2 and C4 diarylated product resulting from different aryl/heteroaryl boronic acids. Csp^2-O and C-C coupling reactions between 2,4-dichloroquinazoline and phenylboronic acid with palladium based catalysts like $Pd(PPh_3)_4$, $Pd(PPh_3)_2Cl_2$ and $Pd_2(dba)_3$; $Pd(PPh_3)_4$ proved as an effective catalyst for monoarylation (hydroxylated) and diarylation. Among the variation of bases such as K_2CO_3, Na_2CO_3, NaO^tBu and Cs_2CO_3, with $Pd(PPh_3)_4$ catalyst revealed that K_2CO_3 turned

out to be the most effective base to give desired products. The effect of different solvents like toluene, acetonitrile, dioxane and tetrahydrofuran along with water as a co-solvent were also studied and observed that better yield of products were obtained in toluene:H_2O (9:1) mixture. Thus, number of 2-aryl-3*H*-quinazolin-4-ones (**1a-9a**) and 2,4-diarylquinazolines (**1b-9b**) were prepared via coupling of 2,4-dichloroquinazoline with variety of aryl boronic acids under the same reaction conditions.

4.2. Characterization :

(a) All the synthesized compounds were characterized by ^{1}H and ^{13}C NMR spectra (JEOL ECS-400 at 400 and 100 MHz NMR spectrometers), Mass Spectra (Waters Micromass Q-Tof Micro, Milford, MA) and Infrared Spectra (Agilent technology cary 630 USA).

(b) Single crystal X-ray crystallography of 2,4-Di-naphthalen-1-yl-quinazoline (**9b)** was grown in ethanol to develop single crystal with Bruker AXS KAPPA APEX II diffractometer with graphite monochromated Mo Kα radiation (λ = 0.7107 Å) using SHELX-97, full-matrix least-square refinement method.

4.3. Biological Evaluation:

(a) Three compounds **2b, 3b** and **9b** submitted to National Cancer Institute (NCI) for *in vitro* anticancer assay were evaluated against 60 human cancer cell lines at single dose of 10 µM which included nine tumor subpanels namely; leukemia, non-small lung, colon, CNS, melanoma, ovarian, renal, prostate and breast cancer cellsand their outputs were reported as a mean graph of the percent growth of treated cells, and presented as percentage growth inhibition (GI %). Preliminary *in vitro* antitumor screening revealed that compounds **2a, 3b** and **9b** showed moderate growth inhibition (20-70%) for some of the cancer cell lines.

REFERENCES

1. Hanahan, D.; Weinberg, R. A. *Cell* **2000**, *100*, 57.
2. Cooper, G. M.; In "Elements of Human Cancer", Jones and Bartlett Publishers, Boston, **1992**, Chapter 1.
3. (a) Baselga, J.; Swain, S. M. *Nat. Rev. Cancer* **2009**, *9*, 463; (b) Brown, C. H. J.; Lain, S.; Verma, C. H. S.; Fersht, A. R.; Lane, D. P. *Nat. Rev. Cancer* **2009**, *9*, 862.
4. Noble, M. E.; Endicott, J. A.; Johnson, L. N. *Science* **2004**, *303*, 1800.
5. Thaimattam, R.; Banerjee, R.; Miglani, R.; Iqbal, J. *Curr. Pharm. Des.* **2007**, *13*, 2751.
6. (a) Glover, D. M.; Leibowitz, M. H.; McLean, D. A.; Parry, H. *Cell* **1995**, *81*, 95–105;

(b) Pan, J.; Wang, Q.; Snell, W. J. *Cell* **2004**, *6*, 445.

7. Bischoff, J. R.; Anderson, L.; Zhu, Y.; Mossie, K.; Ng, L.; Souza, B.; Schryver, B.; Flanagan, F.; Clairvoyant, F.; Ginther, C.; Chan, C. S.; Novotny, M.; Slamon, D. J.; Plowman, G. D. *EMBO J.* **1998,** *17*, 3052.
8. Tong, T.; Zhong, Y.; Kong, J.; Dong, L.; Song, Y.; Fu, M.; Liu, Z.; Wang, M.; Guo, L.; Lu, S.; Wu, M.; Zhan, Q. *Clin. Cancer Res.* **2004**, *10*, 7304.
9. Wang, X. X.; Liu, R.; Jin, S. Q.; Fan, F. Y.; Zhan, Q. M. *Cell Res.* **2006**, *16*, 356.
10. (a) Bansal, Y.; Silakari, O. *Bioorg. Med. Chem.* **2012**, *20*, 6208; (b) Michael, J. P. *Nat. Prod. Rep.* **2008**, *25*, 166; (c) Marzaro, G.; Guiotto, A.; Chilin, A. *Expert Opin. Ther. Pat.* **2012**, *22*, 223.
11. (a) Raghavendra, N. M.; Thampi, P.; Gurubasavarajaswamy, P. M.; Sriram, D. *Chem. Pharm. Bull.* **2007**, *55*, 1615; (b) Verhaeghe, P.; Azas, N.; Gasquet, M.; Hutter, S.; Ducros, C.; Laget, M.; Rault, S.; Rathelot, P.; Vanelle, P. *Bioorg. Med. Chem. Lett.* **2008**, *18*, 396; (c) Alagarsamy, V.; Solomon, V. R.; Sheorey, R. V.; Jayakumar, R. *Chem. Biol. Drug Des.* **2009**, *73*, 471; (d) Smits, R. A.; Adami, M.; Istyastono, E. P.; Zuiderveld, O. P.; van Dam, C. M. E.; de Kanter, F. J. J.; Jongejan, A.; Coruzzi, G.; Leurs, R.; de Esch, I. J. P. *J. Med. Chem.* **2010**, *53*, 2390; (e) Kasibhatla, S.; Baichwal, V.; Cai, S. X.; Roth, B.; Skvortsva, I.; Skvortsov, S.; Lucas, P.; English, N. M.; Sirisoma, N.; Drewe, J.; Pervin, A.; Tseng, B.; Carlson, R. O.; Pleiman, C. M. *Cancer Res.* **2007**, *67*, 5865; (f) Font, M.; Gonzalez, A.; Palop, J. A.; Sanmartin, C. *Eur. J. Med. Chem.* **2011**, *46*, 3887; (g) Liu, F.; Lovejoy, D. B.; Hassani, A. A.; He, Y.; Herold, J. M.; Chen, X.; Yates, C. M.; Frye, S. V.; Brown, P.J.; Huang, J.; Vedadi, M.; Arrowsmith, C. H.; Jin, J. *J. Med. Chem.* **2011**, *54*, 6139; (h) EI-Azab, A.S.; Al-Omar, M.A.; Abdel-Aziz, A.A.M.; Abdel-Aziz, N.I.; EI-Sayed, M.A.-A.; Aleisa, A.M.; Sayad-Ahmed, M.M.; Abdel-Hamide, S.G. *Eur. J. Med. Chem.* **2010**, *45*, 4188; (i) Noolvi, M. N.; Patel, H. M.; Bhardwaj, V.; Chauhan, A. *Eur. J. Med. Chem.* **2011**, *46*, 2327; (j) Xu, J. Y.; Zeng, Y.; Ran, Q.; Wei, Z.; Bi, Y.; He, Q. H.; Wang, Q. J.; Hu, S.; Zhang, J.; Tang, M. Y.; Hua, W. Y.; Wu, X. M. *Bioorg. Med. Chem. Lett.* **2007**, *17*, 2921; (k) Peifer, C.; Buhler, S.; Hauser, D.; Kinkel, K.; Totzke, F.; Schachtele, C.; Laufer, S. *Eur. J. Med. Chem.* **2009**, *44,* 1788.

PUBLICATIONS

1. **Alka Sharma**, Vijay Luxami and Kamaldeep Paul, "Synthesis, single crystal and antitumor activities of benzimidazole-quinazoline hybrids", *Bioorganic & Medicinal Chemistry Letters*, **2013**, *2,* 3288-3294.
2. Kamaldeep Paul, **Alka Sharma** and Vijay Luxami, "Synthesis, in vitro evaluation and molecular modeling of benzimidazole-primary amine substituted quinazoline hybrids", *Bioorganic & Medicinal Chemistry Letters*, **2014**, *24*, 624-629.
3. **Alka Sharma**, Vijay Luxami and Kamaldeep Paul, "Csp^2–O and C-C bond formation via Pd-Catalyzed coupling reaction of 2,4-dichloroquinazoline", *Journal of Heterocyclic Chemistry* **2015 (DOI: 10.1002/jhet.2330)**.
4. **Alka Sharma**, Vijay Luxami and Kamaldeep Paul, "Purine-Benzimidazole hybrids: Synthesis, single crystal determination and in vitro evaluation of anticancer activities. *European Journal of Medicinal Chemistry* **2015**, *93*, 414-422.
5. Vijay Luxami, Richa Rani, **Alka Sharma** and Kamaldeep Paul, Quinazoline-benzimidazole hybrid as dual optical sensor for Cyanide and Pb^{2+} ions and Aurora kinase Inhibitor. *Journal of Photochemistry and Photobiology A: Chemistry*, **2015,** *311,* 68-75.

PAPERS PRESENTED AT CONFERENCES

1. **Alka Sharma**, Vijay luxami, Kamaldeep Paul "Coupling of bicyclic heterocycles and quinazoline : Aurora kinase inhibitors". National conference on emerging trends in chemistry-biology interface (ETCBI-2011) held at kumaun University, Nainital on 03-05 November, **2011**.
2. **Alka Sharma**, Vijay luxami, Kamaldeep Paul "Synthesis and biological evolution of benzimidazole based substituted quinazoline as potential anticancer agents". National symposium on chemistry in 21st Century celebrating international year of chemistry-2011 held at Guru Nanak Dev University, Amritsar on 23-24 December, **2011**.
3. **Alka Sharma**, Vijay luxami, Kamaldeep Paul "Perspectives and challenges In drug research: synthesis and bioevaluation of heterocyclic moieties as novel anticancer agents". Chemical Research Society of India- 2012 held at CDRI, Lucknow on 21-22 July, **2012**.
4. **Alka Sharma**, Vijay luxami, Kamaldeep Paul "Heterocyclic moieties as anticancer: synthesis, characterization and *in-vitro* evolution". Chemical Constellatio Cheminar-

2012 held at Dr. B R Ambedkar National Institute of Technology, Jalandhar on 10-12 Sept, **2012**.

5. **Alka Sharma**, Vijay luxami, Kamaldeep Paul "Ligand free palladium-catalyzed monoarylation/oxidation and diarylation of 2,4-dichloroquinazoline with different boronic acids "NCIMSF-2013 held at Thapar university, Patiala on 26-28 Oct, **2013**.